Theses and Dissertations   1. Thesis and Dissertation Collection, all items

2009-06

Relationship of grain boundary structure and mechanical properties of Inconel 690

Marra, Joseph J.

Monterey California. Naval Postgraduate School

http://hdl.handle.net/10945/4304

Relationship of Grain Boundary Structure and Mechanical Properties of Inconel 690

By
Joseph J. Marra
Lieutenant, United States Navy
B.S. Electrical Engineering/Computer and Systems Engineering 2002
Rensselaer Polytechnic Institute

SUBMITTED TO THE DEPARTMENT OF NUCLEAR SCIENCE AND ENGINEERING,
AND THE DEPARTMENT OF MECHANICAL ENGINEERING IN PARTIAL
FULFILLMENT FOR THE REQUIREMENTS FOR THE DEGREE OF
MASTER OF SCIENCE IN NUCLEAR SCIENCE AND ENGINEERING
AND
MASTER OF SCIENCE IN NAVAL ARCHITECTURE/MARINE ENGINEERING
AT THE
MASSACHUSETTS INSTITUTE OF TECHNOLOGY

June 2009
© 2009 Massachusetts Institute of Technology
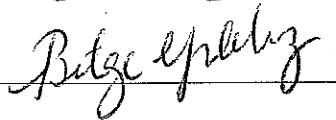
Signature of Author: _____
Joseph Marra
Department of Mechanical Engineering
May 8, 2009
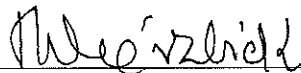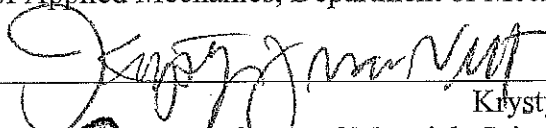
Certified by: _____
Bilge Yildiz, Ph.D.
Assistant Professor of Nuclear Science and Engineering
May 8, 2009
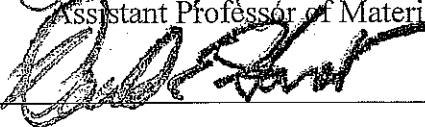
Certified by: _____
Tomasz Wierzbicki, Ph.D.
Professor of Applied Mechanics, Department of Mechanical Engineering
May 8, 2009

Certified by: _____
Krystyn Van Vliet, Ph.D.
Assistant Professor of Materials Science and Engineering
May 8, 2009

Accepted by: _____
David E. Hardt
Chairman, Department Committee of Graduate Studies
May 8, 2009

Accepted by: _____
Jacquelyn C. Yanch
Professor of Nuclear Science and Engineering
Chair, Department Committee on Graduate Students
May 8, 2009

Relationship of Grain Boundary Structure and Mechanical Properties of Inconel 690
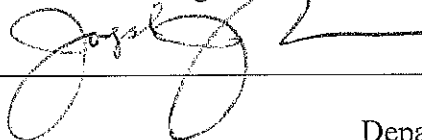
By
Joseph J. Marra
Lieutenant, United States Navy

Submitted to the Department of Nuclear Science and Engineering and
the Department of Mechanical Engineering in partial fulfillment for the requirements for
the degrees of Master of Science in Nuclear Science and Engineering and
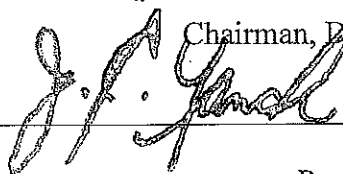Master of Science in Naval Architecture/Marine Engineering

ABSTRACT

Stress corrosion cracking (SCC), failure due to environmentally assisted crack nucleation and propagation, is an important metallurgical problem with impact on current and future designs of ship structural components and nuclear reactors. SCC occurs in the presence of tensile stress, corrosive environment, and a material with susceptibility. The initiation of SCC is difficult to detect and control due to the highly localized nature of chemical and mechanical conditions. As a result, its inhibition has been a particularly challenging problem. SCC mechanism is dependent on the microstructure, particularly the grain boundaries, for a given alloy composition. Therefore, inhibition could be sought from an improved fundamental understanding of the structural and mechanical characteristics at the material's grain boundaries.

This thesis investigated the relationship between the structural nature and the nanoscale mechanical properties on and near the grain boundaries to identify their role in the resistance to stress corrosion cracking. Inconel 690, an austenitic Ni-alloy, was chosen as the material of interest for its relevance in current applications in the nuclear energy technology. An integrated approach to probe the structural, mechanical and chemical information at the nanoscale consistently at select grain boundaries was developed. Grain boundary engineering was accomplished on Inconel 690 through thermomechanical processing (TMP) to produce samples with a desirable distribution of grain boundary structures. Crystallographic structure of the boundaries was identified using electron backscatter diffraction and orientation image mapping. Nanoindentation at ambient conditions was performed to extract mechanical properties with high spatial resolution at and near the selected grain boundaries. Inherent and tip-induced mechanical properties of grain boundaries were characterized on the solution annealed Inconel 690. Mechanical properties governed by the presence of chromium carbide precipitates at the boundaries were characterized on the TMP Inconel 690.

Hardness measured on and near the $\Sigma 3$, low angle, and high angle grain boundaries of the TMP Inconel 690 revealed the distribution of chromium carbide precipitates at each respective grain boundary. Chromium carbide precipitates led to continuously high hardness on the $\Sigma 3$ grain boundaries and discontinuous with large variations in the hardness on low and high angle grain boundaries. These results are consistent with the higher relative cracking susceptibility for low and high angle grain boundaries relative to $\Sigma 3$ grain boundaries.

Inherent hardness of the solution annealed Inconel 690 were found to be the same for both the grain boundary and bulk regions, and did not vary with grain boundary type, specifically the Σ3 and high angle boundaries. This finding is attributed to the weak dependence of the dislocation mobility on the diffusion path during high temperature annealing of the sample, which resulted in an approximately uniform distribution of dislocations prior to nanoindentation. On the other hand, greater hardness was induced at the grain boundaries due to the pile-up of dislocations created by the indentations towards the grain boundaries. The relative increase in hardness induced by the indentations, and the spatial extent of this increase were found to be equivalent for different grain boundary types. These results indicate comparable ease of dislocation mobility and absorption at the different grain boundaries of Inconel 690 when indented at room temperature.

Thesis Advisor: Assistant Professor Bilge Yildiz
Thesis title: Relationship of Grain Boundary Structure and Mechanical Properties of Inconel 690

Table of Contents

List of Figures

9

List of Tables

1. Introduction

1.1. Background

Stress corrosion cracking (SCC), the failure of a material due to environmentally assisted crack nucleation and propagation, is a serious metallurgical problem with impact on current and future nuclear system designs. SCC results from the combination of a material with known susceptibility, the presence of tensile stress and a corrosive environment, shown graphically in Figure 1.1.
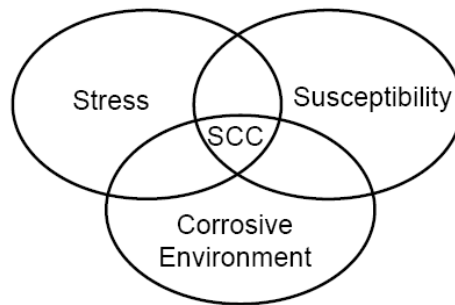
Figure 1.1 – SCC requires the combination of stress, a corrosive environment and material susceptibility.

Inhibition of SCC has been a particularly difficult problem. Conditions that cause this phenomenon to occur are highly localized and thus are difficult to detect and control through the life of components in systems with long designed service lives in harsh environments. Concentrations of ions that pose a specific risk of SCC can be extremely small and difficult to detect. Furthermore, while the applied stresses can obviously result in SCC, residual stress from component fabrication can often provide a sufficient stress intensity to result in failure.

Though the commonly used definition depicted in Figure 1.1 is accurate, it is in fact an oversimplification of this phenomenon. In order to analyze this problem thoroughly, we must

first clearly describe the necessary elements that lead to material failure from SCC. While each element will be discussed individually, the fact that the combined effect from of each element is necessary for SCC can not be understated.

1.1.1. Stress

The presence of stress is the fundamental component of the SCC process. However, an important distinction is that crack propagation does not occur as a result of local stresses that exceed the critical stress intensity required by fracture mechanics. In fact, stress required to induce fracture and crack growth is much less than the material's critical stress intensity. This phenomenon is known as subcritical crack growth. Stress, which can be either residual or applied, must be tensile in order to induce SCC; compressive stress is actually used as a method of SCC inhibition [1]. Sufficient stress to induce SCC can be substantially below the yield strength of the material.

1.1.2. Material

The most common materials studied when discussing SCC susceptibility are metallic alloys. However, other materials, such as pure metals, ceramics and polymers have all been known to be susceptible to SCC [1]. The scope of this thesis will include only polycrystalline metallic alloys. Though discoveries from this thesis can be applied to advance the knowledge of SCC mechanisms, specific results gathered will be relevant to contemporary applications in the nuclear industry.

1.1.3. Corrosive environment

The corrosive environment that contributes to SCC primarily serves to provide a sufficient concentration of a chemical species. Due to the presence of these chemical species,

highly localized general corrosion of the material occurs. The material is "pulled" apart due to the presence of tensile stress, resulting in more material exposure and subsequent localized general corrosion of the newly exposed material. This process continues and, over time, cracks propagate from these sites, form branches, and lead to the material failure, as shown in Figure 1.2.
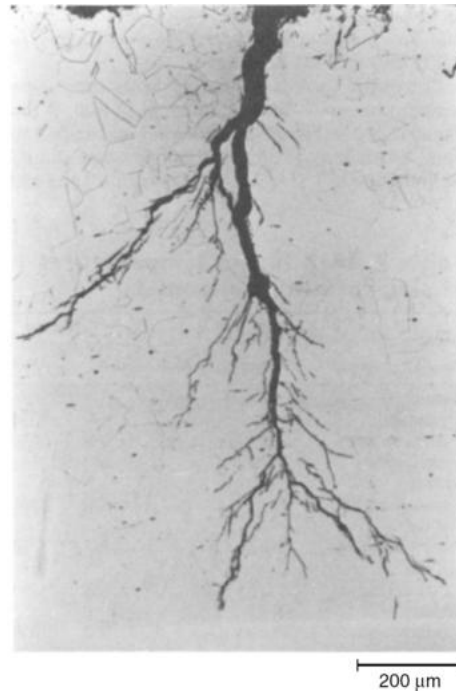
Figure 1.2 – Chloride SCC of a type 304 stainless steel tube, showing the development of cracks into branches [2].

Beyond contributing to the initial mechanism of general corrosion, SCC susceptibility is greatly sensitive to temperature and the amount of circulation of O_2 (or other gaseous environments) in the vicinity of cracks. The change of any of these factors can result in an environment thought to be free from susceptibility to an environment that will cause local failure.

1.1.4. Common susceptible material and environment combinations

When in the presence of tensile stress, the known combinations of materials and environments that are susceptible to SCC are numerous. New combinations are constantly being discovered as materials in all types of engineering systems progress through their designed service lives. For the purpose of understanding the robust challenge SCC presents, examples of combinations of commonly used materials and accompanying corrosive environments that are known to be susceptible are shown in Table 1.1.

Alloy	Environment
Carbon steel	Nitrate, caustic, and carbonate solutions
High strength steels	Aqueous electrolytes containing H_2S
Austenitic stainless steels	High concentrated chloride solutions
High-nickel alloys	High-purity steam
a-brass	Ammoniacal solutions
Aluminum alloys	Aqueous Cl^-, Br^- and I^- solutions
Titanium alloys	Aqueous Cl^-, Br^- and I^- solutions, organic liquids and N_2SO_4
Magnesium alloys	Aqueous Cl^-
Zirconium alloys	Aqueous Cl^-, organic liquids, and I_2

Table 1.1 – Examples of commonly occurring combinations of material and corrosive environments that exhibit susceptibility to SCC. Table taken from reference [2].

By no means are the examples shown in Table 1.1 inclusive of the materials and environments that can combine to result in component failure through SCC. These examples do, however, show how failure from SCC covers a wide range of materials and environments making inhibition difficult and expensive to incorporate into design.

1.1.5. Microstructure

SCC failure occurs through a process that causes a material to fracture. Fracture phenomenon is closely related to the microstructural components such as the crystalline structure, size and distribution of types of grain boundaries [1]. Therefore, thoroughly

understanding microstructure is an important aspect of understanding and preventing SCC. The

microstructural components that are known to be associated with fracture phenomena can be

analyzed macroscopically, microscopically and atomistically, shown schematically in Figure 1.3.
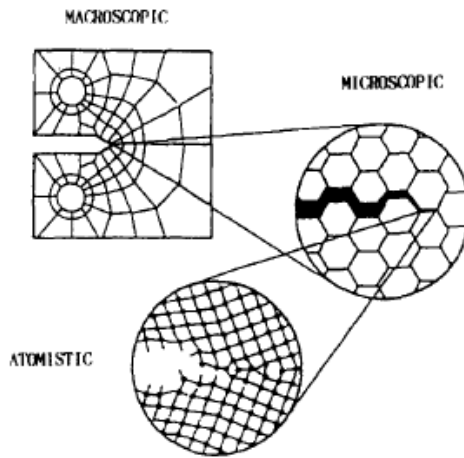
Figure 1.3 – The length scales at which microstructural components can be studied.

 The most basic aspect of microstructure is the crystalline structure of the material.

Atoms in a crystalline material are uniquely arranged, known as a crystal lattice. Figure 1.4

shows an examples of a face centered cubic crystal lattice, which will be relevant to the

discussion of Inconel 690 in this thesis.
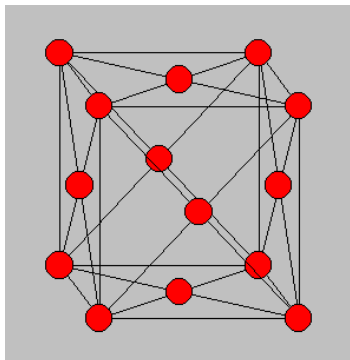
Figure 1.4 – Face centered cubic (FCC) crystal lattice [3].

The lattice parameters, or the distances and angles between atoms in the lattice, are determined by the lowest energy configuration for the material. The properties of a crystal lattice also effect how the lattice handles shear stress. When shear stress is applied to the lattice, parts of the lattice glide along each other, resulting in a deformation of the material. The paths that the lattice glides along are known as slip planes and can be distinctly identified for different types of crystal lattices. The face centered cubic crystal lattice that will be discussed in this thesis contains twelve (12) different slip planes.

The interfaces between smaller crystals of differing orientation are known as grain boundaries and are the most important aspect of microstructure. The stress field that exists due to the misorientation of neighboring grains results acts as a barrier to the translation of dislocation. Thus, the networks formed by grain boundaries drastically affect the macroscopic mechanical properties of a material. The effects on the mechanical properties of a material are not homogeneous, however. Grain boundaries do not exhibit the same resistance to fracture; some are strong while some are weak. In addition to exhibiting varying mechanical properties, grain boundaries can vary based on their chemical composition. Chemical constituents can either enrich at or segregate from grain boundaries depending on material type and the environment conditions. As a result of these effects, grain boundaries are known to be sites of preferential crack initiation and propagation.

1.2. Stress corrosion cracking related component failures in the nuclear industry

SCC was identified as a major problem in the nuclear industry by the Nuclear Regulatory Commission as early as the 1970s. Specifically, in 1975, the NRC became aware of the issue of tube "denting," or the degradation of a tube in the form of a diameter reduction, in steam generators, a vital component in nuclear power plants [4]. Steam generators house numerous

tubes that contain high pressure, high temperature water that has been heated in the reactor core. As the water from the reactor core flows into through the steam generator tubing, it boils water external to the tubing, forming steam that drives the power plants turbine and generates electricity. This is shown schematically in Figure 1.5.
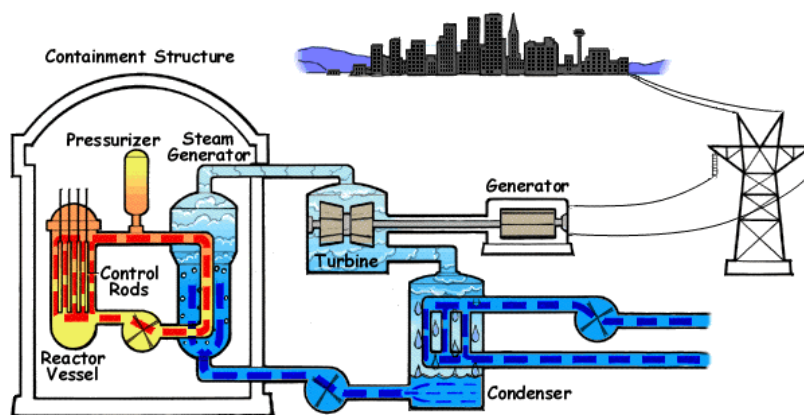
Figure 1.5 – Schematic of a nuclear power plant showing the function of the steam generator.

There are two materials used in pressurized water nuclear reactor steam generators in the United States: Inconel 600 and Inconel 690, two members of a family of austenitic nickel-chromium-based super alloys. In this capacity, they are exposed to temperatures ranging from 278 ºC to 324 ºC and pressures ranging from 7 MPa to 15.5 MPa. In addition their functionality, steam generator tubes serve as the primary enclosure of radioactive material inside of the nuclear plant. Steam generator tube failure can result in contamination of steam that could potentially contaminate the atmosphere. Thus, maintaining the structural integrity of these components is vital to avoid this potentially catastrophic result. In order to improve their mechanical properties and corrosion resistance of Inconel 600 and Inconel 690, these alloys are either mill-annealed or thermally treated. Steam generator tubing in the Unites States is mill-annealed Inconel 600, thermally treated Inconel 600, or thermally treated Inconel 690 [5].

Despite being designed to resist corrosive processes, examples of steam generator tube failures due to SCC in the nuclear industry in the United States are well documented. The first of such accidents caused by SCC was the failure of Inconel 600 steam generator tubes at the Robert E. Ginna Nuclear Power Plant near Rochester, New York, on January 25, 1982 [6]. The accident resulted in the release of 90 curies of radiation to the environment. Metallographic analysis was performed following the accident and revealed the presence of an intergranular stress corrosion crack in the steam generator tubing.

A similar accident occurred in the steam generator tubing at Fort Calhoun, near Omaha, Nebraska, in February, 1984. Fort Calhoun's two steam generators, each comprised of 5,005 mill annealed Inconel 600 tubes, were hydrostatically tested following the detecting of approximately 0.2 gallons per day in steam generator B. The failed tube exposed during hydrostatic testing was found to be a 1.25" long axial "fishmouth" opening at a "U" bend of the tube bottom. This section was removed for laboratory analysis and determined to have failed via transgranular SCC from the outside of the tubing. The analysis revealed a degradation of 95% of the tubing wall thickness [7].

Arkansas Nuclear One Unit 2, located on Lake Dardanelle in Russellville, Arkansas, shut down on March 9, 1992 after discovering of a primary-to-secondary leak of 0.25 gallons per minute. Further inspection revealed a circumferentially-oriented intergranular SCC extending 360 degrees around the outer diameter of the tube at the hot leg expansion transition location, located near the top of the tubesheet. Cracks extended as deep as 94 percent into the tube wall, rendering it below standards for normal operating conditions and requiring replacement. Following these findings, Arkansas Nuclear One management conducted a full inspection of the

remaining tubes and found indications of circumferential cracking on the hot leg side of 488 tubes [8].

McGuire Nuclear Station, near Charlotte, North Carolina, shut down in August, 1993 following the failure of a steam generator tubes containing kinetically welded sleeves made of Inconel 690. The failure resulted in a primary-to-secondary leak of about 200 gallons per day. The tube was removed and analyzed, which revealing 120 degree to 180 degree circumferential cracks located just above the weld that joined the sleeve and the tube. Cracking through the entire tubing wall was also found to exist for 270 degrees around the tube circumference. The remaining 90 degrees of the tubing had experienced cracking through 50% of the wall [9].

On February 15, 2000, Indian Point Nuclear Power Plant in Buchanan, New York, also experienced a steam generator tube rupture and was forced to shut down. The rupture resulted in a primary-to-secondary leak of 19,197 gallons and a discharge of radioactive steam into the surrounding atmosphere. Subsequent analysis of Indian Point's four steam generators, each made up of 3,260 Inconel 600 tubes, revealed that a single tube had failed via a crack approximately 3 inches in length at the inner radius of a U-bend [4].

In addition to expensive repairs, susceptibility to SCC of steam generator components even caused the premature decommissioning of a nuclear generating station. Commonwealth Edison completed the shutdown of Zion Nuclear Power Station, located near Chicago, Illinois, in the spring of 1998 after the announcement of its plan to shut down the site rather than repair failing steam generator tubes [10].

As discussed in Chapter 1.2, the two materials used in steam generators are Inconel 600 and Inconel 690, two austenitic nickel-based super alloys. Inconel 690 has been used extensively to replace degraded steam generator tubing, originally made of Inconel 600, in operating nuclear

reactors and has been proposed as the standard material for use in steam generators of new

generation nuclear reactors. Inconel 690 is preferred due to its high strength, metallurgical

stability, desirable fabrication properties and strong resistance to corrosion by oxidizing acids

and salts in aqueous, high temperature environments.

The mechanical properties and chemical composition of Inconel 690 are summarized in

Table 1.2 and Table 1.3.

Inconel 690 properties	
Young's modulus (E)	211 GPa
Hardness (H)	1.67 GPa
Poisson's ratio (υ)	0.29
Shear modulus (μ)	81.8 GPa

Table 1.2 – Properties of Inconel 690

Inconel 690 Chemical Composition	
Ni	59.47%
Cr	29.50%
Fe	10.24%
Mn	0.15%
Si	0.04%
C	0.03%
Co	0.003%
S	0.001%
Cu	< 0.01%

Table 1.3 – Inconel 690 chemical composition

1.3. Summary

In conclusion, SCC is a phenomenon that can affect all engineering systems. It occurs

when specific electrochemical, metallurgical, mechanical and chemical conditions are present

locally and simultaneously. Materials can exhibit decreased susceptibility depending on their

microstuctural characteristics. Developing an understanding of how the synergy of these factors

works can be effective step in inhibiting SCC. Therefore, this study aims to understand the

relationship between microstructural characteristics and mechanical properties. First, a detailed

explanation of the proposed mechanisms governing of SCC is discussed in Chapter 2. This review is followed by the thesis problem statement and objective in Chapter 3, and an explanation of the approach to measuring and analyzing mechanical properties and their relationship to individual grain boundaries in Chapter 4. A discussion of the experimental procedure follows in Chapter 5. Finally, in Chapters 6 and 7, the results and corresponding conclusions from the recorded experimental data are discussed.

2. Background: stress corrosion cracking mechanisms

To preface the discussion of results and the conclusions deduced from those results, this section provides an explanation of the proposed mechanisms of crack initiation and propagation. Specifically, this section contains a review of factors that affect crack initiation and propagation, and the relationship of those processes to environmental factors, material composition, stress and microstructure. The discussion of these concepts uses reference [11] throughout this section.

2.1. Overview

SCC has long been thought to occur when the alloy involved was known to be susceptible, in a particular environment and in the presence of tensile stress, as shown in Figure 1.1. More recently, the known environments and susceptible material that can result in stress corrosion cracking have grown to include a wide range of combinations. Therefore, the distinguishing requirement for SCC to occur has been narrowed to include only the presence of tensile stress. SCC serves to reduce the amount of strain that causes failure and, thus, the maximum stress that can be applied prior to failure. SCC susceptibility is generally inversely proportional to the general corrosion rate of the material.

SCC occurs over a long time scale and can best be described as occurring in three distinct stages. Figure 2.1 shows the logarithmic crack propagation rate, V or $\frac{da}{dt}$, shown as a function of stress intensity, which exemplifies the three stages of SCC.
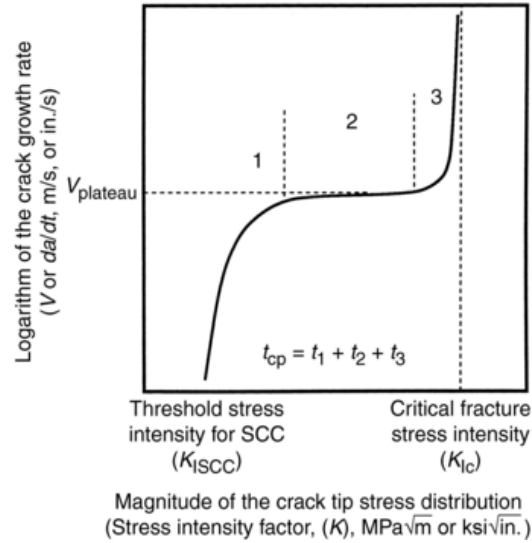
Figure 2.1 - Three stages of SCC, taken from reference [1].

No crack propagation occurs below the threshold stress intensity, K_{ISCC}. The threshold stress intensity is a function of the material as well as the local environmental conditions. The region above the threshold stress intensity is referred to as stage 1. In stage 1, small cracks propagate despite predictions by fracture mechanics that failure should not occur. Crack growth increases approximately quickly with increasing stress intensity. This stage is also referred to as subcritical crack growth and occurs over a large time scale. At higher stress intensities, known as stage 2, crack growth becomes independent of stress intensity and instead depends strictly on the environmental conditions. Crack propagation proceeds at a constant velocity, shown in Figure 2.1 as $V_{plateau}$, which is characteristic of the equilibrium between the environment and the amount of material available for the corrosion reaction to proceed. At even higher stress intensities, known as stage 3, crack growth increases exponentially with increasing stress intensity until fracture occurs at some critical stress intensity, known as the critical fracture intensity (K_{IC}) or the fracture toughness of the material. The total crack propagation time, t_{cp}, is simply the sum of the time of each stage.

2.2. Parameters that affect stress corrosion cracking

The mechanisms that were proposed to explain SCC involve a series of processes and chemical reactions. Crack tip propagation velocities in the aforementioned stages of SCC are affected by a number of rate-determining steps, as follows[11]: mass transport along the crack to the crack tip, reactions in the solution near the crack, surface absorption near the crack, surface diffusion, surface reactions, absorption into the bulk, bulk diffusion to the plastic zone ahead of the crack tip, chemical reactions in the bulk, and rate of interatomic bond rupture.

Therefore, any environmental factors that affect these rate-determining steps will have a result on the velocity of crack propagation. These include[11]: temperature, pressure, solute species, solute concentration and activity, pH, electrochemical potential, solution viscosity, agitation, and flow rate. Changes in these environmental factors affect crack propagation rates, and can also re-initiate crack propagation after it has stopped, or stop crack propagation from proceeding any further. Another important consideration regarding environmental factors is the role of the bulk regions of the material. Crack propagation occurs due to local conditions at the crack, which include interactions between chemical species contributed from the environment and the material. Through diffusion, chemical species are supplied to crack site and provide the means for the continuation of the corrosion process. If bulk regions can not sustain sufficient conditions, crack propagation will not continue.

2.3. The relationship between stress corrosion cracking and microstructure

The microstructure of a material is an important factor in a materials susceptibility to SCC. Cracking can occur in different forms depending on conditions at grain boundaries and grain interiors. Cracks can grow across grain boundaries, known as transgranular SCC (TGSCC), and along grain boundaries, known as intergranular SCC (IGSCC), as shown in

Figure 2.2 and Figure 2.3. Figure 2.2 shows a micrograph of TGSCC in 316 stainless steel used in a chemical processing piping system. Figure 2.3 shows a micrograph that illustrates IGSCC in an Inconel heat exchanger tube. Cracks can clearly been seen occurring along the gain boundaries.

Figure 2.2 - Transgranular SCC in 316 austenitic stainless steel [12].

Figure 2.3 – Intergranular SCC in Inconel [12].

Many studies have been conducted relating the effects of microstructure and SCC susceptibility. Four such studies are important to this research. The first study, performed by Watanabe [13], is a study of the relationship between grain boundary character distribution and fracture. Watanabe observed that fracture occurred in a heterogeneous manner. Specifically, high energy grain boundaries exhibited less resistance to intergranular fracture than low energy

boundaries. Watanabe also observed that grain boundaries formed networks and proposed that, because intergranular fracture is a percolative process, the propagation of cracks depended more heavily upon the connectivity of the grain boundary network rather than only the distribution of grain types. Watanabe proposed that because the frequency of grain boundary types could be identified, grain boundary networks could be described by the types of junctions formed by the grain boundaries, known as triple junctions. The frequency of the types of triple junctions, made up of 0, 1, 2 or 3 low energy boundaries, could then be used to predict the materials resistance to percolation. Grain boundary networks made up of high energy grain boundaries, and thus less resistant triple junctions, would be more susceptible to fracture, while grain boundary networks composed of low energy grain boundaries would be more resistant to fracture.

Following Watanabe's work, Tsurekawa et al [14] analyzed the correlation between grain boundary connectivity and grain boundary character distribution in type 304 austenitic stainless steel. In this study, Tsurekawa et al observed that the frequency of triple junctions that consisted of two low energy grain boundaries increased with the increasing frequency of coincident site lattice boundaries, a specific type of low energy boundary, as shown in Figure 2.4.
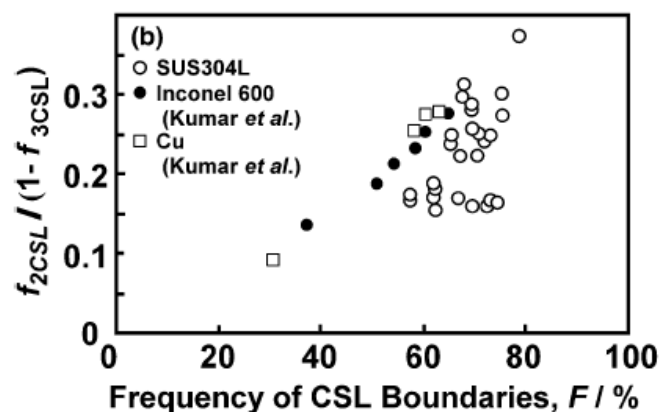
Figure 2.4 - Tsurekawa et al [14] observed an increased frequency of triple junctions composed of two low energy boundaries, denoted as $f_{2CSL}/(1-f_{3CSL})$, with increasing frequency of coincident site lattice boundaries.

Additionally, Tsurekawa et al's study displayed these effects by conducting ferric sulfate-sulfuric acid tests on austenitic stainless steel specimens with different amounts of percolation resistant triple junctions. SEM micrographs of the surfaces and cross-sections of these specimens, shown in Figure 2.5, validate the prediction that the frequency of percolation resistant triple junctions, which follows from an increased frequency of low energy boundaries, results in an increased resistance to a percolative process such as intergranular corrosion.
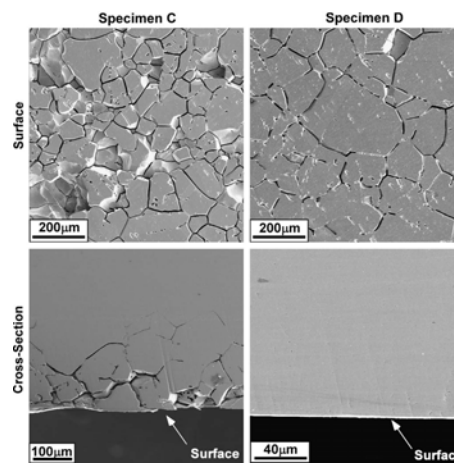
Figure 2.5 – SEM micrographs taken from a study of the correlation of grain boundary character distribution and grain boundary connectivity in austenitic stainless steel. Specimens underwent ferric-sulfate sulfuric acid tests for 48 hours. Due to the difference in frequency of percolation resistant triple junctions (specimen C – 10%, specimen D – 19%), specimen D exhibited less susceptibility to intergranular cracking than specimen C. [14]

Another study, performed by Tan et al [15], analyzed attempts at optimized grain boundary character distribution of Inconel 617, an austenitic solid-solution alloy proposed as a candidate alloy for used in new generator nuclear reactors. The alloy was grain boundary engineered by undergoing thermomechanical processing; specifically, samples were divided into three sets, reduced in thickness by 5%, 9% and 13% respectively, and annealed at 1100 ˚C for 90 minutes. This resulted in an increase in the fraction of $\Sigma 3^n$ ($\Sigma 3$, $\Sigma 9$ and $\Sigma 27$) grain boundaries, as

shown in Figure 2.6. The importance of this conclusion, that an increased fraction of $\Sigma 3^n$ boundaries is promoted by thermomechanical processing, can be seen when combined with results from Watanabe [13].
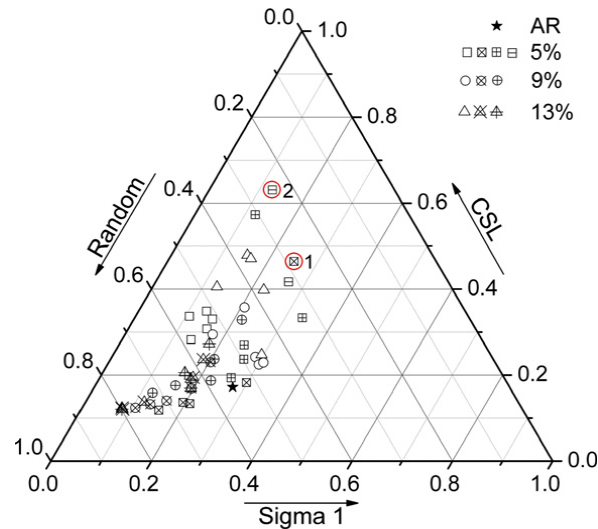
Figure 2.6 - Grain boundary character distribution of as received (AR), 5%, 9% and 13% width-reduction Inconel 617 in the study of Inconel 617 by Tan et al [15]. The open, diagonally crossed, crossed, and horizontal-line-through symbols indicate the number of thermomechanical processing cycles, from 1 to 4, each respective sample has undergone.

Finally, another work by Tan et al [16] studied the employment of grain boundary engineering as a method of improving the corrosion resistance of Incoloy 800H and Inconel 617. Following grain boundary engineering treatments by thermomechanical processing, the mechanical properties and microstructure were thoroughly analyzed using a variety of techniques. The results indicated that the grain boundary engineering resulted in decreased oxide exfoliation in Incoloy 800H and the oxidation rate of Inconel 617. Additionally, grain boundary engineering resulted in increased strength of Incoloy 800H at both room and high temperatures without a substantial decrease in ductility.

Given the aforementioned results correlating grain boundary type to SCC resistance, a systematic characterization of how mechanical properties vary in the vicinity of grain boundaries at the nanoscale is a vital aspect in developing a thorough understanding of the initiation of SCC.

2.4. SCC mechanisms and the role of grain boundaries

Models of how intergranular stress corrosion can occur will be discussed in the subsequent sections. Each proposed model describes how the tensile stress, a corrosive environment and the properties that result in susceptibility combine to result in material failure. The importance of microstructural components, specifically grains and grain boundaries, to the mechanism of SCC will be the focus of the discussion.

2.4.1. Crack initiation

SCC can initiate at existing surface features such as grooves, scratches, or preexisting cracks [1]. These features are commonly produced during fabrication or preparation processes such as grinding or welding. Crack initiation can also occur through a process known as slip dissolution. In this case, the slip planes of the crystalline structure allow shear stress to translate the surface of the material. Here, grain boundaries can play an important role in slip dissolution. This results in the rupture of the natively formed protective oxide layers, thus exposing the material.

Sites of pitting corrosion can also be areas where stress corrosion crack initiation occurs [1]. Pits form as a result of dissolution of the metal due to a local lack of oxygen in a small area. The area becomes anodic and the adjacent area, which contains a higher relative concentration of oxygen, becomes cathodic, resulting in highly localized galvanic corrosion. Following the

29

formation of pits, cracks will initiate based on the combined effects of the geometry of the pit, the chemistry of the exposed material, and the stress conditions on the pit interior. Pits can also occur as the result of the differing chemistry between grain boundaries and the bulk region of the materials. Specific constituents that enrich at or deplete from the grain boundaries provide the necessary anodic conditions for localized galvanic corrosion. Crack initiation generally occurs when the ratio of the depth of the pit to the width of the pit is approximately 10, which can typically only result when the pit walls exhibiting a capability of forming a passivating film to cause crack growth in the lateral direction to be relatively slow.

2.4.2. Crack propagation

Crack initiation and crack propagation are different processes, but are related. The occurrence of crack initiation and the velocity of crack propagation depend on the previous mentioned factors: the surrounding environment and the mechanical and metallurgical properties of the material. Several mechanisms have been proposed as a way to explain SCC crack propagation can probably be attributed to a combination of these. These mechanisms are divided into two categories, both of which include microstructure as an important factor: dissolution models and mechanical fracture models.

2.4.2.1. Dissolution models of crack propagation

Dissolution models propose that cracks advance through preferential dissolution of the material at crack tips. There are two models that describe crack propagation this way: the active path dissolution model and the film rupture model.

Active path dissolution describes the corrosion along a path that is more susceptible to corrosion relative to passivity of the bulk material. The active path refers to the grain

boundaries, where elemental segregation makes passivation more difficult. As a result, a form of crevice corrosion occurs where the grain boundaries corrode uniformly throughout the affected region while the surrounding grain walls and surface remain passive. While stress is not required for this type of intergranular corrosion to occur, the presence of stress serves to open the cracks. This leads to diffusion of corrosion products that would serve to form a protective oxide layer, and thus an increase in crack growth.

Active path is not generally accepted as a good explanation for the mechanism that governs SCC. Active path was proposed as an initial explanation of grain boundary attack, and is based on the preferential dissolution of a specific phase in the material and the development of galvanic cells along the slip planes. The main reasoning is that preferential dissolution enables the continuation of the corrosion reaction at the surface by serving as a source of bare metal. However, the active path model does not take into account the possibility of crack tip blunting, hence its lack of acceptance as the governing SCC mechanism.

The film rupture model is generally accepted as the most accurate description of the governing mechanism of SCC. In the film rupture model, susceptibility is attributed to the rupture of the oxide film on the material surface. The oxide layer is ruptured by the translation of shear stress along the crystalline slip planes, as shown in Figure 2.7.
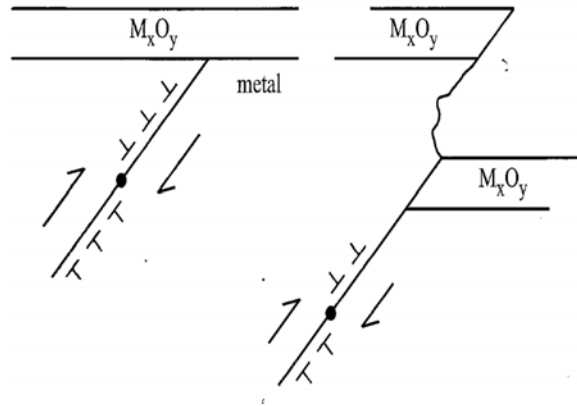
Figure 2.7 - Depiction of the surface oxide film and slip plane, which is the basis for the film rupture model. The susceptibility of the material is dependent upon the slip mechanism, which is impacted by the stacking fault energy [11].

The slip can be predicted by the stacking fault energy of the material. In materials with high stacking fault energy, where the distance between the Shockley partials is low, the material will exhibit wavy slip which results in a longer time to failure of the oxide layer. Conversely, in materials with low stacking fault energy, the distance between the Shockley partial partials is higher, resulting in a lower time to failure of the oxide layer from planar slip in the material. Cracks can be expected to grow transgranularly along the active slip plane, although experimental work to date has shown that cracks can also grow intergranularly [1].

In addition to affecting the nature of the slip that results in the oxide layer rupture, repassivation of the oxide layer will occur and will control the crack propagation rate. An intermediate rate of repassivation is required, as repassivation that occurs too quickly will result subcritical crack growth, while a lower repassivation rate will result in a blunted crack tip. The exposed surface resulting from the oxide rupture will begin to repassivate and the repassivation rate will be affected by alloy composition.

2.4.2.2. Mechanical fracture models of crack propagation

In mechanical fracture models of SCC, crack initiation and propagation occurs as a result localized corrosion combined with ductile deformation and fracture. Initial localized corrosion results in stress concentrations, and the material proceeds to fail by mechanical fracture induced by the presence of tensile stress. These models include the corrosion tunnel model, adsorption-induced cleavage model, adsorption enhanced plasticity and film-induced cleavage and rupture model.

The first of such models, known as the corrosion tunnel model, proposes that active corrosion forms along parallel slip planes that intersect with the surface of the material, as shown in Figure 2.8. The anodic dissolution of the material continues along these slip planes, forming tunnels. After the sufficient amount of material is dissolved, the weakened area between the tunnels succumbs to brittle fracture and fails. The process begins again with the dissolution of material along slip planes and repeats.
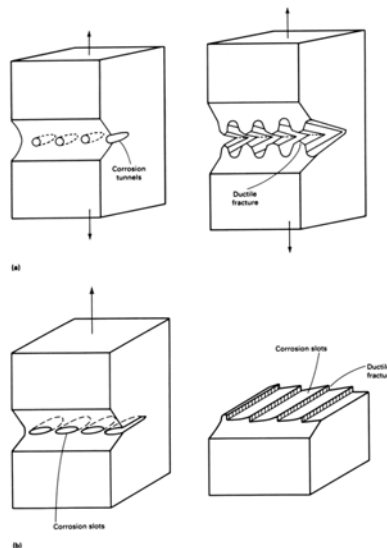
Figure 2.8 – The corrosion tunnel model of SCC [1].

Change in the mechanical properties of the material at the surface due to the electrochemical interactions with the environment is another model proposed to explain the mechanism of SCC. In this model, known as the adsorption-enhanced cleavage model, the absorption of ions from the local environment can serve to weaken the bonds of the crystal lattice, and as result, the stress required to initiate cracks is reduced. Cracks then propagate until they reach regions where absorption has not affected the bonds of the crystal lattice [1]. This model builds on the assumption that adsorption occurs at mobile defect sites, and results in bond weakening at crack tips, which occur both along and across grain boundaries. The nature of these mobile defect sites is not yet characterized [1].

Similar to the adsorption-enhanced cleavage model is the adsorption enhanced plasticity model. Ions from the local environment are absorbed and serve to reduce the shear stress requirement for dislocations to translate. Tensile stress then allows dislocations to translate more easily. The difference between this model and the adsorption-enhanced cleavage model is that this model proposes that the critical shear stress is decreased, while the previous model proposes the decrease in the general strength of the absorption region [1].

Another mechanical fracture model of SCC is the film-induced cleavage model, shown schematically in Figure 2.9. In this model, a thin, brittle, layer, such as a protective oxide, forms at the surface of the material. Due to the brittleness of the layer, cracks initiate under applied or residual stress and propagate, usually along grain boundaries. Cracks then cross into the ductile material below the surface layer and continue to propagate until it is eventually blunted. The protective layer then reforms in the blunted region, and the process repeats [1].
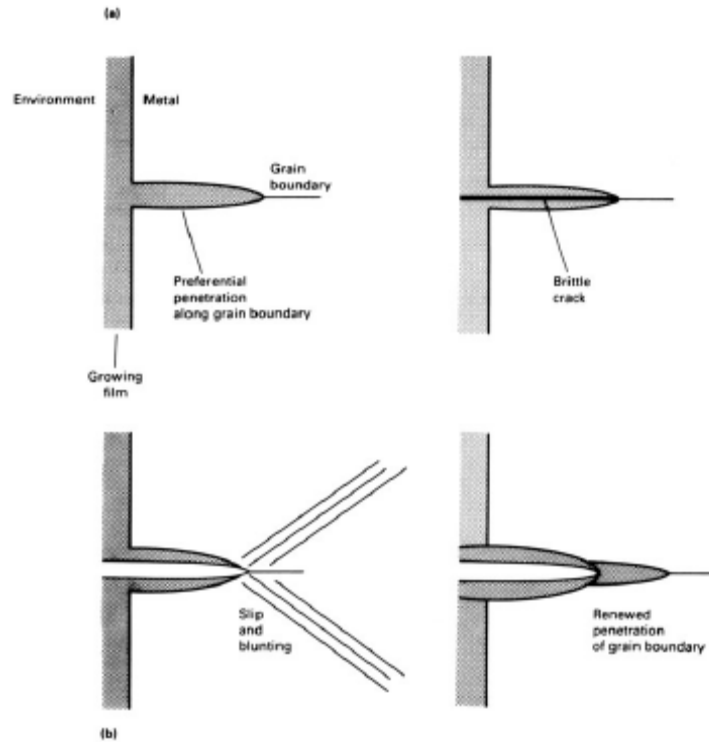
Figure 2.9 – Schematic showing the mechanism of SCC proposed in film induced cleavage and rupture model [1].

2.5. Summary

In conclusion, SCC is an ongoing and challenging problem in the nuclear industry. It occurs when certain critical local environmental, mechanical and metallurgical conditions occur simultaneously. Several models for how SCC initiates and proceeds have been proposed. However, because cracking initiation is difficult to detect at an atomistic level, the accuracy of these models is difficult to verify. It is generally agreed upon that there is no universal model for SCC and that it is likely that more than one of the aforementioned mechanisms of crack initiation and propagation occur simultaneously. Despite the lack of a universal model, the importance of microstructure, specifically grain boundaries, is common to many of the proposed models. From this, it is possible that microstructure can be controlled to develop materials that are less

susceptible to SCC, as has been established in literature. Control of the distribution of types of grain boundaries is achieved through processing, known as grain boundary engineering. These processing methods are effective by increasing the density of stored dislocations and causing chemical agglomerations in the vicinity of grain boundaries, both of which may result in grain boundaries that are stronger and more resistant to percolative processes such as intergranular corrosion and cracking.

3. Problem statement and thesis goal

3.1. Problem statement

Despite the uncertainties in the proposed models explained in Chapter 2, it is evident that the microstructural characteristics of a material play an important in all of the proposed SCC models. Therefore, understanding their effect on SCC behavior at a fundamental level is needed. The nanoscale correlations between the microstructural, chemical, and mechanical properties, is, as of yet, unexplored systematically. The proposed models of SCC provide a high level understanding of how microstructural properties contribute to susceptibility. This is exemplified by the finding of Tsurekawa et al [14], who showed that a grain boundary network with an increased frequency of percolation resistant triple junctions is thus less susceptible to intergranular failure. However, this high level description lacks an accurate explanation of the chemical and mechanical nature of grain boundaries on an appropriately small scale. Particularly, the proposed models of SCC crack initiation lack a thorough understanding of the role of interface structure at the nanoscale due to the challenge in observing and measuring such small scale and highly localized deformation and electrochemical phenomenon.

3.2. Research goals

3.2.1. Relationship between grain boundary structure and mechanical properties

This thesis specifically aimed to identify the relationship between the structure of grain boundaries and their mechanical properties in Inconel 690, an important alloy used in the design of nuclear reactor steam generators in the United States. Specifically, the hardness and elastic modulus in the vicinity of grain boundaries, and their relation to grain size, crystalline orientation, slip systems, and presence of precipitates, are important. This relationship serves to

enhance the understanding of the mechanism of intergranular SCC in Inconel 690 and, perhaps, other polycrystalline materials with face centered cubic structure.

3.2.2. Correlated microstructural, compositional, and mechanical property measurements at grain boundaries

A technical objective is to enable correlated measurement of nanoscale mechanical properties of grain boundaries with well-defined structure with the analysis of the chemical nature of those same grain boundaries.   As has been stressed in previous sections, many combinations of materials and environments exhibit SCC susceptibility. Thus, the development of this approach serves as a template for identifying mechanical properties of grain boundaries with known chemical composition and structure.

4. Approach

4.1. Overview

The methodology to integrate measurement of crystalline orientation, mechanical properties, and chemical composition of grain boundaries of interest follows in this chapter. Grain boundary engineering was accomplished on Inconel 690 through thermomechanical processing to produce samples with a high fraction of coincident grain boundary structures. Next, crystalline orientation of grain boundaries was identified using electron backscatter diffraction analysis. Nanoindentation was used to extract mechanical properties at and near the selected grain boundaries. For some grain boundaries, chemical analysis using transmission electron microscopy (TEM) was performed by an accompanying research in this group on the same samples [17].   Figure 4.1 shows the integration of these techniques in this approach schematically.
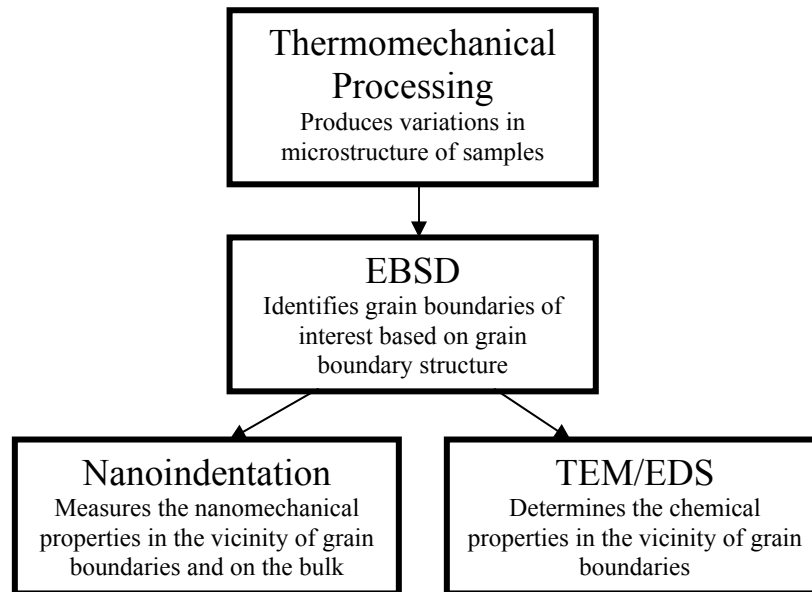
Figure 4.1 – Schematic representation of approach to grain boundary characterization in this thesis and a collaborating thesis [17]. The focus of this thesis was on nanoindentation.

The approach to prepare samples, conduct and coordinate these measurements follows. This thesis focused on the measurement of mechanical properties near grain boundaries using nanoindentation, and thus, the approach to conduct nanoindentation measurements is described in detail.

4.2. Sample preparation

Samples were first thermomechanically processed (TMP) to produce two samples with differing microstructure. Sample surfaces were then polished mechanically and electrolytically to reveal grain boundaries optically and reduce surface roughness, an important parameter that can affect nanoindentation data.

Mechanical polishing is accomplished by placing the sample in contact with a rotating polishing wheel. The polishing wheel is first fitted with sandpaper, and then with polishing mat containing a fine particle polishing suspension. Sample surfaces are affected by mechanical polishing, leaving behind a deformed layer whose depth is on the order of the grit size used in polishing, an effect identified by Langitan and Lawn [18]. This must be removed by electrolytic polishing to ensure that the data collected during nanoindentation experiments does not contain an artifact of mechanically deformed structure.

Subsequent electrolytic polishing was accomplished by constructing an electrolytic cell consisting of the sample to be polished as the anode, a platinum mesh cathode and electrolyte solution. Using an external source, direct current is applied to the system resulting in dissolution of the anode, thus brightening and leveling the sample surface. The mechanism of electrolytic polishing is affected by several factors related to the set up including the surface area of the sample and surface area of the cathode, the spatial orientation of the sample and cathode in the electrolyte solution, the spacing between the sample and the cathode, the depth of the sample and

cathode below the surface of the solution, the composition of the sample, electrolyte solution, and cathode, the degree of agitation and temperature of the electrolyte solution, the mechanical processing applied to the sample before electrolytic polishing, and the current density and voltage. When placed in the electrolytic solution and set up as the anode of the electrolytic polishing set up, a viscous layer, known as the polishing film, forms on the surface of the sample. With a fully formed polishing film, the resistance of the surface and film will vary depending on the height of the surface underneath the film. Using the analogy that surface roughness can be thought of as a series of hills and valleys, the polishing action is controlled by the lower resistance of the polishing film over a "hill" and a higher resistance of the polishing film over a "valley."

Of particular importance is the determination of the ideal current density and voltage used to accomplish the electrolytic polishing, an example of which is shown in Figure 4.2 [19].
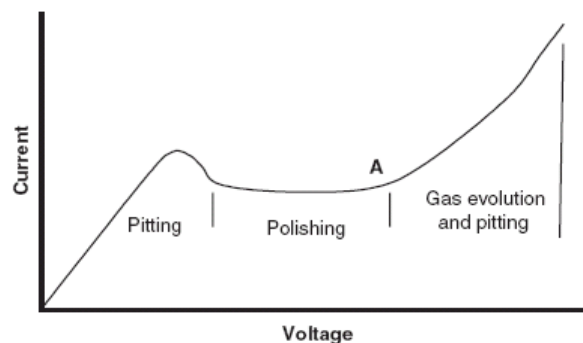
Figure 4.2 – Ideal current and voltage relationship for electrolytic polishing [19].

Figure 4.2 shows three very distinguishable regions. In the first region, current density increases approximately linearly with voltage. The polishing film does not yet form and some areas of the sample dissolve in the electrolyte solution resulting in a dull surface with pitting

41

likely to occur. In the second region, the polishing film forms on the sample surface and results in a "plateau" where current density remains approximately constant with increasing voltage. Finally, in the third region, the relationship between voltage and current density is approximately exponential. Gas bubbles evolve and disrupt the polishing film. Therefore, despite the complexity of the electrolytic polishing mechanism, determination of an appropriate current density and voltage can be used to ensure that the sample surface is polished without unwanted side effects such as pitting or gas streaking.

4.3. Coordinated measurement of mechanical properties, structure and elemental composition

4.3.1. Fiduciary marking of the sample surface

An important aspect of this research centered on the ability to structurally identify specific grain boundaries on chemical and mechanical measurements would be coordinated. To accomplish this, a 10 x 10 grid of microindentations was performed on the sample surface. These indents were used as fiduciary markers for navigating the sample surface. An extra indent at one corner of the grid was also created to allow for easy orientation of the sample. Microindentations were separated by distances on the order of 100 μm and were easily visible optically. Using these markers, the location of specific grain boundaries could be easily found over the course of this research effort.

4.3.2. Orientation image mapping

Determination of the crystalline orientation of areas of interest on the sample surface was accomplished using electron backscattered diffraction (EBSD). This work was done by a collaborating member of the research group [17].   EBSD is a technique that uses a scanning

electron microscope (SEM) that is equipped with a backscatter diffraction camera. The diffraction camera is fitted with a phosphor screen and CCD camera. Electrons are impinged on the area of interest on the surface of the polished sample, which is tilted toward the diffraction camera. The electrons interact with the lattice planes on the surface of the sample, undergo backscatter diffraction, and collide with the phosphor screen. The collisions of the backscattered electrons with the phosphor screen produce a diffraction pattern, which are detected by the CCD camera. These patterns can then be indexed to recognize the crystallographic orientation of the plane that formed the pattern.

EBSD analysis was conducted on a "square" created by 4 of the 100 indents that make up the microindentation grid. An appropriate "square" was chosen that contained several types of grain boundaries that were of interest to this research: $\Sigma 3$, low angle and high angle grain boundaries. This coordination is shown in Figure 4.3.
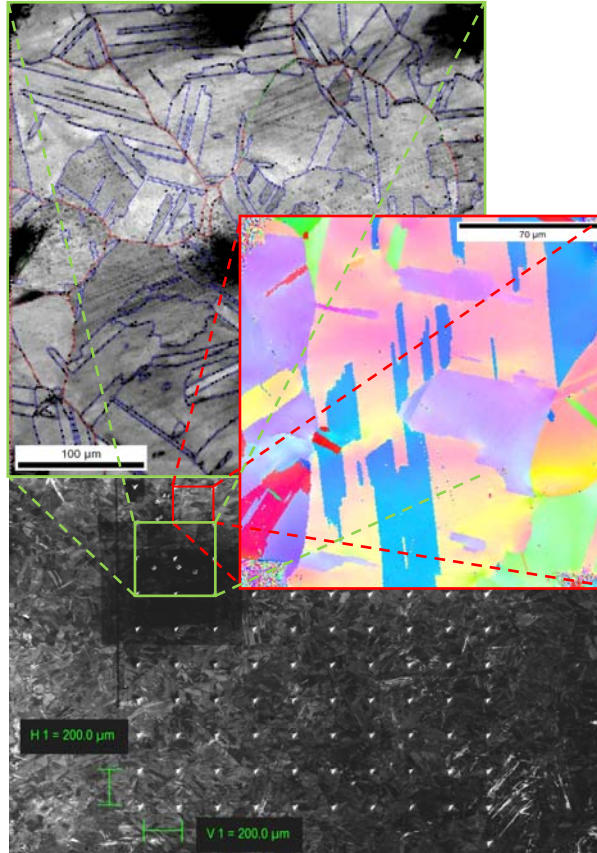
Figure 4.3 - SEM image of the surface of a sample with a grid of micro-indents for positioning. Using the grid to navigate, EBSD is carried out to produce information about boundary type and orientation.

4.3.3. Grain boundary imaging and elemental characterization

After the completion of the EBSD analysis, grain boundaries were chosen based on neighboring grain size, location from microindents to eliminate the chance of performing measurements on area in the microindentation impact volume, crystalline orientation, and grain boundary length. These grain boundaries were removed from the sample using a Focused Ion Beam (FIB). FIB focuses a beam of gallium ions, accelerated to between 5 and 50 keV, on the sample surface. The gallium ion beam is destructive to the sample surface and is essentially used as a site specific micro-machining tool. The micro-machining capability is used to mill trenches in the surface of the sample and create a membrane to be analyzed in a transmission electron microscopy (TEM) and scanning transmission electron microscopy (STEM). TEM analysis

44

provides imaging data such as grain boundary structure, dislocation accumulation, and precipitate formation, while STEM uses Electron Dispersive X-ray Spectroscopy (EDS) to provide elemental composition of the samples at the grain boundaries at atomistic resolution.

4.4. Nanoindentation

The measurement of mechanical properties at the nanoscale was accomplished using nanoindentation and is the focus of this thesis. Nanoindentation consists of contacting a material of unknown properties with a material of known properties. The response of the unknown material is then used to characterize its mechanical properties, using a well known procedure established by Oliver and Pharr [20]. Due to high resolution capability, nanoindentation allows for the determination of mechanical properties in the vicinity of grain boundaries. Indentations are made with a diamond indenter tip of known geometry. An optical image of the tip used in this thesis, a cube corner tip, is shown in Figure 4.4.
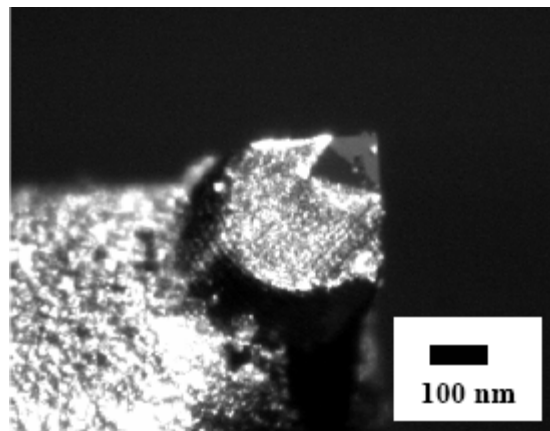
Figure 4.4 – Optical image of a cube corner tip [21].

Specification of the load applied to the tip over time, known as a load function, is defined for each indentation. The load function contains a loading segment, which forces the indenter tip into the surface of the material, a plateau or holding segment, which minimizes the impact of

creep or thermal drift on the measurement, and an unloading segment, which removes the indenter tip from the surface of the material and corrects for elasticity.

During the indentation, the displacement of the indenter tip into the material and the materials response to the applied force are recorded. The material response follows Kick's law, $P = Ch^2$, where P is the applied force, h is the displacement of the indenter tip into the material, and C is a constant that depends on the elastic and plastic properties of the material. An example of the materials response is shown in Figure 4.5 [22]. From this plot of load as a function of indentation depth, known as the load-displacement curve, mechanical properties such as elastic modulus and hardness can be extracted, using relationships discussed in reference [23].
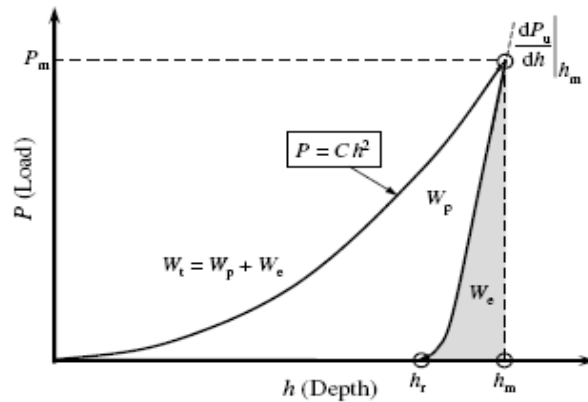
Figure 4.5 - Typical load-displacement curve recorded during indentation experiments [22]. P is the applied load. The total work done by the indenter tip is W_t, which is the sum of the plastic work, W_p, and elastic work, W_e. h_m is the maximum indentation depth and h_f is the final depth of the indent after elastic recovery.

As shown in Figure 4.6, the elastic modulus, E, is descriptive the elastic behavior of the material, which occurs below the yield stress. Hardness is a measure of resistance against plastic deformation, which occurs above the yield stress and is descriptive of the density of dislocations.

Ultimate strength

σ_{Yield}

X
Tensile strength

Proportional limit stress

σ

ε
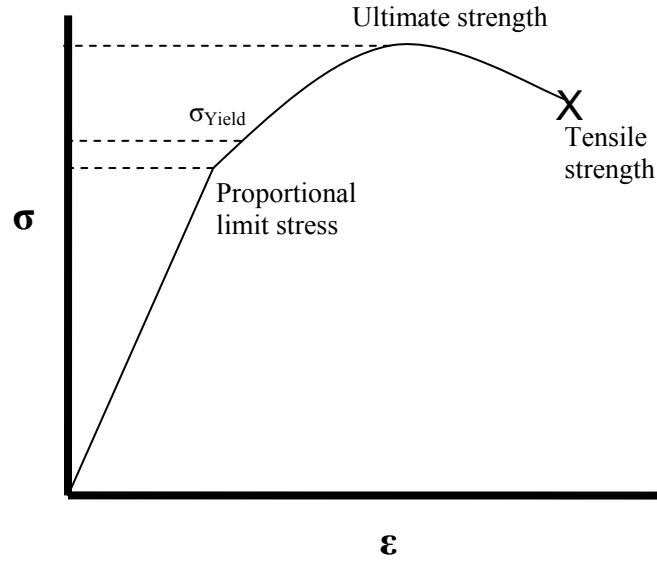
Figure 4.6 – Stress (σ) as a function of non-dimensional strain (ε). Below the yield stress (σ_{Yield}), the slope is equal to the elastic modulus, E, and the material deforms elastically. Above the yield stress, deformation is plastic.

The elastic modulus of the material obtained through nanoindentation is determined from the stiffness of the material. The stiffness is equal to the slope of the unloading segment at the maximum indentation depth of the load-displacement curve. From the measured stiffness, the reduced modulus, E_r, is given by

$$E_r = \frac{\sqrt{\pi}}{2}\frac{S}{\sqrt{A}} \qquad (4.1)$$

where the stiffness, S, is equal to $\dfrac{dP}{dH}\bigg|_{h_m}$ which is the slope of the unloading segment of the

load-displacement curve, and A is the area created by the indentation, which is a function of

indentation depth, and will be discussed in Chapter 4.4.1 [23]. The elastic modulus is then

determined by

$$E_r = \left[\frac{1-v^2}{E} + \frac{1-v_i^2}{E_i} \right]^{-1} \tag{4.2}$$

where, E is the elastic modulus, E_r is the reduced elastic modulus, E_i is the elastic modulus of the

indenter tip, v is the Poisson's ratio of the material, and v_i is the Poisson's ratio of the indenter

tip.

The hardness of the material is given by

$$H = \frac{P}{A} \tag{4.3}$$

where H is the measured hardness, P is the maximum load, and A is the area.

4.4.1. Tip area function

The area created by the indentation is an important parameter in the determination of the

mechanical properties of the material, specifically hardness. For the cube corner indenter tip, the

relationship between area created by the indentation and indentation depth is given by [21]:

$$A = 2.598 h_f^2 \tag{4.4}$$

The description of the indenter geometry, and thus the area it will create as described in equation

(4.4), will inevitably be incorrect because of imperfections in fabrication or blunting of the tip

over time. Therefore, each indentation measurement is accompanied with a characterization of

the tip geometry, and this more accurate relationship between area (A) and depth (h_c) is used. First, indentations of a comparable depth to the indentations made in the sample to be measured are made in fused silica, a material with known elastic modulus and hardness. The response to the indentation by fused silica can then be used to solve for an accurate area function for the imperfect indenter tip. This characterization accompanied every set of indentation measurements throughout this research to ensure that an accurate description of the tip geometry was always used.

4.4.2. Indentation size effect

In materials that are isotropic, measured values of hardness and elastic modulus should be expected to remain constant independent of indentation depth. However, these measured values may exhibit indentation depth dependence or variations due to an inability to accurately describe the indenter geometry with an area function at lower indentation depths. Even when these effects are accounted for and minimized, hardness and elastic modulus variation with depth can still be observed. This is known as the indentation size effect [23].

The indentation size effect is caused by substantial strain gradients created in the vicinity of the indenter tip during an indentation. Inside these strain gradients, dislocations are nucleated and form circular dislocation loops. These dislocations are known as geometrically necessary dislocations and serve to increase the yield strength and the hardness of the material. The density of geometrically necessary dislocations, ρ_G, is inversely proportional to the depth of indentation. Therefore, the measured hardness increases as indentation depth decreases. The increase in hardness behaves as

$$\frac{H}{H_o} = \sqrt{1 + \frac{h^*}{h}} \qquad (4.5)$$

49

where H is the measured hardness, H_o is the hardness that would be measured at infinite depth (without the presence of the indentation size effect), h is the indentation depth, and h^* is a length that is characteristic of the depth dependence of the hardness [24]. The value of h^* is determined by [24]:

$$h^* = 40.5b\alpha^2 \tan^2 \theta \left(\frac{\mu}{H_o} \right)^2 \qquad (4.6)$$

where h^* is determined from the Burger's vector of geometrical necessary dislocations (b), the angle of the interior angle of the indenter tip (θ), shear modulus (μ) and hardness at infinite depth (H_o). α is a fitting parameter that describes the relative ease of dislocation movement in the material [24]. Characterization of the Inconel 690 samples to determine the presence of an indentation size effect was completed and is discussed explicitly in Chapter 5.

4.4.3. Frame compliance

In addition to inaccuracies in the measurement resulting from an indenter tip that has imperfections, the measurement of the displacement of the indenter tip into the material will include displacements of the instrument that result from reaction forces during the indentation. This displacement, known as the frame compliance, or C_f, is directly proportional to the load used to create the indentation and must be accounted for in the total measured displacement. The method of determining this displacement begins by considering the load frame and the sample as springs in series. Therefore, the total compliance, C, can be expressed as

$$C = C_s + C_f \qquad (4.7)$$

where the total measured compliance, C, is the sum of the frame compliance, C_f, and sample compliance, C_s [20]. The compliance of the sample, C_s, is equal to the inverse of the stiffness, S, which is recorded during the indentation measurement. Substituting equation (4.1) into equation (4.7) yields

$$C = C_f + \frac{\sqrt{\pi}}{2E_r}\frac{1}{\sqrt{A}} \qquad\qquad (4.8)$$

For a given material, E_r is assumed to remain constant. Therefore, a plot of the C vs $\sqrt{A}$, is a linear relationship and the intercept of this relationship is the frame compliance, C_f. Because frame compliance can vary over time, characterization of the load frame on fused silica accompanied each nanoindentation measurement.

5. Experimental procedure

This chapter explicitly describes the experimental procedure followed and conditions used to conduct nanoindentation measurements. Samples were received from Special Metals and prepared for analysis. EBSD analysis was conducted on the sample surface. Nanoindentation, and in some cases, TEM and STEM, was then conducted on grain boundaries in those areas [17].

5.1. Sample preparation

5.1.1. Thermomechanical processing

Thermomechanical processing (TMP) was used to create two samples with distinctly different microstructural features: a sample that had undergone solution annealing, and another sample that, after solution annealing, was cold-rolled, thermally treated and furnace cooled.

The as received bar was cut into two 2 cm (length) x 1.2 cm (width) segments, referred to as Sample I and Sample II, using a slow speed saw equipped with a Buehler IsoCut Diamond Wafering Blade. Sample I and Sample II were then solution annealed at 1107 ºC for 15 minutes and water quenched. Following annealing, Sample II was cold rolled to achieve a 5% thickness reduction. By cold-rolling, the absorbed energy by Sample II serves to nucleate and translate dislocations. Subsequently, Sample II was annealed at 950 ºC and furnace cooled. This thermal treatment and cooling served to drive recrystallization and force development of a new microstructure with differing properties relative to Sample I. Table 5.1 summarize the TMP completed on Samples I and II.

	Thickness reduction	Annealing temperature	Cooling method
Sample I	0%	1107 ˚C	Water quenched
Sample II	5%	950 ˚C	Furnace cooled

Table 5.1 – Summary of TMP on Sample I and Sample II

5.1.2. Mechanical polishing

Each sample was mechanically polished to ensure a polished surface capable of revealing grain boundaries when viewed with an optical microscope and to reduce surface roughness. Each sample was polished using a Buehler Ecomet3/Automet 2 variable speed grinder/polisher. Samples were polished using CarbiMet waterproof paper of progressively increasing grit sizes to an eventual surface roughness of 9 μm. Samples where then polished using polycrystalline diamond abrasive MetaDi Supreme of progressively decreasing particle size to an eventual surface roughness of 50 nm, as described in Table 5.2.

Surface	Abrasive	Load	Base speed	Time
CarbiMet abrasive discs	60 to 1200 grit SiC water cooled	6 lb	150 rpm	Until planar
Trident cloth	9 μm MetaDi Supreme diamond suspension	6 lb	150 rpm	15 mins
Trident cloth	3 μm MetaDi Supreme diamond suspension	6 lb	150 rpm	15 mins
Trident cloth	1 μm MetaDi Supreme diamond suspension	6 lb	150 rpm	15 mins
MicroCloth	MasterPrep 0.05 μm alumina suspension	6 lb	150 rpm	15 mins

Table 5.2 – Summary of mechanical polishing procedure for each sample

5.1.3. Electrolytic polishing

Electrolytic testing to determine ideal conditions and polishing were conducted using a

ParStat 2273 electrochemical potentiostat. Inconel 690 samples were used as the anode, while a

1 cm^2 platinum mesh, positioned parallel to the anode at a distance of approximately 1 cm was

used as the counter electrode. The anode and cathode were connected to the leads of the

potentiostat with nickel wire; the nickel wire was spot welded to the anode and to the cathode by

threading it through the platinum mesh. The electrolyte solution consisted of 60 mL H_2SO_4 and

40 mL deionized H_2O. The potential and current density relationship for each sample was

determined potentiodynamically by increasing cathodic potential from 0 to 10 V at a rate of 20

mV/s. Following completion of electrolytic polishing, samples were quickly removed from the

electrolyte solution and thoroughly rinsed with deionized water.

Though desirable to obtain an electrolytically polished surface for both Samples I and II,

this was not feasible due to time constraints and safety concerns. Sample I was successfully

electrolytically polished with the conditions described in Chapter 4.2. First, evolution of

hydrogen gas was not evident at the platinum cathode when Sample I was placed in the

electrolyte solution. The ideal polishing current was determined to be approximately 400 mA

using the aforementioned procedure. The current and voltage relationship built during this

procedure is shown in Figure 5.1.
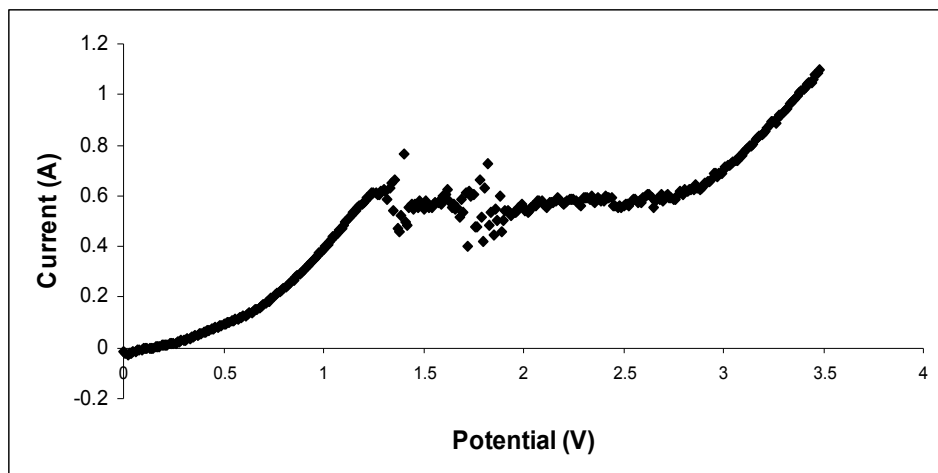
Figure 5.1 – Current-Voltage relationship for Sample I to determine ideal electrolytic polishing conditions.

Sample I was electrolytically polished at 400 mA for 180 seconds. Dissolution of the sample into the electrolyte solution was evident. Immediately upon completion, Sample I was removed from the electrolyte solution and rinsed thoroughly with deionized water. Visual inspection of the surface of Sample I revealed no corrosion of the surface.

Electrolytic polishing on Sample II was not successfully accomplished using the same electrolyte solution. TMP resulted in the formation of chromium carbide precipitates throughout the sample. As a result, Sample II experienced severe general corrosion when placed into the H_2SO_4 electrolyte solution. The surface was recovered by repeating the mechanical polishing procedure discussed in Chapter 4.2. The effect of not electrolytically polishing Sample II on the measurements of hardness and elastic modulus was insignificant, and is discussed more thoroughly in Chapter 5.4.4.

5.2. Fiduciary marking using microindentation

To coordinate measurements taken on grain boundaries of interest, the surfaces of Sample I and Sample II were marked with a 10 x 10 grid of microindentations using a Micro Materials NanoTest 600 Microindenter. Indents were made using a load of 3 N, which achieved depths of approximately 9 μm, to ensure that indents were easily visible in an optical microscope. Figure 5.2 displays the grids for Sample I as an example.
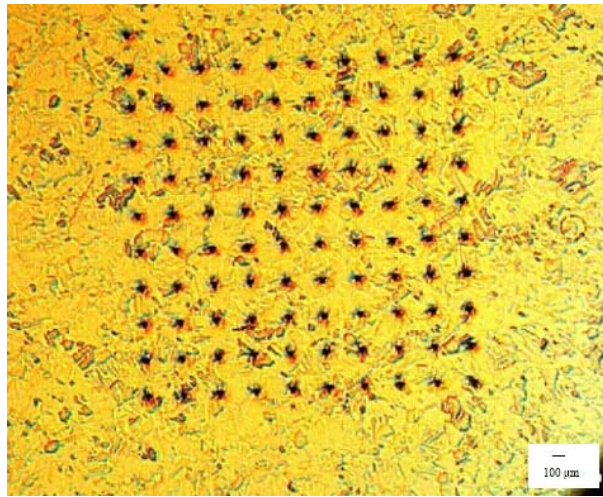
Figure 5.2 – Microindentation grid of Sample I

5.3. Electron backscatter diffraction analysis

Electron backscatter diffraction was conducted to identify the crystallographic orientation and grain boundary structures of the mapped areas of the surfaces. Optical images and the corresponding inverse pole figure (IPF) images are shown in Figure 5.3 and Figure 5.4 for Sample I and Sample II, respectively.
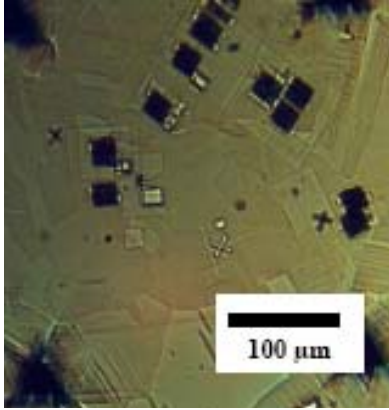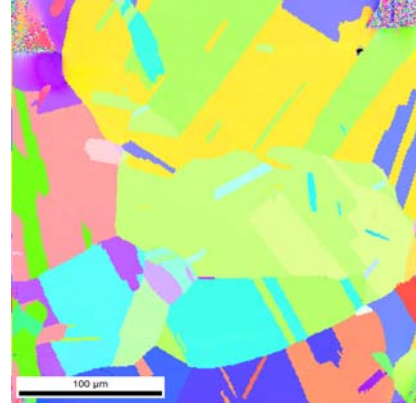
|Optical image|Inverse pole figure image|

Figure 5.3 – Optical image and inverse pole figure of Sample I
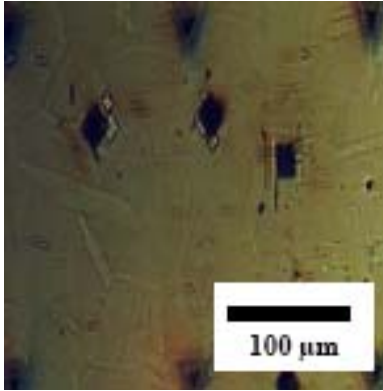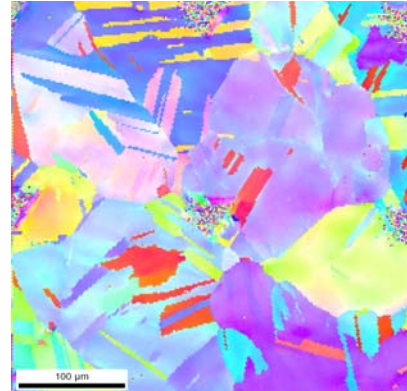
|Optical image|Inverse pole figure image|

Figure 5.4 – Optical image and inverse pole figure of Sample II

5.4. Nanoindentation

Nanoindentation experiments were conducted using a Hysitron TI 900 TriboIndenter. Indents were made using a cube corner indenter tip with a radius of curvature of approximately 100 nm. A load function with 10 s loading segment of 17.5 μN/s to a peak load of 175 μN, a holding segment of 10 s at peak load, and an unloading segment of 17.5 μN/s, as shown in Figure 5.5.
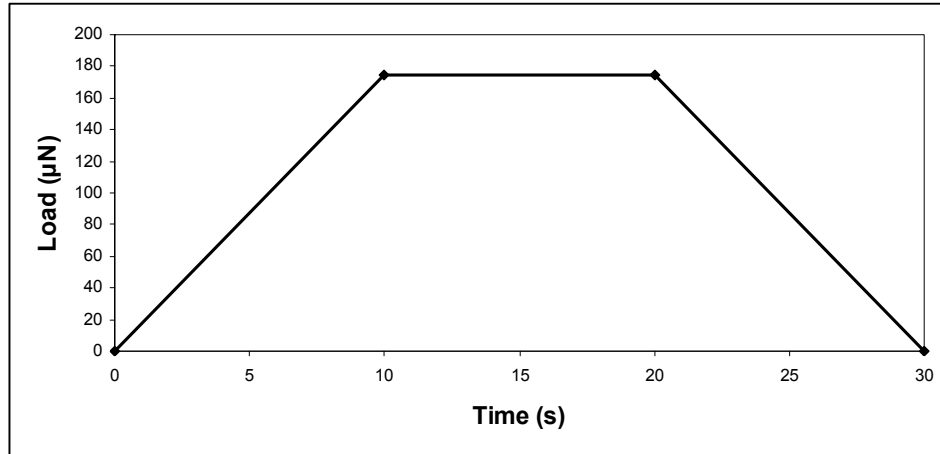
Figure 5.5 - Load function used for nanoindentation measurements

Nanoindentations were made on, 500 nm away from and 5 μm away from grain boundaries. For each grain boundary that was characterized, 50 indents were made, an example of which is shown in Figure 5.6: 10 on the grain boundary itself, 10 indents located 500 nm on both sides of the grain boundary (20 total), and a grid of 10 indents centered 5 μm from the grain boundary, with 1.55 μm separation between indents, on both sides of the grain boundary.
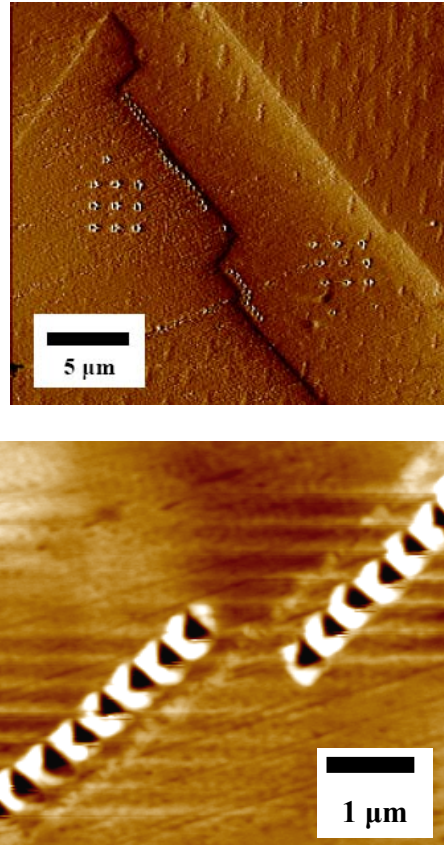
Figure 5.6 – In situ images of nanoindentations showing (left) 50 indents: 10 on the grain boundary, 10 located 500 nm on both sides of the boundary, and a grid of 10 centered 5 μm on both sides of the grain boundary and (right) indents 500 nm away from the boundary.

Two grain boundaries on Sample I were measured using an automated indentation scheme. This was done as way to determine if the measurement technique resulted in hardening of the grain boundary. Rows of 14 indents were conducted approaching the grain boundary from both directions, as shown in Figure 5.8.
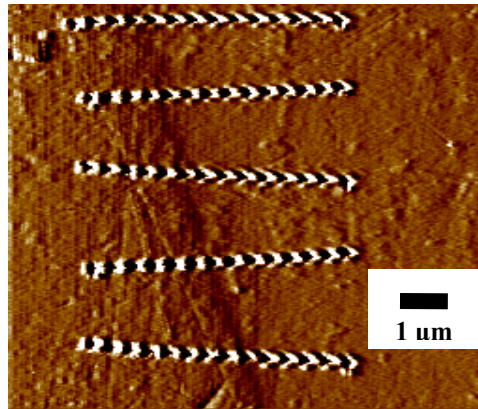
Figure 5.7 – Rows of indents completed by approaching the grain boundary from the left and right using automation.

Indenter geometry was characterized after each set of indentation measurements. Area functions were determined with the analysis method described in Chapter 4.4.1, using 40 indentations made on fused silica. Indentation depths on fused silica ranged from 40 nm to 120 nm to ensure similarity to indentation depths achieved on Samples I and II. The selection of the appropriate indentation depth is discussed in Chapter 5.4.1. The in situ imaging feature of the Hystron TriboIndenter was used to capture appropriately scaled images of the indentations after they were completed.

Frame compliance was also characterized after each set of indentation measurements. Frame compliance was determined with the analysis method described in Chapter 4.4.3, using 50 indentations made on fused silica. Indentation depths on fused silica ranged from 300 nm to 400 nm.

5.4.1. Indentation depth

Indentation depth of nanoindentation measurements can be unreliable if an appropriate indentation depth is not selected. Deep indentations risk being affected by inhomogeneties below the surface. For indentations in the bulk regions, the depth of the grains is unknown so

indentations may interact with different types of grains below the surface. For indentations on and near grain boundaries, the position of the grain boundary below the surface is also unknown. Therefore, deep indentations near the boundary might interact with a grain boundary below the surface, while deep indentations on the boundary might interact with a grain. Conversely, shallow indentations can be unreliable if the indentation depth is on the order of the asperity height of the surface roughness.

Therefore, an indentation depth for nanoindentation measurements was selected that was as shallow as possible. This depth was determined by performing 30 indentations over progressively increasing peak loads. The resulting data was analyzed to determine the minimum peak load where the standard deviation of the data set would be acceptable. This data analysis is summarized in Table 5.3.

Peak Load (μN)	Average indentation depth (nm)	Elastic Modulus (GPa)		Hardness (GPa)	
		Mean $\left(\overline{X}\right)$	Standard Deviation (σ)	Mean $\left(\overline{X}\right)$	Standard deviation (σ)
50	25.26	94.42	18.67	3.77	1.00
80	31.51	133.80	25.35	4.20	0.30
105	36.98	146.36	27.37	4.65	0.28
130	43.23	154.17	27.83	4.65	0.28
175	*60.12*	*151.69*	*20.02*	*4.31*	*0.18*
210	73.51	164.18	17.77	4.09	0.11
250	86.09	163.72	17.92	3.98	0.19

Table 5.3 – Comparison of indentation data gathered at progressively increasing peak loads. The italicized row shows the optimized indentation conditions for minimum indentation depth.

The italicized row in Table 5.3 identifies the indentation data measured at a peak load of 175 μN, which yielded an average indentation depth of 60.12 nm. This data yielded a standard deviation of 20.02 GPa for elastic modulus and 0.18 for hardness. These respective values were an improvement over the next lowest peak load of 130 μN, but not a significant improvement

from the next highest peak load of 210 µN. 175 µN was determined as the optimal load for indentation measurements and was used throughout this thesis.

5.4.2. Indentation lateral separation

Individual nanoindentation measurements create a stress field in the material in a three dimensional spherical volume of radius equal to the indentation depth. This stress field, also associated with dislocation hardening, can impact nanoindentation data if the neighboring indents do not have adequate lateral separation to avoid the overlapping of their impact volume. In this thesis, it is desirable to perform indentation measurements in small distances from grain boundaries. To identify the minimum lateral separation between indents, 4 sets of 30 indentations, at lateral separations of factors of 10, 7, 4, and 2 times the indentation depth of 100 nm were done on Sample I. The results of these indentation sets are summarized in Table 5.4.

Lateral separation as a function of indentation depth (h_c)	Elastic Modulus (GPa)		Hardness (GPa)	
	Mean $(\overline{X})$	Standard Deviation (σ)	Mean $(\overline{X})$	Standard deviation (σ)
$10h_c$	131.42	9.62	2.80	0.18
$7h_c$	143.44	13.43	2.80	0.15
$4h_c$	153.94	26.93	3.40	1.07
$2h_c$	170.18	37.51	4.58	1.94

Table 5.4 – Comparison of elastic modulus (E) and hardness (H) for indentation sets of 30 indents with different lateral separations between indents.

Table 5.4 shows a significant increase in the standard deviation of the elastic modulus and hardness when the lateral separation between indents is below 7hc to 4hc. This increase is the result of the overlapping impact volume of neighboring indents. Therefore, indentation measurements in this thesis were done maintaining a minimum lateral separation of $7h_c$.

5.4.3. Indentation size effect

The presence of an indentation size effect, as discussed in Chapter 4.4.2, was characterized using Sample I. Indentations at varying depths were done to observe the behavior of the measured hardness as a function of depth, as shown in Figure 5.8.
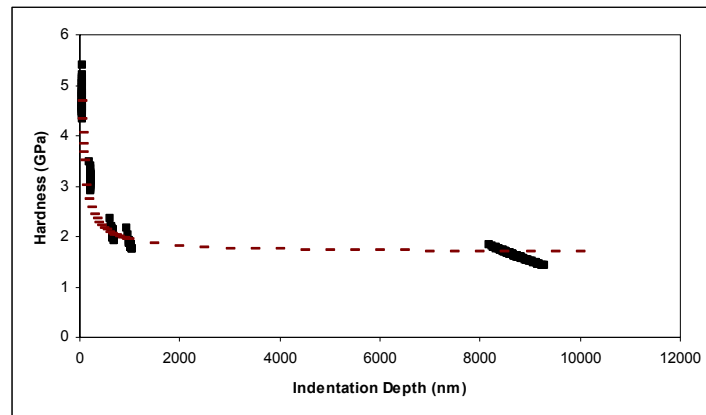
Figure 5.8 – Hardness as a function of indentation depth, showing the indentation size effect encountered in nanoindentation measurements. Measured hardness is shown as black squares; theoretical indentation size effect is shown as a burgundy dashed line.

The measured hardness as a function of indentation depth shown in Figure 5.8 aligns well with the theoretical prediction of the indentation size effect from equation 4.5. The theoretical prediction (dashed curve in Figure 5.8) from equation 4.5 is plotted with the fitting parameter that describes ease of dislocation movement, α, equal to 0.7, which is similar to values used by Nix and Gao [24]. While this behavior is indicative of an indentation size effect in Inconel 690, an explicit determination of whether or not Inconel 690 experiences an actual indentation size effect is not important to the results in this thesis. This is because measured hardness values are compared between sets of indentations done at approximately the same indentation depths (within 5 nm.) This characterization does, however, reconcile the difference between the published hardness of Inconel 690 (1.67 GPa) and the measured values of hardness (between 3 and 6 GPa) in this thesis. Additionally, the data collection and development of a relationship

between the depth dependence on measured hardness in this thesis serves to further characterize Inconel 690 for any future work on this material.

5.4.4. Effect of electrolytic polishing

As mentioned in Chapter 5.1.3, electrolytic polishing was accomplished on Sample I. However, when placed in the electrolytic solution, general corrosion of Sample II occurred and therefore did not allow for electrolytic polishing. Although it is possible to alter the electrolyte solution to allow for electrolytic polishing, omitting electrolytic polishing of the TMP sample was determined to be a more appropriate solution due safety concerns associated with hazardous chemicals needed for electrolytic polishing of chromium-carbide precipitated surfaces.

The hardness and elastic modulus of each sample were compared. 50 indents were done on each sample using the exact specifications of the indents done throughout this thesis: a peak load of 175 μN which achieved indentation depths of approximately 50-60 nm. This data is summarized in Table 5.5.

	Sample I		Sample II	
	Mean (GPa)	Standard deviation (GPa)	Mean (GPa)	Standard deviation (GPa)
Elastic modulus (E)	166.38	16.93	168.56	20.15
Hardness (H)	4.73	0.24	4.85	0.36

Table 5.5 – Comparison of Elastic modulus (E) and hardness (H) of solution annealed sample and TMP sample. The solution annealed sample underwent mechanical and electrolytic polished, while the TMP sample only underwent mechanical polishing.

As shown in Table 5.5, only small differences in the values of hardness and elastic modulus between the Sample I and Sample II is evident. Additionally, the standard deviations of each respective data set are comparable. The effect of not electrolytically polishing Sample II

was found to be negligible, likely due to the high value of hardness of Inconel 690. Sample II

was analyzed using nanoindentation without being electrolytically polished.

6. Results and discussion

6.1. Nanoindentation results

Nanoindentation measurements to determine hardness (H) and elastic modulus (E) at different relative positions of 10 grain boundaries on Sample I and Sample II were conducted. This thesis focuses on the behavior of dislocations and the relationship of that behavior to grain boundaries. Due to this focus, the analysis and discussion of the results that follows concentrates on the measured values of hardness instead of elastic modulus.

On Sample I, two nanoindentation schemes were used. The first scheme, shown in Figure 5.6, was used to characterize differences in the inherent hardness at the bulk regions and regions near the grain boundary as a function of grain boundary structure. Inherent hardness differences reflect differences in the density of stored dislocations that arise during processing of the sample. The distribution of the stored dislocation density is therefore dependent on the annealing temperature and time. The second scheme, shown in Figure 5.7, was used to characterize the induced hardness of two grain boundaries, one Σ3 grain boundary and one high angle boundary. Induced hardness occurs when dislocations are created by nanoindentations and accumulate. These dislocations move towards grain boundaries and are absorbed by, glide through or piled up alongside the grain boundary. The resulting density of dislocations alongside the boundary then contributes to the hardness measurement at that location. Grain boundaries that did not show statistically significant differences in inherent hardness between the bulk regions and the grain boundary were chosen to isolate the induced grain boundary hardening effect.

On Sample II, the nanoindentation scheme shown in Figure 5.6 was used to characterize inherent hardness near, alongside and on grain boundaries. TMP resulted in the formation of chromium carbide precipitates at grain boundaries on Sample II. The presence of these

66

precipitates dominated the blocking of dislocations near the boundary.   This nanoindentation scheme was used to characterize inherent hardness differences between bulk regions and regions near the grain boundary due to the presence of chromium carbide precipitates.

6.1.1. Sample I

Six boundaries on Sample I were characterized using procedure described in 5.4: four $\Sigma 3$ grain boundaries and two high angle boundaries. In situ imaging was done at an appropriate scale to capture the indentation scheme for each data set. For each data set, a comparison of the magnitudes of the elastic modulus (E) and hardness (H), and the ratio of the E and H measured at the bulk and at the grain boundary is included. Inherent and induced mechanical properties for grain boundary (4) and grain boundary (6) were characterized.

Grain Boundary (1)

Grain boundary type: Σ3 Misorientation angle: 59.3° Misorientation direction: <1 -1 -1>	*Neighboring grain orientations* Left grain: <0 1 2> Right grain: <-1 0 2>
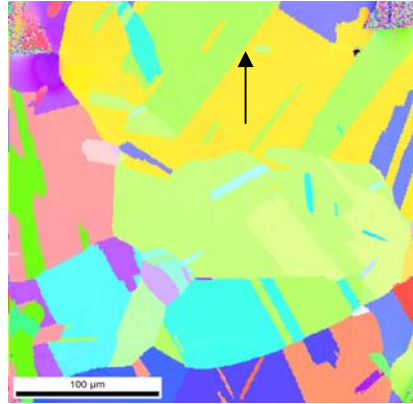
(A)
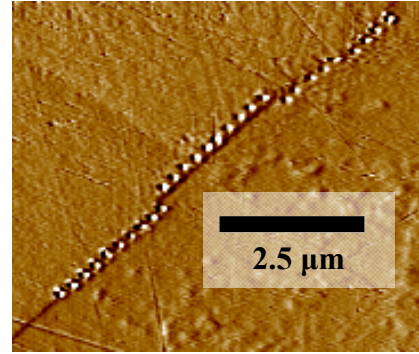
(B)

Figure 6.1 – (A) IPF plot showing orientation of grains that form. Grain boundary (1) is marked by a black arrow. (B) In situ image of grain boundary (1).

	5 μm left of GB	*500 nm left of GB*	*Grain Boundary*	*500 nm right of GB*	*5 μm right of GB*
E (GPa)	200.1	228.4	211.9	217.2	199.7
H (GPa)	3.27	4.67	4.37	4.61	3.38

Table 6.1 - E and H measured at different positions relative to grain boundary (1).

	$\dfrac{500\ nm\ from\ GB}{5\ \mu m\ left\ of\ GB}$	$\dfrac{500\ nm\ from\ GB}{5\ \mu m\ right\ of\ GB}$
E	1.14	1.09
H	1.43	1.36

Table 6.2 – Ratio of bulk to near grain boundary regions for E and H on grain boundary (1).
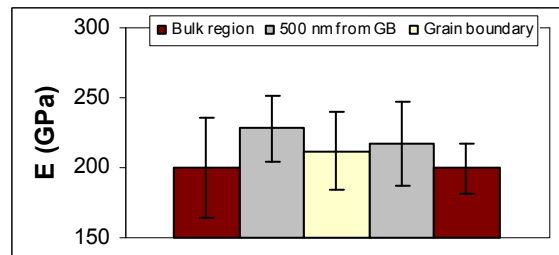
Figure 6.2 - Difference in E as a function of position relative to grain boundary (1).
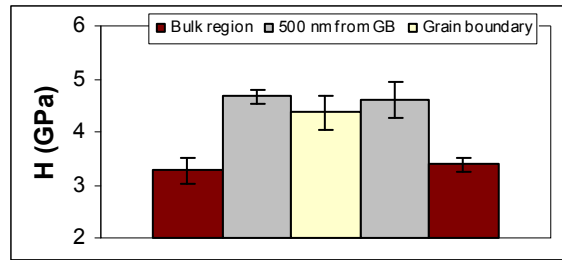
Figure 6.3 - Difference in H as a function of position relative to grain boundary (1).

Grain Boundary (2)

Grain boundary type: High angle Misorientation angle: 43.6˚ Misorientation direction: <0 -2 -1>	*Neighboring grain orientations* Left grain: <-1 0 3> Right grain: <1 -1 1>
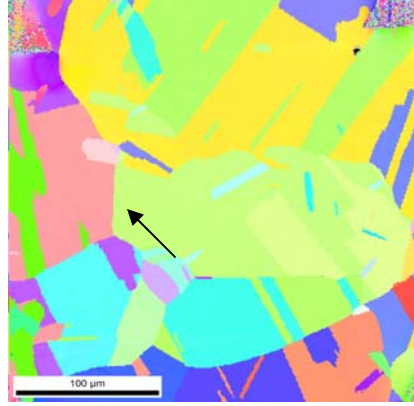
(A)
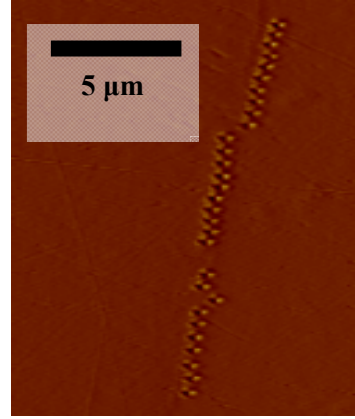
(B)

Figure 6.4 – (A) IPF plot showing orientation of grains that form. Grain boundary (2) is marked by a black arrow. (B) In situ image of grain boundary (2).

	5 μm left of GB	*500 nm left of GB*	*Grain Boundary*	*500 nm right of GB*	*5 μm right of GB*
E (GPa)	186.7	205.1	201.6	208.7	207.8
H (GPa)	3.64	3.77	3.48	3.44	3.51

Table 6.3 - E and H measured at different positions relative to grain boundary (2).

	$\dfrac{500\ nm\ from\ GB}{5\ \mu m\ left\ of\ GB}$	$\dfrac{500\ nm\ from\ GB}{5\ \mu m\ right\ of\ GB}$
E	1.10	1.00
H	0.98	0.96

Table 6.4 - Ratio of bulk to near grain boundary regions for E and H on grain boundary (2).
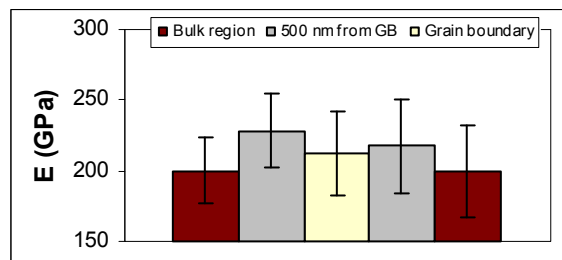
Figure 6.5 - Difference in E as a function of position relative to grain boundary (2).

70
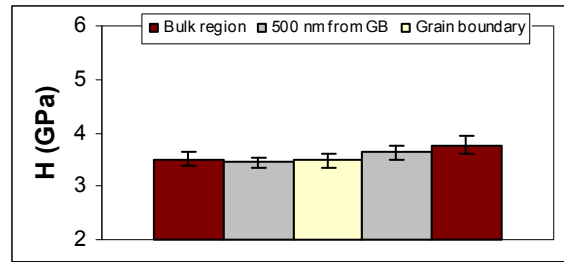
Figure 6.6 - Difference in H as a function of position relative to grain boundary (2).

Grain Boundary (3)

Grain boundary type: CSL (Σ3) Misorientation angle: 59.3˚ Misorientation direction: <1 -1 -1>	*Neighboring grain orientations* Left grain: <0 1 2> Right grain: <1 0 2>

(A)

(B)

Figure 6.7 – (A) IPF plot showing orientation of grains that form. Grain boundary (3) is marked by a black arrow. (B) In situ image of grain boundary (3).

	5 µm left of GB	*500 nm left of GB*	*Grain Boundary*	*500 nm right of GB*	*5 µm right of GB*
E (GPa)	193.7	187.1	195.9	177.3	183.2
H (GPa)	4.78	4.62	4.75	4.81	4.93

Table 6.5 - E and H measured at different positions relative to grain boundary (3).

	$\dfrac{500\ nm\ from\ GB}{5\ \mu m\ left\ of\ GB}$	$\dfrac{500\ nm\ from\ GB}{5\ \mu m\ right\ of\ GB}$
E	0.97	0.97
H	0.97	0.97

Figure 6.8 - Ratio of bulk to near grain boundary regions for E and H on grain boundary (3).
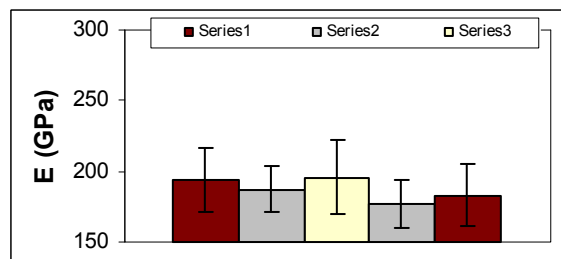
Figure 6.9 - Difference in E as a function of position relative to grain boundary (3).
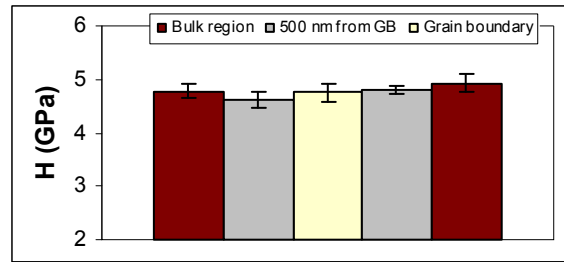
Figure 6.10 - Difference in H as a function of position relative to grain boundary (3).

Grain Boundary (4)

Grain boundary type: CSL (Σ3)	*Neighboring grain orientations*
Misorientation angle: 59.9˚	Left grain: <-3 1 3>
Misorientation direction: <-1 1 -1>	Right grain: <1 2 -1>

(A)

(B)
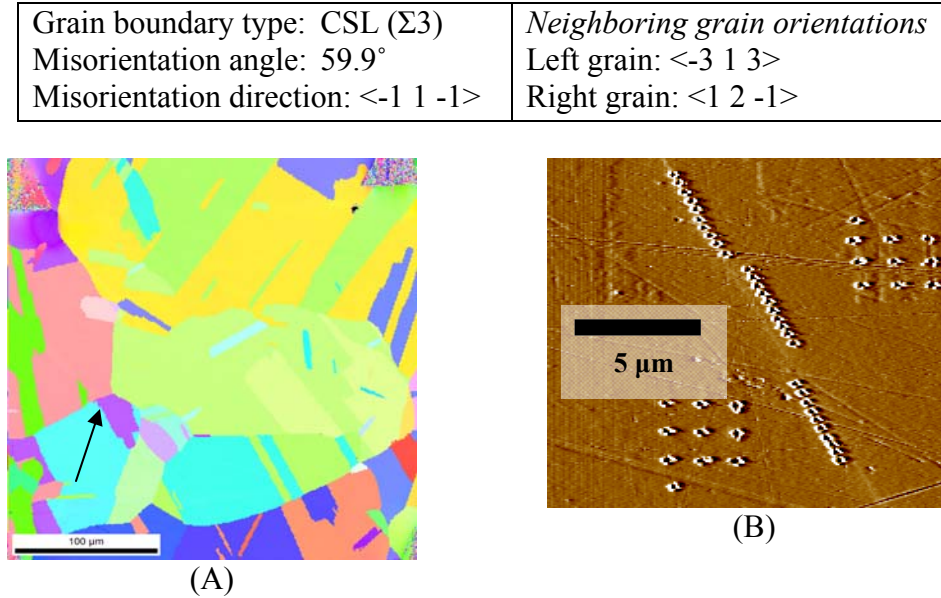
Figure 6.11 – (A) IPF plot showing orientation of grains that form. Grain boundary (4) is marked by a black arrow. (B) In situ image of grain boundary (4).

	5 μm left of GB	*500 nm left of GB*	*Grain Boundary*	*500 nm right of GB*	*5 μm right of GB*
E (GPa)	200.1	186.0	202.71	207.24	212.95
H (GPa)	4.61	4.45	4.43	4.33	4.54

Table 6.6 - E and H measured at different positions relative to grain boundary (4).

	$\dfrac{500\ nm\ from\ GB}{5\ \mu m\ left\ of\ GB}$	$\dfrac{500\ nm\ from\ GB}{5\ \mu m\ right\ of\ GB}$
E	0.97	0.93
H	0.95	0.96

Table 6.7 - Ratio of bulk to near grain boundary regions for E and H on grain boundary (4).
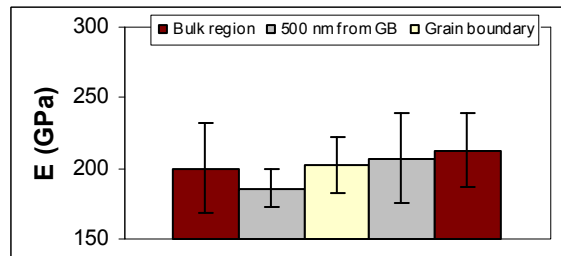
Figure 6.12 - Difference in E as a function of position relative to grain boundary (4).

74
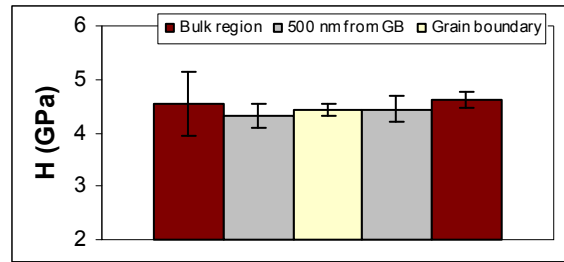
Figure 6.13 - Difference in H as a function of position relative to grain boundary (4).

Grain Boundary (5)

Grain boundary type: CSL (Σ3) Misorientation angle: 59.3˚ Misorientation direction: <1 -1 -1>	*Neighboring grain orientations* Left grain: <-1 0 2> Right grain: <0 1 2>

(A)   (B)

Figure 6.14 – (A) IPF plot showing orientation of grains that form. Grain boundary (5) is marked by a black arrow. (B) In situ image of grain boundary (5).

	5 μm left of GB	*500 nm left of GB*	*Grain Boundary*	*500 nm right of GB*	*5 μm right of GB*
E (GPa)	190.9	189.0	194.7	182.5	168.5
H (GPa)	4.19	4.32	4.07	4.71	4.40

Table 6.8 - E and H measured at different positions relative to grain boundary (5).

	$\dfrac{500 \text{ nm from GB}}{5 \text{ μm left of GB}}$	$\dfrac{500 \text{ nm from GB}}{5 \text{ μm right of GB}}$
E	1.08	0.99
H	1.07	1.03

Table 6.9 - Ratio of bulk to near grain boundary regions for E and H on grain boundary (5).
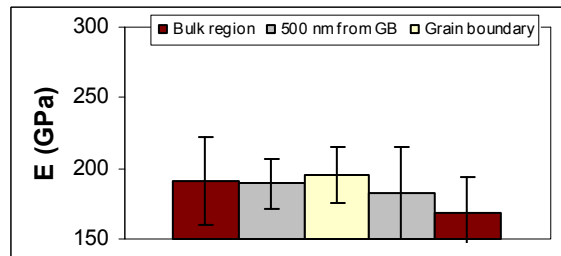
Figure 6.15 – Bar chart showing difference in E as a function of position relative to grain boundary (5).
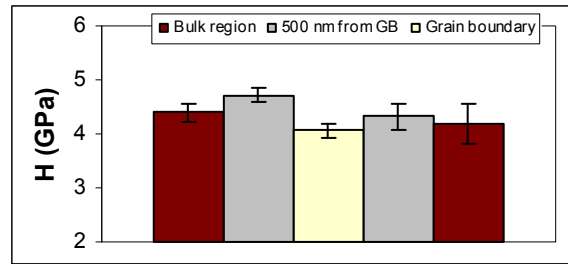
Figure 6.16 - Bar chart showing difference in H as a function of position relative to grain boundary (5).

Grain Boundary (6)

Grain boundary type: High Angle	*Neighboring grain orientations*
Misorientation angle: 59.6˚	Left (top) grain: <-1 4 0>
Misorientation direction: <1 1 1>	Right (bottom) grain: <-1 1 1>
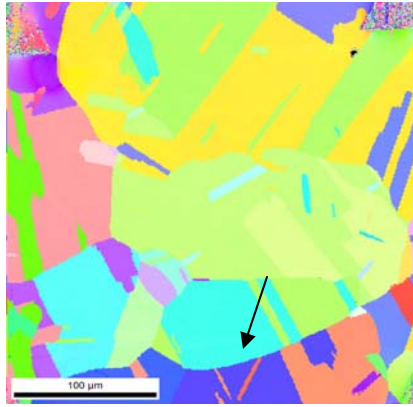
(A)
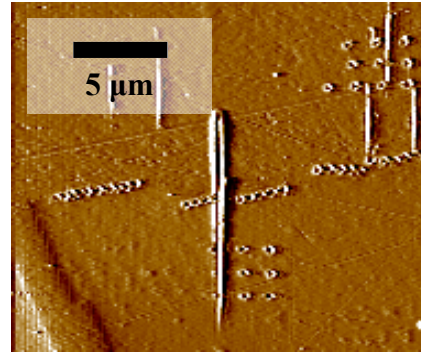
(B)

Figure 6.17 – (A) IPF plot showing orientation of grains that form. Grain boundary (6) is marked by a black arrow. (B) In situ image of grain boundary (6).

	5 μm left of GB	*500 nm left of GB*	*Grain Boundary*	*500 nm right of GB*	*5 μm right of GB*
E (GPa)	208.7	212.7	215.1	202.5	202.5
H (GPa)	4.24	4.26	4.60	4.48	4.74

Table 6.10 - E and H measured at different positions relative to grain boundary (6).

	$\dfrac{500\ nm\ from\ GB}{5\ \mu m\ left\ of\ GB}$	$\dfrac{500\ nm\ from\ GB}{5\ \mu m\ right\ of\ GB}$
E	1.00	1.02
H	0.95	1.00

Table 6.11 - Ratio of bulk to near grain boundary region for E and H on grain boundary (6).
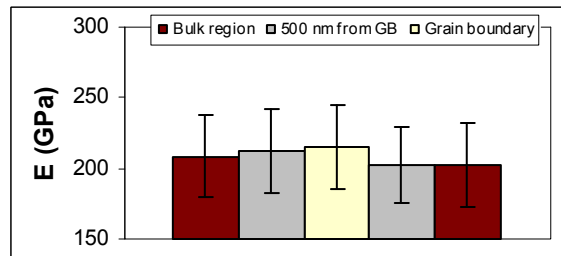
Figure 6.18 – Difference in E as a function of position relative to grain boundary (6).
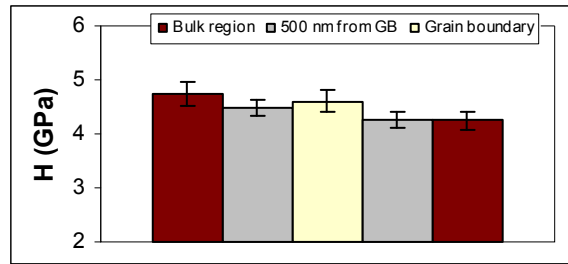
Figure 6.19 - Difference in H as a function of position relative to grain boundary (6).

Grain Boundary (4) – Induced hardness
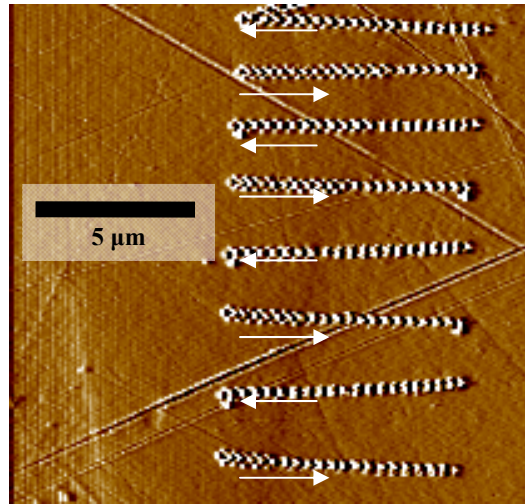
Figure 6.20 – In situ image of induced hardness measurement on grain boundary (4). Arrows indicate the direction nanoindentations were done in.

(A)

(B)
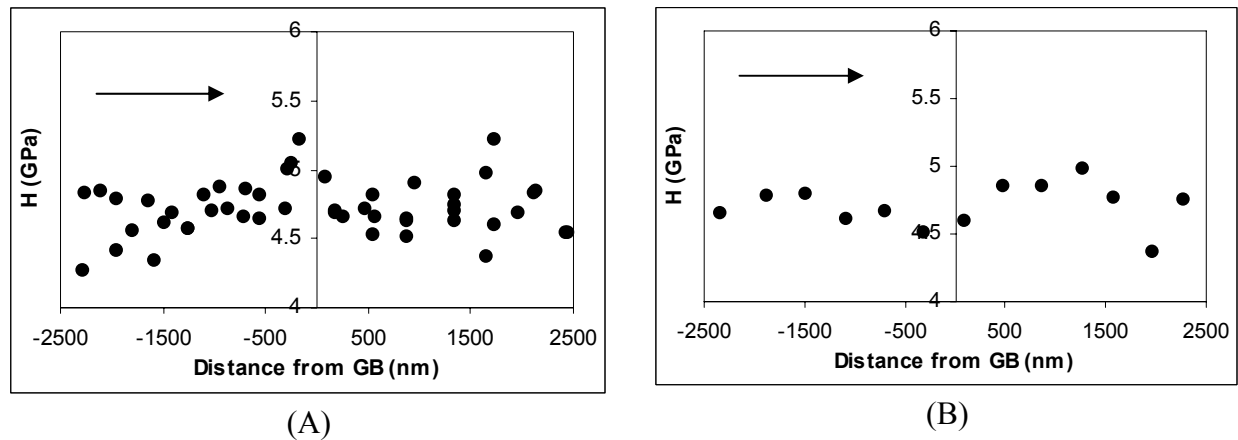
Figure 6.21 - Measurements of tip-induced hardening effect on grain boundary (4) for indentations approaching the grain boundary from left to right. (A) 4 of 5 indentation rows showed an increased hardness near the grain boundary relative to the bulk region of ~14.4% (4.57 GPa to 5.23 GPa) beginning at 2.5 μm from the left of the grain boundary. (B) 1 of 5 indentation rows did not show an increase in hardness approaching the grain boundary.

(A)   (B)
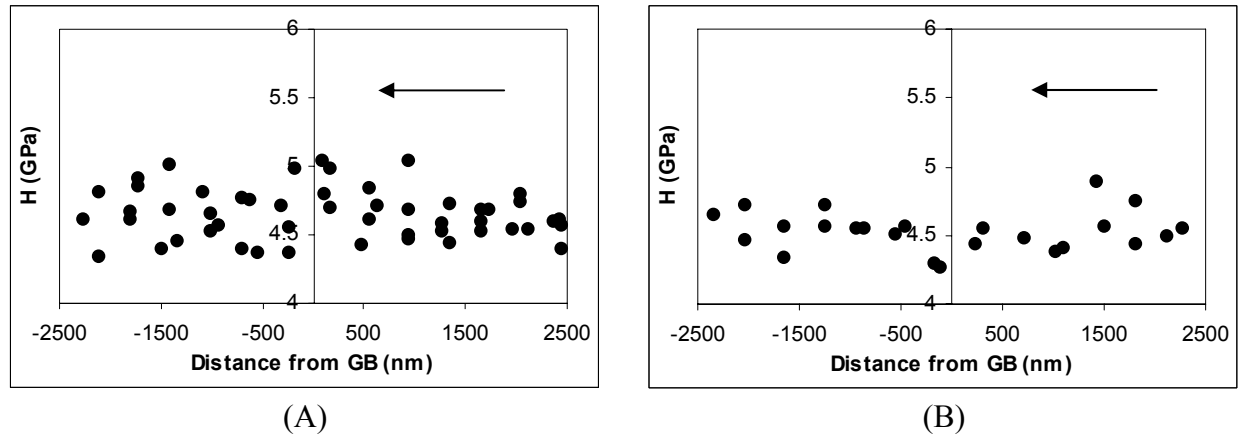
Figure 6.22 – Measurements of tip-induced hardening effect on grain boundary (4) for indentations approaching the grain boundary from right to left. (A) 4 of 6 indentation rows showed an increased hardness near the grain boundary relative to the bulk region of ~9.6% (4.60 GPa to 5.04 GPa) beginning at 2.5 μm from the right of the grain boundary. (B) 2 of 6 indentation rows did not show an increase in hardness approaching the grain boundary.

Grain Boundary (6) – Induced hardness
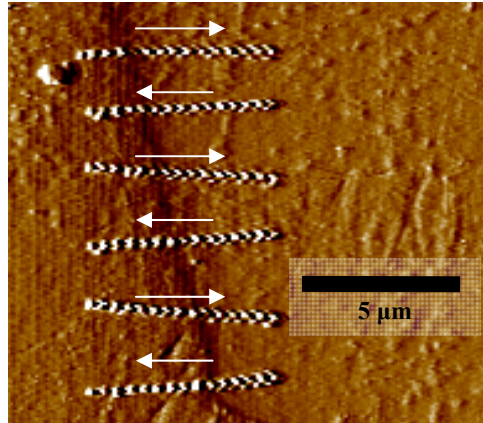
Figure 6.23 – In situ image of induced hardness measurement on grain boundary (6). Arrows indicate the direction nanoindentations were done in.
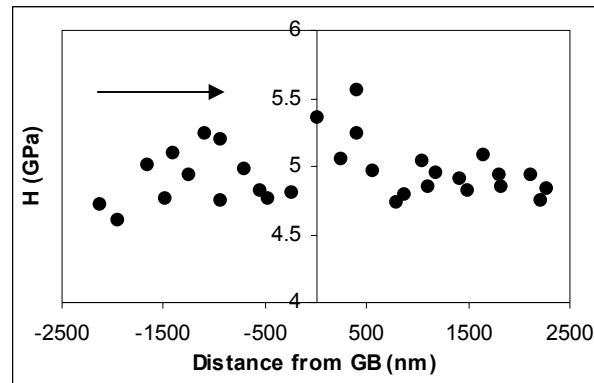
Figure 6.24 – Measurements of tip-induced hardening effect on grain boundary (6) for indentations approaching the grain boundary from left to right. 3 of 3 indentation rows showed an increased hardness near the grain boundary relative to the bulk region of ~13.5% (4.90 GPa to 5.56 GPa) beginning at 2.5 μm from the left of the grain boundary.
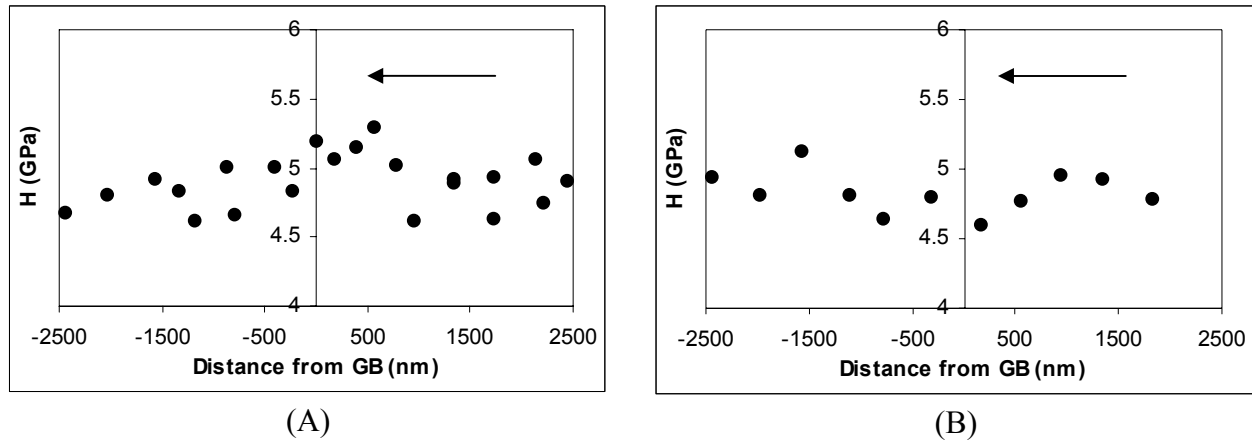
Figure 6.25 - Measurements of tip-induced hardening effect on grain boundary (6) for indentations approaching the grain boundary from right to left. (A) 2 of 3 indentation rows showed an increased hardness near the grain boundary relative to the bulk region of ~9.47% (4.75 GPa to 5.20 GPa) beginning at 2.5 μm from the right of the grain boundary. (B) 1 of 3 indentation rows did not show an increase in hardness approaching the grain boundary.

6.1.2. Sample II

Four boundaries on Sample II were characterized using the aforementioned procedure: one $\Sigma 3$ grain boundary, one low angle boundary and two high angle boundaries. In situ imaging was done at an appropriate scale to capture the indentation scheme for each data set. For each data set, a comparison of the magnitudes of the elastic modulus (E) and hardness (H), and the ratio of the E and H measured at the bulk and at the grain boundary is included.

Grain Boundary #1

Grain boundary type: CSL (Σ3) Misorientation angle: 54.2˚ Misorientation direction: <4 3 0>	*Neighboring grain orientations* Left grain: <-1 0 2> Right grain: <0 -1 2>
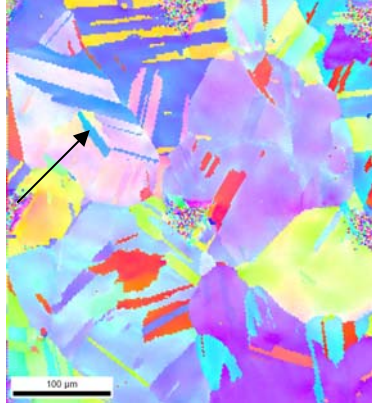
(A)
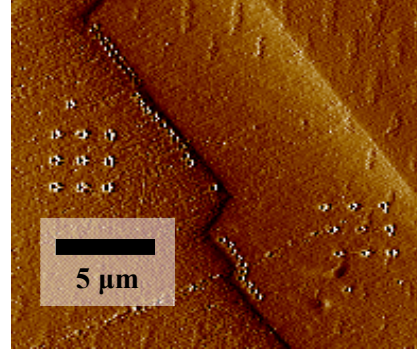
(B)

Figure 6.26 - (A) IPF plot showing orientation of grains that form. Grain boundary (1) is marked by a black arrow. (B) In situ image of grain boundary (1).

	5 μm left of GB	*500 nm left of GB*	*Grain Boundary*	*500 nm right of GB*	*5 μm right of GB*
E (GPa)	204.6	201.6	216.5	220.5	205.0
H (GPa)	4.33	4.68	5.85	5.17	4.18

Table 6.12 - E and H measured at different positions relative to grain boundary (1).

	$\dfrac{500\ nm\ from\ GB}{5\ \mu m\ left\ of\ GB}$	$\dfrac{500\ nm\ from\ GB}{5\ \mu m\ right\ of\ GB}$
E	0.99	1.08
H	1.08	1.24

Table 6.13 - Ratio of bulk to near grain boundary region for E and H on grain boundary (6).
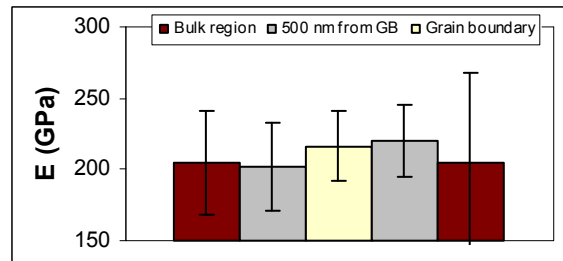
Figure 6.27 – Difference in E as a function of position relative to grain boundary (6).
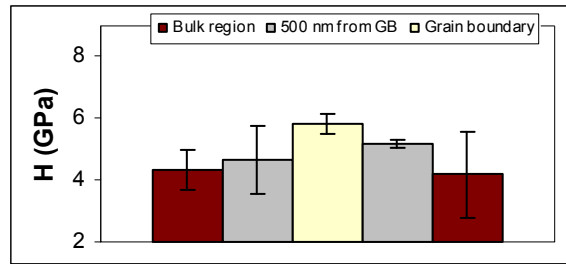
Figure 6.28 – Difference in E as a function of position relative to grain boundary (6).

Grain Boundary #2

Grain boundary type: High angle Misorientation angle: 12.1˚ Misorientation direction: <4 3 0>	*Neighboring grain orientations* Left grain: <-2 1 1> Right grain: <-3 1 1>
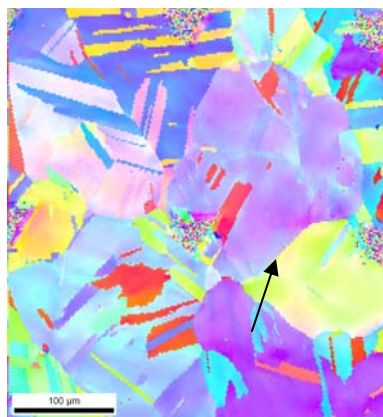
(A)
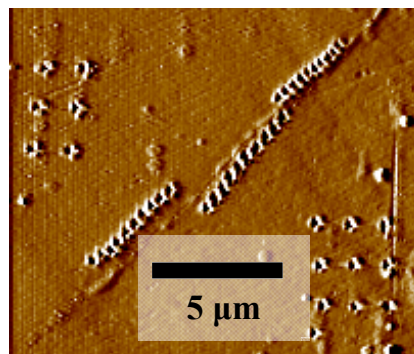
(B)

Figure 6.29 - (A) IPF plot showing orientation of grains that form. Grain boundary (2) is marked by a black arrow. (B) In situ image of grain boundary (2).

	5 µm left of GB	*500 nm left of GB*	*Grain Boundary*	*500 nm right of GB*	*5 µm right of GB*
E (GPa)	198.0	192.0	204.5	186.8	209.9
H (GPa)	3.66	3.62	3.43	3.24	3.91

Table 6.14 - E and H measured at different positions relative to grain boundary (2).

	$\dfrac{500\ nm\ from\ GB}{5\ \mu m\ left\ of\ GB}$	$\dfrac{500\ nm\ from\ GB}{5\ \mu m\ right\ of\ GB}$
E	0.97	0.89
H	0.99	0.83

Table 6.15 - Ratio of bulk to near grain boundary region for E and H on grain boundary (2).
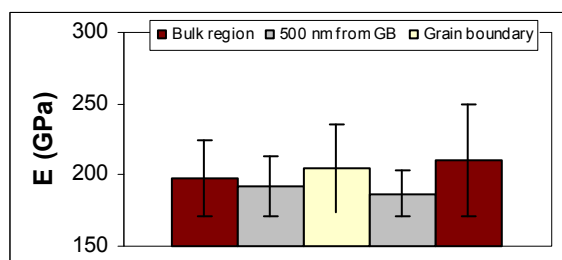
Figure 6.30 – Difference in E as a function of position relative to grain boundary (2).
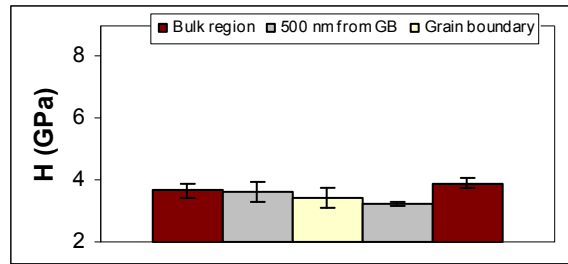
Figure 6.31 – Difference in E as a function of position relative to grain boundary (2).

Grain Boundary #3

Grain boundary type: Low angle Misorientation angle: 58.8˚ Misorientation direction: <-1 1 -1>	*Neighboring grain orientations* Left grain: <2 -1 0> Right grain: <-1 2 2>
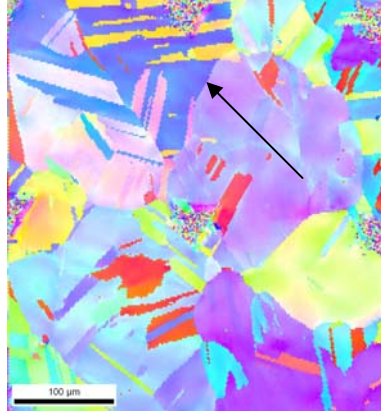
(A)
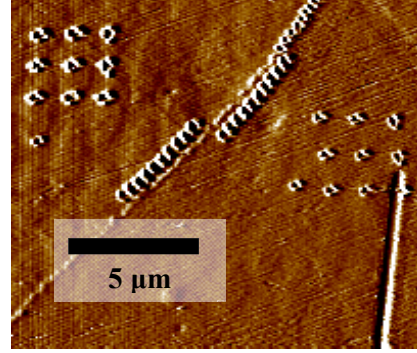
(B)

Figure 6.32 - (A) IPF plot showing orientation of grains that form. Grain boundary (3) is marked by a black arrow. (B) In situ image of grain boundary (3).

	5 μm left of GB	*500 nm left of GB*	*Grain Boundary*	*500 nm right of GB*	*5 μm right of GB*
E (GPa)	222.0	166.6	220.6	186.7	208.9
H (GPa)	5.10	2.94	5.48	3.06	4.48

Table 6.16 - E and H measured at different positions relative to grain boundary (3).

	$\dfrac{500\ nm\ from\ GB}{5\ \mu m\ left\ of\ GB}$	$\dfrac{500\ nm\ from\ GB}{5\ \mu m\ right\ of\ GB}$
E (GPa)	0.99	1.08
H (GPa)	1.08	1.24

Table 6.17- Ratio of bulk to near grain boundary region for E and H on grain boundary (3).
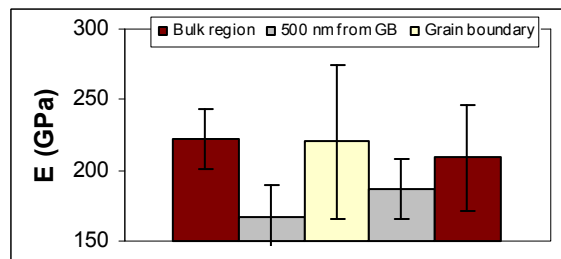
Figure 6.33– Difference in E as a function of position relative to grain boundary (6).
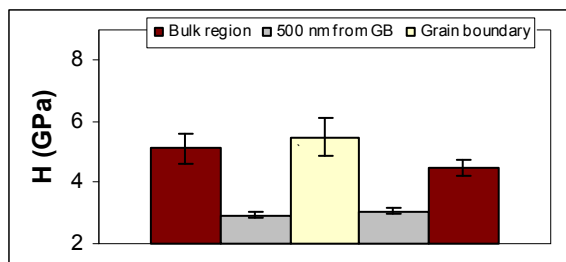
Figure 6.34– Difference in E as a function of position relative to grain boundary (3).

Grain Boundary #4

Grain boundary type: High angle	Neighboring grain orientations
Misorientation angle: 51.5˚	Left grain: <-2 0 1>
Misorientation direction: <-3 1 -1>	Right grain: <2 1 3>
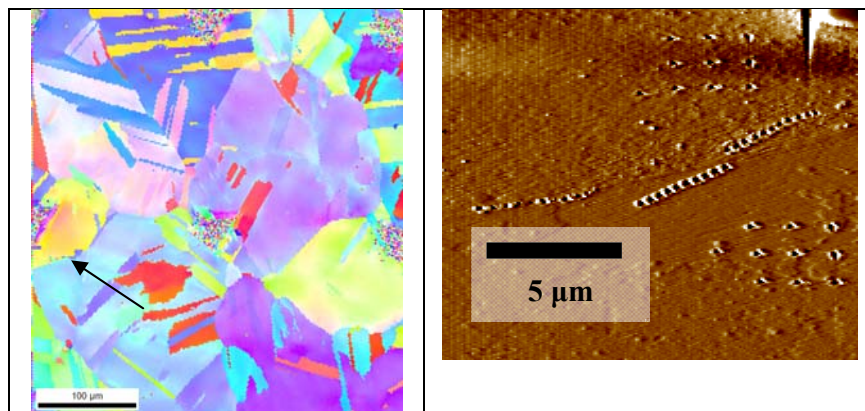
Figure 6.35 - (A) IPF plot showing orientation of grains that form. Grain boundary (4) is marked by a black arrow. (B) In situ image of grain boundary (4).

	5 µm left of GB	*500 nm left of GB*	*Grain Boundary*	*500 nm right of GB*	*5 µm right of GB*
E (GPa)	198.0	211.9	218.4	205.6	218.3
H (GPa)	4.79	5.73	6.27	4.65	4.77

Table 6.18 - E and H measured at different positions relative to grain boundary (4).

	$\dfrac{500\ nm\ from\ GB}{5\ µm\ left\ of\ GB}$	$\dfrac{500\ nm\ from\ GB}{5\ µm\ right\ of\ GB}$
E	1.07	0.89
H	1.20	0.97

Table 6.19 - Ratio of bulk to near grain boundary region for E and H on grain boundary (4).
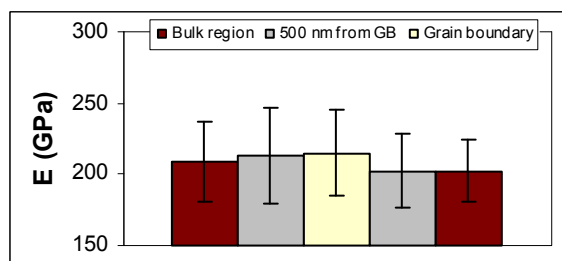
Figure 6.36 – Difference in E as a function of position relative to grain boundary (4).
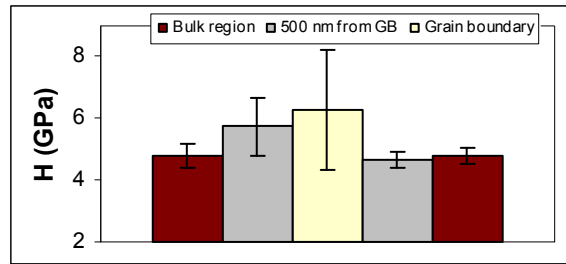
Figure 6.37 – Difference in E as a function of position relative to grain boundary (4).

6.2. Discussion of nanoindentation results

6.2.1. Sample I

A discussion of the correlation of measured inherent and tip-induced hardness values to grain crystalline orientation, grain boundary size, and grain boundary structure is presented here.

6.2.1.1. Grain boundary orientation

Figure 6.38 shows hardness of the bulk regions of neighboring grains of the grain boundaries on Sample I.
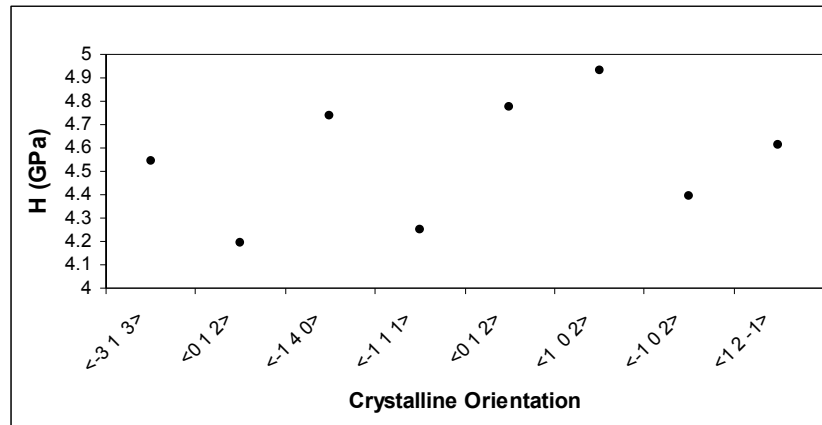
Figure 6.38 – Hardness (H) as a function for different crystalline orientations. Two data sets completed with the NorthStar cube corner tip are not included.

Hardness in the bulk regions does not show a strong dependence on crystalline orientation. This is in agreement with the work of Alexandreanu et al [28] and Vlassak and Nix [25], who both observed negligible differences due to the complicated three dimensional stress field created when using a three-sided pyramidal indenter tip for indentation measurements.

6.2.1.2. Grain boundary size

Figure 6.39 shows the hardness of the bulk regions of neighboring grains of each grain boundary observed from Sample I.
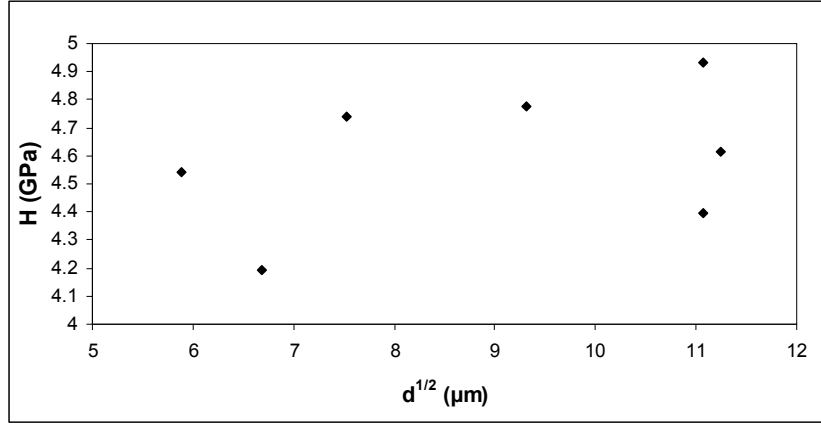
Figure 6.39 – Hardness measured in the bulk region of grains as a function of the square root of grain size ($d^{1/2}$). Two data sets completed with the NorthStar cube corner tip are not included.

Figure 6.39 shows that hardness in the bulk regions does not show a dependence on grain size. Hardness is expected to increase with decreasing grain size according to the Hall-Petch relationship,

$$\sigma_y = \sigma_o + \frac{K}{\sqrt{d}}$$

where σ_y is the resulting yield stress, σ_o is an initial value of yield stress, K is a material dependent constant, and d is the grain size. Grain size is determined by approximating the grains as rectangles and taking the square root of the area. This does not agree with the observations of Alexandreanu et al [28], who observed the expected decreasing hardness with increasing average grain size.

The Hall-Petch effect is likely not observed on Sample I for several reasons. First, grain size is approximated using a two dimensional image. The third dimension of grain is hidden making grain size approximation difficult. This rationale can also be used when considering that the sample surface is where the larger Inconel 690 bar was cut. Thinking of the image as a two dimensional cross section reveals how grain depth or height would be impossible to consider when approximating grain size. Finally, sizes of grains are of similar orders of magnitude, and

thus, the increased yield strength resulting from the Hall-Petch relationship would likely be negligible. Therefore, for the purposes of the analysis in this thesis, hardness can be considered to be independent of grain size evident on the surface of Sample I.

6.2.1.3. Grain boundary type – Inherent hardness

Figure 6.40 and Figure 6.41 summarize the measurements taken on grain boundaries on Sample I as a function of grain boundary type.
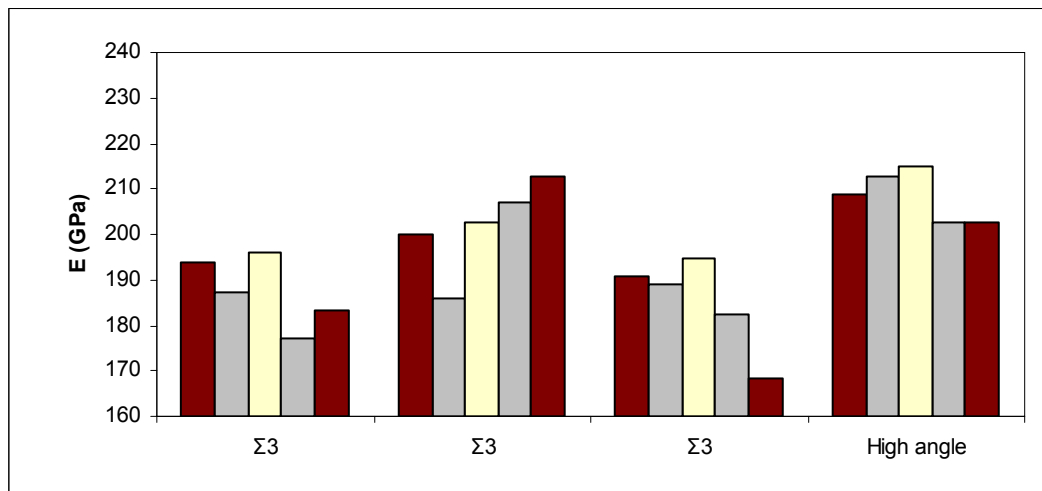
Figure 6.40 – Summary of elastic modulus (E) measured on grain boundaries on Sample I. Two data sets completed with the NorthStar cube corner tip are not included.
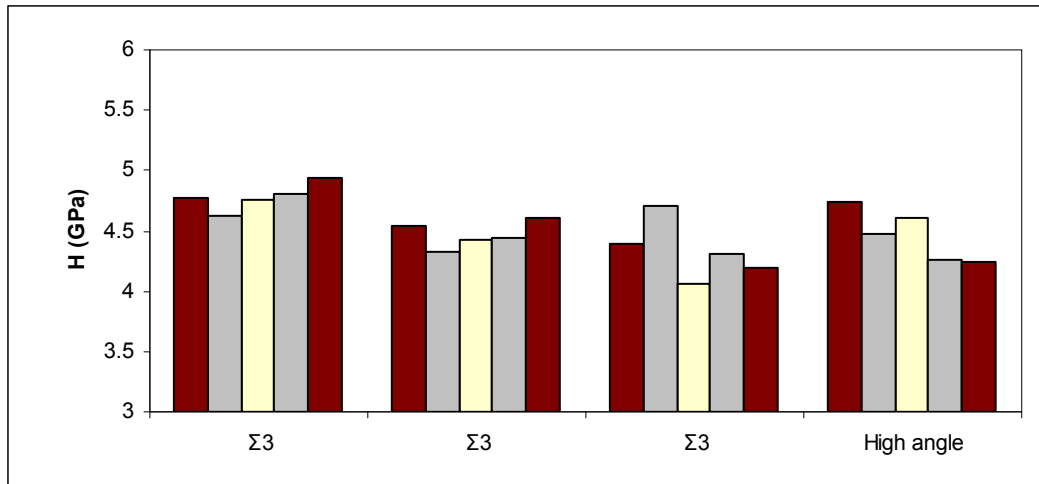
Figure 6.41 - Summary of hardness (H) measured on grain boundaries on Sample I.

The first two data sets presented from Sample I show a significantly decreased elastic modulus and hardness in the bulk region of the grain boundary relative to the region in the vicinity of the grain boundary. These data sets were compiled using a specific cube corner tip with a small radius of curvature, known as a NorthStar cube corner tip. During the course of the measurements taken, however, the NorthStar cube corner tip experienced a sudden and severe degradation. Because the exact timing of the degradation could not be localized with a high degree of confidence, the data collected using this tip is potentially affected by the tip degradation.

The remaining data sets were analyzed using a cube corner indenter tip verified to be of sound structural quality. Hardness on the grain boundary, near the grain boundary and in the corresponding bulk region of the show only slight differences for each characterized grain boundary.

The absence of significant differences in inherent hardness between the bulk and grain boundary regions indicates the uniformity in the distribution of stored dislocation density. This could be caused by the high temperature annealing at $1107^{o}C$ which enables the annihilation and

absorption of strain-induced dislocations in the lattice and at the ground boundaries. Nix and Gao

[24] describe the hardness measured by nanoindentation in terms of statistically stored

dislocations, ρ_s, and geometrically necessary dislocations, ρ_G, induced by the indenter tip as

$$H = 3\sqrt{3}\alpha\mu b\left(\sqrt{\rho_S + \rho_G}\right) \tag{6.1}$$

where H_o is the hardness at infinite depth, b is the Burger's vector of geometrically necessary

dislocations, μ is the shear modulus, and α is a non-dimensional constant that describes the ease

of dislocation movement. The absence of statistically significant trends on the inherent hardness

measurements indicates that the total dislocation density remained similar near the grain

boundary and away from the grain boundary upon the last annealing stage of the sample

processing.

Comparable stored dislocation densities between these boundaries are consistent with

expectations due to the role of high temperature annealing. As shown in Figure 6.42, dislocation

mobility depends exponentially on temperature with an Arrhenius behavior. At high

temperatures, dislocation mobility is high and less dependent on diffusion path. Thus, it is

expected that at the relatively high temperature used for annealing Sample I (1107 ºC), diffusion

of dislocations and subsequent absorption of dislocations at the grain boundaries are comparable

for CSL and high angle grain boundaries. This leads to comparable dislocation densities and thus

hardness, which remain in the lattice upon high temperature annealing.
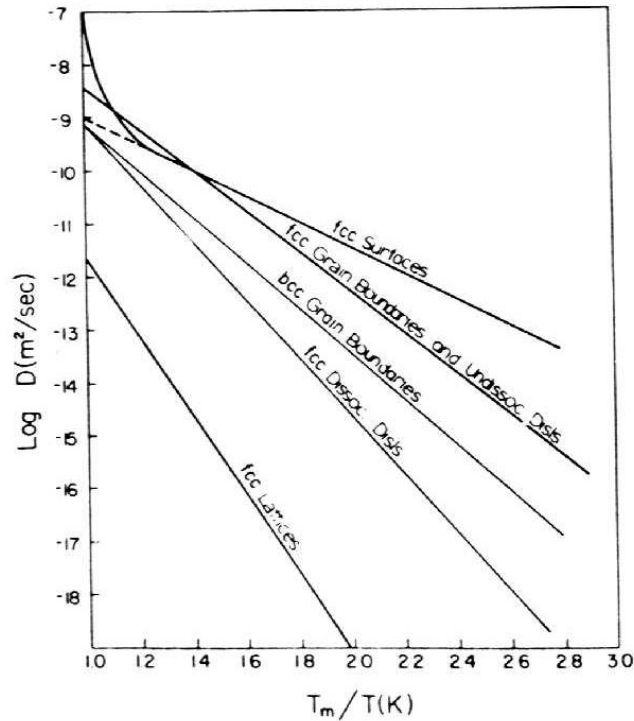
Figure 6.42 - Dislocation mobility (log D) as a function of reciprocal temperature for various diffusion paths in metals [26].

Furthermore, geometrically necessary dislocations that result from a single indent during nanoindentation at room temperature are substantially less than the density of stored dislocations. Therefore, the density of geometrically necessary dislocations (ρ_G) introduced by a single indent would have a negligible effect on the total dislocation density, and thus the hardness.

6.2.1.4. Grain boundary type – Induced hardness

Figure 6.21 and Figure 6.22 show the results of the induced hardness measurements approaching grain boundary (4), a $\Sigma 3$ grain boundary. The measurements on grain boundary (4) reveal an increased hardness near the grain boundary relative to 2.5 μm away from the grain boundary of approximately 14.4% when approaching it from left to right, and of approximately 9.6% when approaching it from right to left. For comparison, inherent hardness near the grain

98

boundary was within 3% of hardness measured away from the grain boundary independent of direction.

Figure 6.24 and Figure 6.25 show the results of the induced hardness measurements completed on grain boundary (6), a high angle boundary. In this case, induced hardness measurements revealed an increased hardening at the boundary relative to 2.5 μm away from the grain boundary of approximately 13.5% when approaching the grain boundary from left to right, and 9.5% when approaching the grain boundary from right to left. When measured manually, hardness near the grain boundary was within 5% of the hardness away from the grain boundary to the left, and within less than 1% of the hardness away from the grain boundary to the right.

Figure 6.21, Figure 6.22, Figure 6.24, and Figure 6.25 show that few indentation rows did not exhibit an increased hardness in the vicinity of grain boundaries (4) and (6). These rows are potentially affected by single indent outliers, which can occur due to inhomogeneities on the sample surface or subsurface. To quantify the dislocation-boundary interaction leading to the hardening, analysis was done using only indentation rows that showed increased hardness in the vicinity of grain boundaries.

6.2.1.5. Interpretation of induced hardness variation

The observed increase in hardness in the vicinity of grain boundaries in this work is consistent with two other studies probing the grain boundary hardness in metals using nanoindentation. The first reviewed here, performed by Soifer et al, used a similar nanoindentation scheme as the induced hardness measurements on Sample I to examine the hardness of bi-crystal copper in the vicinity of grain boundaries [27]. Soifer et al found increased hardness in a region that extends a few microns from the grain boundary in one direction, which is similar to the induced hardness found on Sample I grain boundaries 4 and 6.

The measurement technique, similar to the indentation scheme in this thesis shown in Figure 5.7, and results of their study are shown in Figure 6.43 and Figure 6.44.
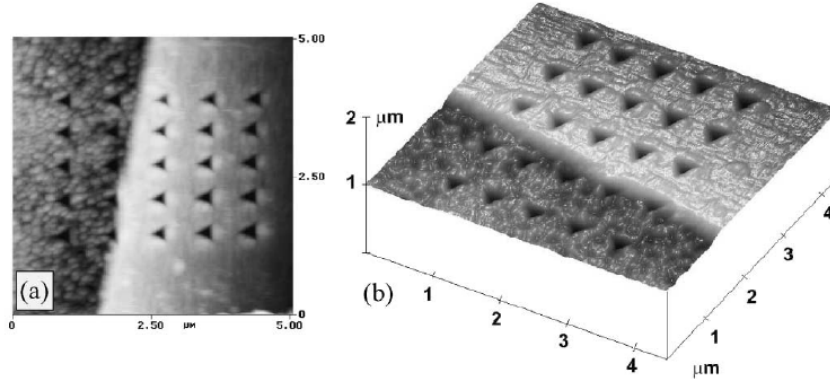
Figure 6.43 – Array of indentations performed by Soifer et al on a grain boundary in bi-crystal copper [27].
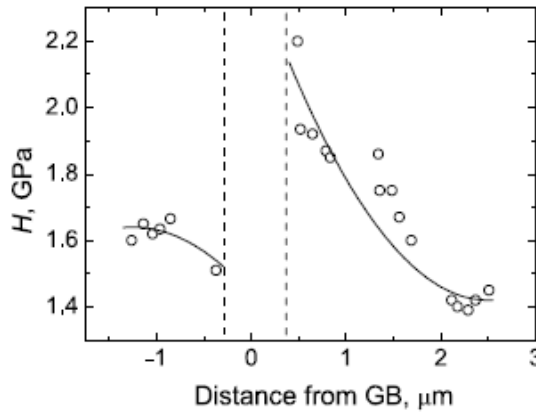
Figure 6.44 – Hardness trends in the vicinity of a single crystal copper grain boundary measured by Soifer et al [27].

Soifer et al discussed three mechanisms that can potentially explain the results seen on the Σ3 and high angle grain boundaries in their work, shown in Figure 6.20 through Figure 6.25. The first explanation considers the absorption of lattice dislocations by the grain boundary during grain boundary migration that occurred during the thermal treatment of the sample. Soifer et al propose that migrating grain boundaries absorb dislocations so the regions behind the

grain boundary that are swept during migration would have a decreased dislocation density. Additionally, migrating grain boundaries repel lattice dislocations in front of the grain boundary, thus resulting in the hardness profile shown in Figure 6.44. As explained by Nix and Gao [24], this increased density of dislocation results in an increased hardness, and thus, the migration of grain boundaries results in the non-uniform distribution of hardness shown in Figure 6.44. This explanation is not valid for the results in this thesis, as the high temperature annealing resulted in a uniform density of dislocations, as described in Chapter 6.2.1.3.

The second mechanism suggests that the results could possibly be governed by the anisotropy in the elastic moduli of the lattice in the surrounding grain boundaries. The elastic field around a grain boundary results in a long range interaction between the grain boundary and dislocations. If the energy of the elastic deformation field in the neighboring grain created by the dislocation is less than if the grain boundary were absent, then the dislocation is attracted by the grain boundary. If the energy from the elastic field would be greater without the grain boundary, dislocations are repelled. Thus, depending on crystalline orientation of neighboring grains, grain boundaries either repulse or attract dislocations. If dislocations are attracted, they glide toward and either are absorbed by the grain boundary, piled-up alongside the grain boundary, or glide through the grain boundary. The resulting depletion or build up of dislocations, leads to a non-uniform distribution of the density of dislocations. This results in differing values of hardness.

The third mechanism suggests that the anisotropy of slip transfer through grain boundaries could cause local hardness variations. Dislocations are induced by the nanoindenter tip during measurements, and the resulting hardness measurement is directly proportional to the ease with which these dislocations are able to propagate away from the tip. Dislocations glide on slip planes. The alignment of these slip planes from one grain to another will govern how easily

dislocations can pass through grain boundaries. Dislocations that can not glide easily through

grain boundaries pile up in the regions adjacent to the grain boundary.

The third mechanism explaining Soifer et al's results aligns well with the result from the

study conducted by Soer et al [28]. Soer et al examined the mechanical response of iron-silicion

and molybdenum body centered cubic (bcc) crystals using nanoindentation. For each of the

materials, increased hardness was found in regions that extended to approximately 1 μm from the

grain boundary, as shown in Figure 6.45. This increase in hardness was attributed to pile-up of

dislocations between the indenter tip and the grain boundary, caused by the grain boundary

obstructing motion of dislocations. Soer et al also observed differing yield excursions, which

indicates the slip transfer of dislocations induced by the indenter tip. In indentations near the

grain boundary, these yield excursions were suppressed, indicating that dislocations were not

capable of gliding away from the indenter tip. Yield excursions were more evident in

indentations conducted away from the grain boundary. This further supports that regions near the

grain boundary resulted in dislocation pile-up and, thus, an increased hardness.
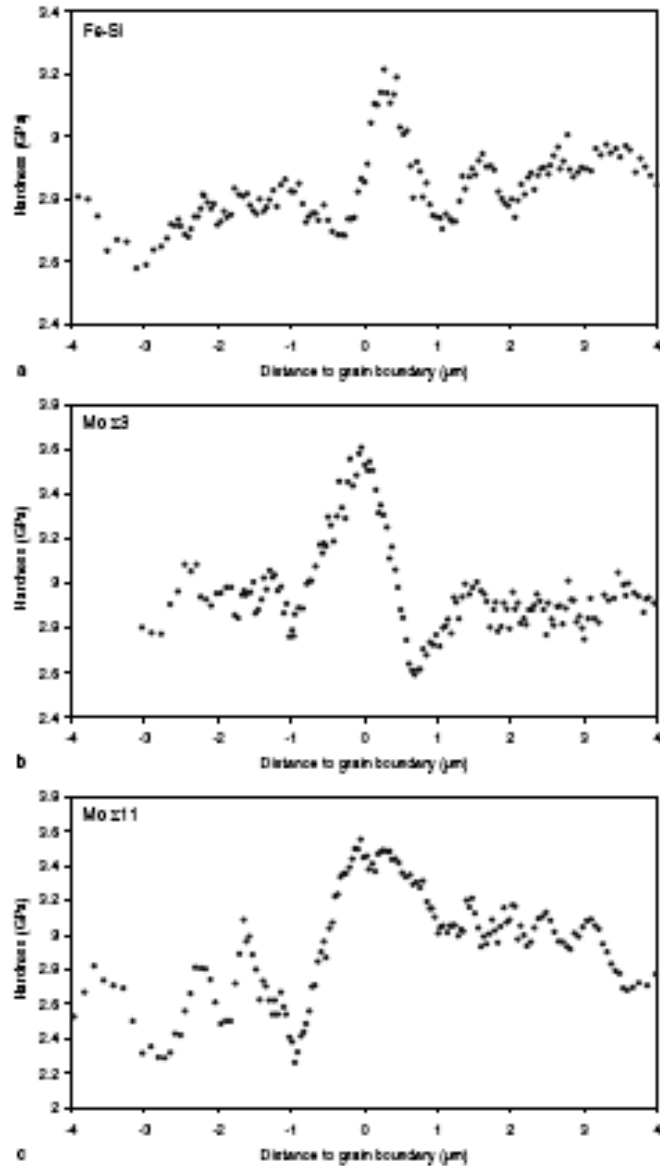
Figure 6.45 – Nanohardness of (a) Fe-Si, (b) a Σ3 grain boundary in Mo and (c) a Σ11 grain boundary in Mo by Soer et al [28]. Increased hardness was observed in regions that extend approximately 1 μm from the grain boundary in each direction.

The similarity in technique and results between these two studies and this thesis validate

the hypothesis that the alteration of the measurement technique from "measuring hardness with

nanoindentations along a grain boundary" to "measuring hardness with nanoindentations

stepping toward the grain boundary" leads to an increased hardness in the vicinity of the grain

103

boundary. The inherent hardness measurement of grain boundary (4) (Σ3 grain boundary) and grain boundary (6) (high angle grain boundary) showed no significant difference between bulk and near-grain boundary region. Therefore, the induced increase in hardness probed directly the dynamic interaction between dislocations introduced by the indenter tip and the grain boundary.

6.2.1.6. Analysis of induced grain boundary hardness

The increase in the induced hardness for each boundary is used for the following analytical comparison of the ease of dislocation movement through grain boundaries as a function of grain boundary type at the environmental conditions of the measurements in this thesis.

Hardness is related to dislocation density and ease of dislocation movement, given by

$$H = 3\sqrt{3}\alpha\mu b\left(\sqrt{\rho_S + \rho_G}\right) \tag{6.1}$$

Induced hardness measurements give the ratio of hardness near the grain boundary relative to hardness the bulk regions. This ratio, combined with equation 6.1, reduces to

$$\frac{H_{GB}}{H_{Bulk}} = \frac{\alpha_{GB}\left(\sqrt{\rho_S + \rho_G}\right)_{GB}}{\alpha_{Bulk}\left(\sqrt{\rho_S + \rho_G}\right)_{Bulk}} \tag{6.2}$$

The ratio of the relative grain boundary hardness for a Σ3 and a high angle boundary, respectively, is expressed as:

$$\frac{\left.\dfrac{H_{GB}}{H_{Bulk}}\right|_{\Sigma3}}{\left.\dfrac{H_{GB}}{H_{Bulk}}\right|_{HA}} = \frac{\left(\left.\dfrac{\alpha_{GB}\left(\sqrt{\rho_S + \rho_G}\right)_{GB}}{\alpha_{Bulk}\left(\sqrt{\rho_S + \rho_G}\right)_{Bulk}}\right)\right|_{\Sigma3}}{\left(\left.\dfrac{\alpha_{GB}\left(\sqrt{\rho_S + \rho_G}\right)_{GB}}{\alpha_{Bulk}\left(\sqrt{\rho_S + \rho_G}\right)_{Bulk}}\right)\right|_{HA}} \tag{6.3}$$

From induced hardness measurements for a Σ3 and high angle boundary, the relative grain boundary hardness for each grain boundary and direction are:

$$\left.\frac{H_{GB}}{H_{Bulk}}\right|_{\Sigma 3, Left\ to\ right} = 1.144 \qquad\qquad (6.4)$$

$$\left.\frac{H_{GB}}{H_{Bulk}}\right|_{\Sigma 3, Right\ to\ left} = 1.096 \qquad\qquad (6.5)$$

$$\left.\frac{H_{GB}}{H_{Bulk}}\right|_{HA, Left\ to\ right} = 1.135 \qquad\qquad (6.6)$$

$$\left.\frac{H_{GB}}{H_{Bulk}}\right|_{HA, Right\ to\ left} = 1.095 \qquad\qquad (6.7)$$

Averaging the induced hardness for both grain boundary types yields

$$\left.\frac{H_{GB}}{H_{Bulk}}\right|_{\Sigma 3} = 1.120 \qquad\qquad (6.8)$$

$$\left.\frac{H_{GB}}{H_{Bulk}}\right|_{HA} = 1.115 \qquad\qquad (6.9)$$

From Figure 6.38 and Figure 6.39, hardness in the bulk regions (H_{Bulk}) is found to not depend on grain size and crystalline orientation in this thesis. Therefore, H_{Bulk} is assumed constant in Sample I. Additionally, from inherent hardness measurements on grain boundary (4) and (6), the total density of dislocations ($\rho_S + \rho_G$) is approximately equal for grain boundary and bulk regions. Thus, equation 6.3 reduces to

$$\frac{H_{GB,\Sigma 3}}{H_{GB,HA}} = \frac{\alpha_{\Sigma 3}}{\alpha_{HA}} \qquad\qquad (6.10)$$

Substituting the values of induced hardness from equations 6.8 and 6.9 gives

$$\left(\frac{1.120}{1.115}\right) = \frac{\alpha_{\Sigma 3}}{\alpha_{HA}} \qquad (6.11)$$

Equation 6.11 can be simplified rearranged as

$$\alpha_{\Sigma 3} = 1.004\,\alpha_{HA} \qquad (6.12)$$

which gives the ease of dislocation motion through a Σ3 grain boundary in terms of the ease of dislocation motion through a high angle grain boundary, where $\alpha_{\Sigma 3}$ and α_{HA} are the non-dimensional constants in the Nix and Gao expression for hardness for Σ3 grain boundaries and high angle grain boundaries, respectively. From equation 6.12, the ease of dislocation motion through a high angle boundary and a Σ3 grain boundary is found to be equal, within the error limits of the measurements. We note here that the nanoindentation measurements were conducted at room temperature, where the dislocation mobility and absorption is small for both types of boundaries. The lack of difference in the dislocation mobility at the Σ3 and high angle boundary at room temperature could explain the similarity in α for both types of boundaries.

6.2.2. Sample II

Measurements on Sample II show the precipitate induced hardness at different types of grain boundaries that result from thermomechanical processing. Figure 6.46 and Figure 6.47 summarize the measurements taken on grain boundaries on Sample II.
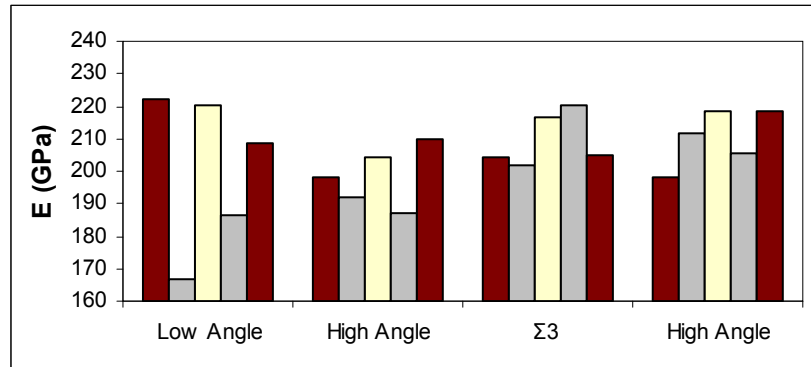
Figure 6.46 - Summary of elastic modulus (E) measured on grain boundaries on Sample II.
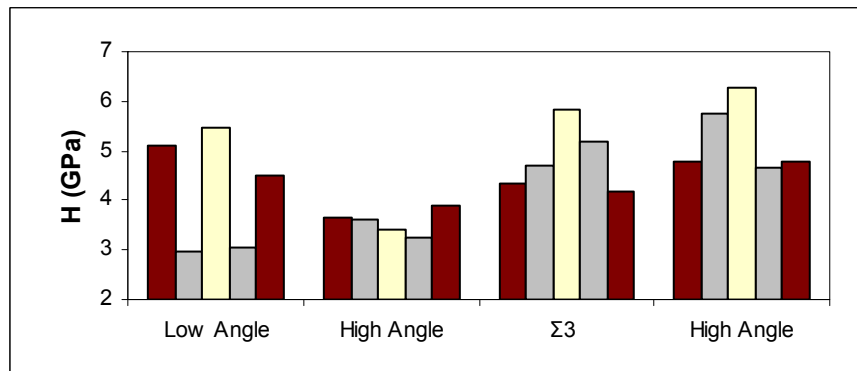
Figure 6.47 - Summary of hardness (H) measured on grain boundaries on Sample II.

Grain boundaries measured on Sample II show substantial differences in elastic modulus and hardness measured in the bulk regions of grains, near the grain boundaries, and on the grain boundaries. The two leftmost data sets presented in Figure 6.46 and Figure 6.47, which show a decreased hardness near the grain boundary relative to the bulk of the grain boundary, can be attributed to sensitization which occurred during thermal treatment. Nanoindentations were

performed approximately 500 nm from the grain boundary, so it is likely that these indentations

for these two data sets landed in depleted chromium regions. The two rightmost data sets shown

in Figure 6.46 and Figure 6.47 indicate the formation of precipitates at the grain boundary. In

these data sets, increased hardness at and near the grain boundary relative to the grain interior is

expected from the formation of chromium carbide precipitates. These results align with

observations made in the collaborative work [17] that characterized the grain boundaries using

TEM and STEM. In that work, precipitation of chromium carbides was identified at the grain

boundaries. The distribution of carbides present at the grain boundaries was found to depend on

grain boundary type. $\Sigma 3$ grain boundaries were observed to have a thin, continuous distribution

of carbides. Low angle grain boundaries were found to have an intermediate concentration of

carbides distributed semi-continuously. High angle grain boundaries were found to have a

coarse, discontinuous concentration of carbides. The distributions of carbides along these grain

boundaries are correlated with the energy of the grain boundary, which affects the diffusion rate

and, thus, carbide growth at the grain boundaries. These results align well with the profiles of

the hardness values measured on these types of grain boundaries, as shown in Figure 6.48

through Figure 6.51.
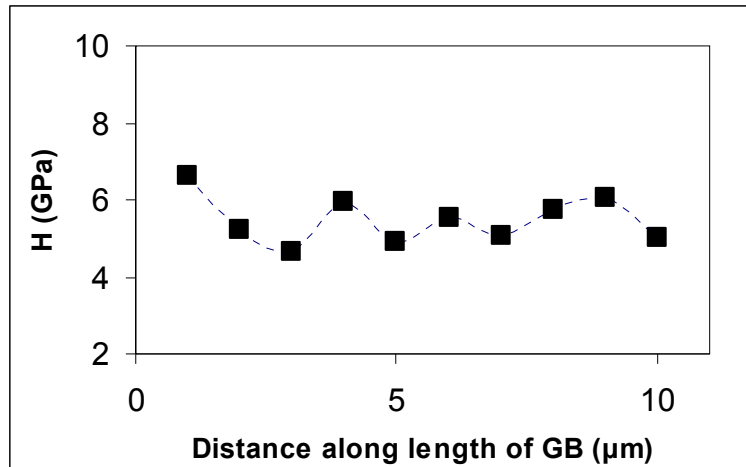
Figure 6.48 - Hardness profile along a low angle grain boundary on Sample II, showing intermediate coarseness of carbides.
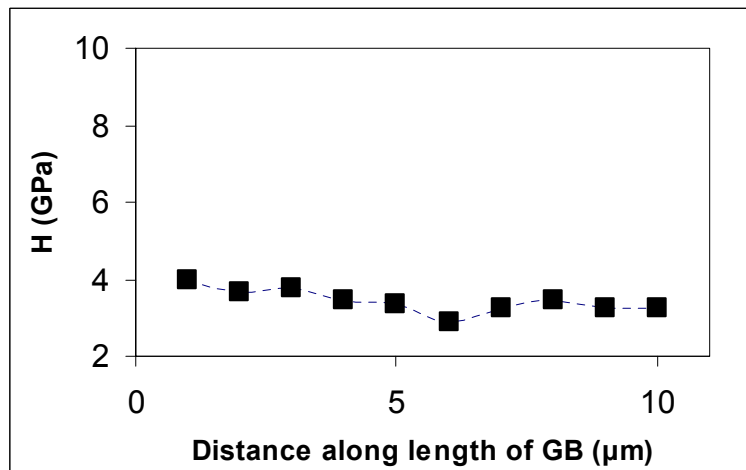
Figure 6.49 - Hardness profile along a high angle grain boundary on Sample II.
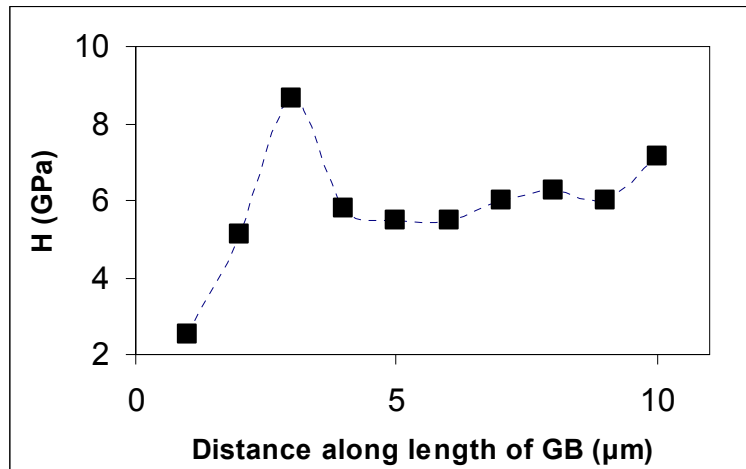
Figure 6.50 – Hardness profile along a Σ3 grain boundary on Sample II, showing a mostly continuous level of carbides. The spike seen in is likely caused by an outlying nanoindentation measurement; the remaining hardness profile shows the approximately constant and continuous hardness profile.
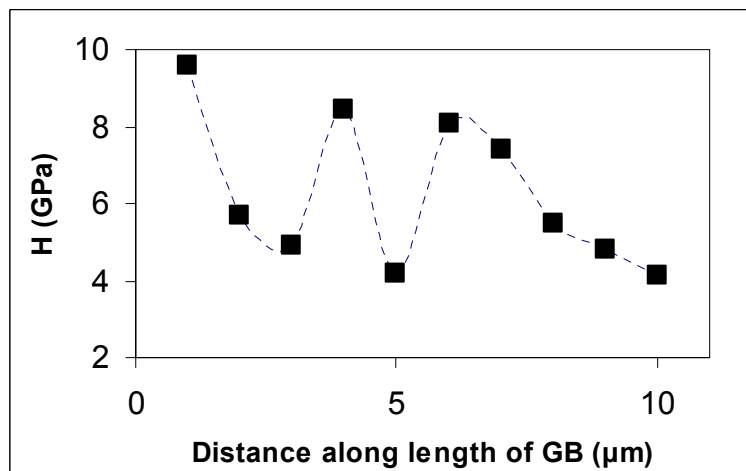
Figure 6.51 - Hardness profile along a high angle grain boundary on Sample II, showing a coarse and discontinuous distribution of carbides.

The presence and varying distribution of chromium carbides at Σ3, low angle and high angle boundaries dominate the difference in hardness between the bulk regions and the regions near the grain boundary. This variation is most significant in the case of the high angle grain boundary.

6.3. Coordinated measurement of structure, mechanical properties and elemental composition

The procedure to characterize and correlate variations between mechanical and structural properties and elemental composition using EBSD, nanoindentation, TEM and STEM was successfully accomplished as described in Chapter 4. Two aspects of the procedure specific to this thesis that were learned over time are reviewed here.

Accounting for the effects of sample processing was the first aspect that became better understood while developing this procedure. TMP resulted in metallurgical changes in the samples. Though, as discussed in Chapter 5.1.3, it was not necessary to complete an accurate analysis in this thesis, electrolytic polishing requirements should be considered when conducting these types of experiments. In this case, had electrolytic polishing been an absolute necessity, a different and more hazardous electrolyte solution would have been required. The overall procedure would be improved by considering this issue ahead of time and allotting for time to determine ideal polishing conditions for different samples.

The sensitivity of nanoindentation measurements to inhomogeneities on the sample surface was the second aspect of this procedure that must be well understood to ensure success. In order to ensure that nanoindentation measurements were not affected by other contributors of this procedure (FIB, EBSD, microindentation), nanoindentation were appropriately spaced far enough away from sites of FIB work and microindentations such that the impact volume of the sample created by the nanoindentation would not be affected. As a result, space along grain boundaries became very limited. Understanding this prior to choosing grain boundaries to examine enabled a smooth accomplishment of the correlated characterization of each sample.

7. Conclusions

This thesis aimed to identify the relationship between the structure of grain boundaries and their mechanical properties in Inconel 690, an important alloy used in the design of nuclear reactor steam generators in the United States. The hardness and elastic modulus in the vicinity of grain boundaries, and their relation to grain size, crystalline orientation, slip systems, and presence of precipitates was considered. Additionally, the correlated measurement of nanoscale mechanical properties of grain boundaries with the analysis of the chemical nature of those same grain boundaries was conducted. An approach for identifying mechanical properties of grain boundaries with known chemical composition and structure was developed.

The following conclusions are made:

- A quantitative assessment of the combined effect of the ease of slip transfer and the attraction or repulsion of dislocations by grain boundaries was conducted. Inherent hardness of the solution annealed Inconel 690 were found to be the same for both the grain boundary and bulk regions, and did not vary with grain boundary type, specifically the $\Sigma 3$ and high angle boundaries. This finding is attributed to the weak dependence of the dislocation mobility on the diffusion path during high temperature annealing of the sample, which resulted in an approximately uniform distribution of dislocations prior to nanoindentation. On the other hand, greater hardness was induced at the grain boundaries due to the pile-up of dislocations created by the indentations towards the grain boundaries. The relative increase in hardness induced by the indentations, and the spatial extent of this increase were found to be equivalent for different grain boundary types. These results indicate comparable ease of dislocation mobility and absorption at the different grain boundaries of Inconel 690 when indented at room temperature.

- Properties of grain boundaries on the TMP sample (Sample II) were dominated by the presence of chromium-carbide precipitates. Chromium-carbides were identified along $\Sigma 3$, low angle and high angle boundaries. Their distributions, in term of continuity and coarseness, was found to depend on grain boundary type using TEM and STEM in a collaborative work. Those findings were consistent with hardness profiles along $\Sigma 3$, low angle and high angle grain boundaries identified using nanoindentation.   These results are consistent with observations of relative stress corrosion cracking susceptibility for these types of boundaries. The results support why $\Sigma 3$ grain boundaries are least susceptible to cracking, while low angle and high angle boundaries are much more susceptible. The coarseness and distribution of chromium carbide precipitates along grain boundaries act as stress concentrators and sites for crack initiation. Precipitate formation also indicates the occurrence of sensitization, which results regions of depleted chromium in the vicinity of the grain boundaries, and increase cracking probability.

Appendix A Minimum indentation depth

Data set	Indent	hc(nm)	Pmax(µN)	S(µN/nm)	A(nm^2)	hmax(nm)	heff(nm)	Er(GPa)	E(GPa)	H(GPa)	A	hf(nm)	m	X(mm)	Y(mm)	Drift Correction
hmin10	1	5.87963	54.91852	3.097506	6091.8	20.52137	19.17707	35.16205	33.22375208	9.015155	2.250271	1.43E-05	1.081621	-141.584507	-96.200505	-1.693638
hmin10	2	21.72358	54.42354	8.427562	15367.63	26.83606	26.56693	60.23283	58.2259088	3.54144	0.000824	3.674963	3.544854	-141.574507	-96.200505	-0.317996
hmin10	3	22.54633	54.75107	13.07573	15879.46	26.35028	25.68675	91.93544	91.54359606	3.447916	0.004336	10.97842	3.512666	-141.564507	-96.200505	0.089584
hmin10	4	24.188	54.79835	13.86172	16915.88	27.75348	27.15291	94.42883	94.24917685	3.239462	0.229529	17.57362	2.423164	-141.554507	-96.200505	0.205879
hmin10	5	22.05953	54.63452	13.23756	15576.03	26.08711	25.15495	93.97546	93.75627689	3.507603	2.753135	18.59753	1.588817	-141.544507	-96.200505	0.224706
hmin10	6	21.26661	54.75419	12.92325	15085.47	24.81741	24.44427	93.2239	92.94011512	3.629598	0.01586	11.11649	3.145663	-141.554507	-96.190505	0.173941
hmin10	7	22.68232	54.65417	13.54871	15964.54	26.39534	25.70775	95.00676	94.87812376	3.423473	0.582729	17.16713	2.117209	-141.574507	-96.191005	0.162097
hmin10	8	24.22017	54.93375	14.5283	16936.4	27.82498	27.05604	98.90974	99.14378855	3.243532	0.740598	19.1707	2.085431	-141.564507	-96.190505	0.183307
hmin10	9	20.75634	54.49991	16.79577	14772.14	23.83117	23.18998	122.4371	125.5460444	3.689371	0.009964	11.73608	3.52986	-141.554507	-96.190505	0.145582
hmin10	10	21.37803	54.60347	14.42175	15154.13	25.15089	24.21767	103.7976	104.5308841	3.603207	0.35903	15.4537	2.314721	-141.544507	-96.190505	0.09006
hmin10	11	20.30808	54.70851	10.69144	14498.38	24.95281	24.14586	78.67042	77.36211194	3.773423	10.69144	19.02882	1	-141.554507	-96.180505	0.050123
hmin10	12	20.38113	54.85445	13.7366	14542.9	23.82471	23.37611	100.9226	101.3561415	3.771907	0.008247	9.871905	3.381709	-141.574507	-96.180505	0.01801
hmin10	13	21.36029	55.14613	15.21413	15143.19	24.70113	24.07879	109.5401	110.9247992	3.641645	0.03816	13.07996	3.034441	-141.564507	-96.180505	0.040034
hmin10	14	22.58967	54.61213	15.84589	15906.56	26.34913	25.17451	111.3174	112.9180832	3.433308	0.05288	14.90535	2.97963	-141.554507	-96.180505	0.005841
hmin10	15	20.97099	54.77084	14.59867	14903.72	24.3745	23.78481	105.95	106.9191283	3.674977	2.378016	17.42386	1.695454	-141.544507	-96.180505	-0.014536
hmin10	16	22.76488	54.70406	11.39036	16016.26	27.08601	26.36688	79.74281	78.49548986	3.415532	0.604387	16.78977	1.994125	-141.554507	-96.170505	-0.039825
hmin10	17	22.7154	54.71398	12.82936	15985.26	26.66189	25.91396	89.9042	89.3489395	3.422777	0.174225	15.46447	2.450201	-141.574507	-96.170505	-0.035419
hmin10	18	20.14766	54.66556	12.32641	14400.74	24.52986	23.47378	91.00787	90.54035342	3.796025	1.865545	16.01771	1.681251	-141.564507	-96.170505	-0.035902
hmin10	19	21.86456	54.89623	13.72139	15454.98	25.39812	24.86514	97.79094	97.91777492	3.552008	0.043547	13.22271	2.908943	-141.554507	-96.170505	0.021609
hmin10	20	21.96981	54.90218	13.50453	15520.3	25.51581	25.01891	96.04268	96.0072147	3.537444	0.125884	14.51287	2.584217	-141.544507	-96.170505	-0.002697
hmin10	21	21.29601	54.66347	12.74891	15103.58	25.24795	24.51178	91.91111	91.51726292	3.61924	0.00311	9.165314	3.579187	-141.584507	-96.160505	-0.026411
hmin10	22	21.49718	54.5326	15.03019	15227.65	24.9483	24.21833	107.9152	109.1084131	3.581157	0.432844	15.9242	2.286016	-141.574507	-96.160505	-0.035263
hmin10	23	22.82127	54.58158	12.91783	16051.62	26.92094	25.99024	90.33685	89.81569275	3.400379	0.861911	17.70216	1.96154	-141.564507	-96.160505	-0.039243
hmin10	24	21.84106	54.87396	10.57879	15440.42	26.65716	25.73144	75.4295	73.95067184	3.553917	9.521582	20.33939	1.039498	-141.554507	-96.160505	-0.044676
hmin10	25	18.82441	54.80508	14.42312	13601.83	22.39183	21.67426	109.5709	110.9592738	4.029244	0.123993	11.63795	2.641267	-141.544507	-96.160505	-0.038763
hmin10	26	20.72846	54.71119	14.93095	14755.07	24.47998	23.47667	108.9059	110.2151864	3.707958	1.841218	16.88593	1.798644	-141.584507	-96.150505	-0.059432
hmin10	27	20.73554	54.71829	10.98825	14759.41	25.33472	24.47033	80.13619	78.91181848	3.70735	7.274732	18.72392	1.153963	-141.574507	-96.150505	-0.0292
hmin10	28	20.46366	54.66556	16.91438	14593.24	23.9667	22.88758	124.0552	127.4065555	3.745951	0.001689	9.826527	4.041295	-141.564007	-96.150505	-0.047377
hmin10	29	20.97098	54.62195	13.4305	14903.71	24.75459	24.02123	97.47195	97.56869778	3.664989	0.049591	12.40523	2.856154	-141.554507	-96.150505	-0.049539
hmin10	30	20.35675	54.5222	12.7162	14528.04	24.05253	23.57247	93.47351	93.21104366	3.752895	2.191791	16.51872	1.645145	-141.544507	-96.150505	-0.039492
hmin20	1	22.3074	80.35828	5.162344	15730.31	33.69483	33.98208	36.4681	34.49834689	5.108499	0.0365	0.000624	2.183023	-130.845006	-101.366005	-1.464372
hmin20	2	31.37431	79.93913	15.22002	21709.96	35.90781	35.31349	91.52098	91.09510478	3.682142	0.017081	19.30673	3.047609	-130.834506	-101.366005	0.025305
hmin20	3	29.37646	79.97948	17.33645	20333.25	33.08913	32.83649	107.7188	108.8892615	3.933433	0.017976	18.3421	3.141823	-130.824506	-101.366005	0.390893
hmin20	4	31.01216	79.90192	19.03482	21457.8	34.80967	34.16041	115.1307	117.2178791	3.723678	0.245812	23.78301	2.472181	-130.814506	-101.366005	0.475591
hmin20	5	28.75728	79.61809	18.16716	19913.61	33.15679	32.04418	114.0635	116.0113839	3.998174	3.72643	25.1132	1.581502	-130.804506	-101.366005	0.461487
hmin20	6	28.10235	79.87718	23.66618	19473.31	31.77135	30.63372	150.2599	158.3778329	4.10188	0.243171	21.7019	2.64634	-130.844506	-101.356005	0.401353
hmin20	7	28.4939	79.59734	23.85879	19736.1	32.18846	30.99604	150.4709	158.6338555	4.033083	0.701767	23.27417	2.314581	-130.834506	-101.356005	0.335827
hmin20	8	29.33341	79.72265	21.67442	20303.96	32.95767	32.09205	134.7696	139.8760064	3.926458	0.742373	23.90913	2.224713	-130.824506	-101.356005	0.261535
hmin20	9	28.35241	79.47274	21.41878	19640.99	31.92666	31.13523	135.4091	140.6286089	4.046269	0.109713	20.71146	2.809321	-130.814506	-101.356005	0.230172
hmin20	10	27.88537	79.30886	19.9091	19328.24	31.34571	30.87303	126.8791	130.667641	4.103263	2.72482	23.93867	1.740751	-130.805006	-101.356005	0.155479
hmin20	11	30.07142	79.43594	22.78556	20808.18	33.28947	32.6861	139.9515	146.0010924	3.817534	0.556125	24.47198	2.356153	-130.844506	-101.346005	0.107353
hmin20	12	28.49674	79.68448	20.21004	19738.02	32.39897	31.45386	127.453	131.3325922	4.037107	0.161526	21.02536	2.644935	-130.834506	-101.346005	0.078382
hmin20	13	24.88521	79.62816	20.47592	17362.34	28.81165	27.80186	137.681	143.3101008	4.586258	0.977183	19.64736	2.096881	-130.824506	-101.346005	0.073823
hmin20	14	28.25115	79.67095	22.65033	19573.02	31.82086	30.88922	143.4433	150.1656315	4.070447	0.119947	20.93996	2.828558	-130.814506	-101.346005	0.035426
hmin20	15	26.99942	79.84331	19.0044	18740	31.07408	30.1504	122.9998	126.1923473	4.260582	2.819466	23.00637	1.700431	-130.804506	-101.346005	0.037488
hmin20	16	28.31824	79.3527	19.82823	19618.05	32.14954	31.31975	125.427	128.9884059	4.044883	0.11383	20.37155	2.735677	-130.844006	-101.336005	0.049105
hmin20	17	26.33668	79.4421	20.27958	18304.23	30.35777	29.27469	132.8061	137.5711656	4.340095	0.312944	19.68191	2.448798	-130.834506	-101.336005	-0.009122
hmin20	18	25.12826	79.87327	20.02488	17518.88	29.01082	28.11979	134.0453	139.0247309	4.559268	2.957404	21.28136	1.71445	-130.824506	-101.336005	-0.004
hmin20	19	26.79031	80.04055	21.53383	18602.11	30.12903	29.57804	139.8863	145.9244522	4.302766	0.01316	16.84752	3.424974	-130.814506	-101.336005	-0.011367
hmin20	20	24.67351	79.4017	22.74584	17226.38	28.30166	27.29163	153.5465	162.3776265	4.60931	0.851996	19.5547	2.216364	-130.805006	-101.336005	-0.045535
hmin20	21	24.43535	80.03946	19.60208	17073.83	28.29843	27.49776	150.9242	162.6978746	4.687843	0.149406	16.71013	2.641947	-130.844506	-101.326005	-0.051074
hmin20	22	27.40474	79.59929	24.42187	19008.31	31.19474	29.84925	156.943	166.5390824	4.187605	0.01988	18.65563	3.434316	-130.834506	-101.326005	0.009793
hmin20	23	27.91079	79.55032	19.92634	19345.21	31.78649	30.90496	126.9333	130.730351	4.112145	0.923514	22.53309	2.097044	-130.824506	-101.326005	0.043196
hmin20	24	26.49382	79.56408	19.88227	18407.23	30.51113	29.49514	129.8394	134.1056238	4.322437	0.387823	20.02063	2.367587	-130.814506	-101.326005	-0.042558
hmin20	25	27.32331	79.63768	24.1333	18954.29	30.56403	29.79824	155.3094	164.5340113	4.201564	0.190954	20.75636	2.740041	-130.805006	-101.326005	-0.057178
hmin20	26	26.16861	79.40786	19.00011	18194.29	29.86482	29.30311	124.8025	128.2677902	4.364438	2.20241	21.84583	1.784322	-130.844506	-101.316005	-0.047921
hmin20	27	28.05406	79.35886	19.73174	19440.99	31.73316	31.07047	125.3837	128.9384796	4.082039	0.002552	15.80553	3.795648	-130.834506	-101.316005	-0.009349
hmin20	28	26.1533	79.58764	20.21561	18184.29	30.5936	29.10601	132.823	137.5910147	4.376724	0.661167	20.39355	2.213003	-130.824506	-101.316005	-0.066156
hmin20	29	28.58199	79.92914	18.87341	19795.41	32.49317	31.75825	118.851	121.4437116	4.037762	0.20322	21.07578	2.522417	-130.814506	-101.316005	-0.006365
hmin20	30	26.84731	79.54081	23.03738	18639.67	30.11455	29.43683	149.5026	157.4599848	4.267287	0.016569	17.59556	3.429582	-130.805006	-101.316005	-0.052938
hmin30	1	26.66194	104.8652	7.628605	18517.65	36.84548	36.97168	49.66919	47.55186253	5.662989	0.006365	0.000285	2.689549	-132.069006	-95.112505	-1.470191
hmin30	2	33.10738	104.7486	16.90835	22932.79	38.16831	37.75369	98.92536	99.16092058	4.567633	0.012276	18.72032	3.072336	-132.058506	-95.112505	-0.069417
hmin30	3	36.36736	104.9695	27.77383	25306.83	39.98282	39.20194	154.6862	163.7708689	4.147871	0.001269	23.61837	4.123249	-132.048506	-95.112505	0.342749
hmin30	4	31.84476	104.34	20.93762	22039.25	36.52129	35.58229	124.9579	128.4470384	4.734282	20.93762	30.59892	1	-132.038006	-95.112505	0.424727
hmin30	5	33.60515	104.5634	22.68367	23289.01	38.24939	37.06237	131.696	136.2720242	4.489816	10.49624	31.11764	1.289632	-132.028506	-95.112505	0.400265
hmin30	6	34.15901	104.5316	25.41251	23688	37.8869	37.24405	146.2912	153.5829241	4.41285	1.524492	29.00002	2.004194	-132.068506	-95.102505	0.35675
hmin30	7	32.50053	104.1951	24.43671	22501.55	36.84592	35.69844	144.3349	151.2334319	4.630575	5.808224	29.14869	1.536102	-132.058506	-95.102505	0.304708
hmin30	8	31.49474	104.4589	22.05769	21794.06	36.05698	35.04653	132.381	137.0733534	4.792999	22.05769	30.31081	1	-132.048506	-95.102505	0.260761
hmin30	9	32.58843	104.3362	24.31749	22563.8	36.72519	35.80636	143.4324	150.1526191	4.624054	2.339529	27.91745	1.838657	-132.038506	-95.102505	0.222315
hmin30	10	36.17191	104.4089	23.7203	25161.75	40.39684	39.47316	132.4905	137.2014845	4.149509	2.269293	31.40254	1.833537	-132.068506	-95.092505	0.159935
hmin30	11	33.26307	104.1871	27.60053	23043.97	37.43408	36.09418	161.0919	171.6612684	4.521229	0.161076	25.67142	2.761129	-132.058506	-95.092505	0.127213
hmin30	12	31.44741	104.4937	21.11357	21760.99	36.16758	35.15925	126.8111	130.5888202	4.801882	14.76702	29.54581	1.134229	-132.058506	-95.092505	0.088759

Data set	Indent	hc(nm)	Pmax(µN)	S(µN/nm)	A(nm^2)	hmax(nm)	heff(nm)	Er(GPa)	E(GPa)	H(GPa)	A	hf(nm)	m	X(mm)	Y(mm)	Drift Correction
hmin30	13	32.79746	104.4629	22.93812	22712.14	36.73072	36.21305	134.8539	139.9752022	4.599429	12.13612	30.5559	1.242206	-132.048506	-95.092505	0.057356
hmin30	14	30.67148	104.9652	25.95723	21221.65	34.47916	33.70431	157.8714	167.6815946	4.946138	2.141911	25.99751	1.905844	-132.038506	-95.092505	0.052109
hmin30	15	33.97365	104.9857	27.29585	23554.16	37.94959	36.85831	157.5787	167.3211739	4.457205	2.18714	29.43213	1.930776	-132.068506	-95.092505	0.011588
hmin30	16	32.15936	104.5159	24.21656	22260.55	36.1177	35.39627	143.8067	150.6006552	4.695118	0.715084	25.85751	2.210151	-132.068506	-95.082505	-0.001408
hmin30	17	31.21115	104.7713	24.87216	21596.21	35.47295	34.37045	149.9545	158.0075524	4.851375	0.286043	23.81739	2.505242	-132.058506	-95.082505	-0.009738
hmin30	18	29.79814	104.6778	27.71736	20620.93	33.70338	32.6306	171.0144	184.088221	5.076289	0.163758	22.2177	2.757204	-132.048506	-95.082505	-0.017503
hmin30	19	31.3364	104.7288	21.12837	21683.5	36.08225	35.05399	127.1265	130.9541817	4.829883	15.1267	29.47477	1.125572	-132.038506	-95.082505	0.016443
hmin30	20	33.60995	104.2224	23.86372	23292.45	37.38366	36.8855	138.5368	144.3233411	4.474513	0.010783	22.03248	3.400882	-132.028506	-95.082505	-0.018237
hmin30	21	33.72854	104.5306	25.67249	23377.66	37.50171	36.78232	148.7655	156.5678977	4.471389	0.489591	27.14362	2.367242	-132.068506	-95.072505	-0.051239
hmin30	22	32.59206	104.9079	25.13406	22566.38	36.67741	35.72251	148.2404	155.9331633	4.648858	0.714292	26.39561	2.234557	-132.058006	-95.072505	-0.046209
hmin30	23	32.3448	104.3432	24.57255	22391.41	36.2362	35.52955	145.4937	152.6240856	4.659968	3.092902	28.08625	1.752877	-132.048506	-95.072505	-0.021284
hmin30	24	32.61313	104.8989	24.55146	22581.31	36.65296	35.81759	144.7564	151.738813	4.645387	2.566237	28.07279	1.812661	-132.038506	-95.072505	0.010719
hmin30	25	33.78885	104.5604	22.19206	23421.04	38.31814	37.32256	128.4782	132.5222333	4.464379	16.92522	32.12005	1.104188	-132.058506	-95.072505	0.003237
hmin30	26	32.33147	104.4833	23.79342	22381.99	36.23691	35.62492	140.9102	147.1422194	4.668184	0.051987	22.60957	2.963917	-132.069006	-95.062505	-0.053973
hmin30	27	33.24148	104.6928	32.81249	23028.54	36.9328	35.63445	191.5759	210.6614577	4.54622	0.01536	24.11214	3.611288	-132.058506	-95.062505	0.005143
hmin30	28	32.75343	105.0345	26.11169	22680.87	36.65568	35.77031	153.6173	162.4640458	4.630973	9.419692	30.15096	1.396978	-132.048506	-95.062505	-0.036902
hmin30	29	31.9144	104.6108	21.39938	22088.16	36.35734	35.58077	127.5723	131.4708227	4.736058	10.50325	29.40759	1.262798	-132.038506	-95.062505	-0.042907
hmin30	30	34.08613	105.1282	23.42659	23635.34	38.37468	37.4518	135.0091	140.1577557	4.447922	11.27882	31.71655	1.278034	-132.028506	-95.062505	-0.049095
hmin40	1	43.20009	129.787	16.48826	30605.68	49.11607	49.1037	83.50427	82.48894456	4.240617	0.006766	24.78042	3.090053	-130.980506	-98.648005	-0.877974
hmin40	2	41.6959	129.4121	22.52432	29400.91	46.80224	46.00498	116.3875	118.642044	4.401636	0.230735	32.16492	2.408878	-130.970006	-98.647505	-0.098184
hmin40	3	37.84303	129.6235	24.55386	26413.79	42.80099	41.8024	133.8564	138.8029969	4.907419	0.08264	27.28381	2.750175	-130.960506	-98.647505	0.104636
hmin40	4	38.58009	129.4326	24.15356	26974.34	43.3965	42.59915	130.2989	134.6409821	4.798359	17.5649	36.61627	1.116471	-130.951006	-98.647505	0.150825
hmin40	5	32.67007	129.8788	28.32089	22621.69	37.20014	36.10955	166.832	178.8194575	5.741338	4.530269	28.51755	1.655483	-130.940506	-98.647505	0.161315
hmin40	6	39.55953	129.9498	27.60638	27727.16	43.87149	43.08996	146.8898	154.3037643	4.686733	16.78404	37.49477	1.188635	-130.980506	-98.637505	0.137106
hmin40	7	36.34161	129.4826	30.69183	25287.7	40.36908	39.5057	171.0027	184.0734659	5.120378	0.476717	29.31914	2.414567	-130.970006	-98.637505	0.10242
hmin40	8	37.36252	129.6641	29.26619	26051.11	41.58187	40.6854	160.6527	171.1169665	4.977298	1.316399	31.5104	2.07087	-130.960506	-98.637505	0.10934
hmin40	9	36.29629	129.311	23.59765	25254.04	41.31325	40.40616	131.5643	136.1181164	5.120408	23.59765	34.92633	1	-130.950506	-98.637505	0.076328
hmin40	10	36.99246	130.0133	23.49789	25773.26	42.02233	41.14219	129.6818	133.9220445	5.044504	15.47457	34.77853	1.150132	-130.940506	-98.637505	0.038412
hmin40	11	38.51851	129.8334	30.99766	26927.3	42.48527	41.65988	167.366	179.2658489	4.821628	0.83361	32.23463	2.250272	-130.981006	-98.627505	0.009336
hmin40	12	37.22079	129.4613	28.34164	25944.55	41.53303	40.64671	155.8966	165.2539821	4.989925	1.793024	31.71775	1.954725	-130.970006	-98.627505	0.02225
hmin40	13	37.69168	129.3664	25.8609	26299.32	42.24261	41.44348	141.2883	147.5925737	4.919002	5.972007	33.85297	1.517375	-130.960506	-98.627505	0.017063
hmin40	14	37.93141	130.0692	25.54357	26480.74	42.62086	41.75045	139.0758	144.962256	4.911844	4.243993	33.49447	1.621347	-130.950506	-98.627505	-0.002442
hmin40	15	40.31192	129.8082	27.16565	28311.64	44.93534	43.89572	143.0449	149.6890741	4.584977	1.277661	34.18305	2.032622	-130.940506	-98.627505	-0.015398
hmin40	16	38.28406	129.4303	30.8617	26748.59	42.5151	41.42947	167.1877	179.2658489	4.838773	3.240618	33.8128	1.816139	-130.981006	-98.617505	-0.036069
hmin40	17	38.47956	129.6591	31.26252	26897.58	42.43832	41.59013	168.8893	181.4055653	4.820475	1.487326	32.98212	2.075506	-130.970506	-98.617505	-0.01997
hmin40	18	40.79498	129.5711	29.71875	28689.75	45.03787	44.06491	155.454	164.7112173	4.516285	1.15077	34.80947	2.122853	-130.960506	-98.617505	-0.024973
hmin40	19	39.24889	129.5167	28.43199	27487.4	43.40542	42.66538	151.9411	160.4205096	4.711857	9.888915	36.32226	1.392464	-130.950506	-98.617505	-0.015313
hmin40	20	39.26031	129.9898	28.08851	27496.2	43.58151	42.73121	150.0815	158.1614718	4.727554	4.290879	35.00884	1.66867	-130.940006	-98.617505	-0.030887
hmin40	21	38.24286	130.1338	33.65894	26717.23	42.11239	41.24585	182.4482	198.7251307	4.870783	0.51418	31.64022	2.457764	-130.981006	-98.607505	-0.061026
hmin40	22	37.96798	129.9887	25.84489	26508.46	42.32672	41.74016	140.6427	146.8239171	4.903669	25.84489	36.71059	1	-130.970006	-98.607505	-0.026772
hmin40	23	38.96188	130.0025	27.65237	27266.7	43.72825	42.48786	148.3716	156.0917327	4.767814	17.96002	37.01388	1.164352	-130.960506	-98.607505	-0.01881
hmin40	24	39.22277	129.524	23.5652	27467.29	43.98708	43.34508	125.9782	129.6261415	4.715572	23.5652	37.84867	1	-130.950506	-98.607505	-0.044022
hmin40	25	39.22334	129.4804	25.7739	27467.73	43.73216	42.99112	137.7855	143.4337459	4.713911	11.27871	36.45835	1.30039	-130.940506	-98.607505	-0.039361
hmin40	26	41.8125	129.3509	24.72821	29493.52	46.42203	45.73568	127.5746	131.4735106	4.385739	16.60098	39.73968	1.146265	-130.980506	-98.597505	-0.008305
hmin40	27	39.42153	129.7878	32.27851	27620.53	43.18285	42.43718	172.0808	185.4388493	4.698961	1.759026	34.22416	2.042597	-130.971006	-98.597505	0.026664
hmin40	28	39.95678	129.5742	25.11273	28035.08	44.48497	43.82656	132.8856	137.6642816	4.621859	4.285836	35.5188	1.610124	-130.960506	-98.597505	-0.007098
hmin40	29	39.40566	129.3859	27.22785	27608.28	44.00481	42.96964	145.1873	152.2560011	4.68649	6.974087	35.88251	1.491409	-130.950506	-98.597505	0.007665
hmin40	30	39.52154	129.4393	31.47856	27697.78	43.76734	42.60553	167.5819	179.7609349	4.673273	0.25494	31.82971	2.620589	-130.940006	-98.597505	-0.034909
hmin50	1	54.90793	150.5987	17.4964	38361.45	61.05785	61.36349	79.14727	#DIV/0!	3.925783	0.00305	33.42823	3.245488	-134.472006	-3.5665	-1.44293
hmin50	2	59.49325	164.6338	30.73235	42509.01	64.11038	63.51102	132.0657	#DIV/0!	3.872917	1.627754	52.99868	1.962348	-134.462006	-3.5665	-0.114586
hmin50	3	57.90182	168.7695	34.05589	41047.15	62.1264	61.61657	148.9311	#DIV/0!	4.111603	0.114514	47.83676	2.781021	-134.451506	-3.5665	0.234769
hmin50	4	53.78906	170.4849	28.89875	37379.27	58.89807	58.2136	132.4337	#DIV/0!	4.560948	20.50453	51.59966	1.121122	-134.442006	-3.5665	0.326967
hmin50	5	55.82156	169.5427	36.35167	39172.13	60.11448	59.31953	162.7311	#DIV/0!	4.328145	2.274503	50.2156	1.951976	-134.431506	-3.5665	0.324701
hmin50	6	53.01471	169.8529	30.15032	36706.34	57.90653	57.23986	139.43	#DIV/0!	4.627345	20.32574	50.81189	1.141018	-134.442006	-3.5565	0.267882
hmin50	7	55.27142	169.3187	30.47601	38683.04	60.52281	59.43827	137.288	#DIV/0!	4.377079	30.38438	53.8763	1.001109	-134.462006	-3.5565	0.242894
hmin50	8	55.61974	168.8776	32.33278	38992.37	60.37107	59.53074	145.0735	#DIV/0!	4.331041	14.33199	52.78902	1.291961	-134.452506	-3.5565	0.246648
hmin50	9	55.64627	168.3291	32.08868	39015.98	60.67991	59.58058	143.9346	#DIV/0!	4.314362	17.06924	53.13675	1.228391	-134.442006	-3.5565	0.182511
hmin50	10	55.50916	167.8417	29.60693	38894.06	60.48267	59.76092	133.0107	#DIV/0!	4.315357	29.60693	54.09191	1	-134.431506	-3.5565	0.115737
hmin50	11	54.46575	167.0922	28.27472	37971.89	59.73349	58.89795	128.5589	#DIV/0!	4.400418	28.26955	52.98796	1.000066	-134.472006	-3.5465	0.070837
hmin50	12	56.24761	167.065	37.2036	39552.84	60.79328	59.61553	165.7414	#DIV/0!	4.223844	5.36891	52.00776	1.694169	-134.462006	-3.5465	0.06889
hmin50	13	54.53571	166.3542	36.90427	38033.4	59.3712	57.9165	167.6598	#DIV/0!	4.373897	9.122746	51.09854	1.512507	-134.452506	-3.5465	0.000477
hmin50	14	53.69633	166.8497	29.40119	37298.39	59.00225	57.95253	134.8822	#DIV/0!	4.473375	27.84127	52.16493	1.019853	-134.442006	-3.5465	-0.010357
hmin50	15	53.37002	166.6327	33.36389	37014.42	57.99417	57.11582	153.6477	#DIV/0!	4.50183	14.65254	50.62433	1.299753	-134.431506	-3.5465	-0.010318
hmin50	16	54.71566	166.0217	34.23656	38191.84	59.25096	58.3526	155.2172	#DIV/0!	4.347047	6.460432	50.64428	1.589591	-134.472006	-3.5365	-0.046217
hmin50	17	55.88744	165.2195	30.03796	39230.89	61.15375	60.01271	134.3666	#DIV/0!	4.211466	22.72088	53.95474	1.101376	-134.462006	-3.5365	-0.045937
hmin50	18	57.54995	165.9192	34.05674	40727.14	61.71373	61.20384	149.5189	#DIV/0!	4.073923	19.51722	55.32023	1.207674	-134.452506	-3.5365	0.011861
hmin50	19	52.88531	166.6194	34.48386	36594.44	57.43563	56.50916	159.7141	#DIV/0!	4.553135	0.028176	41.148	3.179175	-134.442006	-3.5365	-0.028493
hmin50	20	55.22439	166.8736	35.21202	38641.37	60.0755	58.77872	158.7083	#DIV/0!	4.318521	1.380928	48.87009	2.090633	-134.431506	-3.5365	-0.033516
hmin50	21	54.47823	165.9903	31.14905	37982.86	59.40274	58.47491	141.6074	#DIV/0!	4.370138	1.326954	47.66472	2.028593	-134.472006	-3.5265	-0.020537
hmin50	22	54.48459	166.1087	31.80751	37988.45	59.02827	58.40132	144.5901	#DIV/0!	4.372611	12.97257	51.50529	1.320495	-134.462006	-3.5265	-0.049421
hmin50	23	55.42347	165.8376	30.23779	38817.64	60.59661	59.53681	135.978	#DIV/0!	4.272191	30.23779	54.05236	1	-134.452506	-3.5265	-0.063537
hmin50	24	52.62726	166.5482	32.36205	36371.74	57.56189	56.48707	150.3449	#DIV/0!	4.579055	10.41499	49.26937	1.402473	-134.442006	-3.5265	-0.063324

Data set	Indent	hc(nm)	Pmax(µN)	S(µN/nm)	A(nm^2)	hmax(nm)	heff(nm)	Er(GPa)	E(GPa)	H(GPa)	A	hf(nm)	m	X(mm)	Y(mm)	Drift Correction
hmin50	25	56.10021	167.2022	37.1044	39420.94	60.46531	59.47991	165.5758	#DIV/0!	4.241456	4.806979	51.68935	1.728829	-134.432006	-3.5265	0.045351
hmin50	26	55.54239	166.0685	34.4623	38923.59	60.22766	59.15653	154.7649	#DIV/0!	4.266526	13.25212	52.65079	1.350063	-134.472006	-3.5165	-0.031358
hmin50	27	57.49436	166.3227	36.3601	40676.69	61.83507	60.9251	159.7302	#DIV/0!	4.088895	5.770576	53.33796	1.658639	-134.462006	-3.5165	-0.047293
hmin50	28	56.9048	165.8935	30.56025	40143.43	61.74153	60.97611	135.1402	#DIV/0!	4.13252	30.52449	55.54534	1.000435	-134.452006	-3.5165	-0.059218
hmin50	29	55.01247	166.177	30.7627	38453.82	59.70435	59.0639	138.9919	#DIV/0!	4.321469	30.76026	53.66184	1.00003	-134.442006	-3.5165	-0.0622
hmin75	1	71.44288	206.439	33.41494	54068.24	77.03061	76.07641	127.3223	#DIV/0!	3.81812	12.77429	67.89673	1.323991	-134.462006	-6.435	-0.22575
hmin75	2	68.44613	209.9795	38.06456	51042.81	73.46282	72.58343	149.2754	#DIV/0!	4.113793	5.136988	63.36723	1.670691	-134.452006	-6.435	0.103845
hmin75	3	68.18637	211.4144	41.0494	50784.48	73.01657	72.04906	161.3898	#DIV/0!	4.162973	21.47899	65.68516	1.23565	-134.442006	-6.435	0.225159
hmin75	4	69.02482	211.5604	37.04288	51620.55	74.47234	73.30824	144.4536	#DIV/0!	4.098376	4.967969	63.79643	1.665457	-134.432006	-6.435	0.262117
hmin75	5	68.12111	211.6374	43.61139	50719.67	73.05352	71.76071	171.572	#DIV/0!	4.172688	2.888384	62.42987	1.922773	-134.472006	-6.425	0.240755
hmin75	6	69.16106	211.6449	37.11197	51757.02	73.98341	73.43822	144.5321	#DIV/0!	4.089201	9.250393	65.04646	1.471497	-134.432006	-6.425	0.189166
hmin75	7	68.45702	210.2298	48.97822	51053.65	72.90364	71.67625	192.0545	#DIV/0!	4.117821	0.343998	60.33648	2.64188	-134.452006	-6.425	0.128869
hmin75	8	67.91535	210.0047	35.23824	50515.62	73.21909	72.38503	138.9108	#DIV/0!	4.157222	35.23824	66.42546	1	-134.442006	-6.425	0.085733
hmin75	9	68.12671	209.8482	45.26217	50725.23	72.5461	71.60392	178.0567	#DIV/0!	4.136959	6.462386	63.76666	1.690419	-134.452006	-6.425	0.057379
hmin75	10	68.2405	209.6488	35.28081	50838.26	73.96005	72.69722	138.6366	#DIV/0!	4.123838	30.23769	66.42863	1.054912	-134.472006	-6.415	0.008532
hmin75	11	69.85015	209.021	42.09803	52449.9	74.49205	73.57398	162.8637	#DIV/0!	3.985156	8.151515	65.74591	1.576618	-134.432006	-6.415	0.008527
hmin75	12	68.81229	209.9327	43.63388	51408	73.3807	72.42071	170.5074	#DIV/0!	4.083658	4.745853	63.90744	1.769457	-134.452006	-6.415	0.067328
hmin75	13	67.59797	209.8181	34.67073	50201.63	73.28278	72.13677	137.1005	#DIV/0!	4.179507	34.617	66.08168	1.000554	-134.442006	-6.415	0.011561
hmin75	14	67.82814	209.1795	41.39728	50429.25	72.37402	71.61787	163.3298	#DIV/0!	4.14798	4.57973	62.76362	1.752284	-134.432006	-6.415	-0.013027
hmin75	15	69.89976	208.3933	39.95779	52499.95	74.6805	73.81126	154.5101	#DIV/0!	3.9694	6.935719	65.45307	1.602617	-134.472006	-6.405	-0.035493
hmin75	16	67.49987	208.834	39.72651	50104.77	72.09605	71.44246	157.2446	#DIV/0!	4.167947	12.41699	64.03373	1.409363	-134.462006	-6.405	-0.006997
hmin75	17	69.53829	208.3831	42.7931	52135.78	74.17996	73.19045	166.0507	#DIV/0!	3.996931	4.440164	64.51561	1.781447	-134.452006	-6.405	-0.038934
hmin75	18	65.59311	208.9078	33.02883	48239.71	71.33191	70.33687	133.2372	#DIV/0!	4.330619	23.46224	63.26629	1.117876	-134.442006	-6.405	-0.04114
hmin75	19	69.98804	209.0594	35.86585	52589.07	74.88719	74.35973	138.5697	#DIV/0!	3.975339	19.61873	67.30189	1.210831	-134.472006	-6.405	-0.009136
hmin75	20	68.52616	208.611	41.2811	51122.52	73.01505	72.31623	161.7633	#DIV/0!	4.080608	6.162739	63.94157	1.657224	-134.472006	-6.395	-0.05615
hmin75	21	70.02049	208.4675	39.08629	52621.86	74.7443	74.02063	150.965	#DIV/0!	3.961614	30.94958	68.68013	1.00131	-134.462006	-6.395	0.020933
hmin75	22	67.24083	208.8052	36.78931	49849.42	72.2327	71.49761	145.9911	#DIV/0!	4.188719	24.59024	65.00669	1.143632	-134.452006	-6.395	-0.021853
hmin75	23	65.77607	208.5913	36.50154	48417.22	70.77019	70.06201	146.9759	#DIV/0!	4.308205	24.528	63.53915	1.141441	-134.442006	-6.395	-0.06289
hmin75	24	68.24713	208.8075	40.7626	50844.84	73.17451	72.08902	160.1671	#DIV/0!	4.106759	14.56781	65.08296	1.367697	-134.432006	-6.395	-0.006733
hmin75	25	69.07784	208.7819	40.8667	51673.63	73.84984	72.90947	159.2832	#DIV/0!	4.040395	4.129436	63.82585	1.778018	-134.472006	-6.385	0.002137
hmin75	26	71.52308	208.7243	44.26453	54150.36	75.7236	75.05962	168.535	#DIV/0!	3.854533	6.178404	67.07183	1.693985	-134.462006	-6.385	-0.019188
hmin75	27	69.15374	208.8793	40.54155	51749.68	73.64239	73.01791	157.8997	#DIV/0!	4.03634	7.684915	64.89492	1.576598	-134.452006	-6.385	-0.061575
hmin75	28	67.62007	208.1005	40.5086	50223.47	72.30887	71.47297	160.1507	#DIV/0!	4.143492	5.645907	62.86498	1.67562	-134.442006	-6.385	-0.074607
hmin75	29	68.87618	208.2029	38.00739	51471.86	74.08346	72.98465	148.4287	#DIV/0!	4.044985	12.37826	65.3688	1.390271	-134.432006	-6.385	-0.099219
hmin100	1	84.39924	253.223	38.57594	68071.77	89.97879	89.32244	130.999	#DIV/0!	3.719941	2.22253	76.96042	1.883229	-144.023507	-6.0255	0.25523
hmin100	2	85.03842	258.1585	42.27307	68775.35	90.56454	89.61861	142.8178	#DIV/0!	3.753649	10.91674	80.76195	1.450266	-144.013507	-6.0255	0.676964
hmin100	3	86.09828	259.0363	40.05113	69950.7	92.00072	90.94901	134.1694	#DIV/0!	3.703127	20.16767	82.98943	1.230677	-144.003507	-6.0255	0.746496
hmin100	4	77.88348	259.6394	40.95422	61124.61	83.68306	82.63829	146.766	#DIV/0!	4.247707	4.550482	71.85628	1.700701	-144.023507	-6.0255	0.689949
hmin100	5	78.08353	258.8866	36.52954	61331.81	83.80856	83.39881	130.6881	#DIV/0!	4.221083	36.52954	76.31176	1	-144.033507	-6.015	0.580622
hmin100	6	81.96806	257.0665	42.94275	65431.71	87.43275	86.45775	148.7409	#DIV/0!	3.928775	25.29503	79.36997	1.184007	-144.023507	-6.015	0.492705
hmin100	7	80.39776	255.7438	50.71895	63756.83	85.62098	84.17954	177.9679	#DIV/0!	4.011237	0.108624	69.57785	2.8958	-144.013507	-6.015	0.370381
hmin100	8	82.17333	255.3029	46.84695	65652.41	87.33486	86.26062	161.991	#DIV/0!	3.888705	3.015248	75.90995	1.899303	-144.003507	-6.015	0.336221
hmin100	9	78.73103	255.4421	44.68608	62005.1	83.91796	83.0183	158.9986	#DIV/0!	4.119695	2.834179	72.20893	1.89005	-143.993507	-6.015	0.274071
hmin100	10	83.02597	253.9176	43.72175	66573.49	88.10757	87.38165	150.1349	#DIV/0!	3.814094	15.47511	79.50772	1.355803	-144.033507	-6.005	0.190395
hmin100	11	82.82545	252.3527	41.46442	66356.25	88.4032	87.38996	142.6164	#DIV/0!	3.802998	24.80812	80.22224	1.177738	-144.023507	-6.005	0.124835
hmin100	12	87.07335	252.9101	52.17915	71041.6	91.37364	90.70856	173.4504	#DIV/0!	3.560027	0.07431	76.03385	3.027613	-144.013507	-6.005	0.143698
hmin100	13	84.18938	253.248	43.50578	67841.63	89.60053	88.55515	147.9904	#DIV/0!	3.732928	11.57808	80.12889	1.447557	-144.003507	-6.005	0.163898
hmin100	14	78.32329	253.8505	43.90741	61580.65	83.91232	82.65942	156.7655	#DIV/0!	4.122244	14.41729	74.67643	1.380783	-143.993507	-6.005	0.03642
hmin100	15	77.2084	253.0377	43.75999	60428.23	82.24411	81.5452	157.7219	#DIV/0!	4.187409	7.227368	72.30063	1.598743	-144.033507	-5.995	-0.019928
hmin100	16	78.01933	252.2202	49.15841	61265.27	83.05637	81.8674	175.9647	#DIV/0!	4.116855	0.121287	67.2523	2.848523	-144.023507	-5.995	-0.015861
hmin100	17	78.60274	252.6246	50.35644	61871.38	83.02804	82.36528	179.368	#DIV/0!	4.083061	0.339719	69.41469	2.581482	-144.013507	-5.995	-0.032527
hmin100	18	80.86563	251.6293	44.00497	64253.37	86.0723	85.15428	153.8114	#DIV/0!	3.916204	9.943074	76.56354	1.50235	-143.993507	-5.995	-0.042657
hmin100	19	76.17374	252.1577	41.66146	59369.45	81.71172	80.71315	151.4913	#DIV/0!	4.247264	19.70168	73.10782	1.25655	-143.993507	-5.995	-0.062969
hmin100	20	81.83927	252.2865	44.05663	65293.44	86.77118	86.13408	152.7606	#DIV/0!	3.863888	10.04916	77.54946	1.499125	-144.033507	-5.985	-0.072375
hmin100	21	79.86602	251.7144	42.38815	63195.06	84.94343	84.31976	149.3956	#DIV/0!	3.983134	15.95185	76.40217	1.333304	-144.023507	-5.985	-0.051375
hmin100	22	82.71727	251.8054	47.93416	66239.21	87.59193	86.65713	165.0146	#DIV/0!	3.801456	4.006128	77.04503	1.829779	-144.013507	-5.985	-0.052332
hmin100	23	82.62285	251.6224	38.54096	66137.14	88.12956	87.51938	132.7806	#DIV/0!	3.804555	22.77288	79.83027	1.17774	-144.003507	-5.985	-0.052368
hmin100	24	79.12496	251.9395	50.13031	62416.71	83.93905	82.89423	177.7808	#DIV/0!	4.036411	0.360058	70.01294	2.563088	-143.993507	-5.985	-0.066449
hmin100	25	83.75225	251.6342	42.04754	67363.61	88.87596	88.24063	143.5366	#DIV/0!	3.735461	19.83747	80.71037	1.258292	-144.033507	-5.975	-0.059601
hmin100	26	77.83621	251.6926	48.05392	61075.7	82.86249	81.76449	172.2778	#DIV/0!	4.120994	0.586492	69.21393	2.396192	-144.023507	-5.975	-0.04745
hmin100	27	79.61859	251.6773	47.4184	62934.59	84.62728	82.36528	167.47	#DIV/0!	3.99903	1.24328	72.0707	2.172093	-144.013507	-5.975	-0.062719
hmin100	28	79.70732	251.6487	43.41859	63027.93	85.04125	84.05423	153.2301	#DIV/0!	3.992654	14.01305	76.02073	1.386071	-144.003507	-5.975	-0.049266
hmin100	29	76.31637	252.9379	39.08185	59514.8	81.96969	81.17038	141.9376	#DIV/0!	4.25	39.08185	74.69837	1	-143.993507	-5.975	-0.03466

Appendix B Minimum indentation lateral separation

Data set	Indent	hc(nm)	Pmax(µN)	S(µN/nm)	A(nm^2)	hmax(nm)	heff(nm)	Er(GPa)	H(GPa)	A	hf(nm)	m	X(mm)	Y(mm)	Drift Correc
2h$_c$	1	95.90168	255.1813	45.73079	93794.02	100.9981	100.0867	132.2988	2.720656	45.73079	94.50666	1	-140.548	-98.34401	-0.143143
2h$_c$	2	95.8124	281.3445	50.25042	93681.8	100.7179	100.0115	145.4611	3.003193	11.754	91.64309	1.494673	-140.5475	-98.34401	-0.135768
2h$_c$	3	95.04355	291.8843	45.39636	92717.31	100.7624	99.86582	132.0917	3.14811	43.80093	93.3559	1.012478	-140.547	-98.34401	-0.124356
2h$_c$	4	94.04499	477.7914	56.26362	91469.78	101.4359	100.414	164.8252	5.223489	56.23153	91.92044	1.000182	-140.5475	-98.34401	-0.057505
2h$_c$	5	95.05857	294.0184	43.38709	92736.11	101.2096	100.141	126.2324	3.170484	43.38709	93.36441	1	-140.5465	-98.34401	-0.118642
2h$_c$	6	94.51819	462.341	60.96391	92060.24	101.0509	100.2061	178.0211	5.022157	29.9014	90.89727	1.227452	-140.5465	-98.34401	-0.02558
2h$_c$	7	96.86239	291.0739	51.00156	95004.53	102.0963	101.1428	146.6041	3.06379	2.560771	89.95585	1.960154	-140.546	-98.34401	-0.139997
2h$_c$	8	94.77272	412.807	51.4827	92378.37	101.6046	100.7865	150.0759	4.468655	39.08549	92.06114	1.08817	-140.546	-98.34401	-0.161494
2h$_c$	9	95.08955	627.8472	65.53187	92774.91	103.015	102.2751	190.6216	6.767424	65.53187	92.69436	1	-140.546	-98.34401	-0.065334
2h$_c$	10	95.93744	264.4424	45.85948	93838.98	101.0281	100.2622	132.6393	2.818044	31.44874	93.72346	1.133947	-140.5455	-98.34401	-0.081201
2h$_c$	11	95.64067	428.6125	60.01406	93466.07	101.7068	100.9971	173.9245	4.585755	37.44196	92.74678	1.155201	-140.5455	-98.34401	-0.135364
2h$_c$	12	95.30146	289.4027	44.59906	93040.46	100.9193	100.1682	129.5462	3.110504	40.34604	93.45398	1.034711	-140.545	-98.34401	-0.044111
2h$_c$	13	94.9328	607.157	62.95715	92578.65	103.6653	102.1658	183.3262	6.558283	38.79524	91.12201	1.145147	-140.545	-98.34401	-0.096206
2h$_c$	14	92.26155	908.2709	77.88162	89256.14	102.4499	101.0082	230.9674	10.17601	33.29171	86.56735	1.238262	-140.545	-98.34401	-0.093948
2h$_c$	15	96.10444	261.7529	40.13654	94049.05	102.2308	100.9956	115.9571	2.783153	38.06793	94.3544	1.018346	-140.5445	-98.34401	-0.151125
2h$_c$	16	94.07866	442.0934	57.74465	91511.75	100.9433	99.82067	169.1251	4.831001	24.61548	90.09866	1.269854	-140.5445	-98.34401	-0.097457
2h$_c$	17	95.0178	287.7499	48.06656	92685.05	100.219	99.50766	139.8856	3.104598	30.17897	92.54917	1.162366	-140.544	-98.34401	-0.128717
2h$_c$	18	93.66541	413.7437	52.06857	90997.08	100.6253	99.62501	152.9314	4.54678	52.06857	91.67888	1	-140.544	-98.34401	-0.172938
2h$_c$	19	95.51022	758.8613	71.92204	93302.31	104.2584	103.4236	208.6175	8.133361	31.2547	90.33666	1.24033	-140.544	-98.34401	-0.131563
2h$_c$	20	96.49467	252.0208	49.56719	94540.57	100.9706	100.308	142.8302	2.665742	4.380837	91.05002	1.820849	-140.5435	-98.34401	-0.037738
2h$_c$	21	93.97219	508.2168	60.21553	91379.06	101.2494	100.3022	176.49	5.561634	60.21553	91.8622	1	-140.5435	-98.34401	-0.078659
2h$_c$	22	95.12953	293.8045	42.3389	92824.99	101.0701	100.334	123.1238	3.165145	41.18164	93.32932	1.00942	-140.543	-98.34401	-0.168407
2h$_c$	23	94.14206	439.166	53.25954	91590.79	101.1684	100.3264	155.9216	4.794871	53.25954	92.08062	1	-140.543	-98.34401	-0.194953
2h$_c$	24	93.2577	680.709	72.52483	90490.3	101.538	100.2971	213.6095	7.522453	28.57119	88.31397	1.27672	-140.543	-98.34401	-0.119668
2h$_c$	25	95.84406	281.2608	43.75888	93721.59	101.201	100.6647	126.643	3.001025	43.75888	94.23718	1	-140.5425	-98.34401	-0.069398
2h$_c$	26	95.40803	538.2112	59.79823	93174.1	103.1644	102.1584	173.5704	5.776403	54.50071	92.89795	1.028884	-140.5425	-98.34401	-0.102805
2h$_c$	27	95.98476	265.1699	49.45094	93898.49	100.8111	100.0065	142.9816	2.824006	18.68603	92.80292	1.343375	-140.542	-98.34401	-0.110116
2h$_c$	28	95.15183	446.2702	56.22231	92852.93	102.1675	101.105	163.4729	4.806206	30.02542	91.59416	1.198205	-140.542	-98.34401	-0.225874
2h$_c$	29	94.45099	673.3903	70.4639	91976.31	102.7342	101.6184	205.856	7.321346	28.88261	89.53943	1.263949	-140.542	-98.34401	-0.145276
2h$_c$	30	95.50063	271.8029	49.17848	93290.28	100.4448	99.64578	142.6566	2.913518	6.662695	90.42094	1.669091	-140.5415	-98.34401	-0.115267
4h$_c$	1	96.33801	264.5278	49.02933	94343.13	101.4639	100.3845	141.4281	2.80389	49.02933	94.98918	1	-140.5505	-98.24501	-0.128318
4h$_c$	2	95.96311	273.5307	42.40608	93871.27	101.4832	100.8008	122.63	2.913892	42.40608	94.35055	1	-140.55	-98.24501	-0.070881
4h$_c$	3	95.04576	290.5269	49.06217	92720.06	100.0024	99.48696	142.7561	3.133377	22.62908	91.986	1.26671	-140.5495	-98.24501	-0.082348
4h$_c$	4	96.81867	290.9426	48.18189	94949.34	102.1743	101.3475	138.5392	3.064188	48.18189	95.30907	1	-140.549	-98.24551	-0.076133
4h$_c$	5	95.46259	284.4313	47.77747	93242.55	100.729	99.92753	138.628	3.050446	36.86706	93.42864	1.091654	-140.5485	-98.24551	-0.078167
4h$_c$	6	99.1303	493.4365	62.17613	97883.47	105.9431	105.0824	176.0775	5.04106	21.14657	94.49041	1.334656	-140.5485	-98.24551	-0.081602
4h$_c$	7	95.89875	297.2889	52.73306	93790.34	100.8891	100.127	152.5593	3.169718	11.81245	91.62892	1.507382	-140.548	-98.24551	-0.112553
4h$_c$	8	96.1816	303.3203	42.90389	94146.17	102.4965	101.4839	123.8883	3.221801	22.83951	92.95402	1.206533	-140.5475	-98.24551	-0.081319
4h$_c$	9	95.6614	261.4741	48.57328	93492.1	100.8038	99.69871	140.7488	2.796751	22.87316	92.87127	1.268315	-140.547	-98.24551	-0.117025
4h$_c$	10	95.98073	273.8131	48.265	93893.42	100.9741	100.2356	139.5563	2.916211	25.97022	93.3262	1.218397	-140.5465	-98.24551	-0.103993
4h$_c$	11	95.24526	551.2669	70.88128	92970	102.0918	101.0783	205.9657	5.929514	15.88361	89.72416	1.459896	-140.5465	-98.24551	-0.066018
4h$_c$	12	97.18398	270.3119	54.17801	95410.94	101.9254	100.926	155.4028	2.833133	2.639891	90.9051	2.008461	-140.546	-98.24551	-0.096605
4h$_c$	13	95.61041	269.3627	54.2237	93428.08	101.6286	99.33613	157.1757	2.883102	14.83165	92.0726	1.462175	-140.5455	-98.24551	-0.117192
4h$_c$	14	94.91929	271.2587	41.54407	92561.74	100.471	99.81635	120.984	2.930571	36.59122	93.0009	1.043806	-140.5455	-98.24551	-0.118156
4h$_c$	15	96.19853	280.773	51.90938	94167.49	100.7281	100.2552	149.8753	2.981634	12.98894	92.25896	1.478349	-140.545	-98.24551	-0.113443
4h$_c$	16	96.19744	529.4199	64.68021	94166.11	103.6274	102.3363	186.7493	5.622192	33.18205	92.44392	1.208575	-140.545	-98.24551	-0.108593
4h$_c$	17	96.33505	271.4459	46.91171	94339.4	101.546	100.6748	135.3223	2.877333	30.03255	93.97673	1.157568	-140.544	-98.24551	-0.09368
4h$_c$	18	95.9626	270.4377	49.24065	93870.62	100.8562	100.0817	142.3947	2.880962	22.97113	93.10848	1.269671	-140.5435	-98.24551	-0.120611
4h$_c$	19	95.71419	256.4629	39.79845	93558.41	101.6035	100.5472	115.2815	2.741206	39.79845	94.10318	1	-140.543	-98.24551	-0.11059
4h$_c$	20	97.05464	270.4011	50.43145	95247.41	102.0025	101.076	144.7804	2.838934	18.96858	93.86471	1.344941	-140.5425	-98.24551	-0.121024
4h$_c$	21	95.74028	543.7545	67.72692	93591.18	103.1015	101.7618	196.1456	5.80989	20.25678	90.75075	1.371468	-140.5425	-98.24551	-0.104699
4h$_c$	22	95.54288	264.5734	45.95621	93343.3	100.8606	99.86068	133.2716	2.834413	32.87122	93.41655	1.119341	-140.542	-98.24551	-0.096658
4h$_c$	23	96.2494	287.0398	44.76794	94231.53	101.7664	101.0582	129.2123	3.046112	44.76794	94.64647	1	-140.5415	-98.24551	-0.115856
4h$_c$	24	96.83018	269.7394	44.55691	94963.86	102.4845	101.3705	128.1064	2.840443	42.642	95.22204	1.015641	-140.541	-98.24551	-0.102534
4h$_c$	25	95.87055	294.0808	43.5401	93754.88	101.5877	100.9362	125.9875	3.136699	30.17826	93.34823	1.123442	-140.5405	-98.24551	-0.120003
4h$_c$	26	93.2112	557.0913	57.35675	90432.55	101.2728	100.4958	168.9884	6.160296	40.83405	89.78986	1.102252	-140.5405	-98.24551	-0.149383
4h$_c$	27	95.39784	270.3371	46.78357	93161.32	100.6277	99.73169	135.8033	2.901817	46.67615	93.94841	1.000835	-140.54	-98.24551	-0.088331
4h$_c$	28	96.15975	274.4076	48.04859	94118.66	100.8058	100.443	138.7643	2.915549	21.8761	93.16546	1.274297	-140.5395	-98.24551	-0.135839
4h$_c$	29	96.65257	259.1239	52.05908	94739.7	101.4109	100.3857	149.853	2.735114	6.394289	91.81076	1.722741	-140.539	-98.24551	-0.113699
4h$_c$	30	95.67445	277.075	50.54155	93508.49	100.7816	99.78604	146.4394	2.9631	20.05928	92.52545	1.324412	-140.5385	-98.24551	-0.140138

$7h_c$	1	97.2535	273.5189	47.27888	95498.88	102.5819	101.5924	135.551	2.864106	7.411808	92.25045	1.614799	-140.5545	-98.14601	-0.146428
$7h_c$	2	95.98144	250.9785	49.51796	93894.32	100.8767	99.78277	143.1785	2.672989	9.619017	91.81663	1.571716	-140.5545	-98.14651	-0.086375
$7h_c$	3	95.39963	276.1485	46.00947	93163.57	100.6766	99.90113	133.5546	2.964125	32.01154	93.13603	1.127141	-140.553	-98.14651	-0.081919
$7h_c$	4	96.39269	243.4466	47.57701	94412.03	101.1501	100.2304	137.1887	2.578555	9.503708	92.24347	1.560887	-140.5525	-98.14651	-0.093795
$7h_c$	5	96.1749	260.7147	43.71602	94137.74	101.3847	100.6478	126.239	2.769503	43.71602	94.68394	1	-140.552	-98.14651	-0.10135
$7h_c$	6	95.79153	245.2014	46.9585	93655.57	100.848	99.70777	135.9509	2.618119	43.63618	94.34242	1.027519	-140.551	-98.14651	-0.087832
$7h_c$	7	95.93348	263.0803	46.48743	93834	101.3192	100.1779	134.4591	2.803677	34.8115	93.93065	1.103909	-140.5505	-98.14651	-0.088827
$7h_c$	8	95.85103	275.3903	45.90729	93730.35	101.2933	100.3502	132.8545	2.938112	35.60316	93.81348	1.089658	-140.55	-98.14651	-0.133648
$7h_c$	9	95.90952	258.2565	44.04721	93803.87	101.4574	100.3069	127.4215	2.753154	44.01143	94.442	1.000293	-140.549	-98.14651	-0.133
$7h_c$	10	96.47001	260.8624	47.26818	94509.48	101.729	100.6091	136.2279	2.760172	25.33727	93.86637	1.221778	-140.5485	-98.14651	-0.057992
$7h_c$	11	95.92094	282.0011	50.07119	93818.23	101.1678	100.1449	144.8369	3.005824	11.69373	91.72937	1.494241	-140.5475	-98.14651	-0.104215
$7h_c$	12	96.11767	241.7277	44.09106	94065.7	101.9294	100.2295	127.3707	2.569775	44.09106	94.74705	1	-140.547	-98.14651	-0.106609
$7h_c$	13	96.67072	249.4268	48.71134	94762.6	101.461	100.5111	140.1995	2.632123	17.75397	93.54172	1.361072	-140.546	-98.14651	-0.104695
$7h_c$	14	95.48727	258.3589	45.08375	93273.51	100.6474	99.78525	130.7904	2.769906	45.08375	94.05461	1	-140.5455	-98.14651	-0.083574
$7h_c$	15	94.63557	277.8337	46.45266	92206.9	100.1667	99.12132	135.5388	3.013155	33.25263	92.43756	1.117498	-140.545	-98.14651	-0.139576
$7h_c$	16	97.14629	272.862	55.22052	95363.28	101.7608	100.8523	158.4327	2.86129	0.377182	88.08026	2.584739	-140.544	-98.14651	-0.110613
$7h_c$	17	95.75608	284.9063	48.50228	93611.03	101.4017	100.1616	140.4538	3.043512	15.13042	91.96513	1.39537	-140.5435	-98.14651	-0.151352
$7h_c$	18	96.28853	231.7151	55.16749	94280.81	100.8718	99.43868	159.1866	2.457712	0.276178	87.8836	2.751072	-140.543	-98.14651	-0.065388
$7h_c$	19	95.83669	262.633	51.08546	93712.32	100.5091	99.69248	147.8542	2.802545	9.016688	91.46669	1.60002	-140.542	-98.14651	-0.108949
$7h_c$	20	95.00588	259.5422	43.64957	92670.13	99.82933	99.46541	127.0413	2.80071	26.15915	92.45756	1.178574	-140.5415	-98.14651	-0.109814
$7h_c$	21	95.43941	270.1239	43.29438	93213.46	100.6844	100.1188	125.6397	2.897906	39.3302	93.66918	1.033724	-140.5405	-98.14651	-0.107229
$7h_c$	22	96.81299	274.0206	48.67426	94942.16	101.9672	101.0353	139.9602	2.886184	30.00546	94.43622	1.172186	-140.54	-98.14651	-0.098567
$7h_c$	23	96.93227	266.3947	52.8885	95092.8	101.9485	100.71	151.9575	2.801419	16.64259	93.59282	1.412997	-140.5395	-98.14651	-0.125621
$7h_c$	24	95.7139	258.4667	48.09862	93558.04	100.9975	99.74416	139.3243	2.762635	12.17545	91.81476	1.4756	-140.5385	-98.14651	-0.121768
$7h_c$	25	96.34433	272.8867	55.66592	94351.1	101.2708	100.021	160.5649	2.892248	2.391524	89.96152	2.052023	-140.538	-98.14651	-0.129432
$7h_c$	26	95.38983	283.4526	43.62035	93151.27	100.7953	100.2635	126.628	3.042928	37.26468	93.4122	1.054336	-140.5375	-98.14651	-0.138874
$7h_c$	27	96.60128	260.2446	54.39047	94675	101.0629	100.1898	156.6174	2.74882	3.455442	90.90874	1.939727	-140.5365	-98.14651	-0.090429
$7h_c$	28	96.1826	271.7086	46.42585	94147.42	101.214	100.572	134.0573	2.88599	16.83963	92.68907	1.346926	-140.536	-98.14651	-0.136478
$7h_c$	29	95.74124	238.0015	39.61267	93592.39	101.3759	100.2474	114.7225	2.542958	39.61267	94.23919	1	-140.535	-98.14651	-0.097318
$7h_c$	30	95.70777	256.6423	43.57812	93550.34	100.849	100.1247	126.2353	2.74336	43.57812	94.23546	1	-140.5345	-98.14651	-0.071001
$10h_c$	1	95.47105	237.7039	40.02354	93253.15	100.7608	99.92537	116.1231	2.549018	23.97317	92.9242	1.178828	-140.559	-98.04451	-1.189738
$10h_c$	2	96.29537	238.3777	40.49924	94289.43	101.5076	100.7099	116.8558	2.528149	25.33165	93.3165	1.164601	-140.558	-98.04451	-0.185922
$10h_c$	3	96.72049	266.0525	40.67515	94825.39	102.256	101.6262	117.0312	2.80571	33.94505	94.6785	1.062187	-140.5575	-98.04451	0.051319
$10h_c$	4	96.09789	262.8908	39.9317	94040.81	101.6637	101.0355	115.3704	2.795497	39.92784	94.45179	1.000033	-140.5565	-98.04451	0.157133
$10h_c$	5	95.97664	280.6269	42.95312	93888.27	101.9982	100.8766	124.2007	2.988945	37.81799	94.05632	1.043927	-140.555	-98.04451	0.022194
$10h_c$	6	97.71511	261.4167	49.70207	96083.48	102.5379	101.6599	142.0643	2.720725	4.218202	92.06225	1.824754	-140.554	-98.04451	0.006633
$10h_c$	7	96.14637	257.8549	44.69832	94101.83	101.4577	100.473	129.1002	2.740169	14.24999	92.45063	1.390645	-140.553	-98.04451	0.004652
$10h_c$	8	96.70049	256.8348	41.19329	94800.16	101.9472	101.3766	118.5378	2.709223	33.28772	94.67829	1.074338	-140.552	-98.04451	-0.018131
$10h_c$	9	95.4625	270.3176	44.22601	93242.43	101.2838	100.0466	128.3234	2.899084	44.22601	93.93445	1	-140.551	-98.04451	-0.067178
$10h_c$	10	96.20104	267.6203	43.75813	94170.64	101.6607	100.788	126.3385	2.841866	43.75813	94.67206	1	-140.55	-98.04451	-0.066249
$10h_c$	11	95.69332	252.4701	47.11942	93532.19	100.4093	99.71188	136.5068	2.699286	10.85506	91.63907	1.506659	-140.549	-98.04451	-0.085708
$10h_c$	12	95.04775	251.9959	39.14024	92722.55	101.1605	99.87646	113.8848	2.717742	39.14024	93.43818	1	-140.548	-98.04451	-0.094132
$10h_c$	13	95.85009	279.1537	46.96501	93729.17	101.1841	100.308	135.9164	2.978301	15.26244	92.10118	1.38072	-140.547	-98.04451	-0.136553
$10h_c$	14	95.62613	256.3062	40.73788	93447.81	101.3703	100.3448	118.0725	2.742774	40.73788	94.05323	1	-140.546	-98.04451	-0.087142
$10h_c$	15	95.79007	292.9056	47.36295	93653.74	101.1391	100.4283	137.1232	3.127538	34.02366	93.53306	1.114959	-140.545	-98.04451	-0.130355
$10h_c$	16	96.40871	258.8049	46.12083	94432.21	101.3053	100.6173	132.9756	2.740643	15.73984	92.91927	1.371842	-140.544	-98.04451	-0.079691
$10h_c$	17	94.7054	291.3862	46.13573	92294.19	100.2815	99.44228	134.5504	3.157145	42.89895	92.96556	1.025472	-140.543	-98.04451	-0.156425
$10h_c$	18	95.61789	301.8018	45.77113	93437.47	101.4018	100.5632	132.6679	3.229987	45.77113	93.96946	1	-140.542	-98.04451	-0.16556
$10h_c$	19	95.53667	274.4284	49.33526	93335.5	100.487	99.70856	143.0767	2.940236	17.31267	92.12286	1.363717	-140.541	-98.04451	-0.132455
$10h_c$	20	97.34431	234.0047	42.26759	95613.79	102.9251	101.4965	121.1106	2.447394	25.17084	94.9349	1.185206	-140.54	-98.04451	-0.096374
$10h_c$	21	95.94057	276.3037	45.81367	93842.91	100.9859	100.4638	132.5041	2.944321	14.46465	92.09162	1.388191	-140.539	-98.04451	-0.142171
$10h_c$	22	95.7669	248.4903	40.74204	93624.62	101.1817	100.3412	117.973	2.654113	40.73146	94.24156	1.000092	-140.538	-98.04451	-0.081231
$10h_c$	23	94.7084	254.8656	43.84383	92297.94	99.96678	99.06818	127.8637	2.761335	40.32958	93.08013	1.030108	-140.537	-98.04451	-0.122541
$10h_c$	24	95.10682	277.0256	45.92576	92796.54	100.2182	99.63085	133.575	2.9853	45.92576	93.59882	1	-140.536	-98.04451	-0.138472
$10h_c$	25	95.72724	257.7203	43.16802	93574.8	101.2666	100.2049	125.0309	2.754164	38.93868	94.01523	1.036761	-140.535	-98.04451	-0.126467
$10h_c$	26	95.91115	251.1284	44.51154	93805.92	101.3427	100.1426	128.7634	2.677107	23.81838	93.25553	1.220698	-140.534	-98.04451	-0.12269
$10h_c$	27	96.60824	257.1712	43.76876	94683.77	101.9973	101.015	126.0263	2.716106	43.76876	95.13932	1	-140.533	-98.04451	-0.153229
$10h_c$	28	96.76641	265.0562	46.62188	94883.36	101.8846	101.0303	134.1003	2.793495	20.70314	93.73573	1.283081	-140.532	-98.04451	-0.110921
$10h_c$	29	96.24894	264.1763	42.63013	94230.95	101.6412	100.8966	123.0424	2.803498	41.64194	94.64831	1.008293	-140.531	-98.04451	-0.128165
$10h_c$	30	95.05865	243.4597	46.44086	92736.21	99.73492	98.99042	135.1171	2.625292	11.43024	91.1863	1.488666	-140.53	-98.04451	-0.12058

Appendix C Indentation size effect

h_max(nm)	H(GPa)	h_max(nm)	H(GPa)	h_max(nm)	H(GPa)	h_max(nm)	H(GPa)	h_max(nm)	H(GPa)
9285.305	1.42029	8538.28	1.679689	685.9684	1.911352	218.8353	3.145272	53.76396	5.039747
9250.093	1.431124	8524.544	1.685106	687.5606	1.917473	219.1637	3.146014	53.54199	5.067062
9231.309	1.436954	8519.43	1.68713	677.7204	1.966786	218.5591	3.150094	53.34506	5.123032
9189.889	1.449937	8518.582	1.687465	677.6842	1.971658	218.0452	3.150885	52.68363	5.1393
9174.228	1.454891	8508.845	1.69133	678.9619	1.972596	219.3429	3.152229	52.64841	5.212961
9164.158	1.45809	8507.58	1.691833	678.1261	1.972968	217.8086	3.154033	50.92609	5.38613
9162.396	1.458651	8504.078	1.693226	677.293	1.975094	218.8952	3.154169		
9143.942	1.464545	8500.667	1.694586	674.4732	1.981511	218.2128	3.157765		
9134.723	1.467502	8500.136	1.694797	676.8304	1.984025	218.1961	3.159901		
9118.405	1.472759	8491.575	1.698216	673.4618	1.986561	217.3961	3.185085		
9117.111	1.473178	8486.004	1.700447	672.0574	1.997714	217.8455	3.187222		
9080.541	1.485067	8481.245	1.702356	672.2895	1.998503	216.4791	3.192554		
9077.629	1.48602	8476.382	1.70431	670.2082	2.007423	217.1863	3.196462		
9030.727	1.501496	8458.586	1.711489	671.744	2.008354	217.6478	3.198537		
9008.859	1.508794	8456.117	1.712488	671.9231	2.009212	216.8074	3.201732		
8982.447	1.51768	8448.812	1.715451	671.8266	2.011941	216.4462	3.205515		
8967.356	1.522792	8402.014	1.734614	668.6451	2.012782	216.5931	3.206206		
8944.053	1.530738	8400.926	1.735063	970.3993	2.01631	215.5976	3.213053		
8929.687	1.535667	8386.971	1.740842	668.0802	2.021055	216.6542	3.213198		
8929.373	1.535775	8380.015	1.743733	668.783	2.023245	216.4034	3.220733		
8928.902	1.535937	1041.777	1.748841	666.205	2.03112	215.8109	3.227945		
8911.801	1.541837	1037.053	1.762688	666.2727	2.031374	216.8036	3.230632		
8881.405	1.552409	1037.324	1.763409	667.7965	2.035361	215.6196	3.23459		
8836.7	1.568156	8329.666	1.764877	664.4443	2.048237	215.1635	3.242215		
8835.329	1.568643	8321.992	1.768133	662.3408	2.059612	214.4004	3.259909		
8819.013	1.574453	1035.869	1.770899	664.2722	2.063088	214.425	3.268496		
8810.948	1.577336	8314.803	1.771191	661.5434	2.063486	211.4199	3.354894		
8810.826	1.57738	1035.686	1.771617	664.015	2.065829	209.6665	3.391037		
8806.538	1.578917	1035.082	1.774134	660.7408	2.069302	207.1678	3.482771		
8799.06	1.581601	1036.243	1.777281	662.6142	2.06999	59.4015	4.32848		
8796.699	1.58245	1032.862	1.779537	662.3353	2.070335	59.0443	4.371931		
8793.508	1.583599	1032.464	1.782351	660.1533	2.072179	58.15173	4.444117		
8788.131	1.585537	1029.794	1.789678	659.9835	2.072898	58.18427	4.45207		
8784.366	1.586897	1028.219	1.791994	659.5274	2.078226	58.02959	4.460051		
8783.217	1.587312	8261.566	1.794092	657.3848	2.094375	58.29608	4.467431		
8782.492	1.587574	1029.049	1.794603	655.863	2.111594	57.96899	4.476171		
8782.2	1.58768	1028.216	1.795554	654.6213	2.114653	58.64269	4.504994		
8775.461	1.590119	1028.089	1.79712	654.2857	2.11474	57.52222	4.508219		
8760.564	1.595531	8246.835	1.800507	654.8525	2.119151	57.37467	4.510912		
8760.089	1.595705	1027.362	1.800879	655.0994	2.120504	57.41502	4.52706		
8744.714	1.601321	1026.839	1.803576	653.6615	2.124733	57.43927	4.538742		
8739.633	1.603183	1025.244	1.805036	657.4001	2.127271	57.43698	4.556785		
8729.732	1.606822	1024.643	1.806154	652.8237	2.127987	57.65825	4.557561		
8727.022	1.60782	1024.68	1.807417	652.0847	2.135292	57.37963	4.566715		
8726.114	1.608154	1024.628	1.808463	650.1924	2.148384	56.91568	4.578672		
8722.198	1.609599	1024.513	1.808693	935.9128	2.157423	56.85327	4.581826		
8721.92	1.609701	1023.959	1.810905	647.5164	2.163749	56.9488	4.596968		
8712.816	1.613067	1023.83	1.812795	647.6056	2.168724	56.37972	4.598474		
8711.335	1.613616	1023.141	1.813789	644.7349	2.187944	57.11098	4.615845		
8710.268	1.614011	1022.137	1.817089	643.3387	2.199961	56.73455	4.623707		
8704.585	1.616119	1021.789	1.817253	642.6743	2.201631	56.96581	4.625005		
8691.058	1.621154	1021.717	1.817764	620.4958	2.366759	56.56161	4.64616		
8681.624	1.624679	1021.894	1.818856	228.1599	2.91104	56.61197	4.65275		
8679.822	1.625354	1021.487	1.819424	226.7045	2.937936	56.59793	4.692326		
8671.891	1.628328	1020.644	1.819506	226.632	2.955677	55.23247	4.7132		
8670.661	1.62879	1021.383	1.821162	225.6874	2.980254	55.65306	4.715328		
8666.497	1.630355	1020.748	1.821267	225.0445	3.008226	56.35678	4.716072		
8654.968	1.634702	8194.907	1.823398	223.5099	3.013476	55.8265	4.728463		
8653.485	1.635262	1020.406	1.824807	222.8445	3.028281	56.26663	4.762217		
8651.661	1.635952	1019.791	1.825301	223.0969	3.050518	56.17908	4.7722		
8644.184	1.638783	1019.453	1.827785	221.6349	3.069805	55.99345	4.7824		
8638.543	1.640924	1019.646	1.829781	221.8315	3.071367	55.34733	4.808904		
8618.815	1.648445	1018.38	1.831964	221.4636	3.0886	55.69859	4.818917		
8609.899	1.651861	1016.886	1.835939	220.4906	3.096287	55.0599	4.84207		
8606.612	1.653122	1015.99	1.838897	220.7714	3.098871	54.88837	4.843584		
8595.139	1.657539	1015.221	1.84148	220.7279	3.105911	54.34703	4.861429		
8593.7	1.658094	1014.997	1.845764	219.7686	3.109787	54.99551	4.875014		
8589.244	1.659815	1014.134	1.846394	220.9347	3.115642	55.30262	4.884852		
8584.631	1.661599	1008	1.870152	220.3077	3.115734	55.15923	4.893157		
8558.933	1.671592	1007.6	1.870756	219.3787	3.131219	54.23126	4.965799		
8558.352	1.671819	1006.402	1.87556	218.6724	3.13431	53.63033	4.99836		
8551.092	1.674659	1001.74	1.88865	220.349	3.137596	53.329	5.019629		
8541.657	1.678361	996.8655	1.90615	218.7905	3.14465	53.02233	5.038013		

Appendix D Effect of electrolytic polishing

Data set	Indent	hc(nm)	Pmax(µN)	S(µN/nm)	A(nm^2)	hmax(nm)	heff(nm)	Er(GPa)	E(GPa)	H(GPa)	A	hf(nm)	m	X(mm)	Y(mm)
Electrolytically polished	1	50.58494	153.9595	20.46092	34630.98	56.3476	56.22837	97.41539	97.50681843	4.445715	0.008322	32.7901	3.114901	-133.267006	-98.177505
Electrolytically polished	2	51.67453	165.3733	34.09189	35554.88	56.14159	55.31264	160.1903	170.5445495	4.651213	0.026197	39.82248	3.193312	-133.257006	-98.178005
Electrolytically polished	3	56.71721	167.8583	33.45199	39974.44	62.01888	60.48062	148.2401	155.9328009	4.19914	1.384131	50.16413	2.055944	-133.247006	-98.178005
Electrolytically polished	4	53.53123	169.0868	33.52228	37154.59	58.37483	57.31424	154.0856	163.0362507	4.550899	16.9094	51.0077	1.250303	-133.237006	-98.178005
Electrolytically polished	5	38.89074	171.184	32.9574	25397.43	43.99502	42.78631	183.2284	199.7366116	6.740211	0.501735	30.65014	2.33653	-133.227006	-98.178005
Electrolytically polished	6	48.44771	169.126	37.49826	32850.57	52.95133	51.83038	183.3051	199.8360579	5.148343	3.096998	43.37777	1.874095	-133.267006	-98.168005
Electrolytically polished	7	52.34832	168.122	30.75254	36131.71	57.19939	56.44851	143.3414	150.0436851	4.653032	30.49534	50.96458	1.00311	-133.257006	-98.168005
Electrolytically polished	8	51.72576	167.7054	29.7462	35598.59	56.82138	55.95417	139.6851	145.685448	4.711013	29.72297	50.31468	1.000286	-133.247006	-98.168005
Electrolytically polished	9	53.61145	166.9219	33.52441	37224.43	58.73908	57.34579	153.9508	162.8714768	4.484203	13.85511	50.76737	1.321202	-133.237006	-98.168005
Electrolytically polished	10	50.88815	167.432	33.86094	34886.98	55.61511	54.59667	160.6209	171.0776481	4.799268	1.987285	44.93208	1.954538	-133.227006	-98.168005
Electrolytically polished	11	51.90382	167.1586	38.47139	35750.7	56.33351	55.16258	180.2729	195.9137705	4.675674	0.568778	44.66134	2.416851	-133.267006	-98.158005
Electrolytically polished	12	50.26709	167.5769	28.92356	34363.53	55.41924	54.61243	138.2413	143.9732102	4.876591	27.61514	48.72165	1.016742	-133.257006	-98.158005
Electrolytically polished	13	48.05865	167.0939	34.81562	32530.98	52.84872	51.65819	171.0253	184.1020719	5.136455	12.81465	45.10327	1.365782	-133.247006	-98.158005
Electrolytically polished	14	52.24258	166.8654	34.79761	36040.91	56.75208	55.83907	162.4001	173.2853813	4.62989	2.076678	46.44784	1.958418	-133.237006	-98.158005
Electrolytically polished	15	49.78056	167.0968	34.02767	33955.96	54.4778	53.46352	163.6097	174.7908299	4.920986	11.89412	46.68363	1.38066	-133.227006	-98.158005
Electrolytically polished	16	49.45123	166.7911	30.45596	33681.31	54.50045	53.55858	147.0323	154.4754188	4.952037	30.45596	48.08211	1	-133.267006	-98.148005
Electrolytically polished	17	46.36235	166.7716	32.48486	31153.78	51.39705	50.21272	163.0649	174.112276	5.353173	32.48486	45.07889	1	-133.257006	-98.148005
Electrolytically polished	18	50.07067	167.6009	31.03041	34198.73	54.69781	54.12156	148.668	156.4499296	4.900794	14.94189	47.31408	1.260369	-133.247006	-98.148005
Electrolytically polished	19	52.79916	166.5532	32.55562	36520.02	57.51237	56.63613	150.9369	159.1995392	4.5606	12.51371	49.76511	1.343056	-133.237006	-98.148005
Electrolytically polished	20	46.84704	167.0262	27.77122	31544.61	52.37976	51.35781	138.5375	144.3240971	5.294922	24.07061	45.03835	1.050729	-133.227006	-98.148005
Electrolytically polished	21	50.68847	166.6217	39.4621	34718.29	54.6725	53.85521	187.6445	205.4925058	4.799247	0.643618	43.72377	2.399495	-133.267006	-98.138005
Electrolytically polished	22	49.23453	166.6198	29.77386	33501.13	54.48245	53.43166	144.1253	150.982184	4.973557	25.5761	47.52614	1.055278	-133.257006	-98.138005
Electrolytically polished	23	52.82626	166.6981	39.58487	36543.43	56.83163	55.98463	183.4676	200.0470426	4.561644	2.386581	47.5831	1.995064	-133.247006	-98.138005
Electrolytically polished	24	51.22205	166.7271	36.29259	35169.88	55.75127	54.66753	171.4618	184.6545121	4.740622	4.599702	46.71352	1.731402	-133.237006	-98.138005
Electrolytically polished	25	52.13455	166.6956	33.33581	35948.25	56.96104	55.88493	155.7783	165.1088624	4.637099	13.1564	49.20097	1.336658	-133.227006	-98.138005
Electrolytically polished	26	49.59966	166.7694	32.20138	33802.39	54.2414	53.48078	155.1799	164.3753881	4.933659	14.68997	46.83672	1.282895	-133.267006	-98.128005
Electrolytically polished	27	50.11725	166.8809	29.36814	34237.78	55.10555	54.37904	140.6237	146.8012582	4.874175	29.36814	48.69066	1	-133.257006	-98.128005
Electrolytically polished	28	51.89919	166.7561	31.16276	35746.74	56.72484	55.91254	146.0335	153.2729455	4.664931	12.92216	48.89061	1.312231	-133.247006	-98.128005
Electrolytically polished	29	51.08549	166.676	32.25846	35054.05	55.96009	54.96066	152.6544	161.2893242	4.75483	2.574645	45.41135	1.848171	-133.237006	-98.128005
Electrolytically polished	30	49.69799	167.3085	33.12808	33887	54.69	53.48575	159.4463	169.6245114	4.937246	11.23121	46.47884	1.38741	-133.227006	-98.128005
Electrolytically polished	31	51.33669	167.1166	36.08727	35267.23	55.36267	54.80986	170.2563	183.1298679	4.73858	12.23167	48.33023	1.399216	-133.267006	-98.117505
Electrolytically polished	32	49.72186	167.5113	35.73044	33906.93	54.36376	53.23801	171.921	185.2363123	4.940327	13.49848	46.86366	1.35966	-133.257006	-98.118005
Electrolytically polished	33	50.1967	166.8991	31.167	34304.43	55.21443	54.21294	149.0921	156.9630317	4.865235	21.21578	48.10764	1.140113	-133.247006	-98.118005
Electrolytically polished	34	52.24427	167.1107	35.52358	36042.36	56.39225	55.77244	165.7849	177.5074431	4.63651	7.057714	48.34722	1.578415	-133.237006	-98.118005
Electrolytically polished	35	46.11349	167.096	32.7314	30953.94	51.1955	49.94229	164.832	176.3158408	5.398214	9.963719	42.68153	1.422265	-133.227006	-98.118005
Electrolytically polished	36	50.35172	166.9577	36.14619	34434.65	54.52947	53.81594	172.5836	186.0766661	4.848538	2.001477	44.61068	1.99293	-133.267006	-98.108005
Electrolytically polished	37	49.64461	166.8825	30.1672	33842.46	54.60663	53.79355	145.2911	152.3806553	4.931157	30.13554	48.25949	1.000387	-133.257006	-98.108005
Electrolytically polished	38	52.51738	166.054	35.98332	36277.1	56.73377	55.97845	167.3862	179.5151001	4.577377	2.983598	47.36501	1.866502	-133.247006	-98.108005
Electrolytically polished	39	52.66043	166.0864	32.13896	36400.33	57.80542	56.53624	149.2499	157.1539658	4.562771	25.26661	50.9056	1.089572	-133.237006	-98.108005
Electrolytically polished	40	49.40766	166.5761	38.99747	33645.05	53.28548	52.61126	188.3695	206.4426136	4.950985	5.224947	45.21896	1.730625	-133.227006	-98.108005
Electrolytically polished	41	50.01206	166.6947	33.9794	34149.62	54.50114	53.69138	162.9137	173.9241526	4.881305	1.658062	43.81509	2.013205	-133.267006	-98.097505
Electrolytically polished	42	50.36854	167.6348	35.21295	34448.79	55.07874	53.93899	168.0932	180.4035876	4.866204	15.6047	47.74236	1.301649	-133.257006	-98.098005
Electrolytically polished	43	52.88027	166.1375	32.85	36590.09	57.68057	56.67337	152.1558	160.6818952	4.540506	11.79394	49.7561	1.367736	-133.247006	-98.098005
Electrolytically polished	44	51.90944	166.8914	36.42555	35755.51	56.07799	55.34573	170.6748	183.658763	4.667572	4.257731	47.28962	1.758317	-133.237006	-98.098005
Electrolytically polished	45	47.41036	167.2291	30.45676	32001.54	51.9439	51.52839	150.8458	159.0889254	5.225659	30.45676	46.03768	1	-133.227006	-98.098005
Electrolytically polished	46	49.68405	167.1618	37.35036	33875.37	54.18393	53.04068	179.7991	195.3031426	4.934611	0.482323	42.10066	2.444422	-133.267006	-98.087505
Electrolytically polished	47	49.11481	166.2664	29.87598	33401.78	54.41156	53.28873	144.8345	151.8326159	4.977771	29.87598	47.72351	1	-133.257006	-98.088005
Electrolytically polished	48	51.74201	166.4355	35.23333	35612.46	56.40978	55.28486	165.4198	177.050684	4.673518	9.251723	48.27486	1.483973	-133.247006	-98.088005
Electrolytically polished	49	49.68607	166.6341	28.26158	33877.05	54.83142	54.10817	136.408	141.3764346	4.91879	25.47646	47.99299	1.037151	-133.237006	-98.088005
Electrolytically polished	50	49.64451	167.507	32.36685	33842.37	54.49486	53.52596	155.8852	165.2399363	4.949623	9.631253	46.13607	1.427925	-133.227006	-98.088005
Solution annealed	1	50.41463	162.5467	29.18375	34487.56	55.23247	54.59195	139.2338	145.1497755	4.7132	10.92836	47.11704	1.34205	-134.587006	-1.6745
Solution annealed	2	49.79194	166.1984	29.17695	33965.47	55.15923	54.06411	140.2671	146.3771522	4.893157	28.97725	48.35361	1.002506	-134.577006	-1.6745
Solution annealed	3	53.44866	167.0577	29.73207	37082.77	58.64269	57.66274	136.7961	142.2642755	4.504994	29.73207	52.04397	1	-134.567006	-1.6745
Solution annealed	4	53.03666	167.378	33.8631	36725.35	57.65825	56.74375	156.5592	166.067393	4.557561	6.966127	49.04484	1.557606	-134.557006	-1.6745
Solution annealed	5	52.64966	167.3433	41.74751	36391.05	56.37972	55.65601	193.8957	213.7314881	4.598474	1.168619	46.61729	2.25491	-134.547006	-1.6745
Solution annealed	6	47.44012	166.949	31.39407	32025.76	52.64841	51.42851	155.4293	164.6808813	5.212961	12.54503	44.37996	1.325449	-134.587006	-1.6645
Solution annealed	7	52.34598	167.1	33.96189	36129.7	56.96581	56.03614	158.3049	168.2157752	4.625005	20.3635	50.17796	1.190633	-134.577006	-1.6645
Solution annealed	8	51.51217	167.0268	28.04038	35416.51	56.35678	55.97966	132.0128	136.6424313	4.716072	27.98689	50.01892	1.000686	-134.567006	-1.6645
Solution annealed	9	52.32983	166.705	32.24286	36115.82	57.11098	56.20755	150.321	158.4519337	4.615845	13.95961	49.48051	1.301093	-134.557006	-1.6645
Solution annealed	10	48.99167	167.1522	33.20124	33299.72	53.329	52.76756	161.2014	171.7970681	5.019629	10.25476	45.62183	1.419346	-134.547006	-1.6645
Solution annealed	11	50.04601	166.9547	28.80396	34178.06	55.30262	54.39319	138.0426	143.7380344	4.884852	28.80018	48.59667	1.000048	-134.587006	-1.6545
Solution annealed	12	52.05571	166.7074	39.23543	35880.69	56.56161	55.24239	183.5198	200.114721	4.64616	0.375333	44.38238	2.555958	-134.577006	-1.6545
Solution annealed	13	51.43931	166.708	34.03254	35354.5	55.65306	55.11317	160.364	170.759489	4.715328	13.73102	48.59132	1.331401	-134.567006	-1.6545
Solution annealed	14	53.533	166.3172	36.0193	37156.13	57.96899	56.99608	165.5598	177.2257884	4.476171	9.502082	50.13384	1.486155	-134.557006	-1.6545
Solution annealed	15	50.87134	166.7755	30.51232	34872.76	55.99345	54.97072	144.7661	151.7505222	4.7824	30.13668	49.47981	1.004587	-134.547006	-1.6545
Solution annealed	16	53.5497	166.0574	31.68712	37170.66	58.29608	57.4801	145.6188	152.7743831	4.467431	11.90017	50.41519	1.348129	-134.587006	-1.644
Solution annealed	17	54.57492	166.4302	30.59719	38067.9	59.0443	58.65446	138.9431	144.8048806	4.371931	30.54207	53.21143	1.000669	-134.577006	-1.6445
Solution annealed	18	52.54806	166.8861	35.42031	36303.52	56.9488	56.08176	164.7073	176.1601232	4.596968	12.16007	49.52138	1.392391	-134.567006	-1.6445
Solution annealed	19	53.04801	166.3023	35.57647	36735.17	57.41502	56.55388	164.4586	175.8496192	4.52706	7.034193	49.16234	1.581246	-134.557006	-1.6445
Solution annealed	20	46.26377	167.3716	32.4708	31074.55	50.92609	50.12967	163.202	174.2829568	5.38613	13.31097	43.32478	1.320178	-134.547006	-1.6445
Solution annealed	21	53.15682	167.1593	32.5857	36829.43	57.43927	57.0042	150.4404	158.5967722	4.538742	9.800239	49.69098	1.425624	-134.587006	-1.6345
Solution annealed	22	53.88879	166.8028	38.16952	37466.34	58.18427	57.16633	174.7153	188.7882259	4.45207	3.868392	49.22706	1.816746	-134.577006	-1.6345
Solution annealed	23	54.94214	166.1775	36.35849	38391.66	59.4015	58.37004	164.4077	175.7861198	4.32848	3.038349	49.83836	1.866671	-134.567006	-1.6345
Solution annealed	24	53.67113	165.6608	33.44701	37276.43	58.15173	57.38583	153.4882	162.3064632	4.444117	6.061225	49.4675	1.598715	-134.557006	-1.6345

120

Solution annealed	25	50.82435	166.2302	27.20334	34833.04	56.17908	55.40734	129.1402	133.2917413	4.7722	27.14496	49.29201	1.000765	-134.547006	-1.6345
Solution annealed	26	52.49202	166.1153	35.7435	36255.27	56.85327	55.97759	166.3207	178.1785092	4.581826	3.571527	47.58797	1.805218	-134.587006	-1.6245
Solution annealed	27	50.2539	167.002	37.41185	34352.45	54.34703	53.60181	178.8402	194.0690287	4.861429	4.888007	45.88684	1.728311	-134.577006	-1.6245
Solution annealed	28	51.02541	166.6926	30.89799	35003.15	56.26663	55.07161	146.3226	153.6207932	4.762217	24.933	49.25184	1.078749	-134.567006	-1.6245
Solution annealed	29	52.74931	166.2178	32.78192	36477	57.43698	56.55212	152.0757	160.5843577	4.556785	13.0156	49.79329	1.332994	-134.557006	-1.6245
Solution annealed	30	47.99442	166.3876	29.31049	32478.35	53.34506	52.25196	144.099	150.9507073	5.123032	28.30446	46.50295	1.012734	-134.547006	-1.6245
Solution annealed	31	48.68224	166.5329	31.06093	33043.89	53.76396	52.70336	151.3923	159.7529615	5.039747	18.60103	46.34824	1.185326	-134.587006	-1.6145
Solution annealed	32	49.39073	167.0046	32.75486	33630.96	54.23126	53.21469	158.249	168.1467934	4.965799	3.021925	44.00238	1.806824	-134.577006	-1.6145
Solution annealed	33	53.62434	166.0729	34.1327	37235.66	58.02959	57.27347	156.7206	166.2656815	4.460051	15.72068	51.01763	1.285754	-134.567006	-1.6145
Solution annealed	34	50.48115	166.4625	29.39569	34543.54	55.69859	54.72826	140.1313	146.2156181	4.818917	29.39569	49.06544	1	-134.557006	-1.6145
Solution annealed	35	48.7583	166.792	34.86814	33106.7	53.02233	52.34593	169.7875	182.537975	5.038013	9.889855	45.38223	1.455774	-134.547006	-1.6145
Solution annealed	36	50.49742	166.1825	30.79028	34557.25	55.34733	54.54535	146.7502	154.1356373	4.808904	19.40477	48.24695	1.166968	-134.587006	-1.6045
Solution annealed	37	51.85071	166.1278	33.50827	35705.3	56.61197	55.56907	157.116	166.7518289	4.65275	5.098187	47.36311	1.655156	-134.577006	-1.6045
Solution annealed	38	48.65187	167.3085	31.88248	33018.83	53.54199	52.58762	155.4555	164.7130706	5.067062	8.176285	44.84714	1.475033	-134.567006	-1.6045
Solution annealed	39	51.42077	165.8208	28.93275	35338.73	56.59793	55.71921	136.3638	141.7539367	4.692326	28.91228	49.98648	1.000258	-134.557006	-1.6045
Solution annealed	40	48.04138	167.1137	33.45773	32516.83	52.68363	51.78746	164.3907	175.7648413	5.1393	9.440701	44.5405	1.450909	-134.547006	-1.6045
Solution annealed	41	53.40726	167.015	38.27847	37046.78	57.52222	56.67963	176.2033	190.6880928	4.508219	1.861116	47.72793	2.051656	-134.587006	-1.594
Solution annealed	42	51.33438	166.7505	31.90451	35265.27	55.8265	55.25429	150.5266	158.7014547	4.728463	20.58467	49.18882	1.160511	-134.577006	-1.5945
Solution annealed	43	52.11896	166.1524	34.68986	35934.88	56.73455	55.7112	162.1359	172.9570484	4.623707	11.45764	48.98896	1.403494	-134.567006	-1.5945
Solution annealed	44	49.24597	167.4982	34.38952	33510.64	53.63033	52.89894	166.4446	178.3337158	4.99836	1.663351	43.06952	2.018106	-134.557006	-1.5945
Solution annealed	45	50.40146	166.9897	34.65932	34476.48	54.88837	54.01498	165.384	177.0058586	4.843584	1.988852	44.52778	1.969104	-134.547006	-1.5945
Solution annealed	46	50.31009	166.5656	31.64448	34399.66	55.0599	54.25783	151.1665	159.478595	4.84207	19.26922	48.04337	1.180636	-134.587006	-1.5845
Solution annealed	47	52.65196	166.1966	37.22168	36393.03	57.37963	56.00075	172.8708	186.4413812	4.566715	3.375658	47.75423	1.846904	-134.577006	-1.5845
Solution annealed	48	52.54626	166.2148	36.06016	36301.96	56.91568	56.00329	167.6862	179.891973	4.578672	3.126837	47.46393	1.852606	-134.567006	-1.5845
Solution annealed	49	53.11084	165.9545	34.74144	36789.58	57.37467	56.69347	160.4797	170.9028075	4.510912	1.489336	46.84849	2.06098	-134.557006	-1.5845
Solution annealed	50	50.08906	166.7944	35.25323	34214.14	54.99551	53.63755	168.8616	181.3706501	4.875014	0.996383	43.27605	2.18998	-134.547006	-1.5845

Appendix E Sample I grain boundaries Inherent mechanical properties

Grain boundary (1)

Indent	hc(nm)	Pmax(µN)	S(µN/nm)	A(nm^2)	hmax(nm)	heff(nm)	Er(GPa)	E(GPa)	H(GPa)	A	hf(nm)	m	X(mm)	Y(mm)	Drift Correcti
bulkleft_000.hys	47.11137	172.47	47.23757	52254.7	50.3039	49.84971	183.087921	199.5543502	3.300564	19.56749	44.8885	1.35882	-132.2745	-5.421657	0.484931
bulkleft_001.hys	48.09573	171.3687	50.86918	53644.46	51.18587	50.62233	194.592958	214.6572338	3.194527	0.434456	41.50934	2.705107	-132.273	-5.421657	0.373526
bulkleft_002.hys	49.88001	170.396	56.68542	56198.41	52.58101	52.1345	211.857676	238.0184983	3.032043	0.771053	44.26762	2.617066	-132.2715	-5.421657	0.330179
bulkleft_003.hys	48.54473	169.7154	48.13107	54282.92	51.53023	51.18931	183.032733	199.482773	3.126498	10.03303	45.47034	1.621894	-132.2745	-5.423157	0.237404
bulkleft_004.hys	48.26694	169.7462	44.47529	53887.58	51.29655	51.12942	169.749813	182.4904424	3.150007	44.19743	47.30256	1.002677	-132.273	-5.423157	0.213334
bulkleft_005.hys	47.23053	168.6119	48.28457	52422.21	50.675	49.84957	186.846726	204.448782	3.216422	9.343113	44.08341	1.651227	-132.2715	-5.423157	0.125906
bulkleft_006.hys	45.41095	169.2089	50.93918	49886.09	48.23027	47.90229	202.06778	224.6667464	3.391906	9.141256	42.28519	1.69099	-132.2745	-5.424657	0.108365
bulkleft_007.hys	46.44019	168.4396	40.98881	51314.91	50.10268	49.52224	160.316553	170.7007715	3.282469	24.52262	44.57156	1.20472	-132.273	-5.424657	0.049732
bulkleft_008.hys	48.3807	168.2657	56.62646	54049.35	51.30548	50.60933	215.803771	243.4797192	3.113187	0.068254	40.55433	3.383808	-132.2715	-5.424657	0.069264
bulkleft_009.hys	40.14555	166.64	28.21253	42808.84	44.89451	44.5755	120.812003	123.6834657	3.892653	22.80273	38.2219	1.07568	-132.2749	-5.427453	-0.168713
bulkright_000.hys	46.08679	168.108	39.50158	50822.63	49.51593	49.27859	155.246096	164.4564343	3.307739	29.34993	44.51827	1.118567	-132.2552	-5.427438	-0.004678
bulkright_001.hys	45.19504	167.6995	48.5426	49588.24	48.43929	47.78605	193.138349	212.727613	3.381841	0.177974	37.59498	2.949927	-132.2537	-5.427438	-0.019963
bulkright_002.hys	47.17128	167.2354	46.96312	52338.89	50.20475	49.84202	181.877738	197.9866577	3.195242	0.678375	40.89305	2.513055	-132.2522	-5.427438	-0.002617
bulkright_003.hys	45.54852	167.8012	46.65956	50076.2	48.70344	48.24573	184.739509	201.7002119	3.350918	11.8469	42.68794	1.545425	-132.2552	-5.428938	-0.021085
bulkright_004.hys	46.74272	167.6137	47.44157	51737.73	49.5801	49.39251	184.749968	201.7723961	3.239679	0.506905	40.16801	2.610914	-132.2537	-5.428938	-0.017701
bulkright_005.hys	43.31152	167.8607	47.35577	47017.7	46.59085	45.97003	193.49823	213.2044671	3.570159	1.604289	38.01918	2.243043	-132.2522	-5.428938	-0.012682
bulkright_006.hys	44.32109	167.5255	43.67768	48389.33	47.64451	47.19771	175.921758	190.3281353	3.462034	7.979097	40.86923	1.649978	-132.2552	-5.430438	-0.03282
bulkright_007.hys	43.06803	167.5824	46.88157	46689.02	46.33273	45.74897	192.2337	211.5305117	3.589331	17.30122	40.72232	1.406219	-132.2537	-5.430438	-0.018342
bulkright_008.hys	44.15895	167.9176	49.95541	48168.07	47.42624	46.67996	201.668341	224.1278538	3.486077	14.40659	41.60065	1.511091	-132.2522	-5.430438	-0.028485
bulkright_009.hys	46.4546	167.1044	42.81945	51335.02	50.19478	49.3815	167.443776	179.5873835	3.255174	37.20289	45.24942	1.058819	-132.2507	-5.42761	-0.01969
GB 001.hys	40.28038	168.3816	47.79071	42985.23	43.5008	42.92286	204.229619	227.5912615	3.917196	3.153766	35.78986	2.024517	-132.2662	-5.431672	-0.053391
GB 002.hys	39.13615	168.0762	41.6531	41496.35	42.59888	42.16251	181.166194	197.0667468	4.050385	9.398851	35.84801	1.564876	-132.2658	-5.431641	-0.085287
GB 003.hys	38.06477	167.9761	41.47469	40118.78	41.3701	41.10234	183.461156	200.0386043	4.18697	17.09331	35.64719	1.346922	-132.2655	-5.431485	-0.089307
GB 004.hys	39.07416	168.5894	38.82478	41416.21	43.02715	42.3309	169.027982	181.5802602	4.070614	30.2939	37.5604	1.098607	-132.2651	-5.431321	-0.091228
GB 005.hys	37.12795	168.5268	40.70383	38927.28	40.67071	40.23319	182.786057	199.1629417	4.329272	40.2536	36.07387	1.00459	-132.2647	-5.431117	-0.079275
GB 006.hys	37.29143	168.2505	51.95221	39134.32	40.28071	39.72035	232.680483	267.3684904	4.299308	0.670665	31.31532	2.595294	-132.2644	-5.430899	-0.105279
GB 007.hys	35.64636	169.0231	44.58042	37067.74	38.97317	38.48992	205.15445	228.8464659	4.559842	20.81392	33.53076	1.307997	-132.264	-5.430711	-0.085349
GB 008.hys	33.81833	169.0946	34.23882	34815.17	37.78206	37.52234	162.58081	173.5100193	4.856922	34.23829	32.58363	1.000006	-132.2637	-5.4305	-0.079678
GB 009.hys	34.32796	168.6417	41.20254	35438.53	37.99518	37.3977	193.919297	213.762852	4.758709	14.2744	31.6299	1.409189	-132.2633	-5.430274	-0.101342
GB 010.hys	34.80904	168.3236	44.09898	36030.25	38.39211	37.67176	205.839985	229.7784843	4.671731	10.11591	31.67825	1.570233	-132.263	-5.430008	-0.097303
GB LEFT 001.hys	34.48111	169.1233	43.86222	35626.56	38.18228	37.37295	205.891556	229.8486525	4.747113	17.4656	32.10474	1.366315	-132.2632	-5.429547	-0.091239
GB LEFT 002.hys	36.07074	169.4271	46.4095	37597.28	39.52355	38.80877	212.0623	238.3005551	4.506367	13.07427	33.31758	1.504146	-132.2628	-5.429313	-0.074071
GB LEFT 003.hys	34.38319	168.9618	42.36082	35506.3	37.85904	37.37467	199.180322	220.7814383	4.758644	23.41819	32.43806	1.237669	-132.2625	-5.429008	-0.064104
GB LEFT 004.hys	36.1282	169.0929	52.00083	37669.17	39.05478	38.56701	237.384352	274.1847904	4.488893	4.275687	32.13973	1.976568	-132.2621	-5.428805	-0.05035
GB LEFT 005.hys	34.72263	169.4257	43.73801	35923.73	38.16859	37.62787	204.457568	227.9004109	4.716261	20.08407	32.54637	1.311811	-132.2618	-5.428547	-0.06057
GB LEFT 006.hys	35.61719	169.3691	37.76759	37031.44	39.51079	38.98058	173.887662	187.7340685	4.573657	35.98203	34.40954	1.019294	-132.2615	-5.428282	-0.033205
GB LEFT 007.hys	34.90189	169.3089	45.40974	36144.82	38.37236	37.69825	211.622005	237.6937988	4.684181	7.809097	31.44233	1.677878	-132.2611	-5.427992	-0.034649
GB LEFT 008.hys	35.80624	169.5178	46.6773	37266.95	39.09204	38.53001	214.229194	241.2950317	4.548744	10.81217	32.80274	1.577024	-132.2608	-5.427641	-0.037375
GB LEFT 009.hys	33.79803	169.5742	38.41371	34790.42	37.58915	37.10885	182.469899	198.7532618	4.874164	26.75529	32.06894	1.141692	-132.2604	-5.42736	-0.058903
GB LEFT 010.hys	34.38734	169.2368	43.48777	35511.39	37.88154	37.30604	204.464572	227.9099123	4.765705	16.71886	31.94273	1.378178	-132.26	-5.427078	-0.066109
GB RIGHT 001.hys	34.32111	169.1081	49.02248	35430.12	37.50004	36.90831	230.751076	264.5928675	4.773004	3.480648	29.98499	2.006991	-132.2592	-5.427258	-0.028298
GB RIGHT 002.hys	34.16291	169.4856	47.02469	35236.25	37.52717	36.86605	221.955521	252.0864441	4.809978	14.16329	31.52594	1.481642	-132.259	-5.427446	-0.05056
GB RIGHT 003.hys	33.65143	169.7891	40.675	34611.8	37.22835	36.78214	193.709235	213.4842231	4.905526	40.675	32.60786	1	-132.2585	-5.427203	-0.032701
GB RIGHT 004.hys	33.98647	170.021	44.05023	35020.44	37.4678	36.88125	208.55576	233.4841007	4.854908	11.13093	30.96321	1.533288	-132.2582	-5.426961	-0.021343
GB RIGHT 005.hys	33.24917	169.7738	41.29771	34123.21	36.81484	36.3324	198.077799	219.3041448	4.975316	33.1522	31.85384	1.089414	-132.2579	-5.426617	-0.030368
GB RIGHT 006.hys	34.61572	169.5986	38.61395	35792.09	38.64158	37.90984	180.83625	196.6406412	4.73844	38.54976	33.51474	1.000671	-132.2576	-5.426305	-0.011504
GB RIGHT 007.hys	35.82181	169.4721	45.97963	37286.37	38.99563	38.58617	210.972191	236.7993544	4.545149	11.06906	32.83655	1.559935	-132.2574	-5.426094	-0.0119
GB RIGHT 008.hys	37.82153	168.6695	39.32077	39808.24	41.63784	41.03871	174.610486	188.6546368	4.23705	39.32077	36.74914	1	-132.257	-5.425742	-0.016172
GB RIGHT 009.hys	39.35311	168.3823	36.92694	41777.25	42.99814	42.77302	160.069357	170.3948579	4.030477	18.84866	37.04949	1.255195	-132.2567	-5.425407	-0.013137
GB RIGHT 010.hys	38.39017	169.4561	41.13411	40535.48	41.86728	41.47987	181.016953	196.8739731	4.180439	26.26445	36.62117	1.17941	-132.2563	-5.425078	-0.021857

Grain boundary (2)

Indent	hc(nm)	Pmax(µN)	S(µN/nm)	A(nm^2)	hmax(nm)	heff(nm)	Er(GPa)	E(GPa)	H(GPa)	A	hf(nm)	m	X(mm)	Y(mm)	Drift Correction
bulkleft_000.hys	42.71969	168.15	49.19036	48673.12	45.76388	45.28345	197.5469	218.5939959	3.454678	2.408107	37.98249	2.135815	-135.8344	4.31257	-0.00579
bulkleft_001.hys	42.15251	168.7226	43.07808	47765.92	46.03141	45.09001	174.6353	188.6862979	3.53228	12.83292	39.32824	1.471091	-135.8329	4.31257	-0.016787
bulkleft_002.hys	42.37718	168.2083	36.91818	48124.2	46.41464	45.79437	149.1054	156.9790458	3.495296	33.58886	41.06825	1.037283	-135.8313	4.31257	-0.006151
bulkleft_003.hys	43.59312	168.0613	49.60886	50087.85	46.64607	46.13392	196.3939	217.0544033	3.35533	6.477362	40.03394	1.80061	-135.8344	4.31102	-0.00241
bulkleft_004.hys	42.95795	168.7193	41.48423	49056.91	46.47687	46.00825	165.9464	177.7096512	3.439256	41.48423	41.94118	1	-135.8329	4.31102	0.006003
bulkleft_005.hys	40.16883	168.4694	40.48233	44663.95	43.8892	43.29	169.7156	182.4472565	3.771933	40.48233	39.12844	1	-135.8313	4.31102	-0.002156
bulkleft_006.hys	42.77046	168.7387	37.18017	48754.77	46.50078	46.17426	149.1893	157.0806184	3.460968	37.18017	41.63586	1	-135.8344	4.30947	-0.00156
bulkleft_007.hys	43.60775	168.3284	49.48342	50111.72	46.92803	46.15903	195.8506	216.3303034	3.359064	3.04385	39.14919	2.06068	-135.8329	4.30947	-0.01393
bulkleft_008.hys	42.52775	168.2229	40.06864	48365.1	45.99556	45.67653	161.426	172.0755915	3.478188	39.85473	41.46893	1.002198	-135.8313	4.30947	-0.010964
bulkleft_009.hys	39.68651	165.1278	39.15089	43926.36	43.69418	42.8498	165.5061	177.1585473	3.759196	2.904454	34.71828	1.927939	-135.8356	4.309813	-0.292238
bulkright_000.hys	40.50064	169.8509	47.76182	45175.14	43.8918	43.16779	199.0975	220.6704043	3.75983	1.760781	35.29367	2.214191	-135.8216	4.317535	0.107735
bulkright_001.hys	41.4791	169.352	58.36478	46700.52	44.58448	43.65531	239.2901	276.9665474	3.62634	0.034058	33.15289	3.619512	-135.82	4.317535	0.118082
bulkright_002.hys	41.67178	169.1902	44.73512	47004.06	45.09924	44.50831	182.8167	199.2026168	3.599481	2.289144	36.62614	2.084103	-135.8185	4.318035	0.099759
bulkright_003.hys	39.60833	170.0475	47.19376	43807.43	42.9819	42.31072	199.777	221.582385	3.881704	24.84743	37.74631	1.266772	-135.8216	4.316485	0.115047
bulkright_004.hys	41.47527	169.3117	37.57055	46694.5	45.38149	44.85515	154.0457	162.9874466	3.625946	37.57055	40.34865	1	-135.82	4.316485	0.082611
bulkright_005.hys	37.96696	169.5423	41.09089	41349.56	41.71635	41.06149	179.0379	194.3232295	4.10022	28.22289	36.31279	1.150911	-135.8185	4.316485	0.036255
bulkright_006.hys	39.36408	168.9018	39.15057	43436.91	43.03832	42.5997	166.4345	178.3211597	3.888439	13.46341	36.54197	1.404149	-135.8216	4.314435	0.046362
bulkright_007.hys	42.01213	169.2413	51.29712	47542.77	45.04773	44.48655	208.4422	233.3286565	3.559769	3.396357	37.73447	2.046559	-135.82	4.314435	0.056349
bulkright_008.hys	40.19121	169.6374	47.59573	44698.34	43.43929	42.86431	199.4606	221.1575288	3.79516	1.515154	34.80575	2.261018	-135.8185	4.314435	0.026874
bulkright_009.hys	39.02664	167.3658	38.90238	42927.78	42.99412	42.25329	166.3573	178.2243288	3.898775	11.46092	35.97451	1.459435	-135.8216	4.319031	-0.129432
GB 000.hys	43.74639	170.8806	42.73466	50338.32	47.18373	46.74538	168.7585	181.2408267	3.394642	42.61864	42.74218	1.001139	-135.8269	4.305196	0.243486
GB 001.hys	44.73998	169.3377	48.29819	51978.05	47.99041	47.36955	187.6963	205.5603298	3.257869	10.9381	41.785	1.592813	-135.827	4.305641	0.13867
GB 002.hys	42.75651	169.6805	40.0041	48732.32	46.55895	45.93769	160.5576	170.9992046	3.481888	39.97682	41.69493	1.000279	-135.8271	4.306117	0.115258
GB 003.hys	42.4703	169.1542	52.08007	48273.11	45.58127	44.90628	210.0167	235.4863483	3.504107	16.81307	40.11832	1.47414	-135.8272	4.306641	0.079422
GB 004.hys	42.52533	168.9308	56.27554	48361.22	45.65084	44.77672	226.7284	258.8433047	3.493105	9.158868	39.51017	1.754431	-135.8271	4.307078	0.078577
GB 005.hys	42.72861	169.0554	47.09497	48687.46	45.86436	45.42086	189.104	207.4065364	3.472257	29.71116	41.13335	1.194404	-135.8271	4.307578	0.032936
GB 006.hys	42.47743	168.7927	42.49382	48284.51	46.42626	45.45655	171.3392	184.4992451	3.495793	41.46523	41.44356	1.010276	-135.8271	4.308031	0.01957
GB 007.hys	43.22233	168.693	40.99626	49484.65	46.84108	46.30846	163.2841	174.3851971	3.408997	30.65462	41.70959	1.117632	-135.8267	4.308446	-0.000702
GB 008.hys	41.3942	168.3339	48.43738	46567.1	44.98099	44.00066	198.873	220.3693027	3.614867	17.47708	39.06808	1.419331	-135.8271	4.308953	-0.005225
GB 009.hys	40.72642	168.0756	39.86653	45524.75	44.50992	43.88839	165.5463	177.2088923	3.69196	36.72326	39.53142	1.033449	-135.827	4.30943	-0.02912
GB left 000.hys	44.28929	168.3284	47.74473	51230.83	47.6955	46.93349	186.8937	204.5101356	3.285686	14.66703	41.72197	1.478198	-135.8271	4.310758	-0.008163
GB left 001.hys	43.11216	168.4281	54.54903	49306.17	46.12399	45.4279	217.6563	246.0595004	3.415964	2.66674	38.70855	2.176205	-135.827	4.31111	-0.012155
GB left 002.hys	42.88197	168.8264	40.86741	48934.35	46.62956	45.98028	163.6835	174.8828652	3.450059	25.16014	41.05069	1.193294	-135.827	4.311559	-0.022492
GB left 003.hys	41.42577	168.7221	41.97007	46616.69	45.06496	44.44081	172.228	185.6255698	3.619349	37.2676	40.22298	1.049196	-135.827	4.311969	-0.025103
GB left 004.hys	43.1794	168.7102	48.05475	49415.06	46.49928	45.8125	191.5321	210.6035999	3.414146	3.92204	38.95395	1.95356	-135.8269	4.312418	-0.036869
GB left 005.hys	43.38995	167.7433	40.45118	49756.85	47.12734	46.50006	160.6718	171.1406136	3.371261	33.76284	42.04836	1.073522	-135.8268	4.312887	-0.044233
GB left 006.hys	43.13996	168.1377	49.3494	49351.17	46.63033	45.69528	196.8194	217.6222146	3.406964	5.174895	39.30241	1.876345	-135.8267	4.313317	-0.019933
GB left 007.hys	42.75599	168.1647	52.55565	48731.5	46.05221	45.1558	210.9353	236.7486786	3.450843	0.846662	37.06	2.53014	-135.8267	4.313785	-0.017788
GB left 008.hys	42.8838	168.299	42.23151	48937.3	46.49005	45.87266	169.142	181.7239401	3.439073	42.23151	41.88751	1	-135.8267	4.314215	-0.01034
GB left 009.hys	41.89528	168.7516	49.1294	47357.45	45.24946	44.47141	200.024	221.9142201	3.563359	16.81699	39.51991	1.441553	-135.8267	4.314184	-0.01647
GB right 000.hys	43.90675	168.4426	52.26639	50601.08	47.04	46.32383	205.8626	229.8092618	3.328834	7.345311	40.56018	1.788414	-135.8261	4.314711	-0.016711
GB right 001.hys	40.71901	168.7636	48.70059	45513.25	44.01173	43.31801	202.2554	224.9200372	3.708011	9.039925	37.53727	1.668165	-135.826	4.31518	-0.004766
GB right 002.hys	40.89556	168.5275	54.59614	45787.58	43.77592	43.21066	226.0596	257.8922481	3.680638	1.362253	35.7903	2.403898	-135.8259	4.315629	-0.01582
GB right 003.hys	40.45074	169.0691	42.93056	45098.07	44.33201	43.40439	179.1111	194.4173948	3.74892	24.20817	38.55582	1.231164	-135.8259	4.316078	-0.012704
GB right 004.hys	41.64373	168.7226	41.04342	46959.8	45.21009	44.72685	167.809	180.0462543	3.592915	40.72453	40.60275	1.00323	-135.8258	4.316606	-0.010947
GB right 005.hys	41.53274	168.7968	40.07153	46784.92	45.03208	44.69203	164.1413	175.4536205	3.607931	39.83658	40.46949	1.002411	-135.8257	4.317055	-0.011855
GB right 006.hys	40.40891	168.5698	40.06548	45033.51	44.20021	43.56442	167.2774	179.3784598	3.743207	40.06548	39.35707	1	-135.8256	4.317524	-0.011912
GB right 007.hys	41.74467	168.7024	49.6499	47119.16	45.146	44.29305	202.6536	225.4579569	3.580335	10.26099	38.74245	1.633569	-135.8256	4.318012	0.004767
GB right 008.hys	40.59969	168.7205	51.86775	45328.34	43.61765	43.03936	215.8477	243.5407172	3.722185	18.18552	38.3501	1.441566	-135.8254	4.318442	0.008738
GB right 009.hys	41.13528	168.7371	38.15512	46161.46	45.06174	44.45207	157.3431	167.0312203	3.655367	38.01429	40.0231	1.001487	-135.8254	4.318832	-0.017137

Grain boundary (3)

Indent	hc(nm)	Pmax(μN)	S(μN/nm)	A(nm^2)	hmax(nm)	heff(nm)	Er(GPa)	E(GPa)	H(GPa)	A	hf(nm)	m	X(mm)	Y(mm)	Drift Correc
bulkleft_000.hys	54.69345	166.8457	37.24459	34060.94	58.6356	58.05325	178.8009	194.0185252	4.898446	8.308748	51.11555	1.548687	-138.5546	8.962222	-0.010872
bulkleft_001.hys	54.40971	166.5814	36.93295	33829.27	58.53804	57.79249	177.9109	192.875394	4.924179	10.26261	51.15248	1.472165	-138.5531	8.962222	-0.006982
bulkleft_002.hys	56.29521	166.1178	33.91406	35382.77	60.47246	59.96886	159.7419	169.9897964	4.694878	11.44327	53.1452	1.393096	-138.5515	8.962222	-0.007497
bulkleft_003.hys	53.21484	166.6526	31.9438	32861.81	57.96153	57.12763	156.1261	165.535644	5.071316	31.9438	51.91058	1	-138.5546	8.960672	-0.000427
bulkleft_004.hys	55.40958	166.5529	40.68629	34648.98	59.28745	58.47976	193.659	213.4176488	4.806862	3.605275	50.78865	1.87882	-138.5531	8.960672	-0.004861
bulkleft_005.hys	53.6834	166.5973	34.29147	33239.62	58.03144	57.3271	166.6453	178.5853114	5.012011	22.57644	51.70413	1.157402	-138.5515	8.960672	-0.006255
bulkleft_006.hys	54.25337	166.3624	35.13596	33701.93	58.25851	57.80448	169.574	182.2686385	4.936286	10.01698	50.9124	1.455618	-138.5546	8.959122	-0.003204
bulkleft_007.hys	52.59054	167.02	35.25109	32361.57	56.82854	56.14405	173.6171	187.3898822	5.16106	18.41028	50.25268	1.243427	-138.5531	8.959122	-0.004318
bulkleft_008.hys	52.78201	166.5942	38.59285	32514.61	56.50344	56.01955	189.628	208.0950426	5.123672	3.161302	47.86468	1.889139	-138.5515	8.959122	0.006028
bulkleft_009.hys	55.48416	162.7412	28.34152	34710.49	60.29749	59.79077	134.7807	139.8890357	4.68853	9.327861	51.86161	1.38087	-138.553	8.964	-0.331256
bulkright_000.hys	54.76735	166.4263	37.47226	34121.41	58.84655	58.09834	179.7344	195.2197775	4.877473	0.125866	45.4996	2.836713	-138.569	8.966593	-0.052254
bulkright_001.hys	56.59765	166.879	34.47536	35635.01	60.83025	60.22804	161.8099	172.5521671	4.683006	23.61899	54.69548	1.142967	-138.5674	8.966593	0.021148
bulkright_002.hys	56.1691	166.2786	34.08572	35277.84	60.29971	59.82779	160.789	171.2858777	4.713402	34.08572	54.94954	1	-138.5659	8.966593	0.001851
bulkright_003.hys	57.58131	166.3536	37.52457	36461.31	61.30563	60.90621	174.1143	188.0225368	4.56247	3.139391	52.5949	1.87479	-138.569	8.965043	-0.009537
bulkright_004.hys	54.47913	166.5367	39.01582	33885.88	58.37097	57.68046	187.7873	205.6795277	4.914634	5.093627	50.2558	1.739432	-138.5674	8.965043	0.002449
bulkright_005.hys	55.48735	165.8697	33.00952	34713.12	60.07045	59.25603	156.9738	166.5769239	4.778299	33.00952	54.23112	1	-138.5659	8.965043	-0.011101
bulkright_006.hys	56.90267	167.2142	38.63016	35890.28	60.86047	60.14911	180.6646	196.4190295	4.659039	2.967192	51.88556	1.909062	-138.569	8.963493	-0.005869
bulkright_007.hys	54.9037	166.6616	40.88146	34233.09	58.70157	57.96122	195.7664	216.2181731	4.868436	7.918732	51.37301	1.616063	-138.5674	8.963493	-0.008352
bulkright_008.hys	53.91881	166.5294	43.91689	33430.2	57.57042	56.76276	212.8124	239.3355434	4.981406	0.812302	47.63493	2.407176	-138.5659	8.963493	-0.020969
bulkright_009.hys	56.08549	165.9191	36.42746	35208.35	60.18405	59.50158	172.0049	185.3426617	4.712492	0.279512	47.7119	2.588419	-138.5691	8.967282	-0.071192
GB 000.hys	56.88085	167.428	40.03349	35871.99	60.88252	60.01749	187.2753	205.0093216	4.667375	0.17264	48.32206	2.796479	-138.5704	8.958368	0.074962
GB 001.hys	59.17946	166.7267	42.28421	37822.92	62.6709	62.13671	192.6351	212.0614267	4.408086	0.003359	46.59656	3.941196	-138.5705	8.957774	0.070423
GB 002.hys	56.90928	166.7315	39.0805	35895.82	60.81157	60.10905	182.7566	199.1247118	4.644871	4.701027	52.57155	1.76673	-138.5707	8.957368	0.036058
GB 003.hys	54.23604	166.8191	32.27914	33687.83	58.63011	58.11206	155.8189	165.1586996	4.951911	15.95627	51.62497	1.255237	-138.5707	8.95668	-0.012196
GB 004.hys	55.80088	167.0711	36.19592	34972.3	59.79969	59.26269	171.4875	184.6870531	4.777241	6.525975	51.81071	1.61447	-138.5708	8.956282	0.002994
GB 005.hys	57.63879	166.7814	31.97055	36509.87	62.18391	61.55133	148.2449	155.938619	4.568118	21.76928	55.59737	1.141323	-138.5709	8.955883	-0.000866
GB 006.hys	54.81291	166.7485	34.07487	34158.71	59.26108	58.48311	163.3497	174.4668973	4.881582	5.574819	50.48505	1.634393	-138.5711	8.955516	-0.006019
GB 007.hys	55.00716	167.049	39.74577	34317.96	59.03667	58.15937	190.0925	208.7061358	4.867683	7.067925	51.27124	1.638885	-138.5683	8.957571	0.009297
GB 008.hys	55.12803	166.8588	45.07825	34417.22	58.93683	57.90418	215.2851	242.7592515	4.84812	0.363019	48.0054	2.674235	-138.5683	8.957813	-0.005038
GB 009.hys	54.50403	166.907	39.93745	33906.2	58.38252	57.63844	192.1656	211.4404488	4.92261	5.168144	50.33478	1.747618	-138.568	8.958039	-0.01988
gb left 000.hys	55.64418	170.9634	33.79063	34842.65	59.89334	59.37221	160.3893	170.7908623	4.820627	22.04374	53.60905	1.159425	-138.5594	8.963461	0.087736
gb left 001.hys	55.67731	166.9448	30.57586	34870.04	60.6372	59.77232	145.0732	152.1190967	4.787627	30.57586	54.31231	1	-138.559	8.963711	0.062146
gb left 002.hys	56.16849	166.8132	31.76989	35277.33	60.74108	60.1065	149.8659	157.9000787	4.728622	27.95478	54.60536	1.047703	-138.5586	8.96404	0.044165
gb left 003.hys	56.09927	166.7288	39.16621	35219.8	59.87129	59.29199	184.9068	201.918029	4.733951	4.151311	51.5909	1.80906	-138.5583	8.964352	0.030472
gb left 004.hys	56.02654	166.468	34.59162	35159.4	60.04395	59.63583	163.45	174.5918754	4.734667	20.88699	53.91093	1.189619	-138.558	8.96468	0.006995
gb left 005.hys	54.04204	166.8609	38.65406	33530.17	58.03935	57.27962	187.0304	204.6888656	4.976439	6.927015	50.24115	1.630494	-138.5577	8.965016	0.012469
gb left 006.hys	54.78852	167.1995	34.99188	34138.74	59.16628	58.3722	167.7947	180.0283266	4.897647	13.42113	51.91204	1.351996	-138.5574	8.96536	-0.001895
gb left 007.hys	55.57673	166.3204	33.28077	34786.92	59.8665	59.32485	158.0958	167.9579602	4.781119	25.40042	53.81934	1.101656	-138.5571	8.96568	0.015299
gb left 008.hys	56.1093	166.1912	36.87883	35228.13	60.038	59.48911	174.0874	187.98825	4.717571	11.63269	53.05284	1.428246	-138.5568	8.966032	-0.002538
gb left 009.hys	54.58308	166.2914	34.10366	33970.74	58.6245	58.24013	163.9394	175.2018217	4.895137	20.81275	52.46272	1.184852	-138.5565	8.966375	-0.002662
gb right 000.hys	57.60826	168.6353	35.26566	36484.07	61.7364	61.19465	163.5819	174.7561567	4.622164	12.03286	54.53589	1.392505	-138.5642	8.961051	0.279814
gb right 001.hys	55.31251	168.6965	33.10018	34569	59.7645	59.13492	157.7327	167.510721	4.879994	32.75829	54.01826	1.003947	-138.5638	8.961465	0.239473
gb right 002.hys	57.5014	168.8345	39.81108	36393.84	61.24646	60.68207	184.8949	201.9024565	4.639095	3.490101	52.74227	1.8722	-138.5635	8.96184	0.219232
gb right 003.hys	58.88546	167.8724	38.05096	37570.66	62.70543	62.19429	173.9306	187.7887302	4.468177	20.01941	56.69225	1.247127	-138.5632	8.962223	0.183027
gb right 004.hys	57.405	167.5566	36.67462	36312.54	61.47642	60.83155	170.5187	183.4614701	4.61429	10.4193	54.15007	1.462436	-138.5628	8.962653	0.116292
gb right 005.hys	57.85076	167.4546	35.31618	36689.22	61.80404	61.40695	163.3576	174.4767405	4.564136	0.616043	50.34801	2.332331	-138.5625	8.962989	0.086518
gb right 006.hys	55.74456	167.3705	34.19769	34925.68	59.70271	59.41522	162.1284	172.9477017	4.792192	5.175398	51.29272	1.659615	-138.5621	8.963286	0.060256
gb right 007.hys	56.9124	167.0484	41.25185	35898.43	60.75643	59.9495	192.9037	212.416876	4.653361	7.372492	53.28662	1.645369	-138.5618	8.963653	0.042595
gb right 008.hys	56.97082	166.4814	36.87086	35947.43	60.86751	60.35727	172.2996	185.7163102	4.631247	1.952753	51.26415	2.013865	-138.5615	8.964043	0.022657
gb right 009.hys	59.29747	165.9179	42.04793	37924.41	62.84839	62.25691	191.3022	210.3002536	4.374962	0.004791	47.0889	3.843971	-138.5611	8.964418	0.014967

Grain boundary (4)

Indent	hc(nm)	Pmax(µN)	S(µN/nm)	A(nm^2)	hmax(nm)	heff(nm)	Er(GPa)	E(GPa)	H(GPa)	A	hf(nm)	m	X(mm)	Y(mm)	Drift Correc
bulkleft_000.hys	41.12723	170.7752	39.94606	27522.96	46.00971	44.33358	213.3345	240.0570147	6.204825	0.686578	34.16521	2.378487	-138.7033	8.768644	0.132201
bulkleft_001.hys	52.32127	168.9451	46.06315	36955.59	56.06039	55.07203	212.2992	238.6272863	4.571572	10.09558	49.22205	1.595005	-138.7017	8.768644	0.178902
bulkleft_002.hys	55.66293	168.4587	47.74844	40028.99	59.05209	58.30896	211.4495	237.4562709	4.208418	7.631078	52.2493	1.717568	-138.7002	8.768644	0.146865
bulkleft_003.hys	55.63923	168.1486	39.51781	40006.77	59.53717	58.83048	175.0495	189.2144506	4.203005	21.37399	53.5538	1.240111	-138.7033	8.767094	0.132704
bulkleft_004.hys	52.56215	168.4715	35.55294	37173.14	56.33381	56.11611	163.3788	174.5031522	4.532076	27.32045	50.89833	1.101121	-138.7017	8.767094	0.102544
bulkleft_005.hys	53.19741	168.5925	46.73651	37749.82	56.60989	55.90288	213.1247	239.7669033	4.466047	0.466585	46.44628	2.621519	-138.7002	8.767094	0.086597
bulkleft_006.hys	53.61516	167.67	40.94612	38131.41	57.3691	56.68633	185.7831	203.0598859	4.397163	13.63772	50.85765	1.423401	-138.7033	8.765544	0.072368
bulkleft_007.hys	54.26511	167.1921	39.23325	38728.82	58.426	57.46123	176.6331	191.2378194	4.316995	38.8493	53.18264	1.004011	-138.7017	8.765544	0.048941
bulkleft_008.hys	53.46229	167.0904	44.73954	37991.56	56.8705	56.26334	203.3681	226.4241461	4.398093	0.638397	46.94682	2.494559	-138.7002	8.765544	0.045759
bulkleft_009.hys	56.39517	167.308	39.86046	40718.47	60.36246	59.54318	175.0175	189.1735488	4.108897	15.65091	53.83437	1.3601	-138.7029	8.76436	0.098848
bulkright_000.hys	50.57348	168.3765	38.25566	35395.67	54.61897	53.87449	180.1588	195.7666831	4.756981	26.6082	48.84646	1.142384	-138.6956	8.778879	0.039673
bulkright_001.hys	53.33212	168.0389	44.75099	37872.67	56.99983	56.14835	203.7392	226.9266053	4.436945	0.035396	43.58725	3.345188	-138.694	8.778879	0.052069
bulkright_002.hys	52.54339	167.5545	35.79285	37156.17	57.02373	56.05431	164.5188	175.9248031	4.509467	23.39125	50.61322	1.16232	-138.6925	8.778879	0.036837
bulkright_003.hys	51.3772	168.1051	36.89547	36108.95	56.01782	54.79439	172.0285	185.3725995	4.655497	29.05746	49.81339	1.093224	-138.6956	8.777329	0.011844
bulkright_004.hys	51.33299	167.7734	41.76436	36069.53	55.16302	54.34584	194.8365	214.9808997	4.651388	2.826247	46.42093	1.972774	-138.694	8.777329	0.004505
bulkright_005.hys	52.02485	167.722	44.65059	36688.73	55.62705	54.84209	206.5359	230.7260609	4.571484	4.949341	47.9741	1.828381	-138.6925	8.777329	0.001075
bulkright_006.hys	51.61945	167.9833	34.02366	36325.3	55.89217	55.32239	158.1653	168.0436757	4.624416	33.83536	50.37459	1.002136	-138.6956	8.775779	0.005548
bulkright_007.hys	50.34876	167.3063	35.8706	35197.46	54.36358	53.84688	169.4017	182.0513253	4.753362	35.8706	49.18272	1	-138.694	8.775779	-0.000529
bulkright_008.hys	51.82108	167.7775	49.1099	36505.84	54.85827	54.38336	227.7313	260.2720091	4.595908	0.004493	40.65323	4.018925	-138.6925	8.775779	-0.002068
bulkright_009.hys	51.25553	164.8295	32.55127	36000.53	56.00898	55.0533	152.0017	160.4942805	4.57853	32.50507	49.98687	1.000542	-138.6958	8.779985	-0.187086
gb 000.hys	53.9759	167.6906	45.39678	38462.43	57.59821	56.74632	205.0886	228.7569798	4.359853	2.009321	48.84151	2.139969	-138.7021	8.777567	0.002604
gb 001.hys	52.79424	167.4138	39.06401	37383.32	56.37665	56.00846	179.0081	194.2849685	4.478301	7.27397	49.06997	1.619014	-138.7024	8.778133	-0.005566
gb 002.hys	51.44781	167.5906	42.51258	36171.95	54.96904	54.40442	198.0461	219.2617737	4.633165	7.396772	47.85758	1.66073	-138.7027	8.778622	-0.016301
gb 003.hys	52.10694	167.0484	39.30081	36762.54	55.92246	55.29482	181.6074	197.6370099	4.543984	18.77489	49.82646	1.286517	-138.7029	8.778993	-0.002005
gb 004.hys	53.75193	167.2973	42.34334	38256.75	57.20481	56.71516	191.8076	210.9674796	4.373013	8.311552	50.32181	1.618172	-138.7031	8.779442	0.000602
gb 005.hys	53.31581	166.6415	38.4671	37857.78	57.11666	56.56485	175.1648	189.361461	4.401776	17.66597	50.9375	1.299002	-138.7032	8.779852	-0.003794
gb 006.hys	53.37387	166.7267	36.78373	37910.79	57.53376	56.77334	167.3822	179.5100343	4.397869	18.78735	51.08253	1.255524	-138.7034	8.78034	-0.000616
gb 007.hys	53.16655	166.6687	40.83415	37721.71	57.14074	56.22775	186.2785	203.7063588	4.418376	8.716607	49.77056	1.582022	-138.7037	8.780829	-0.002663
gb 008.hys	54.07198	167.2421	35.92883	38550.83	58.23094	57.56309	162.1291	172.9485975	4.338224	35.28238	52.87502	1.007144	-138.7039	8.781219	-0.00133
gb 009.hys	54.06324	167.0654	45.7494	38542.78	57.6973	56.80205	206.4661	230.6308881	4.334545	1.520623	48.63214	2.237258	-138.7041	8.781688	-0.001247
gb left 000.hys	54.89607	167.0508	45.67129	39313.11	58.90251	57.63933	204.0842	227.3941301	4.24924	15.27304	52.3727	1.439884	-138.6974	8.76668	0.017021
gb left 001.hys	54.01089	166.8898	45.33109	38494.62	57.87788	56.77207	204.7062	228.2377627	4.335406	1.55585	48.58541	2.223685	-138.6976	8.767149	0.00602
gb left 002.hys	55.93901	166.4676	37.72571	40288.27	59.82347	59.24844	166.5263	178.4362288	4.131913	26.37241	54.21671	1.140316	-138.6977	8.767618	0.008159
gb left 003.hys	53.96842	167.4501	36.982	38455.55	58.14936	57.36433	167.0882	179.1409255	4.354382	17.67858	51.56991	1.279719	-138.698	8.768008	-0.015903
gb left 004.hys	53.95233	167.4754	43.85505	38440.76	57.37973	56.81646	198.1794	219.4400903	4.356714	1.030642	47.92131	2.32928	-138.6982	8.768536	-0.008294
gb left 005.hys	49.67047	167.8473	35.82845	34602.45	53.69299	53.18403	170.6512	183.6289487	4.850733	27.45537	48.01855	1.102616	-138.6984	8.769043	0.001456
gb left 006.hys	56.05401	166.6591	48.63464	40396.51	59.44238	58.62408	214.392	241.520572	4.125582	3.948382	51.89618	1.963342	-138.6986	8.769512	0.006345
gb left 007.hys	52.82355	167.2718	32.08246	37409.91	57.14131	56.73391	146.9634	154.3924214	4.471324	32.08246	51.5201	1	-138.6988	8.770059	-0.012013
gb left 008.hys	54.3816	166.7716	41.64535	38836.37	57.97557	57.38502	187.2329	204.9537527	4.294213	0.926601	48.06768	2.326678	-138.699	8.770606	-0.014072
gb left 009.hys	56.10489	166.3813	50.88851	40444.45	59.45168	58.55703	224.1946	255.2475343	4.113824	0.263335	49.15048	2.877038	-138.6993	8.770555	-0.01139
gb right 000.hys	52.88825	167.3623	40.91926	37468.63	56.71092	55.9558	187.2961	205.0364412	4.466732	5.249027	48.77366	1.755997	-138.6993	8.77284	-0.025075
gb right 001.hys	53.4181	167.4616	38.50274	37951.18	57.14658	56.6801	175.1112	189.2930879	4.412553	22.49077	51.42023	1.209349	-138.6996	8.77327	-0.002392
gb right 002.hys	54.36412	167.5341	39.13788	38820.23	58.39232	57.57458	175.9961	190.4231989	4.315639	24.38285	52.49707	1.186165	-138.6998	8.773661	-0.00192
gb right 003.hys	47.62546	167.527	32.64372	32838.06	52.03175	51.47444	159.6047	169.8202534	5.101612	32.64372	46.34246	1	-138.7	8.774071	0.005583
gb right 004.hys	55.11464	166.7461	41.87179	39516.5	58.66624	58.10136	186.6238	204.1574563	4.219657	17.60381	52.7584	1.341677	-138.7002	8.774539	-0.006624
gb right 005.hys	54.28772	166.5398	36.52026	38749.68	58.53161	57.70787	164.3745	175.7446817	4.297837	21.90825	52.25465	1.195828	-138.7003	8.774989	-0.012822
gb right 006.hys	54.28727	166.7853	39.55546	38749.27	58.15704	57.44964	178.0367	193.0368516	4.304217	20.26315	52.13124	1.261332	-138.7006	8.775477	-0.013952
gb right 007.hys	52.22089	166.9035	36.579	36865.12	56.27227	55.64301	168.7947	181.2863764	4.52741	36.579	51.08019	1	-138.7008	8.775848	-0.02102
gb right 008.hys	53.42635	166.4804	34.49344	37958.71	57.80427	57.04617	156.8612	166.6385438	4.385828	34.49344	52.21974	1	-138.701	8.776317	-0.016153
gb right 009.hys	53.19556	166.991	37.56489	37748.13	56.95969	56.52961	171.3047	184.4555917	4.42382	22.82989	51.22701	1.192827	-138.7012	8.776786	-0.012231

Grain boundary (5)

Indent	hc(nm)	Pmax(µN)	S(µN/nm)	A(nm^2)	hmax(nm)	heff(nm)	Er(GPa)	E(GPa)	H(GPa)	A	hf(nm)	m	X(mm)	Y(mm)	Drift Correction
bulkleft_000.hys	56.12257	175.3515	34.3294	39440.93	60.63942	59.9535	153.1537	161.8981756	4.445926	0.061865	44.95754	2.935832	-140.017135	-2.354356	0.814261
bulkleft_001.hys	55.22589	174.7153	36.70249	38642.7	59.29603	58.79613	165.4233	177.0550304	4.521301	0.041344	44.03315	3.101263	-140.015585	-2.354356	0.717354
bulkleft_002.hys	57.70181	172.2684	36.00406	40865.1	61.97621	61.29033	157.8011	167.5949461	4.215538	0.067377	47.12672	2.960192	-140.014035	-2.354356	0.562794
bulkleft_003.hys	55.14006	170.9941	32.86482	38566.69	59.64432	59.04228	148.2723	155.9716927	4.433725	0.38964	46.51846	2.40706	-140.017135	-2.355906	0.431204
bulkleft_004.hys	57.13647	170.0522	38.209	40352.59	61.11246	60.4744	168.5252	180.9470633	4.214158	7.977543	53.47608	1.572453	-140.015585	-2.355906	0.349125
bulkleft_005.hys	54.34122	169.6705	38.93601	37862.51	58.51734	57.60948	177.2889	192.0777444	4.481227	0.260219	46.06559	2.649092	-140.014035	-2.355906	0.209764
bulkleft_006.hys	56.6607	168.5444	37.03721	39923.59	60.9946	60.07371	164.2322	175.5670114	4.221673	2.704323	51.37874	1.910697	-140.017135	-2.357456	0.185206
bulkleft_007.hys	56.321	166.6652	39.61201	39618.59	60.25108	59.47658	176.3243	190.8427959	4.206741	3.27482	51.50955	1.893558	-140.015585	-2.357456	-0.008505
bulkleft_008.hys	52.82469	166.5147	29.73417	36542.07	57.39414	57.02478	137.8142	143.4677275	4.556793	21.05081	50.72957	1.124121	-140.014035	-2.357456	-0.063102
bulkleft_009.hys	51.37089	164.6178	28.55088	35296.3	56.18363	55.69521	134.6448	139.7292907	4.663881	24.59329	49.61978	1.053706	-140.016913	-2.360625	-0.253954
bulkright_000.hys	58.00789	176.9563	34.37873	41143.84	62.51107	61.86834	150.1662	158.2642162	4.30092	16.57017	55.36014	1.264399	-140.014307	-2.367372	1.048944
bulkright_001.hys	55.58276	178.4775	34.86965	38959.48	59.93405	59.42157	156.5221	166.0218705	4.581105	22.66843	53.48932	1.159001	-140.012757	-2.367372	1.137245
bulkright_002.hys	54.74688	177.6674	37.60319	38219.35	58.9248	58.29048	170.419	183.3353843	4.648625	17.30297	52.19986	1.289075	-140.011207	-2.367372	1.04611
bulkright_003.hys	60.08815	175.5781	51.8074	43061.6	63.41533	62.62994	221.1982	251.0207007	4.077371	0.823886	54.13603	2.506279	-140.014307	-2.368922	0.913088
bulkright_004.hys	60.80193	173.9184	44.901	43729.01	64.56408	63.70696	190.2418	208.9026895	3.977185	5.695354	56.83587	1.773929	-140.012757	-2.368922	0.743297
bulkright_005.hys	59.41113	173.0967	36.47946	42432.98	63.39373	62.96991	156.9031	166.4899826	4.079297	20.09907	57.16217	1.223958	-140.011207	-2.368922	0.601433
bulkright_006.hys	59.52223	171.0144	47.16669	42535.84	62.63491	62.24154	202.6248	225.41904	4.020479	0.391531	52.54009	2.675711	-140.014307	-2.370472	0.468396
bulkright_007.hys	63.65428	169.2335	36.23563	46444.21	67.59868	67.15705	148.9721	156.8177508	3.643801	24.33343	61.7752	1.152342	-140.012757	-2.370472	0.356365
bulkright_008.hys	61.38229	168.9541	42.36224	44275.23	64.86619	64.37353	178.3747	193.4708987	3.815996	8.894916	58.02195	1.592547	-140.011207	-2.370472	0.276198
bulkright_009.hys	51.29452	169.1222	38.75268	35231.41	55.21208	54.56763	182.9244	199.3422753	4.800325	10.87573	48.1343	1.474134	-140.015054	-2.368219	0.101801
GB 000.hys	55.81184	166.6337	34.38968	39163.46	60.21084	59.44593	153.9651	162.8890241	4.254826	34.38968	54.60048	1	-140.021503	-2.373672	-0.029724
GB 001.hys	58.48627	166.3305	36.87574	41581.24	62.79089	61.86919	160.2238	170.5859189	4.000134	27.51577	56.84304	1.114305	-140.021796	-2.373848	-0.014051
GB 002.hys	57.40537	166.6682	34.94775	40595.99	61.59965	60.98217	153.6783	162.538574	4.105533	34.94775	56.2131	1	-140.02205	-2.374141	-0.020915
GB 003.hys	57.81123	166.7243	43.05059	40964.65	61.26338	60.7158	188.4557	206.5556059	4.069957	9.606614	54.60802	1.577115	-140.022304	-2.374434	-0.020444
GB 004.hys	56.84955	166.4895	36.18681	40093.62	60.73782	60.30017	160.1207	170.4583815	4.152518	21.74672	54.80434	1.194531	-140.022596	-2.374668	-0.019554
GB 005.hys	59.39907	166.4924	44.34727	42421.82	63.00535	62.21478	190.7687	209.5966707	3.924687	0.71575	53.00179	2.453993	-140.022948	-2.374942	-0.020556
GB 006.hys	60.00145	166.2865	43.21487	42980.85	63.35071	62.88738	184.6845	201.6286724	3.868851	0.357761	52.70426	2.646408	-140.023261	-2.375293	-0.01216
GB 007.hys	59.0865	166.2858	48.4359	42133.1	62.43961	61.66133	209.0694	234.1873806	3.946678	0.064856	50.49375	3.252903	-140.023573	-2.375567	-0.015213
GB 008.hys	55.87968	167.1628	42.95088	39223.96	59.4355	58.79864	192.1459	211.4144739	4.261751	2.782486	51.02557	1.997217	-140.023846	-2.375918	-0.005222
GB 009.hys	57.58685	166.3981	44.75561	40760.64	60.902	60.37529	196.4092	217.0748721	4.082323	0.344902	50.39142	2.685335	-140.02412	-2.37627	-0.002741
GB left 000.hys	50.90156	168.6211	39.41569	34898.32	54.76336	54.11008	186.9397	204.5703865	4.831781	1.73648	45.1726	2.089162	-140.009237	-2.360215	0.09826
GB left 001.hys	52.84022	167.8769	37.7232	36555.48	57.18622	56.17789	174.8103	188.9093877	4.592387	10.35158	49.59727	1.478716	-140.009511	-2.360508	0.066793
GB left 002.hys	50.7817	168.1897	35.87116	34797.01	54.84007	54.29824	170.3764	183.2815688	4.833452	18.86579	48.47573	1.241814	-140.009823	-2.360859	0.03866
GB left 003.hys	52.94477	167.1212	31.94002	36645.84	57.38105	56.86903	147.1283	155.4355502	4.56044	31.89431	51.63386	1.000539	-140.010096	-2.361172	0.032967
GB left 004.hys	51.30767	167.9568	35.08916	35242.58	55.54864	54.8976	165.6052	177.2826077	4.765735	7.73491	47.52362	1.540555	-140.010409	-2.361543	-0.005869
GB left 005.hys	51.5808	167.2846	33.52386	35474.97	56.13788	55.32331	157.6986	167.4687322	4.715568	15.94666	48.97644	1.271913	-140.010682	-2.361836	-0.002786
GB left 006.hys	50.05312	168.043	31.33273	34184.02	54.77926	54.0755	150.1487	158.2429485	4.915835	31.33273	48.71233	1	-140.010995	-2.362168	-2.60E-05
GB left 007.hys	51.74737	167.1256	33.14838	35617.03	56.29023	55.52868	155.621	164.915951	4.692293	23.53035	49.84202	1.127915	-140.011229	-2.362481	-0.013121
GB left 008.hys	52.74091	166.9051	38.55688	36469.75	57.01848	55.98752	178.8835	194.1247373	4.576537	1.180602	46.47326	2.197896	-140.011483	-2.362793	-0.002755
GB left 009.hys	52.35607	166.9472	44.38839	36138.36	56.13839	55.17686	206.8807	231.1959795	4.619667	0.382143	45.22534	2.645938	-140.011796	-2.363125	-0.002885
GB right 000.hys	52.17616	167.612	38.96179	35983.93	55.86402	55.40263	181.9782	198.1166716	4.657968	16.42922	49.67673	1.330998	-140.017264	-2.370098	-0.024271
GB right 001.hys	50.87482	166.7439	40.09588	34875.7	54.92288	53.99379	190.2274	208.8837082	4.781092	1.359336	44.92327	2.181133	-140.017577	-2.370371	-0.028211
GB right 002.hys	52.9869	167.1876	35.09532	36682.28	57.13286	56.55976	162.3513	173.2247103	4.557722	35.09532	51.79594	1	-140.017831	-2.370684	-0.024123
GB right 003.hys	56.18837	166.6011	42.37864	39499.8	59.61685	59.13681	188.9228	207.1685733	4.217769	0.320771	48.66928	2.662645	-140.018104	-2.371016	-0.014088
GB right 004.hys	57.23878	166.4567	39.95863	40445.11	60.94374	60.36307	176.0404	190.4798061	4.115619	11.56388	54.23504	1.471061	-140.018358	-2.371348	-0.009138
GB right 005.hys	56.39573	166.4868	39.9437	39685.6	60.12557	59.52176	177.6506	192.5414415	4.195143	12.93812	53.55845	1.430724	-140.018632	-2.371641	-0.005944
GB right 006.hys	57.23126	166.1678	43.61164	40438.31	60.67017	60.08889	192.1502	211.4201021	4.109168	1.128412	51.32568	2.299951	-140.018905	-2.371895	-0.005918
GB right 007.hys	55.76798	166.556	35.85416	39124.37	59.79558	59.25201	160.6019	171.0541162	4.257091	35.54918	54.591	1.003367	-140.019159	-2.372168	-0.005111
GB right 008.hys	56.38802	166.8542	36.35834	39678.68	60.73122	59.82989	161.7187	172.4389026	4.205135	23.65657	54.48274	1.165169	-140.019432	-2.372461	-0.002265
GB right 009.hys	57.65215	166.1951	35.467	40819.97	61.6589	61.16659	155.5331	164.8082133	4.071417	35.467	56.48068	1	-140.019764	-2.372774	-0.017326

126

Grain boundary (6)

Indent	hc(nm)	Pmax(µN)	S(µN/nm)	A(nm^2)	hmax(nm)	heff(nm)	Er(GPa)	E(GPa)	H(GPa)	A	hf(nm)	m	X(mm)	Y(mm)
bulkbottom_000.hys	48.83794	168.0533	39.66919	33172.51	52.80634	52.01522	192.9741	212.5100828	5.066042	18.7284	46.54501	1.291249	-140.056924	1.503386
bulkbottom_001.hys	51.02843	167.7952	36.95972	35005.7	54.82797	54.43339	175.0226	189.180085	4.793367	36.95972	49.89344	1	-140.055374	1.503386
bulkbottom_002.hys	53.387	166.6131	48.30498	37029.17	56.85352	55.97389	222.4102	252.7271497	4.499509	0.389601	46.62529	2.710376	-140.053824	1.503386
bulkbottom_003.hys	51.18864	166.9926	46.26047	35141.52	54.61447	53.89601	218.6425	247.4371775	4.752004	0.442285	44.38599	2.634475	-140.056924	1.501836
bulkbottom_004.hys	49.98241	167.1192	36.53279	34124.79	54.23456	53.41329	175.2196	189.4314279	4.897297	30.41431	48.51068	1.071725	-140.055374	1.501836
bulkbottom_005.hys	50.61396	166.9732	40.96784	34655.44	54.26587	53.67074	194.9809	215.1729064	4.818095	16.35354	48.13627	1.357915	-140.053824	1.501836
bulkbottom_006.hys	50.27309	167.954	39.19591	34368.57	54.22424	53.48683	187.3246	205.0737933	4.886847	29.84516	48.73611	1.10869	-140.056924	1.500286
bulkbottom_007.hys	51.40737	167.1347	35.57247	35327.33	55.82181	54.93119	167.6847	179.8900191	4.731033	35.53926	50.23104	1.000367	-140.055374	1.500286
bulkbottom_008.hys	51.82005	167.1062	33.94877	35679.1	56.07766	55.51178	159.2399	169.3694769	4.683588	33.94877	50.58947	1	-140.053824	1.500286
bulkbottom_009.hys	55.71747	166.1335	34.55134	39079.37	59.85446	59.3237	154.8552	163.9777514	4.251182	13.38145	52.84285	1.347845	-140.056694	1.505563
bulktop_000.hys	57.82485	169.4811	45.54106	40977.05	61.19873	60.61598	199.3277	220.9791898	4.136002	6.466152	54.12005	1.745513	-140.050541	1.515128
bulktop_001.hys	58.70016	169.2313	42.96889	41777.5	62.216	61.654	186.2592	203.6812277	4.050776	0.70602	52.09468	2.427171	-140.048991	1.515128
bulktop_002.hys	57.4828	169.3767	50.82997	40666.2	60.47136	59.98196	223.3253	254.0184379	4.165048	0.99445	51.82516	2.447857	-140.047441	1.515128
bulktop_003.hys	56.67783	168.8417	47.3756	39939	60.22454	59.35075	210.0347	235.5110807	4.227489	5.207451	52.77027	1.846429	-140.050541	1.513578
bulktop_004.hys	56.56263	168.0139	44.5673	39835.43	59.75074	59.39004	197.8411	218.9873824	4.2177	1.430997	50.96163	2.235718	-140.048991	1.513578
bulktop_005.hys	57.70236	168.0911	47.56007	40865.6	61.54813	60.35308	208.4483	233.3370539	4.113267	5.572397	53.89718	1.826645	-140.047441	1.513578
bulktop_006.hys	54.90401	168.4004	39.59106	38357.98	58.80796	58.09413	179.1035	194.4076337	4.390232	20.08685	52.71739	1.264075	-140.050541	1.512028
bulktop_007.hys	53.03776	168.0505	36.91266	36726.3	57.11759	56.45225	170.656	183.635032	4.575753	36.91266	51.89959	1	-140.048991	1.512028
bulktop_008.hys	57.09507	167.409	37.95643	40315.17	61.01719	60.40299	167.4889	179.6440286	4.152507	30.71593	55.62269	1.083832	-140.047441	1.512028
bulktop_009.hys	53.12773	164.499	33.28359	36804.21	57.64394	56.83449	153.715	162.5833735	4.46957	1.484887	46.76172	2.038053	-140.051835	1.511781
GB 000.hys	50.06214	169.2784	40.92389	34191.57	53.83541	53.16445	196.0885	216.64734	4.95088	11.65656	47.05123	1.477903	-140.065979	1.507813
GB 001.hys	53.81997	168.8329	41.4462	37406.24	57.53788	56.87512	189.8661	208.4082942	4.513495	0.570969	46.82977	2.465999	-140.065452	1.507774
GB 002.hys	56.65114	168.4024	39.81041	39915	60.45792	59.82373	176.5482	191.1292716	4.219024	33.83885	55.31578	1.065681	-140.065003	1.507774
GB 003.hys	54.74398	168.4466	40.95584	38216.79	58.31779	57.82864	185.6195	202.8465518	4.407658	14.52129	52.07035	1.400061	-140.064514	1.507774
GB 004.hys	53.00146	168.4756	51.7408	36694.88	56.40509	55.44357	239.3124	276.9991343	4.591254	1.771051	48.03641	2.274825	-140.063987	1.507715
GB 005.hys	53.98937	167.325	48.21015	37554.25	57.37543	56.59243	220.4163	249.922275	4.455553	0.175275	46.35466	2.949737	-140.063343	1.507695
GB 006.hys	51.16586	167.4978	37.39817	35122.19	55.24531	54.52493	176.8049	191.4578205	4.769003	10.62936	47.96138	1.465481	-140.062249	1.507715
GB 007.hys	51.25068	167.3376	37.20194	35194.18	55.36892	54.62425	175.6972	190.0412743	4.754696	37.20194	50.12616	1	-140.062679	1.50752
GB 008.hys	51.5136	167.8665	44.20308	35417.73	55.07912	54.36181	208.1024	232.8639494	4.739617	4.982114	47.45161	1.819615	-140.061721	1.507598
GB 009.hys	52.25989	167.0193	37.70993	36055.76	56.36132	55.58168	175.9556	190.3714419	4.632249	7.180499	48.47478	1.604608	-140.061155	1.507617
gb bottom 000.hys	55.21018	167.6588	40.71838	38628.78	58.98067	58.29833	183.5565	200.1624359	4.340257	2.368077	50.00631	2.013836	-140.058569	1.506578
gb bottom 001.hys	54.75888	167.5246	39.78529	38229.93	59.78175	57.91692	180.2833	195.9272459	4.382027	11.76289	51.76221	1.461676	-140.058042	1.506617
gb bottom 002.hys	51.93608	167.7851	35.37917	35778.29	55.92698	55.49294	165.7192	177.4251841	4.689578	25.96789	50.18927	1.118332	-140.057475	1.506734
gb bottom 003.hys	53.50537	167.2948	46.99596	37132.09	57.28447	56.17519	216.083	243.8679785	4.505396	1.096361	47.76864	2.361546	-140.056929	1.506871
gb bottom 004.hys	51.65979	168.1409	38.75495	35542.3	55.67489	54.91371	182.1332	198.3172977	4.730726	38.70061	50.57268	1.000569	-140.056245	1.506852
gb bottom 005.hys	53.49043	166.7407	41.62632	37119.09	56.99654	56.49467	191.4274	210.4654778	4.492048	0.84138	47.05648	2.356216	-140.055561	1.5065
gb bottom 006.hys	55.35769	166.9482	39.89047	38759.55	59.31571	58.49656	179.5207	194.9445818	4.307279	23.5729	53.44087	1.208003	-140.055034	1.506578
gb bottom 007.hys	52.81243	167.6939	40.01981	36531.48	56.48436	55.95513	185.5138	202.7087682	4.590394	9.571387	49.51388	1.537192	-140.054487	1.506715
gb bottom 008.hys	54.17826	167.4903	47.48249	37719.6	57.53043	56.82382	216.6131	244.6055429	4.440405	2.837573	49.5663	2.057465	-140.053862	1.506852
gb bottom 009.hys	55.13055	167.1675	32.94559	38558.27	59.6233	58.93609	148.6529	156.4317085	4.335451	32.94559	53.86204	1	-140.053257	1.50693
gb top 000.hys	56.03248	166.7328	43.37103	39360.39	59.45643	58.91573	193.689	213.4573512	4.236056	5.271564	52.03242	1.790507	-140.051499	1.508024
gb top 001.hys	53.52685	166.7551	36.87081	37150.78	57.34478	56.91886	169.4859	182.1574739	4.488604	20.42065	51.37403	1.226003	-140.050874	1.508082
gb top 002.hys	55.84634	166.9482	53.3851	39194.22	58.60981	58.19177	238.9152	276.4183938	4.259511	0.481251	49.65967	2.728312	-140.050229	1.508004
gb top 003.hys	57.15806	166.5266	46.05094	40372.1	60.64413	59.87016	203.0639	226.012584	4.124794	0.661489	50.80253	2.507546	-140.049702	1.507945
gb top 004.hys	53.29548	167.1058	37.96766	36949.7	57.36678	56.59643	175.0021	189.1539332	4.52252	13.66171	50.49987	1.385183	-140.049155	1.507809
gb top 005.hys	57.78451	166.8803	47.95496	40940.33	61.26707	60.39447	209.9871	235.4458343	4.076184	4.754736	53.81962	1.889358	-140.048081	1.508414
gb top 005x.hys	55.35592	167.051	36.6282	38757.99	59.26363	58.77646	164.8427	176.3293104	4.310105	36.6282	54.21574	1	-140.048667	1.508492
gb top 006.hys	58.16153	166.6202	42.72527	41284.08	61.71699	61.08638	186.3066	203.743167	4.035944	7.146025	54.54659	1.676954	-140.047436	1.508395
gb top 007.hys	56.32268	166.8942	45.60419	39620.1	60.02403	59.0674	202.9933	225.9171934	4.212361	2.986608	51.69656	2.014097	-140.046909	1.508629
gb top 008.hys	55.15968	166.7743	40.39628	38584.05	59.06148	58.25602	182.21	198.4167099	4.322365	16.17969	52.662	1.354991	-140.046362	1.508766
gb top 009.hys	55.60507	166.5527	41.27399	38979.32	59.34953	58.63154	185.2227	202.3293399	4.272848	7.813757	52.06932	1.626205	-140.045913	1.50859

Appendix F Sample I grain boundaries - Induced mechanical properties

Grain boundary (4)

Data Set	Row	Indent	hc(nm)	Pmax(µN)	S(µN/nm)	A(nm^2)	hmax(nm)	heff(nm)	Er(GPa)	H(GPa)	A	hf(nm)	m	X(mm)	Y(mm)	Drift Correc
1	4	1	49.25412	167.9492	36.05024	36406.55	53.41446	52.74818	167.3991	4.61316	34.95368	48.03288	1.012138	-136.0928	7.712641	-0.004893
1	4	2	48.15776	167.943	43.84828	35453.96	51.66496	51.03033	206.3265	4.736932	10.8853	45.12754	1.541159	-136.0932	7.712641	-0.015256
1	4	3	48.64973	167.9757	45.47451	35879.97	52.22734	51.42011	212.7045	4.681601	3.650463	44.24359	1.942834	-136.0936	7.712641	-0.00288
1	4	4	48.2102	167.6202	43.92972	35499.27	51.68428	51.07194	206.5778	4.721793	0.232821	40.4485	2.784178	-136.094	7.712641	-0.004565
1	4	5	48.66646	168.3009	42.63868	35894.5	52.33675	51.62682	199.3997	4.688765	24.23079	46.77991	1.227954	-136.0944	7.712641	-0.01511
1	4	6	48.43926	168.0947	45.90933	35697.43	52.05061	51.18535	215.2867	4.708873	3.612521	44.03684	1.95237	-136.0948	7.712641	-0.013848
1	4	7	46.17355	168.3543	34.40478	33759.67	50.4469	49.84356	165.9031	4.986845	7.514531	42.3095	1.539655	-136.0952	7.712641	-0.02123
1	4	8	46.13381	168.0935	39.32041	33726.12	50.28387	49.34004	189.701	4.984075	39.32041	45.06507	1	-136.0956	7.712641	-0.020765
1	4	9	51.28977	167.2794	38.61274	38206.49	55.17355	54.53894	175.0237	4.378297	34.52922	50.0121	1.044922	-136.096	7.712641	-0.015767
1	4	10	49.47798	167.4777	49.16577	36602.5	53.03766	52.03277	227.6891	4.575581	1.049234	43.8244	2.409699	-136.0964	7.712641	-0.014986
1	4	11	50.61717	167.5289	35.30415	37607.27	54.80897	54.17615	161.2964	4.454695	35.30415	49.43085	1	-136.0968	7.712641	-0.015459
1	4	12	46.85487	168.5171	34.45778	34337.14	51.27628	50.52277	164.7555	4.907722	34.45778	45.63223	1	-136.0972	7.712641	-0.016022
1	4	13	51.73835	167.4115	32.5807	38608.62	56.33877	55.59213	146.9106	4.336119	22.42273	49.74343	1.13824	-136.0976	7.712641	-0.018468
1	4	14	49.29788	167.8148	43.04933	36444.82	53.12836	52.22153	199.7944	4.604628	2.221158	44.14905	2.070823	-136.098	7.712641	-0.028048
1	4	15	51.44044	167.3495	44.29605	38341.34	55.0975	54.27393	200.4316	4.364728	2.056445	46.27906	2.116176	-136.0984	7.712641	-0.018749
1	4	16	49.3807	167.9017	46.226	36517.3	52.89407	52.10485	214.3245	4.597869	2.185399	44.38774	2.124643	-136.0988	7.712641	-0.013703
1	4	17	50.59077	167.7169	39.89796	37583.84	54.4646	53.7435	182.3412	4.462474	18.89184	48.31661	1.290996	-136.0992	7.712641	-0.015076
1	4	18	48.21909	168.6644	38.27759	35506.94	52.07972	51.52385	179.9794	4.750181	12.86221	45.31392	1.409314	-136.0996	7.712641	-0.011557
1	4	19	49.9671	167.2873	40.39335	37032.35	53.8572	53.07319	185.9748	4.517328	20.64137	47.83827	1.26403	-136.1	7.712641	-0.000395
1	4	20	49.54471	167.7547	44.27702	36661.01	52.82898	52.38628	204.8854	4.575835	1.980554	44.32685	2.127197	-136.1004	7.712641	0.001009
1	5	1	50.314	168.0214	49.58837	37338.63	53.41837	52.85524	227.3712	4.499936	2.464303	45.62409	2.134141	-136.1004	7.710641	-0.004778
1	5	2	46.37165	168.1441	44.19881	33927.11	50.31162	49.22485	212.6043	4.956038	5.325141	42.39104	1.796354	-136.1	7.710641	-0.013004
1	5	3	48.50453	168.3699	44.88553	35753.99	51.98622	51.31785	210.3192	4.70912	0.270118	40.98262	2.755256	-136.0996	7.710641	-0.01499
1	5	4	47.99477	168.2522	42.10851	35313.35	51.7084	50.99153	198.5341	4.764549	4.712284	43.76722	1.80803	-136.0992	7.710641	-0.002049
1	5	5	47.88453	167.9887	45.85563	35218.39	51.69389	50.6321	216.4924	4.769913	8.021522	44.492	1.676053	-136.0988	7.710641	-0.011978
1	5	6	49.34338	167.9467	50.51816	36484.63	52.96559	51.83674	234.3297	4.603219	1.033218	43.74297	2.434595	-136.0984	7.710641	-0.001148
1	5	7	48.54036	168.0032	39.13716	35785.06	52.3453	51.75987	183.3045	4.694785	39.13716	47.46719	1	-136.098	7.710641	0.003311
1	5	8	47.46629	168.5495	44.70835	34859.19	50.98362	50.29377	212.1606	4.835153	3.693391	43.02981	1.926792	-136.0976	7.710641	-0.003151
1	5	9	47.45998	168.8044	38.3569	34853.79	51.64634	50.76064	182.0343	4.843215	38.25672	46.35512	1.001054	-136.0972	7.710641	-0.006604
1	5	10	49.75857	167.9788	51.73996	36848.8	53.12535	52.19352	238.8082	4.558596	0.155129	42.29687	3.048315	-136.0968	7.710641	-0.010578
1	5	11	48.53025	167.5971	37.3192	35776.3	52.43252	51.89844	174.8113	4.684586	36.80963	47.38288	1.005489	-136.0964	7.710641	-0.001301
1	5	12	48.40112	167.7582	44.16797	35664.4	51.90898	51.24976	207.2167	4.703798	1.399262	42.75302	2.237051	-136.096	7.710641	-0.012832
1	5	13	48.9485	168.3878	45.92886	36139.84	52.29145	51.69821	214.056	4.65934	2.911669	44.27653	2.024312	-136.0956	7.710641	-0.0086
1	5	14	46.11109	168.8223	39.0824	33706.95	50.26083	49.35083	188.6063	5.008532	21.8807	44.05561	1.225844	-136.0952	7.710641	-0.004293
1	5	15	48.66717	168.3988	45.40008	35895.12	52.05362	51.44908	212.3116	4.691413	0.524566	41.94276	2.562891	-136.0948	7.710641	-0.002547
1	5	16	48.69604	167.6885	34.39565	35920.19	53.01789	52.3525	160.7937	4.668363	34.39552	47.47721	1.000001	-136.0944	7.710641	-0.015643
1	5	17	48.87654	167.6261	44.54164	36077.17	52.75011	51.69906	207.7709	4.646321	3.850758	44.50326	1.91207	-136.094	7.710641	-0.01207
1	5	18	47.36528	167.8561	35.32839	34772.7	51.72229	50.92876	167.857	4.827239	22.36955	45.35511	1.173077	-136.0936	7.710641	-0.010178
1	5	19	49.44461	168.5955	43.54567	36574.84	53.15072	52.35018	201.7384	4.609601	4.363191	45.17207	1.853998	-136.0932	7.710641	-0.000555
1	5	20	47.30964	168.2204	41.71302	34725.1	51.33738	50.33424	198.3283	4.844347	8.410798	43.86401	1.604401	-136.0928	7.710641	-0.011763
1	6	1	50.83582	167.7859	52.30484	37801.57	54.07108	53.2417	238.3536	4.438595	0.216573	43.75617	2.956979	-136.0928	7.708641	-0.008392
1	6	2	49.38896	167.9654	44.01595	36524.53	53.05436	52.25097	204.0575	4.598701	11.5439	46.44293	1.522019	-136.0932	7.708641	-0.006175
1	6	3	49.94718	168.2847	46.88875	37014.79	53.5445	52.63895	215.9314	4.546418	7.432078	46.4797	1.716134	-136.0936	7.708641	0.001829
1	6	4	49.27874	167.5809	45.04787	36428.08	52.97166	52.06879	209.1178	4.600322	3.031954	44.63054	1.999496	-136.094	7.708641	-0.018205
1	6	5	49.38842	167.5208	37.67868	36524.05	53.56731	52.72294	174.6791	4.58659	37.67868	48.27691	1	-136.0944	7.708641	-0.007054
1	6	6	50.47793	167.7736	39.72164	37483.77	54.67664	53.64573	181.7776	4.475901	20.61891	48.3398	1.256218	-136.0948	7.708641	-0.029963
1	6	7	49.23807	168.1532	43.88126	36392.53	53.05774	52.11207	203.8017	4.620543	6.601017	45.52869	1.717999	-136.0952	7.708641	-0.015022
1	6	8	45.69858	168.0607	42.84402	33359.74	49.25411	48.64054	207.8327	5.037831	2.839578	40.84554	1.987194	-136.0956	7.708641	-0.001363
1	6	9	51.37784	167.1011	35.83687	38285.29	55.61822	54.87496	162.274	4.364629	35.36357	50.18775	1.00523	-136.096	7.708641	-0.020973
1	6	10	48.0471	167.9533	39.96566	35358.47	51.9122	51.19893	188.3107	4.750014	30.79352	46.55583	1.104859	-136.0964	7.708641	-0.021612
1	6	11	48.70648	167.2811	43.27493	35929.26	53.39579	51.60563	202.2772	4.655847	6.004383	44.86527	1.743704	-136.0968	7.708641	-0.032236
1	6	12	45.85215	167.7671	46.05008	33488.81	49.57116	48.58451	222.9541	5.009648	0.092906	37.30824	3.095202	-136.0972	7.708641	-0.02429
1	6	13	47.27416	168.5631	39.14876	34694.75	50.98563	50.50344	186.2177	4.85846	20.30188	45.10087	1.254745	-136.0976	7.708641	-0.029298
1	6	14	47.53108	167.9776	46.28691	34914.72	51.22631	50.25287	219.4768	4.811083	2.68504	42.78656	2.057369	-136.098	7.708641	-0.017821
1	6	15	47.68719	168.017	39.11207	35048.7	51.5349	50.90903	185.1014	4.793815	15.54536	45.09827	1.352666	-136.0984	7.708641	-0.011437
1	6	16	46.62022	167.943	42.80506	34137.75	50.18186	49.5628	205.2639	4.919569	10.38622	43.50239	1.544667	-136.0988	7.708641	-0.019471
1	6	17	45.60252	168.604	41.29619	33279.12	49.18736	48.66462	200.5668	5.066362	11.41033	42.57724	1.490981	-136.0992	7.708641	-0.005321
1	6	18	47.9292	168.6185	39.83946	35256.85	51.89223	51.10353	187.9864	4.782573	35.69122	46.68228	1.04	-136.0996	7.708641	-0.013331
1	6	19	45.47703	167.9135	44.23216	33173.93	48.95106	48.32417	215.1664	5.061609	3.317816	40.89559	1.956852	-136.1	7.708641	-0.028087
1	6	20	50.72453	167.4405	33.72315	37702.62	55.18829	54.4484	153.8782	4.441084	33.72315	49.48325	1	-136.1004	7.708641	-0.039124
2	1	1	53.61183	169.5594	39.67223	40309.62	57.30078	56.81734	175.0722	4.206425	0.010766	41.63277	3.55277	-136.1005	7.709266	0.205067
2	1	2	50.64704	169.2752	38.51058	37633.79	54.71139	53.94371	175.8838	4.497959	2.09979	45.09421	2.013285	-136.1001	7.709266	0.167386
2	1	3	51.1816	169.4417	37.0667	38109.82	55.26326	54.61005	168.2288	4.446144	19.91252	48.9586	1.236299	-136.0997	7.709266	0.131946
2	1	4	49.78842	168.5949	38.84863	36875.05	53.74771	53.04326	179.2438	4.57206	4.402241	45.30948	1.782063	-136.0993	7.709266	0.094413
2	1	5	51.22201	168.3486	39.69908	38145.93	54.88252	54.40248	180.0907	4.41328	2.769901	46.14993	1.946071	-136.0989	7.709266	0.086874
2	1	6	50.73601	168.8653	44.96536	37712.82	54.28384	53.5526	205.1485	4.477664	2.665185	45.89758	2.038374	-136.0985	7.709266	0.072069
2	1	7	49.84754	168.3776	42.26918	36927.06	53.36891	52.83514	194.8885	4.559735	3.944938	45.38785	1.869551	-136.0981	7.709266	0.063436
2	1	8	52.43588	167.715	40.47831	39237.86	56.77501	55.54338	181.0525	4.274314	11.14935	49.37177	1.48953	-136.0977	7.709266	0.021711
2	1	9	49.69457	167.8044	34.33198	36792.55	53.83717	53.36034	158.5819	4.560825	25.71614	47.93758	1.109472	-136.0973	7.709266	-0.001606
2	1	10	49.83717	167.8555	39.21652	36917.93	54.01059	53.04734	180.8361	4.546721	24.30288	47.96163	1.188187	-136.0969	7.709266	0.007733
2	1	11	49.63572	167.6522	39.53856	36740.87	53.40486	52.81588	182.7599	4.563098	19.62644	47.42006	1.272533	-136.0965	7.709266	0.00316
2	1	12	49.52969	167.4936	45.81578	36647.84	53.13886	52.27155	212.0439	4.570355	10.03855	46.43759	1.595805	-136.0961	7.709266	0.009155
2	1	13	48.36343	168.2551	42.82971	35631.78	52.08502	51.30978	201.0302	4.722052	19.49626	46.14992	1.313454	-136.0957	7.709266	0.015331
2	1	14	44.80141	168.2631	38.86935	32610.23	48.78236	48.04811	190.7064	5.159826	4.729134	40.43223	1.759296	-136.0953	7.709266	0.001437

```
2  1  15  47.49456  167.7092  35.63766  34883.42  51.86202  51.02402  169.0575  4.807705  26.16481  45.76007  1.118572  -136.0949  7.709266  -0.003536
2  1  16  45.71447  168.443   41.13975  33373.08  49.59838  48.78527  199.5255  5.04727   0.951329  39.34457  2.305756  -136.0945  7.709266  -0.026897
2  1  17  45.1478   167.7646  40.49634  32898.69  48.86349  48.25484  197.816   5.099432  2.920501  40.20754  1.94252   -136.0941  7.709266  -0.015909
2  1  18  48.99192  167.5512  46.24814  36177.67  52.41798  51.70908  215.4313  4.631343  0.068584  40.15828  3.188297  -136.0937  7.709266  -0.019854
2  1  19  48.92023  167.4086  40.04103  36115.21  52.70161  52.05593  186.6788  4.635403  1.70445   43.24305  2.107878  -136.0933  7.709266  -0.031223
2  1  20  50.38416  167.0862  37.59806  37400.72  54.6613   53.71717  172.2504  4.467461  15.56651  47.79011  1.333718  -136.0929  7.709266  -0.022756
2  2  1   48.78663  167.2581  38.8821   35998.93  52.95118  52.01288  181.5682  4.646195  38.41084  47.6899   1.004954  -136.0929  7.707266  -0.019724
2  2  2   48.24049  168.0047  46.02445  35525.44  52.02132  50.97825  216.3484  4.729137  3.684485  43.86909  1.947534  -136.0933  7.707266  -0.015253
2  2  3   49.10549  167.6428  38.46557  36276.73  53.09966  52.37418  178.934   4.621221  18.10129  46.7546   1.28941   -136.0937  7.707266  -0.011937
2  2  4   47.26681  168.0901  47.39961  34688.48  50.74343  49.92649  225.4847  4.845704  0.175632  39.53065  2.931516  -136.0941  7.707266  -0.015578
2  2  5   48.30036  168.3588  40.93852  35577.2   52.06742  51.38471  192.3008  4.732211  14.01892  45.57501  1.412701  -136.0945  7.707266  -0.011646
2  2  6   48.44357  167.9307  46.8184   35701.16  52.63387  51.13371  219.5382  4.703788  7.133301  44.92738  1.730298  -136.0949  7.707266  -0.00889
2  2  7   47.52704  167.6533  35.20531  34911.27  51.86717  51.09866  166.9399  4.802269  27.93739  45.91361  1.088804  -136.0953  7.707266  -0.020632
2  2  8   47.30345  167.6947  33.73622  34719.8   51.66043  51.03152  160.4141  4.829943  33.73622  46.06076  1         -136.0957  7.707266  -0.013315
2  2  9   50.93499  167.5079  44.01907  37889.86  54.63554  53.789    200.3615  4.420916  3.900355  46.55722  1.900425  -136.0961  7.707266  -0.006851
2  2  10  49.04966  167.3015  44.00441  36228.02  52.50507  51.90111  204.8371  4.618014  10.6393   46.00002  1.55213   -136.0965  7.707266  -0.016138
2  2  11  47.35688  167.5516  39.44181  34765.51  51.29219  50.54293  187.4206  4.819477  18.33808  45.03482  1.296615  -136.0969  7.707266  -0.016959
2  2  12  47.13784  168.2309  38.31861  34578.3   51.26323  50.43057  182.5756  4.865215  20.24547  44.96019  1.246011  -136.0973  7.707266  -0.036702
2  2  13  48.35161  167.8888  37.15468  35621.55  52.6552   51.7406   174.4183  4.713125  20.95793  46.23091  1.219323  -136.0977  7.707266  -0.01726
2  2  14  46.46774  168.0873  36.31913  34008.47  50.62708  49.93879  174.4925  4.942514  36.31913  45.31072  1         -136.0981  7.707266  -0.013753
2  2  15  48.28061  167.8205  33.62372  35560.12  52.78729  52.02396  157.9788  4.719347  22.81451  46.30968  1.144885  -136.0985  7.707266  -0.019484
2  2  16  49.13164  167.9203  43.52856  36299.56  52.66744  52.02492  202.4224  4.625959  2.70552   44.25664  2.013706  -136.0989  7.707266  -0.00791
2  2  17  48.98151  167.5541  38.56821  36168.6   53.19749  52.23978  179.6795  4.632584  7.274883  45.23762  1.611782  -136.0993  7.707266  -0.038361
2  2  18  51.17464  166.8711  36.18409  38103.6   55.38516  54.63343  164.2364  4.379404  36.01299  50.01306  1.001874  -136.0997  7.707266  -0.041108
2  2  19  56.14206  165.8978  38.41491  42662.41  60.29193  59.381    164.7828  3.888617  21.78849  54.10808  1.220985  -136.1001  7.707266  -0.037317
2  2  20  49.88988  167.9782  40.57699  36964.32  53.74729  52.99468  186.9921  4.544333  14.09549  47.17199  1.406535  -136.1005  7.707266  0.002606
2  3  1   49.51931  167.0987  36.22861  36638.73  53.73694  52.97856  167.6935  4.560711  36.22861  48.36622  1         -136.1005  7.705266  -0.016873
2  3  2   47.641    167.7976  43.5325   35009.03  50.95125  50.5319   206.1381  4.79298   7.540101  44.10444  1.667504  -136.1001  7.705266  -0.015973
2  3  3   49.01379  167.5098  43.12861  36196.74  52.76234  51.92676  200.8471  4.627759  1.71089   43.55009  2.156733  -136.0997  7.705266  -0.014037
2  3  4   47.65025  167.7231  39.54988  35016.98  51.78785  50.83085  187.2581  4.789766  17.03772  45.21223  1.324896  -136.0993  7.705266  0.00232
2  3  5   47.26559  167.4611  36.77812  34687.44  51.49422  50.68055  174.9598  4.827717  33.03661  45.9347   1.042294  -136.0989  7.705266  -0.012745
2  3  6   46.96394  167.8123  39.17919  34430     51.43343  50.17634  187.0776  4.874014  23.04189  45.00226  1.207994  -136.0985  7.705266  -0.00799
2  3  7   48.07707  167.9714  47.09677  35384.32  51.97133  50.75195  221.8301  4.747058  3.614125  43.72811  1.969385  -136.0981  7.705266  -0.006577
2  3  8   48.46696  168.1495  43.35629  35721.43  52.11288  51.3757   203.2462  4.707245  6.047965  44.62346  1.741022  -136.0977  7.705266  -0.008262
2  3  9   49.25602  168.5616  47.71007  36408.22  52.44313  51.90581  221.5364  4.629768  4.051952  45.05908  1.937914  -136.0973  7.705266  -0.000787
2  3  10  48.24891  167.959   40.49611  35532.72  51.80466  51.35956  190.3417  4.726884  4.220402  43.80428  1.821632  -136.0969  7.705266  -0.006496
2  3  11  48.38336  168.0779  47.35345  35649.03  52.02414  51.04544  222.2095  4.714795  13.10485  45.6642   1.516084  -136.0965  7.705266  0.005155
2  3  12  47.73761  168.2522  48.5066   35092.02  51.11257  50.3391   229.4201  4.7946    2.419445  42.97151  2.124053  -136.0961  7.705266  -0.015352
2  3  13  47.20552  167.8996  39.44908  34636.1   50.79443  50.39761  187.805   4.847532  10.29893  43.99765  1.503711  -136.0957  7.705266  -0.012641
2  3  14  47.15242  167.6509  50.10638  34590.75  50.59328  49.66185  238.6975  4.846698  0.168968  39.64349  2.994218  -136.0953  7.705266  -0.005001
2  3  15  50.95348  167.5084  46.59291  37906.33  54.48461  53.64984  212.0307  4.41901   4.040348  46.72823  1.925262  -136.0949  7.705266  -0.013293
2  3  16  49.38086  167.8919  42.48289  36517.43  53.3463   52.34485  196.9694  4.597582  7.37472   45.78079  1.660952  -136.0945  7.705266  -0.021084
2  3  17  48.20133  168.4719  38.45467  35491.6   52.34089  51.48712  180.8511  4.746811  18.20911  45.85055  1.286578  -136.0941  7.705266  -0.015195
2  3  18  47.23437  168.1897  45.81986  34660.74  50.77178  49.98737  218.0568  4.852455  3.970602  42.94342  1.918981  -136.0937  7.705266  0.003838
2  3  19  48.15968  168.0317  45.62776  35455.63  51.65201  50.92204  214.6947  4.739212  3.164633  43.58273  1.992837  -136.0933  7.705266  -0.01374
2  3  20  50.00307  168.1663  39.32035  37064.05  53.90858  53.21069  180.9572  4.53718   8.267944  46.46247  1.577857  -136.0929  7.705266  -0.00715
2  4  1   50.13556  167.8432  48.18598  37180.94  53.88954  52.74799  221.409   4.514226  12.78375  47.39935  1.535538  -136.0929  7.703266  0.001318
2  4  2   48.63958  168.1039  49.58067  35871.16  51.63316  51.18246  231.9394  4.686325  0.460643  42.11123  2.675476  -136.0933  7.703266  0.002594
2  4  3   49.77117  167.8476  46.15438  36859.88  53.20097  52.49866  212.9957  4.553667  2.762188  45.05708  2.04627   -136.0937  7.703266  -0.015956
2  4  4   50.11827  167.4523  42.08086  37165.67  53.9115   53.10274  193.3964  4.505563  11.22154  47.01007  1.508249  -136.0941  7.703266  0.002504
2  4  5   47.78859  168.0589  42.04467  35135.85  51.66851  50.78645  198.7332  4.783119  10.03056  44.60258  1.547071  -136.0945  7.703266  -0.017858
2  4  6   49.36613  167.7273  50.59218  36504.54  52.67117  51.85259  234.6091  4.594697  1.082534  43.82547  2.421247  -136.0949  7.703266  0.002057
2  4  7   49.65071  167.3531  38.52535  36754.03  53.94104  52.90869  178.0447  4.553326  6.748561  45.79827  1.636847  -136.0953  7.703266  -0.005011
2  4  8   48.08251  167.9425  36.63729  35389.01  52.31189  51.52045  172.5536  4.74561   36.59102  46.93423  1.000501  -136.0957  7.703266  -0.015892
2  4  9   46.81281  168.0453  41.46515  34301.36  50.67022  49.85232  198.3638  4.899086  10.56432  43.68756  1.521155  -136.0961  7.703266  -0.001667
2  4  10  51.33724  167.7897  38.32439  38248.96  55.19333  54.62085  173.6202  4.386777  16.80594  48.86499  1.314681  -136.0965  7.703266  -0.004791
2  4  11  59.37549  166.1079  35.35389  45762.71  63.51382  62.89932  146.4253  3.629765  35.35389  58.20088  1         -136.0969  7.703266  -0.032797
2  4  12  50.80981  167.9803  35.88921  37778.44  55.08781  54.32021  163.5975  4.446459  35.8702   49.63871  1.000208  -136.0973  7.703266  -0.012035
2  4  13  52.12946  167.2088  37.01521  38960.85  56.3927   55.51743  166.1502  4.291713  6.079273  48.06386  1.650007  -136.0977  7.703266  -0.018143
2  4  14  50.23631  167.995   37.40932  37269.93  54.50292  53.60436  171.6862  4.507521  37.40932  49.11363  1         -136.0981  7.703266  -0.011958
2  4  15  49.5843   167.3198  42.38118  36695.74  53.24019  52.54528  196.0199  4.559652  8.983793  46.26278  1.591324  -136.0985  7.703266  -0.014247
2  4  16  48.34512  168.2532  44.82652  35615.93  51.70555  51.16019  210.4494  4.7241    0.248590  40.72796  2.779387  -136.0989  7.703266  -0.020035
2  4  17  51.76212  167.4115  41.84918  38629.98  55.57913  54.76238  188.6512  4.333721  13.4953   49.00676  1.438777  -136.0993  7.703266  -0.002564
2  4  18  50.49432  167.4789  38.65078  37498.3   54.42374  53.74417  176.8428  4.466306  12.53399  47.57214  1.424381  -136.0997  7.703266  -0.025851
2  4  19  48.89498  167.7569  34.90028  36093.22  53.43259  52.50004  162.7612  4.647873  34.90028  47.6933   1         -136.1001  7.703266  -0.013174
2  4  20  54.01366  166.5482  45.80426  40679     57.50386  56.74073  201.2128  4.094205  6.612208  50.39295  1.745771  -136.1005  7.703266  -0.012832
2  5  1   50.33976  167.8316  47.30033  37361.42  53.93057  53.00092  216.814   4.49211   0.37906   43.42962  2.697498  -136.1005  7.701266  -0.015757
2  5  2   47.50694  168.2507  47.25706  34894.03  51.10959  50.17718  224.1434  4.821761  0.184927  39.80633  2.912891  -136.1001  7.701266  0.003212
2  5  3   49.00687  168.2975  43.02307  36190.7   52.55011  51.94072  200.3723  4.650296  16.48234  46.54731  1.378754  -136.0997  7.701266  0.00479
2  5  4   47.87927  168.371   45.00623  35213.87  51.29648  50.68507  212.4959  4.781383  7.469039  44.36415  1.689606  -136.0993  7.701266  -0.005143
2  5  5   47.63069  167.7816  41.98187  35000.19  51.28676  50.62809  198.8206  4.793734  2.648554  42.64607  1.99724   -136.0989  7.701266  -0.015964
2  5  6   49.29608  168.1663  45.75896  36443.25  53.00899  52.05237  212.3745  4.61447   23.20633  47.35041  1.279428  -136.0985  7.701266  -0.007679
2  5  7   48.68963  167.7729  37.76833  35914.63  52.78642  52.02125  176.5741  4.671437  20.2895   46.5183   1.238801  -136.0981  7.701266  -0.010409
2  5  8   50.08789  167.9178  39.85306  37138.86  54.1943   53.24795  183.2239  4.52135   27.48168  48.41035  1.148142  -136.0977  7.701266  -0.012388
2  5  9   49.25544  167.4067  41.03353  36407.71  52.97275  52.31526  190.536   4.598111  41.03353  48.2355   1         -136.0973  7.701266  -0.010032
```

2	5	10	47.17983	168.3523	42.0488	34614.15	50.85043	50.18263	200.2449	4.863685	4.241507	42.80684	1.842226	-136.0969	7.701266	-0.010897
2	5	11	47.08566	167.8845	38.60278	34533.77	51.21891	50.34743	184.0481	4.861459	8.749934	43.61165	1.5488	-136.0965	7.701266	-0.008986
2	5	12	46.08645	168.0645	36.33037	33686.16	50.13163	49.55595	175.3795	4.989127	27.14622	44.40865	1.112689	-136.0961	7.701266	-0.013671
2	5	13	47.9243	167.9899	41.14252	35252.63	51.71812	50.98664	194.1467	4.765316	10.43551	44.77477	1.521352	-136.0957	7.701266	-0.001743
2	5	14	51.44038	167.4493	49.44564	38341.28	54.80515	53.98028	223.7327	4.367338	2.559158	46.79854	2.120676	-136.0953	7.701266	0.002307
2	5	15	48.05096	168.1663	40.94918	35361.8	51.68365	51.13099	192.9358	4.755592	13.77151	45.3017	1.419456	-136.0949	7.701266	-0.003642
2	5	16	47.06692	168.004	34.49398	34517.79	51.43224	50.71982	164.4965	4.86717	34.49398	45.84929	1	-136.0945	7.701266	-0.009371
2	5	17	47.32239	168.0897	44.65626	34736	51.01042	50.14545	212.2889	4.839062	3.571395	42.85013	1.938143	-136.0941	7.701266	-0.010488
2	5	18	49.08361	167.8623	38.0627	36257.63	52.84769	52.39122	177.1066	4.62971	9.489595	45.71673	1.513438	-136.0937	7.701266	-0.006813
2	5	19	48.25316	167.3287	45.21988	35536.39	51.92792	51.02841	212.5336	4.708657	0.597174	41.6931	2.522829	-136.0933	7.701266	-0.010365
2	5	20	51.97802	167.1626	46.48032	38824.28	55.61986	54.67533	209.0029	4.305619	1.03898	46.14928	2.370708	-136.0929	7.701266	-0.010872
2	6	1	50.77602	167.7569	41.63525	37748.39	54.36069	53.79793	189.8658	4.444081	4.804727	46.56364	1.795462	-136.0929	7.699266	-0.010446
2	6	2	48.18713	168.0466	40.83511	35479.34	52.02017	51.27357	192.0794	4.736464	13.19137	45.37365	1.433672	-136.0933	7.699266	0.004994
2	6	3	48.58458	167.535	40.72369	35823.42	52.76489	51.67004	190.6331	4.676691	14.64699	45.93182	1.39482	-136.0937	7.699266	-0.002119
2	6	4	51.2033	167.3051	44.49897	38129.21	54.67314	54.02312	201.9091	4.387845	16.47625	48.76972	1.397272	-136.0941	7.699266	0.004898
2	6	5	46.67273	167.7961	41.1274	34182.33	50.54467	49.73267	197.0903	4.908855	16.11867	44.16546	1.364541	-136.0945	7.699266	-0.01911
2	6	6	49.5625	167.8142	36.77046	36676.61	53.67844	52.98537	170.1137	4.575509	36.77046	48.42154	1	-136.0949	7.699266	0.008365
2	6	7	49.62787	167.6947	35.70583	36733.98	53.98631	53.15029	165.0593	4.56511	35.70583	48.45373	1	-136.0953	7.699266	0.006193
2	6	8	49.82679	167.817	37.43559	36908.8	53.88021	53.18891	172.6452	4.546803	29.39519	48.28041	1.094958	-136.0957	7.699266	0.000705
2	6	9	49.94131	167.7592	45.1366	37009.62	53.60354	52.72883	207.877	4.532853	1.645479	44.55011	2.200533	-136.0961	7.699266	-0.004533
2	6	10	49.89769	167.6077	35.46001	36971.21	54.14851	53.44269	163.3961	4.533467	35.46001	48.71602	1	-136.0965	7.699266	0.013668
2	6	11	50.21406	167.5554	50.20071	37250.27	53.74508	52.71734	230.4518	4.498098	2.256515	45.46234	2.173646	-136.0969	7.699266	-0.006611
2	6	12	47.29171	168.0027	41.82544	34709.76	50.86029	50.30428	198.9068	4.840217	13.75523	44.55635	1.430985	-136.0973	7.699266	-0.000516
2	6	13	48.47912	168.1365	38.0943	35731.97	52.61276	51.78939	178.5527	4.705493	23.16904	46.52357	1.193063	-136.0977	7.699266	-0.001034
2	6	14	49.70724	167.6723	41.37758	36803.69	53.93207	52.74643	191.0972	4.555856	11.59439	46.71959	1.487282	-136.0981	7.699266	-0.014226
2	6	15	51.20703	167.8774	45.86404	38132.54	54.5975	53.95227	208.0939	4.40247	3.357073	46.71652	1.976805	-136.0985	7.699266	-0.008611
2	6	16	49.86701	167.4535	50.15726	36944.2	53.23492	52.37094	231.2041	4.532606	0.150817	42.25441	3.030199	-136.0989	7.699266	-0.023088
2	6	17	50.8617	166.4834	33.21186	37824.6	55.7753	54.62128	151.3006	4.401458	12.51503	47.84261	1.352279	-136.0993	7.699266	-0.122352
2	6	18	49.21702	167.8751	44.35842	36374.13	52.90302	52.05541	206.0699	4.615233	2.660327	44.36575	2.031874	-136.0997	7.699266	-0.004237
2	6	19	49.10046	167.363	36.07851	36272.34	53.13489	52.57961	167.8401	4.614067	26.5612	47.39253	1.11818	-136.1001	7.699266	-0.012397
2	6	20	49.64018	168.0962	48.73421	36744.78	53.31486	52.22711	225.2531	4.574695	0.13423	41.75305	3.036626	-136.1005	7.699266	-0.011706
2	7	1	52.32686	167.363	50.40366	39139.2	55.57655	54.8172	225.7308	4.276097	0.166059	44.83628	3.005891	-136.1005	7.697266	0.005966
2	7	2	47.83141	168.7504	41.41797	35172.68	51.53059	50.88716	195.6685	4.797769	14.30165	45.13799	1.411073	-136.1001	7.697266	0.015113
2	7	3	47.80244	168.1191	44.62615	35147.76	51.4051	50.6279	210.8995	4.783209	10.50637	44.73753	1.563561	-136.0997	7.697266	0.000443
2	7	4	49.47191	167.5064	43.93945	36597.18	53.10478	52.33107	203.5006	4.577029	5.476865	45.52951	1.784151	-136.0993	7.697266	-0.003263
2	7	5	47.10569	168.5756	35.86828	34550.86	51.34452	50.63058	170.9684	4.879057	35.86828	45.93073	1	-136.0989	7.697266	-0.012681
2	7	6	47.64113	168.6055	38.09486	35009.15	51.71514	50.96059	180.3892	4.816042	35.16413	46.39311	1.031979	-136.0985	7.697266	-0.001791
2	7	7	44.37876	168.6993	36.16677	32259.8	48.72058	47.87712	178.4075	5.229396	32.49212	43.01746	1.041843	-136.0981	7.697266	-0.001917
2	7	8	48.75466	167.5971	36.16666	35971.14	53.11877	52.23018	168.9531	4.659211	36.16666	47.59616	1	-136.0977	7.697266	-0.002634
2	7	9	50.03879	168.0626	41.66547	37095.54	53.76174	53.064	191.6683	4.530534	10.80265	46.9498	1.515809	-136.0973	7.697266	-0.005464
2	7	10	50.06074	167.8056	42.63293	37114.9	53.77607	53.01278	190.0676	4.521246	16.47834	47.60233	1.374587	-136.0969	7.697266	-0.007420
2	7	11	48.22112	168.4438	37.67465	35508.7	52.19153	51.57438	177.14	4.743734	22.30997	46.19975	1.202106	-136.0965	7.697266	-0.014362
2	7	12	44.30867	168.0731	34.38926	32201.86	48.79332	47.9742	169.792	5.219359	20.43408	42.13687	1.19437	-136.0961	7.697266	-0.017966
2	7	13	47.24875	167.839	39.69899	34673.04	50.8865	50.4196	188.8941	4.84062	12.66203	44.35677	1.434042	-136.0957	7.697266	0.000898
2	7	14	47.1763	168.6885	36.63188	34611.14	51.14042	50.63002	174.4561	4.873822	29.93199	45.66249	1.078733	-136.0953	7.697266	0.004977
2	7	15	47.40853	168.1785	33.18186	34809.72	51.71461	51.20982	157.5743	4.831366	33.18186	46.14143	1	-136.0949	7.697266	-0.001938
2	7	16	50.17671	167.5824	48.09031	37217.27	53.2934	52.79027	220.8616	4.502813	0.357458	43.27654	2.730108	-136.0945	7.697266	-0.011048
2	7	17	46.60109	168.3691	41.24248	34121.52	50.49496	49.6629	197.8178	4.934396	6.393337	42.75414	1.692321	-136.0941	7.697266	-0.010683
2	7	18	48.34867	168.2429	43.02242	35619	51.98687	51.28161	201.9709	4.723405	1.481405	42.68117	2.19927	-136.0937	7.697266	-0.014514
2	7	19	47.3117	168.3691	39.69439	34726.86	51.27151	50.49292	188.7258	4.848382	15.59949	44.73107	1.358405	-136.0933	7.697266	-0.006511
2	7	20	50.02565	167.5534	34.54046	37083.96	54.52712	53.66385	158.9168	4.518219	34.54046	48.81291	1	-136.0929	7.697266	-0.002465
2	8	1	50.14863	167.2618	51.24449	37192.48	53.42613	52.59663	235.426	4.497195	0.555542	43.95742	2.646821	-136.0929	7.695266	-0.004329
2	8	2	52.56627	167.334	50.43901	39356.02	56.24764	55.05443	225.2661	4.251803	1.638963	47.47662	2.284156	-136.0933	7.695266	0.004528
2	8	3	51.8327	167.7402	51.60364	38693.45	55.20011	54.27061	232.4323	4.335107	5.775383	48.19915	1.867827	-136.0937	7.695266	-0.014394
2	8	4	48.31558	167.6675	44.01385	35590.37	51.92818	51.17265	206.7083	4.711034	1.670705	42.87531	2.178109	-136.0941	7.695266	0.000155
2	8	5	49.83991	167.7432	36.47854	36920.35	53.79927	53.28872	168.2052	4.543381	9.677319	46.46043	1.484924	-136.0945	7.695266	0.005969
2	8	6	49.59012	167.7279	41.429	36700.85	53.13012	52.62654	191.6026	4.570138	5.029016	45.43145	1.777197	-136.0949	7.695266	0.006869
2	8	7	51.10902	168.1822	47.63412	38045.02	54.47048	53.75705	216.3735	4.42061	0.097821	42.77891	3.109329	-136.0953	7.695266	0.003944
2	8	8	49.61213	168.1237	38.59643	36720.16	53.34439	52.87908	178.4554	4.578511	7.279976	45.86062	1.61124	-136.0957	7.695266	-0.00849
2	8	9	51.2628	168.184	49.35825	38182.38	54.36374	53.81836	223.8016	4.404753	4.399122	47.23195	1.932964	-136.0961	7.695266	0.007549
2	8	10	47.50315	167.6507	44.97083	34890.78	51.25118	50.29914	213.3096	4.805013	9.655448	44.33842	1.59891	-136.0965	7.695266	-0.007294
2	8	11	48.48098	167.5824	35.76367	35733.58	52.60359	51.99535	167.6249	4.689773	35.44926	47.29327	1.003468	-136.0969	7.695266	-0.001518
2	8	12	50.70338	167.3198	47.89125	37683.82	54.09078	53.32369	218.5816	4.440096	0.226164	43.30697	2.867045	-136.0973	7.695266	-0.007019
2	8	13	45.68816	168.3979	39.23768	33350.99	50.11886	48.90697	190.3635	5.049263	9.549574	42.35485	1.52668	-136.0977	7.695266	-0.012701
2	8	14	50.97539	167.9788	43.25958	37925.85	54.37132	53.88767	196.811	4.429137	4.291917	46.67889	1.856479	-136.0981	7.695266	-0.00118
2	8	15	47.64613	168.1804	36.35745	35013.44	51.80213	51.11544	172.1515	4.803311	36.35745	46.48969	1	-136.0985	7.695266	-0.007497
2	8	16	48.37875	167.8266	40.1228	35645.03	52.16445	51.51587	188.2897	4.708273	22.24926	46.36167	1.232229	-136.0989	7.695266	-0.005738
2	8	17	47.92295	168.1357	35.77579	35251.47	52.26723	51.44773	168.4945	4.769609	35.77579	46.74802	1	-136.0993	7.695266	-0.000552
2	8	18	47.46064	167.6551	37.71059	34854.35	51.45411	50.79501	178.9657	4.810162	37.71059	46.34918	1	-136.0997	7.695266	-0.006717
2	8	19	48.71493	168.353	44.61455	35936.61	52.47105	51.54506	208.5177	4.684723	8.588381	45.37467	1.635189	-136.1001	7.695266	0.009682
2	8	20	48.71614	168.1103	40.24729	35937.65	52.89775	51.84884	188.1034	4.67783	17.58844	46.22936	1.321418	-136.1005	7.695266	-0.005234
2	9	1	51.64777	167.4209	49.15578	38527.26	54.93524	54.20222	221.8837	4.345519	2.506994	46.96984	2.123469	-136.1005	7.693266	0.000585
2	9	2	49.50159	167.5967	36.02501	36623.2	53.61279	52.99077	166.7864	4.576244	36.00214	48.33737	1.00025	-136.1001	7.693266	0.005103
2	9	3	48.2961	167.8285	47.13568	35573.52	51.71441	50.9665	221.4222	4.717792	12.32103	45.49511	1.536677	-136.0997	7.693266	0.015169
2	9	4	49.11443	168.4728	46.8765	36284.53	52.90795	51.8099	218.0365	4.643102	5.727065	45.31459	1.807282	-136.0993	7.693266	-0.003832

130

2	9	5	45.63141	168.0727	43.33917	33303.36	49.13219	48.53997	210.4124	5.046721	9.615222	42.41691	1.578891	-136.0989	7.693266	0.001121
2	9	6	48.27493	167.359	41.58638	35555.21	52.03927	51.29321	195.4044	4.707017	8.874771	44.91458	1.584999	-136.0985	7.693266	0.005796
2	9	7	47.63057	168.6595	49.35719	35000.08	50.89032	50.19341	233.7495	4.818833	0.724615	41.55595	2.5277	-136.0981	7.693266	0.009669
2	9	8	46.81779	168.4875	34.95718	34305.6	50.99158	50.43265	167.2202	4.911371	32.36392	45.46925	1.029789	-136.0977	7.693266	-0.002786
2	9	9	48.44569	167.7686	40.60975	35703.01	52.20124	51.54412	190.4201	4.699006	12.08084	45.5017	1.462618	-136.0973	7.693266	0.005064
2	9	10	46.22102	168.4103	46.61197	33799.76	49.79992	48.93079	224.634	4.982588	8.140769	42.86103	1.679967	-136.0969	7.693266	-0.000523
2	9	11	48.56937	168.1074	38.68039	35810.23	52.57321	51.82892	181.1016	4.694395	12.85569	45.6783	1.415217	-136.0965	7.693266	0.005923
2	9	12	49.71008	167.5677	34.32267	36806.19	54.16084	53.37168	158.5096	4.552706	26.37009	48.00102	1.100066	-136.0961	7.693266	-0.002902
2	9	13	49.15689	167.8432	34.18596	36321.6	53.48128	52.83917	158.9279	4.621029	34.0508	47.92195	1.001528	-136.0957	7.693266	-0.00169
2	9	14	48.19631	168.2679	43.55827	35487.26	52.12199	51.0936	204.8657	4.741643	3.1271	43.49952	1.965824	-136.0953	7.693266	0.001026
2	9	15	49.8175	167.6077	45.232	36900.63	53.4902	52.59663	208.6237	4.542138	1.122757	43.98266	2.324637	-136.0949	7.693266	-0.001128
2	9	16	48.86359	168.3119	36.30457	36065.89	53.053	52.34067	169.3744	4.666789	24.05004	46.97278	1.157844	-136.0945	7.693266	0.003773
2	9	17	46.41711	168.1169	46.24574	33965.59	50.29147	49.14358	222.3243	4.949622	4.402487	42.27293	1.889985	-136.0941	7.693266	-0.002369
2	9	18	47.62982	167.6546	37.52845	34999.44	52.0403	50.98037	177.7317	4.790209	25.77171	45.85884	1.146423	-136.0937	7.693266	-0.003721
2	9	19	48.56016	167.6947	44.83289	35802.23	51.91697	51.36549	209.931	4.683916	0.916297	42.45602	2.381932	-136.0933	7.693266	-0.010267
2	9	20	47.52159	168.0935	40.43147	34906.59	51.2129	50.63971	191.7347	4.815524	12.25936	44.59152	1.454768	-136.0929	7.693266	-0.000362

Grain boundary (6)

Row	Indent	hc(nm)	Pmax(µN)	S(µN/nm)	A(nm^2)	hmax(nm)	heff(nm)	Er(GPa)	H(GPa)	A	hf(nm)	m	X(mm)	Y(mm)	Drift Correc
1	1	46.25539	168.9896	33.01016	33120.45	51.04939	50.09488	160.7068	5.102274	33.01016	44.97555	1	-135.3774	2.33975	0.08807
1	2	49.0364	168.5241	45.779	35489.14	52.67848	51.79734	215.3046	4.74861	2.900802	44.34987	2.02308	-135.3769	2.33975	0.118834
1	3	48.86034	168.5986	43.78994	35336.91	52.6582	51.74796	206.393	4.771175	0.006274	37.1141	3.800839	-135.3765	2.33975	0.091521
1	4	44.3497	169.0043	35.00549	31541.22	48.73751	47.97066	174.6352	5.358204	17.18188	41.86836	1.263954	-135.376	2.33975	0.082018
1	5	45.21803	169.1703	41.06655	32256.39	49.06495	48.30759	202.5887	5.244551	2.81962	40.23281	1.960174	-135.3756	2.33975	0.058904
1	6	48.59578	168.6431	44.331	35108.75	52.31113	51.44892	209.6209	4.803448	0.412072	41.49322	2.617042	-135.3751	2.33975	0.046524
1	7	47.45348	168.9856	43.02489	34131.55	51.27031	50.3992	206.3368	4.951008	8.963261	44.12079	1.598526	-135.3747	2.33975	0.037208
1	8	46.11586	167.8977	34.83073	33003.62	50.28361	49.73115	169.87	5.08725	20.4749	43.95028	1.199254	-135.3742	2.33975	0.01957
1	9	47.47517	168.7378	39.46389	34149.99	51.5939	50.68199	189.208	4.941079	10.05647	44.21982	1.511352	-135.3738	2.33975	0.019043
1	10	48.18216	168.7417	35.58976	34753.42	52.27169	51.73813	169.1458	4.855399	35.39746	46.98679	1.002119	-135.3733	2.33975	0.025203
1	11	47.4099	168.3544	45.69714	34094.52	51.1138	50.173	219.2712	4.937873	2.775239	42.66874	2.036911	-135.3729	2.33975	0.024819
1	12	46.58915	168.3132	42.64871	33400.71	50.31102	49.54903	206.7583	5.03921	9.07562	43.27395	1.590035	-135.3724	2.33975	0.024839
1	13	49.59526	168.3901	45.21056	35974.37	53.17085	52.38869	211.1923	4.680835	9.092361	46.34543	1.622536	-135.372	2.33975	0.019151
1	14	48.01078	167.992	44.65461	34606.69	51.60652	50.8323	212.6773	4.854321	1.880973	42.74673	2.149259	-135.3715	2.33975	0.009777
2	1	48.06272	167.7403	43.57959	34651.13	51.84898	50.94951	207.4241	4.840834	3.785558	43.62237	1.90362	-135.3715	2.33775	0.005368
2	2	46.81986	168.4169	40.62914	33595.07	50.87507	49.92878	196.397	5.013143	40.62914	45.78356	1	-135.372	2.33775	0.009507
2	3	46.82814	168.0782	37.11846	33602.05	50.81955	50.22426	179.408	5.002023	37.11846	45.6961	1	-135.3724	2.33775	0.008175
2	4	45.38312	168.486	35.77459	32393.2	49.27088	48.91536	176.1094	5.201276	16.78213	42.87514	1.28252	-135.3729	2.33775	-0.009533
2	5	45.76989	168.6598	43.24052	32714.75	49.52308	48.69527	211.8136	5.155468	17.24381	43.3743	1.364175	-135.3733	2.33775	0.003028
2	6	46.58387	167.8008	33.49239	33396.26	50.94315	50.34145	162.3798	5.02454	33.49239	45.33134	1	-135.3738	2.33775	-0.007543
2	7	47.37598	167.8451	44.4393	34065.72	50.87929	50.2087	213.3257	4.927097	4.130741	43.08325	1.88656	-135.3742	2.33775	0.000591
2	8	47.4016	168.4434	53.34546	34087.47	50.77504	49.76979	255.997	4.941504	2.630722	42.93607	2.164217	-135.3747	2.33775	0.013566
2	9	46.31518	168.0327	47.38808	33170.58	50.02563	48.97459	230.53	5.065715	0.518492	39.74911	2.601742	-135.3751	2.33775	0.001999
2	10	47.60006	168.1369	51.34037	34256.22	50.87062	50.05627	245.7673	4.908214	2.496366	43.00001	2.154619	-135.3756	2.33775	7.04E-05
2	11	45.1085	168.1171	38.2721	32165.78	48.93357	48.40301	189.0689	5.226582	29.27863	43.54546	1.10583	-135.376	2.33775	0.009607
2	12	50.6076	168.132	50.66118	36861.26	53.79621	53.09667	233.7895	4.561211	0.178045	43.18484	2.98661	-135.3765	2.33775	0.0052
2	13	47.30081	168.0704	35.89745	34001.92	51.38423	50.81228	172.4831	4.942969	22.11896	45.26847	1.184078	-135.3769	2.33775	-0.009785
2	14	44.98716	168.2969	40.80874	32065.52	48.79741	48.08019	201.9151	5.248532	17.93457	42.63292	1.320855	-135.3774	2.33775	-0.018458
3	1	50.15566	168.0994	44.39834	36464.06	53.61124	52.99528	206.0009	4.610003	3.83516	45.76181	1.910501	-135.3774	2.33575	0.005043
3	2	48.6086	167.2311	39.72439	35119.78	52.71624	51.76593	187.8089	4.761735	13.67842	45.84173	1.407247	-135.3769	2.33575	-0.013463
3	3	45.06241	168.4273	37.77636	32127.69	49.32757	48.40632	186.7305	5.242436	9.601863	41.69682	1.504865	-135.3765	2.33575	-0.008028
3	4	46.89426	167.598	40.03077	33657.85	50.83143	50.0343	193.3239	4.979462	0.078862	37.39116	3.019815	-135.376	2.33575	-0.019735
3	5	48.26441	167.7269	33.15134	34823.94	52.94673	52.05873	157.3972	4.816425	33.15134	46.99955	1	-135.3756	2.33575	-0.002033
3	6	46.5182	168.8528	40.67315	33341.04	50.01588	49.63179	197.3572	5.064413	5.834242	42.51351	1.714648	-135.3751	2.33575	0.001639
3	7	47.17413	168.4273	36.53195	33894.53	51.29085	50.63193	175.8097	4.96916	36.44914	46.01738	1.000897	-135.3747	2.33575	0.013828
3	8	46.43704	168.0356	43.52696	33272.85	50.34744	49.33242	211.421	5.050233	3.065391	41.71805	1.972379	-135.3742	2.33575	0.000454
3	9	47.51816	167.7269	39.04402	34186.53	51.58891	50.74004	187.0948	4.906228	39.04402	46.4442	1	-135.3738	2.33575	0.000837
3	10	47.8307	167.4974	40.43804	34452.83	51.51565	50.93726	193.0246	4.861644	10.86272	44.73054	1.498457	-135.3733	2.33575	-0.003034
3	11	48.01235	167.6879	37.32427	34608.03	52.23563	51.38189	177.7615	4.845347	37.309	46.88843	1.000164	-135.3729	2.33575	0.007452
3	12	47.99214	168.0506	42.85181	34590.74	51.65875	50.93339	204.1381	4.858254	10.23998	44.85401	1.550203	-135.3724	2.33575	0.004362
3	13	45.98673	168.8287	45.01763	32895.67	49.453	48.79944	219.9116	5.132246	0.152481	37.82561	2.926138	-135.372	2.33575	-0.000245
3	14	48.01198	168.5679	45.02673	34607.72	51.56182	50.81978	214.4464	4.870817	3.158267	43.39346	1.983668	-135.3715	2.33575	-0.000556
4	1	49.35035	167.4407	45.70745	35761.34	52.7264	52.09784	214.1484	4.682169	1.078709	43.50553	2.345502	-135.3715	2.33375	-0.021804
4	2	48.38965	168.0234	39.39518	34931.46	52.24325	51.58846	186.7538	4.810088	21.11325	46.28554	1.243335	-135.372	2.33375	-0.001865
4	3	47.38747	167.537	45.88932	34075.47	51.03507	50.12564	220.2548	4.916645	1.059775	41.53203	2.353837	-135.3724	2.33375	-0.018964
4	4	49.92715	167.3507	34.94313	36264	54.22296	53.51907	162.5769	4.614789	34.9338	48.72934	1.000104	-135.3729	2.33375	-0.008553
4	5	49.67656	168.0796	39.65889	36045.22	53.49272	52.85516	185.0766	4.663021	33.23294	48.3148	1.07131	-135.3733	2.33375	0.017487
4	6	48.29195	168.2565	41.13376	34847.57	52.21082	51.35981	195.2302	4.828356	12.45654	45.3964	1.457876	-135.3738	2.33375	0.005497
4	7	46.3716	168.3879	37.6936	33217.91	50.4756	49.72206	183.2383	5.06919	37.57237	45.24902	1.00129	-135.3742	2.33375	0.006863
4	8	44.54182	168.0132	39.39687	31698.82	48.25853	47.7403	196.0537	5.300297	1.05979	38.17355	2.243275	-135.3747	2.33375	0.001753
4	9	49.98052	167.8015	47.5705	36310.68	53.37185	52.62609	221.1848	4.62127	2.932887	45.40546	2.046997	-135.3751	2.33375	0.011138
4	10	47.65592	167.7891	36.96285	34303.79	51.81979	51.06047	176.8191	4.891271	36.96285	46.52107	1	-135.3756	2.33375	-0.005956
4	11	49.86014	167.5308	38.15949	36205.44	53.62222	53.15285	177.6849	4.627226	23.96927	47.96667	1.181287	-135.376	2.33375	-0.003941
4	12	48.77202	167.4978	35.08729	35260.66	53.17852	52.35233	165.5539	4.750273	33.69027	47.50314	1.015803	-135.3765	2.33375	-0.009389
4	13	48.86089	168.0223	43.17204	35337.39	52.62522	51.77984	203.4793	4.754803	7.405452	45.28562	1.66864	-135.3769	2.33375	-0.017697
4	14	48.96761	167.6405	42.04357	35429.62	52.91071	51.95809	197.9024	4.731648	3.003377	44.15314	1.957449	-135.3774	2.33375	0.005327
5	1	51.73718	167.1373	45.93012	37862.91	55.33296	54.46639	209.1344	4.414275	1.646886	46.40925	2.214139	-135.3774	2.33175	-0.007972
5	2	48.46564	167.3378	40.30727	34996.77	52.13877	51.57931	190.8992	4.781521	1.798116	42.87956	2.095542	-135.3769	2.33175	-0.015889
5	3	50.24506	167.4827	43.18828	36542.47	54.1984	53.15354	200.1713	4.583233	8.887149	46.92716	1.605578	-135.3765	2.33175	-0.00122
5	4	49.24278	168.5189	40.66551	35667.97	52.76128	52.3508	190.7752	4.724658	8.929914	45.84838	1.569107	-135.376	2.33175	0.024258
5	5	46.72541	167.8579	41.03651	33515.43	50.95907	49.79325	198.6017	5.008375	21.07917	44.62576	1.263304	-135.3756	2.33175	0.004719
5	6	47.29264	167.889	37.26734	33995	51.76308	50.67139	179.0836	4.938639	34.92387	46.0502	1.025793	-135.3751	2.33175	0.009925
5	7	45.2969	168.1652	39.17791	32321.72	49.27618	48.51616	193.0763	5.202853	15.34612	42.68694	1.35805	-135.3747	2.33175	-0.000237
5	8	48.14699	167.4645	42.32769	34723.28	51.78532	51.11427	201.2561	4.822832	12.23207	45.2574	1.480361	-135.3742	2.33175	0.01242
5	9	42.85849	168.7621	34.62662	30330.16	47.37627	46.51382	176.1601	5.56417	34.62662	41.64005	1	-135.3738	2.33175	0.001779
5	10	49.05984	168.0384	38.84093	35509.42	52.92286	52.30458	182.6218	4.732221	10.71414	45.89462	1.481618	-135.3733	2.33175	-0.013635
5	11	48.03097	168.0247	39.45996	34623.96	51.71586	51.22455	187.8897	4.852844	19.77291	45.82271	1.268601	-135.3729	2.33175	-0.010568
5	12	48.17599	167.7916	42.84173	34748.13	51.7614	51.1134	203.6623	4.828913	5.551527	44.20568	1.763728	-135.3724	2.33175	-0.009573
5	13	47.27842	167.8027	44.36143	33982.93	50.94795	50.11539	213.2112	4.937853	1.325504	41.57684	2.257306	-135.372	2.33175	-0.013699
5	14	48.62122	167.1897	37.78158	35130.66	52.35928	51.94009	178.5961	4.759084	7.674737	44.93553	1.582892	-135.3715	2.33175	-0.014762
6	1	50.28892	167.8059	33.62182	36580.97	54.38922	54.03215	155.7501	4.587245	31.6656	48.92694	1.022888	-135.3715	2.32975	-0.009042
6	2	52.19472	167.2945	42.55797	38272.27	55.92039	55.14295	192.7408	4.371167	27.39371	50.50619	1.179545	-135.372	2.32975	0.024838
6	3	48.53818	167.597	39.08536	35059.17	52.4632	51.75416	184.9474	4.780406	39.08536	47.46619	1	-135.3724	2.32975	0.027671
6	4	47.38112	168.4891	39.40803	34070.08	51.50718	50.58774	189.1616	4.945369	24.72636	45.52752	1.183538	-135.3729	2.32975	0.016224

6	5	48.21476	167.6948	51.80126	34781.36	51.36015	50.64271	246.0945	4.821398	0.156526	40.77634	3.047741	-135.3733	2.32975	0.00691
6	6	45.98251	168.6656	45.22439	32892.14	49.60331	48.77966	220.9335	5.127837	0.438111	39.02988	2.614213	-135.3738	2.32975	0.00752
6	7	48.53359	168.5968	41.01371	35055.22	52.31953	51.61665	194.083	4.809465	32.10708	47.09708	1.099453	-135.3742	2.32975	0.011175
6	8	49.6758	167.2907	49.79577	36044.56	53.30587	52.19545	232.3846	4.641218	0.104008	41.66143	3.135558	-135.3747	2.32975	0.007037
6	9	48.31631	167.6146	33.62027	34868.48	52.65242	52.05545	159.5216	4.807051	27.89914	46.71781	1.070628	-135.3751	2.32975	-0.008071
6	10	50.1136	167.7487	38.60908	36427.2	53.78391	53.3722	179.2303	4.605039	24.64547	48.26321	1.175887	-135.3756	2.32975	-0.013551
6	11	48.71761	167.8607	43.19942	35213.73	52.46725	51.6319	203.9655	4.766909	1.103223	42.7101	2.29605	-135.376	2.32975	0.00064
6	12	47.12441	167.7761	38.89934	33852.43	51.16093	50.35922	187.3191	4.956102	38.83013	46.04302	1.000723	-135.3765	2.32975	-0.015882
6	13	47.47241	168.2316	43.08646	34147.64	51.17378	50.40079	206.5833	4.926596	2.632432	42.53194	2.015322	-135.3769	2.32975	-0.013597
6	14	48.57142	168.0384	39.30984	35087.78	52.41621	51.77746	185.9337	4.789088	16.59381	46.08621	1.331373	-135.3774	2.32975	-0.002067

Appendix G Sample II grain boundaries

Grain boundary (1)

Indent	hc(nm)	Pmax(μN)	S(μN/nm)	A(nm^2)	hmax(nm)	heff(nm)	Er(GPa)	E(GPa)	H(GPa)	A	hf(nm)	m	X(mm)	Y(mm)
bulkleft_000.hys	55.41012	166.3118	41.12413	38806.08	59.13605	58.44322	184.9617	201.9893984	4.285715	13.27937	52.63358	1.436559	-139.414896	-98.806486
bulkleft_001.hys	52.34562	166.8819	37.8841	36129.38	56.66199	55.64941	176.5881	191.1803291	4.619008	37.8841	51.24435	1	-139.413346	-98.806486
bulkleft_002.hys	51.27111	167.2777	36.3006	35211.53	55.07245	54.72721	171.3982	184.5739476	4.750651	36.3006	50.11908	1	-139.411796	-98.806486
bulkleft_003.hys	55.74528	166.5058	44.24311	39104.14	59.57956	58.56785	198.2298	219.5076756	4.258008	6.020336	51.95417	1.757354	-139.414896	-98.808036
bulkleft_004.hys	52.9705	166.9151	39.69168	36668.1	56.71479	56.12447	183.6497	200.2833758	4.552052	39.69168	51.91918	1	-139.413346	-98.808036
bulkleft_005.hys	52.81956	167.1918	38.53012	36537.64	56.69858	56.074	178.5932	193.7515869	4.575877	38.23396	51.72119	1.003125	-139.411796	-98.808036
bulkleft_006.hys	55.22479	166.549	36.9771	38641.72	59.13002	58.60288	166.6631	178.6076685	4.310083	36.9771	54.09876	1	-139.414896	-98.809586
bulkleft_007.hys	50.64764	166.807	48.66461	34683.85	53.98552	53.21841	231.5178	265.6945355	4.809356	3.33782	46.29115	2.020972	-139.413346	-98.809586
bulkleft_008.hys	53.23187	166.5597	49.81855	36894.5	56.75019	55.73936	229.7974	263.2252287	4.514486	2.596056	48.64067	2.123241	-139.411796	-98.809586
bulkleft_009.hys	78.25853	162.6663	39.4185	61562.27	82.06371	81.35352	140.7594	146.9628042	2.642305	9.185628	74.96055	1.549192	-139.413694	-98.80388
bulkright_000.hys	52.6803	167.9184	41.27464	36417.47	56.43474	55.73154	191.6299	210.7327474	4.61093	14.31764	49.99674	1.409625	-139.401525	-98.808408
bulkright_001.hys	54.6184	169.2759	44.38477	38106.16	57.97207	57.47877	201.4518	223.8358995	4.442219	1.990018	49.37805	2.124038	-139.399975	-98.808408
bulkright_002.hys	54.24598	168.9395	49.25198	37778.95	57.39748	56.81856	224.5089	255.6925471	4.471789	2.988637	49.74464	2.062304	-139.398425	-98.808408
bulkright_003.hys	51.3858	168.8685	36.94069	35308.98	55.49963	54.8143	174.1796	188.1056849	4.782592	22.54127	49.37746	1.189331	-139.401525	-98.809958
bulkright_004.hys	50.87697	169.1021	41.90216	34877.53	54.3255	53.9037	198.7918	220.2603958	4.848454	30.69335	49.35656	1.126746	-139.399975	-98.809958
bulkright_005.hys	56.41761	167.8478	44.58655	39705.23	59.81707	59.24102	198.2508	219.535661	4.227347	38.91351	55.25884	1.057813	-139.398425	-98.809958
bulkright_006.hys	51.61234	168.3633	49.09773	35501.85	55.19642	54.1842	230.8717	264.7660818	4.742381	3.038151	47.13462	2.055782	-139.401525	-98.811508
bulkright_007.hys	50.81979	168.3799	44.06728	34829.19	54.21075	53.68552	209.2086	234.3780235	4.834448	10.27774	47.70924	1.564071	-139.399975	-98.811508
bulkright_008.hys	52.85891	167.3871	38.02193	36571.63	56.69894	56.1607	176.1557	190.6272217	4.576966	38.02193	51.75831	1	-139.398425	-98.811508
bulkright_009.hys	294.3334	127.5855	36.57038	531320.9	297.6565	296.95	44.45144	42.3550688	0.240129	7.271939	291.2231	1.641531	-139.398991	-98.812739
bulkright_010.hys	80.72979	162.5633	48.29882	64323.31	83.86367	83.25412	168.728	181.2024051	2.527284	0.325883	73.90152	2.778731	-139.402116	-98.813395
gb 000.hys	48.5271	168.1681	36.74127	32915.95	52.33562	51.95992	179.4261	194.8228496	5.109016	9.102136	45.05262	1.509101	-139.412257	-98.799544
gb 001.hys	31.84299	176.5938	35.65963	20418.12	36.39309	35.55715	221.1077	250.8934369	8.648876	31.74924	30.38554	1.044304	-139.412229	-98.800302
gb 002.hys	43.81692	168.2242	37.0712	29136.33	48.09683	47.22032	192.4217	211.7791248	5.773694	9.431677	40.40677	1.501487	-139.411909	-98.800723
gb 003.hys	45.65346	168.2481	41.23543	30586.02	49.47971	48.7136	208.9026	233.958935	5.500816	9.197395	42.32102	1.56674	-139.41169	-98.801184
gb 004.hys	45.53178	167.6605	41.41368	30489.02	49.46397	48.56811	210.1391	235.6544877	5.499046	2.483184	40.43271	2.009517	-139.411471	-98.801606
gb 005.hys	42.28637	167.9793	40.76502	27951.43	46.31986	45.37688	216.0332	243.7986649	6.009686	1.565557	36.53633	2.145412	-139.411221	-98.802067
gb 006.hys	40.9686	168.3014	35.96798	26948.1	45.45536	44.478	194.1274	214.0389757	6.245391	11.45886	37.83706	1.419246	-139.411026	-98.802442
gb 007.hys	42.26015	168.1691	37.03217	27931.32	46.09623	45.66602	196.3217	216.9581923	6.020809	9.835483	38.91505	1.486618	-139.410792	-98.802817
gb 008.hys	36.47887	169.1299	29.41813	23645.18	41.16791	40.79075	169.5035	182.1796472	7.152827	20.10945	34.2643	1.135198	-139.410573	-98.803216
gb 009.hys	40.63612	168.123	29.69028	26697.4	45.25753	44.88304	160.0958	171.5422016	6.297353	25.16023	38.88122	1.059913	-139.4103	-98.803583
gb left 000.hys	100.7786	160.0392	44.39077	88916.13	104.1409	103.4825	131.8977	136.5078451	1.799889	0.926169	94.8605	2.391528	-139.407573	-98.806888
gb left 001.hys	49.34736	168.5615	40.55789	33594.9	53.05212	52.46442	196.053	216.6000432	5.017472	20.23477	47.17507	1.272681	-139.407866	-98.806516
gb left 002.hys	47.03996	168.9123	36.204	31700.77	51.29514	50.53914	180.1592	195.7671846	5.328335	29.52878	45.50484	1.079033	-139.408159	-98.806009
gb left 003.hys	49.89183	168.0311	39.51673	34048.97	53.96222	53.08094	189.7421	208.2451961	4.934984	15.05741	47.25855	1.369282	-139.40855	-98.805657
gb left 004.hys	46.75153	167.9942	36.32365	31467.42	50.90738	50.22022	181.4236	197.399335	5.338671	21.27604	44.6536	1.203613	-139.408862	-98.805305
gb left 005.hys	49.7354	168.2068	34.14649	33918.24	53.83356	53.42992	164.2723	175.6170699	4.959184	33.37895	48.4608	1.008748	-139.409331	-98.804856
gb left 006.hys	52.33186	167.1876	42.67926	36117.56	56.18278	55.26983	198.9722	220.502359	4.628983	6.799855	48.6389	1.69273	-139.409741	-98.804505
gb left 007.hys	48.82785	167.8424	42.00336	33164.17	52.53283	51.82479	204.3545	227.76065	5.060956	6.722313	45.08584	1.686454	-139.410171	-98.804114
gb left 008.hys	48.50614	166.8782	43.03205	32898.69	52.15276	51.41464	210.2024	235.74133	5.072488	5.632894	44.57831	1.76285	-139.410581	-98.803645
gb left 009.hys	49.02552	167.1837	45.4629	33327.76	52.50436	51.78354	220.6424	250.2396295	5.016351	7.23423	45.50029	1.708629	-139.410815	-98.803235
gb right 000.hys	49.09531	167.1389	43.23984	33385.61	52.751	51.99435	209.6714	235.0126171	5.006315	5.119991	45.04461	1.797939	-139.406167	-98.81177
gb right 001.hys	48.97717	167.2262	40.45404	33287.72	52.89815	52.07747	196.4512	217.1309246	5.023661	12.4303	46.07966	1.450943	-139.405835	-98.812024
gb right 002.hys	47.98665	168.235	46.84341	32471.99	51.72321	50.68022	230.3185	263.9722416	5.180927	1.313852	42.4245	2.298727	-139.405659	-98.812376
gb right 003.hys	47.2539	167.5923	35.00769	31874.33	51.48303	50.84437	173.7312	187.5349245	5.257908	34.57455	46.03386	1.004847	-139.405464	-98.812747
gb right 004.hys	47.01343	168.1156	40.00917	31679.27	50.73571	50.16487	199.1622	220.7570681	5.306801	4.370394	42.59056	1.802581	-139.40519	-98.813118
gb right 005.hys	48.22584	167.2825	40.67225	32668.15	51.98678	51.31054	199.375	221.0427116	5.120661	20.52425	46.08933	1.269461	-139.405288	-98.813509
gb right 006.hys	46.79775	167.8377	40.0653	31504.76	50.53337	49.93958	199.9931	221.8727549	5.327375	3.224854	41.96548	1.903532	-139.405444	-98.813841
gb right 007.hys	47.46457	167.9162	37.88115	32045.67	51.60799	50.78911	187.4879	205.2875317	5.239904	34.36817	46.1844	1.038802	-139.405053	-98.814212
gb right 008.hys	47.82638	167.3395	34.47648	32340.85	51.84895	51.46668	169.8564	182.6250062	5.174244	34.44124	46.61103	1.000396	-139.4048	-98.814544
gb right 009.hys	48.17041	167.0936	34.49904	32622.64	52.3192	51.80298	169.2319	181.8372375	5.122012	31.79565	46.80714	1.031468	-139.404565	-98.814856

Grain boundary (2)

Indent	hc(nm)	Pmax(µN)	S(µN/nm)	A(nm^2)	hmax(nm)	heff(nm)	Er(GPa)	E(GPa)	H(GPa)	A	hf(nm)	m	X(mm)	Y(mm)
bulkleft_000.hys	63.9161	165.8578	51.27995	49309.42	67.01367	66.34187	204.6056	228.1012322	3.363612	0.150983	56.45707	3.056186	-139.214853	-98.907498
bulkleft_001.hys	59.93214	166.1167	39.27674	45363.49	63.7414	63.10418	163.3868	174.5131517	3.661903	4.348469	55.50643	1.796417	-139.213803	-98.907498
bulkleft_002.hys	63.38101	165.711	51.95533	48770.28	66.3629	65.77312	208.443	233.3297961	3.397786	0.048681	54.90215	3.408375	-139.211753	-98.907498
bulkleft_003.hys	62.31301	165.5873	49.31105	47702.72	65.28555	64.83152	200.0357	221.9299275	3.471234	0.01978	52.68467	3.617269	-139.215353	-98.909048
bulkleft_004.hys	60.26054	166.8482	38.78616	45682.82	64.34879	63.48685	160.7812	171.2761625	3.652318	38.78616	59.1851	1	-139.213803	-98.909048
bulkleft_005.hys	59.76138	166.3794	46.32856	45197.87	63.19778	62.45485	193.0744	212.6428857	3.681132	9.868308	56.67313	1.609928	-139.211753	-98.909048
bulkleft_006.hys	61.48859	165.397	38.77511	46886.37	65.15537	64.68775	158.6589	168.6523577	3.527613	38.77511	60.42221	1	-139.214853	-98.910598
bulkleft_007.hys	56.37008	166.9905	36.34431	41968.12	60.22677	59.81609	157.1852	166.8368532	3.978985	31.78774	54.98011	1.052518	-139.213803	-98.910598
bulkleft_008.hys	57.24975	166.4207	45.745	42795.03	60.96682	59.97826	195.9213	216.4245658	3.888785	2.283237	52.31586	2.106208	-139.212253	-98.910598
bulkleft_009.hys	56.4537	167.1895	39.91138	42046.4	60.56016	59.59546	172.4516	185.909181	3.976311	10.01704	53.22661	1.520369	-139.214944	-98.910903
bulkright_000.hys	59.45714	166.5761	34.52466	44903.51	63.66608	63.07578	144.3524	151.2544153	3.709647	34.52466	58.25093	1	-139.202869	-98.912048
bulkright_001.hys	55.88993	169.3419	43.16016	41519.97	59.32775	58.83261	187.6676	205.5227641	4.078564	5.103201	51.7922	1.79439	-139.201319	-98.912048
bulkright_002.hys	59.69599	169.5521	39.05015	45134.53	63.33234	62.95242	162.8558	173.8520221	3.756594	10.04384	56.41611	1.505402	-139.199769	-98.912048
bulkright_003.hys	60.55637	168.7619	45.55021	45971.39	64.10089	63.3351	188.2268	206.2554142	3.67102	15.28124	58.01263	1.436576	-139.202869	-98.913598
bulkright_004.hys	58.71556	168.7189	58.41646	44189.81	61.56648	60.88172	246.2119	287.1688708	3.818051	1.551024	53.90809	2.414517	-139.201319	-98.913598
bulkright_005.hys	58.72626	168.8236	50.12364	44200.07	62.03951	61.25237	211.235	237.1609954	3.819532	9.264992	55.6051	1.676673	-139.199769	-98.913598
bulkright_006.hys	55.19694	168.5941	36.20781	40877.14	59.27196	58.68916	158.6708	168.6669167	4.124411	36.20781	54.03287	1	-139.202869	-98.915148
bulkright_007.hys	54.72452	168.2714	46.58708	40441.61	58.41662	57.43351	205.2514	228.9781659	4.160849	11.0169	51.76049	1.570614	-139.201319	-98.915148
bulkright_008.hys	55.19778	168.361	44.70696	40877.92	58.81309	58.02219	195.914	216.4148468	4.118629	0.632597	48.63265	2.49332	-139.199769	-98.915148
bulkright_009.hys	57.89358	166.9558	47.3494	43405.06	61.65822	60.53811	201.3627	223.7158758	3.846459	0.323983	50.84429	2.749208	-139.202913	-98.915708
gb 000.hys	59.38995	177.6544	45.96922	44838.61	63.30502	62.28842	192.3428	211.6747358	3.962085	22.14803	57.28868	1.293717	-139.203909	-98.90522
gb 001.hys	62.62418	174.8999	45.01178	48012.6	66.06381	65.53842	182.0051	198.1513961	3.642791	9.97643	59.4036	1.578842	-139.204104	-98.90563
gb 002.hys	60.87903	173.173	48.45462	46287.11	64.43653	63.55947	199.5446	221.2703167	3.741279	1.970985	55.76804	2.18008	-139.2043	-98.90602
gb 003.hys	63.88248	170.8131	46.59743	49275.46	67.23699	66.63177	185.9865	203.3253292	3.466495	2.814787	59.15217	2.040417	-139.204593	-98.90643
gb 004.hys	65.04141	169.3356	48.82286	50452.51	68.25482	67.64269	192.5824	211.9916934	3.356337	0.231313	57.68782	2.870187	-139.204807	-98.906821
gb 005.hys	72.67067	168.0009	57.77905	58535.95	75.81347	74.8514	211.5894	237.6488965	2.870047	5.888205	69.21616	1.938079	-139.2051	-98.907134
gb 006.hys	66.1017	167.6137	44.67536	51541.1	69.49324	68.91556	174.3517	188.3248447	3.25204	0.447759	59.1574	2.600918	-139.205335	-98.907505
gb 007.hys	62.90997	166.3718	31.31929	48298.04	67.38874	66.89406	126.2647	129.9565472	3.44469	3.100277	57.46504	1.775001	-139.20555	-98.907915
gb 008.hys	65.91013	167.1623	53.68117	51343.58	69.32403	68.24562	209.9006	235.327099	3.255758	1.01074	60.48332	2.492723	-139.205862	-98.908266
gb 009.hys	65.45281	166.1999	48.11834	50873.56	68.76251	68.0433	189.0164	207.2914134	3.266921	1.785415	60.36258	2.223727	-139.206057	-98.908598
gb left 000.hys	64.53578	165.0118	43.70059	49937.33	68.21223	67.36775	173.2644	186.9414431	3.304378	6.377737	60.82696	1.732217	-139.209202	-98.911684
gb left 001.hys	61.06062	165.7357	44.6122	46465.25	64.66985	63.84689	183.3683	199.9181708	3.566875	8.643977	57.76759	1.636406	-139.210034	-98.91186
gb left 002.hys	63.88732	165.0821	44.71804	49280.35	67.28412	66.65604	178.4764	193.6014393	3.349858	1.150005	58.11005	2.314968	-139.209807	-98.912153
gb left 003.hys	62.61401	165.7239	41.524	48002.45	66.4303	65.60729	167.9199	180.185697	3.452406	0.44569	55.42763	2.550628	-139.210081	-98.912446
gb left 004.hys	62.31811	165.4934	46.77933	47707.8	65.45607	64.97142	189.7554	208.2626076	3.468895	0.012523	51.90815	3.692542	-139.210315	-98.912778
gb left 005.hys	62.21018	165.4459	42.39572	47600.53	65.137	64.6541	172.1674	185.5486957	3.475716	0.700493	55.65609	2.429495	-139.210589	-98.913071
gb left 006.hys	62.88715	165.6555	38.49667	48275.22	66.68787	66.11449	155.2372	164.4455729	3.43148	16.61665	60.42384	1.322449	-139.211382	-98.913423
gb left 007.hys	59.32129	167.5	48.65854	44772.36	62.63183	61.90306	203.7459	226.935721	3.741148	4.393893	55.27601	1.92515	-139.211077	-98.912778
gb left 008.hys	51.88821	167.9797	42.74437	37872.44	55.40352	54.83562	194.6041	214.6720716	4.435408	0.365052	44.51307	2.626689	-139.211194	-98.912973
gb left 009.hys	56.22917	167.6933	34.8127	41836.37	60.18194	59.84193	150.798	159.0308842	4.008315	32.02603	54.86963	1.032237	-139.211468	-98.913247
gb right 000.hys	63.89771	166.0008	46.97044	49290.84	67.71227	66.54832	187.4461	205.2327288	3.367782	3.558168	59.56208	1.976779	-139.205843	-98.90938
gb right 001.hys	65.67828	165.6988	46.06384	51105.04	68.81392	68.37615	180.5357	196.2527404	3.242318	2.728292	60.98923	2.053545	-139.206175	-98.90977
gb right 002.hys	65.74717	165.6706	42.81249	51175.86	68.98852	68.64943	167.6767	179.8799932	3.237279	15.66745	63.24208	1.397365	-139.206448	-98.910102
gb right 003.hys	65.57571	165.7407	46.32407	50999.67	68.88879	68.25909	181.7431	197.8124599	3.249838	3.437128	61.17588	1.979738	-139.206741	-98.910552
gb right 004.hys	65.87917	165.3678	42.88066	51311.7	69.20404	68.77152	167.7213	179.9359866	3.22281	11.96935	62.99662	1.497458	-139.207112	-98.910884
gb right 005.hys	64.89608	165.1456	43.02538	50304.18	68.22273	67.77483	169.9642	182.7610662	3.28294	1.049076	58.88678	2.315604	-139.207366	-98.911235
gb right 006.hys	66.30026	165.2481	48.84101	51746.2	69.29094	68.8378	190.2305	208.887838	3.193434	11.58371	63.4803	1.58347	-139.20762	-98.911587
gb right 007.hys	66.65496	164.8959	41.13309	52113.57	70.52291	69.66159	159.6433	169.8679672	3.164164	23.86837	64.77671	1.218527	-139.207874	-98.911977
gb right 008.hys	66.50603	164.6782	45.33279	51959.17	69.81323	69.23051	176.2042	190.689172	3.169376	1.430453	61.03481	2.256122	-139.208089	-98.912309
gb right 009.hys	64.40885	164.8068	37.5749	49808.41	68.30944	67.69842	149.1699	157.0571968	3.308815	37.5749	63.31233	1	-139.208343	-98.912661

Grain boundary (3)

Indent	hc(nm)	Pmax(µN)	S(µN/nm)	A(nm^2)	hmax(nm)	heff(nm)	Er(GPa)	E(GPa)	H(GPa)	A	hf(nm)	m	X(mm)	Y(mm)
bulkleft_000.hys	51.70038	169.6112	46.0624	37705.06	55.44215	54.46204	210.1752	235.7040832	4.498367	3.016013	47.05312	2.012086	-137.965041	1.287019
bulkleft_001.hys	50.072	169.7886	45.55297	36268.26	53.82677	52.86746	211.9279	238.1152877	4.681465	1.023165	44.09433	2.353763	-137.963491	1.287019
bulkleft_002.hys	46.4374	170.3564	37.63844	33153.2	50.4199	49.83199	183.1487	199.6331286	5.13846	17.671344	44.01011	1.286284	-137.961941	1.287019
bulkleft_003.hys	47.62719	169.3977	40.24211	34159	51.6616	50.78429	192.9137	212.4301017	4.959092	40.242114	46.57483	1	-137.965041	1.285469
bulkleft_004.hys	44.26936	169.7172	40.76776	31355.02	48.24614	47.39163	203.985	227.2596242	5.41276	1.82621	38.67726	2.093278	-137.963491	1.285469
bulkleft_005.hys	45.87447	169.2698	34.79746	32682.02	50.0399	49.52279	170.5407	183.4891896	5.179293	23.889454	43.96791	1.141939	-137.961941	1.285469
bulkleft_006.hys	47.11852	168.4086	45.84886	33727.34	50.43445	49.87336	221.1935	251.0141147	4.993237	0.608606	40.59976	2.524717	-137.965041	1.283919
bulkleft_007.hys	43.89691	168.8157	38.4547	31050.57	47.8931	47.1894	193.3524	213.0111319	5.436798	12.841133	40.99043	1.412069	-137.963491	1.283919
bulkleft_008.hys	42.79511	168.9633	42.85497	30157.6	46.39613	45.75212	218.644	247.4392471	5.602678	0.732011	36.2314	2.414783	-137.961941	1.283919
bulkleft_009.hys	45.59828	168.1626	39.14114	32451.95	49.39563	48.82052	192.5076	211.8927058	5.181895	15.090123	42.96175	1.363673	-137.966225	1.284141
bulkright_000.hys	53.29858	166.099	46.49524	40299.65	56.82527	55.97788	205.2072	228.9181611	4.121598	0.762971	47.14867	2.471514	-137.951057	1.289769
bulkright_001.hys	52.82415	167.0973	37.90557	39861.93	56.49464	56.13034	168.2127	180.5538474	4.191903	36.722229	51.66593	1.012738	-137.949507	1.289769
bulkright_002.hys	50.05058	168.2009	45.60395	37342.88	53.30634	52.81681	209.0901	234.2156922	4.504231	5.546051	46.1718	1.801645	-137.947957	1.289769
bulkright_003.hys	52.04078	167.7668	37.10396	39143.55	56.058	55.43193	166.1594	177.9764498	4.285937	37.103963	50.9104	1	-137.951057	1.288219
bulkright_004.hys	48.63087	168.1103	44.32697	36079.68	51.95484	51.47525	206.7624	231.034679	4.659416	5.266503	44.64122	1.801982	-137.949507	1.288219
bulkright_005.hys	47.5596	168.6562	37.786	35138.22	51.56712	50.90719	178.5977	193.7573323	4.799794	32.742017	46.19034	1.056772	-137.947957	1.288219
bulkright_006.hys	52.71076	167.5976	39.17602	39757.61	56.56395	55.91931	174.0785	187.9769293	4.215484	39.075061	51.63674	1.001052	-137.951057	1.286669
bulkright_007.hys	48.15266	168.085	39.16136	35658.18	51.78029	51.37175	183.7439	200.4058263	4.713785	38.975645	47.07133	1.001934	-137.949507	1.286669
bulkright_008.hys	46.44653	168.8349	51.87501	34170.63	49.83736	48.88752	248.6374	290.7812356	4.940936	0.184083	39.13827	2.995485	-137.947957	1.286669
bulkright_009.hys	50.99583	168.3859	33.99371	38193.75	55.19071	54.71092	154.1123	163.0688187	4.40873	17.130836	48.50798	1.252247	-137.952194	1.286844
gb 000.hys	35.50799	167.5807	26.56501	25226.54	40.96654	40.23923	148.189	155.8710881	6.643031	26.355551	33.91334	1.002784	-137.950717	1.296188
gb 001.hys	43.69792	166.4513	44.23752	31827.33	47.20981	46.51993	219.6977	248.9143342	5.229823	7.041114	40.11265	1.702852	-137.951057	1.295734
gb 002.hys	47.87411	165.2763	59.99881	35413.58	50.33314	49.94011	282.4831	343.3031401	4.66703	12.984697	45.34503	1.668112	-137.95128	1.295211
gb 003.hys	37.81264	160.7187	26.62701	27027.15	43.24415	42.33959	143.5017	150.2355012	5.946565	0.125838	26.65585	2.598397	-137.951475	1.294727
gb 004.hys	45.49548	164.1414	39.77519	33352.42	49.34195	48.59052	192.9671	212.5008885	4.921423	3.763659	40.93581	1.85491	-137.951717	1.294227
gb 005.hys	41.39314	166.2206	41.87189	29912.49	45.11961	44.37044	214.5019	241.6728526	5.556895	3.087362	36.63562	1.948445	-137.951889	1.293703
gb 006.hys	44.83502	165.3016	36.23861	32788.83	48.7416	48.25613	177.3141	192.1100729	5.041399	4.129126	40.1929	1.767681	-137.952069	1.293273
gb 007.hys	40.47853	166.9385	39.84567	29165.18	44.38692	43.62075	206.7205	230.9776052	5.723896	0.206749	32.133	2.741951	-137.952389	1.292789
gb 008.hys	38.49326	167.2024	38.37603	27567.33	42.44741	41.76097	204.7847	228.3443197	6.065237	8.240776	34.93362	1.567002	-137.952663	1.292367
gb 009.hys	45.48446	166.5037	38.15677	33342.99	49.30736	48.75721	185.1417	202.2238237	4.993663	11.812173	42.47471	1.439728	-137.952882	1.291961
gb left 000.hys	67.25491	163.9841	35.63757	54080.04	70.90501	70.70599	135.7764	141.061374	3.032247	10.888126	64.09737	1.436207	-137.956475	1.288758
gb left 001.hys	66.9217	164.6814	47.70506	53730.47	70.2287	69.51076	182.3429	198.5888321	3.064954	0.294309	59.87129	2.79237	-137.956725	1.288391
gb left 002.hys	68.99227	164.2653	44.89772	55919.15	71.96958	71.73626	168.2205	180.5636315	2.93755	0.299845	61.72248	2.737012	-137.957014	1.288055
gb left 003.hys	69.24956	163.9713	46.09528	56193.86	72.34416	71.91748	172.2848	185.6975357	2.917958	1.483608	63.88439	2.258247	-137.957335	1.287688
gb left 004.hys	70.22591	163.882	41.58981	57241.81	73.64721	73.18124	154.0157	162.9508229	2.862977	2.447015	65.20361	2.244556	-137.9576	1.287336
gb left 005.hys	68.23105	163.8096	46.9833	55109.95	71.45988	70.84596	177.3223	192.1205478	2.972414	0.272638	61.06403	2.805619	-137.957913	1.287023
gb left 006.hys	68.90432	163.837	36.64047	55825.38	72.6212	72.25792	137.3979	142.97526	2.934811	36.640469	67.78645	1	-137.958217	1.28671
gb left 007.hys	70.08421	163.795	40.47698	57089.17	74.12473	73.11917	150.095	158.177799	2.869109	13.667664	67.372	1.420239	-137.958507	1.286422
gb left 008.hys	67.95239	164.6429	34.60869	54815.05	71.92404	71.52035	130.9695	135.4232919	3.003607	29.702968	66.48216	1.05905	-137.958866	1.286172
gb left 009.hys	69.80386	163.6316	42.64478	56787.74	73.39431	72.68168	158.5526	168.5211857	2.88146	2.557963	64.9033	2.027158	-137.959132	1.285859
gb right 000.hys	63.38644	164.1806	46.78456	50083.92	66.77642	66.01841	185.2202	202.3260933	3.27811	1.280303	57.88947	2.316407	-137.952733	1.291289
gb right 001.hys	65.15419	163.6044	44.45333	51893.09	68.56116	67.91446	172.8958	186.4730487	3.15272	9.725074	62.04458	1.59492	-137.952983	1.290836
gb right 002.hys	66.21377	163.4588	39.96659	52991.13	69.79708	69.28118	153.8262	162.7192592	3.084644	19.09222	64.00246	1.290678	-137.953288	1.290508
gb right 003.hys	67.96521	163.927	53.78862	54828.6	70.66703	70.25092	203.5268	226.6390671	2.989808	0.0582	59.89484	3.398095	-137.953553	1.290109
gb right 004.hys	67.67746	163.6334	48.67077	54524.79	70.71364	70.19899	184.6741	201.6151112	3.001082	0.831822	61.83726	2.487098	-137.95378	1.28975
gb right 005.hys	68.24311	163.5614	44.38346	55122.73	71.29284	71.007	167.4907	179.6462618	2.967223	4.232262	64.05935	1.88529	-137.954092	1.289391
gb right 006.hys	67.7194	163.7493	41.57859	54569.03	71.28304	70.67314	157.6999	167.4703427	3.000773	1.162566	61.7638	2.262223	-137.954366	1.289039
gb right 007.hys	66.63278	163.911	39.90463	53428.18	70.38839	69.71346	152.9582	161.6597777	3.067875	24.540179	64.80841	1.194148	-137.954702	1.288742
gb right 008.hys	66.30469	164.0849	48.49804	53085.83	69.34365	68.84219	186.4961	203.9905726	3.090936	0.35374	59.53195	2.751798	-137.954967	1.288391
gb right 009.hys	68.18901	164.0438	43.19273	55065.41	71.28613	71.03747	163.082	174.1336031	2.979071	0.640164	61.63704	2.475132	-137.955225	1.288055
gb right 000.hys	63.38644	164.1806	46.78456	50083.92	66.77642	66.01841	185.2202	202.3260933	3.27811	1.280303	57.88947	2.316407	-137.952733	1.291289
gb right 001.hys	65.15419	163.6044	44.45333	51893.09	68.56116	67.91446	172.8958	186.4730487	3.15272	9.725074	62.04458	1.59492	-137.952983	1.290836
gb right 002.hys	66.21377	163.4588	39.96659	52991.13	69.79708	69.28118	153.8262	162.7192592	3.084644	19.09222	64.00246	1.290678	-137.953288	1.290508
gb right 003.hys	67.96521	163.927	53.78862	54828.6	70.66703	70.25092	203.5268	226.6390671	2.989808	0.0582	59.89484	3.398095	-137.953553	1.290109
gb right 004.hys	67.67746	163.6334	48.67077	54524.79	70.71364	70.19899	184.6741	201.6151112	3.001082	0.831822	61.83726	2.487098	-137.95378	1.28975
gb right 005.hys	68.24311	163.5614	44.38346	55122.73	71.29284	71.007	167.4907	179.6462618	2.967223	4.232262	64.05935	1.88529	-137.954092	1.289391
gb right 006.hys	67.7194	163.7493	41.57859	54569.03	71.28304	70.67314	157.6999	167.4703427	3.000773	1.162566	61.7638	2.262223	-137.954366	1.289039
gb right 007.hys	66.63278	163.911	39.90463	53428.18	70.38839	69.71346	152.9582	161.6597777	3.067875	24.540179	64.80841	1.194148	-137.954702	1.288742
gb right 008.hys	66.30469	164.0849	48.49804	53085.83	69.34365	68.84219	186.4961	203.9905726	3.090936	0.35374	59.53195	2.751798	-137.954967	1.288391
gb right 009.hys	68.18901	164.0438	43.19273	55065.41	71.28613	71.03747	163.082	174.1336031	2.979071	0.640164	61.63704	2.475132	-137.955225	1.288055

Grain boundary (4)

Indent	hc(nm)	Pmax(µN)	S(µN/nm)	A(nm^2)	hmax(nm)	heff(nm)	Er(GPa)	E(GPa)	H(GPa)	A	hf(nm)	m	X(mm)	Y(mm)
bulkleft_000.hys	48.53785	168.5014	41.48545	35997.54	52.34284	51.58412	193.7288	213.5101931	4.680916	0.80744	41.99028	2.362027	-138.154103	1.137144
bulkleft_001.hys	49.18699	169.7493	43.27799	36572.38	52.88127	52.12871	200.505	222.5609997	4.641462	6.586838	45.42857	1.708217	-138.152553	1.137144
bulkleft_002.hys	49.74334	169.4388	37.53413	37068.01	53.70951	53.12903	172.7275	186.2594126	4.571026	37.53413	48.61477	1	-138.151003	1.137144
bulkleft_003.hys	45.20894	168.938	34.01959	33107.45	49.61647	48.93337	165.6537	177.3432539	5.102719	21.79128	43.14254	1.166117	-138.154103	1.135594
bulkleft_004.hys	51.45943	168.1972	47.33534	38613.94	55.03509	54.12441	213.4265	240.1841019	4.355868	10.24668	48.41633	1.606412	-138.152553	1.135594
bulkleft_005.hys	48.29791	168.6832	45.03679	35786	51.86911	51.107	210.9336	236.7462332	4.713665	3.96	43.96129	1.907834	-138.151003	1.135594
bulkleft_006.hys	43.69429	169.3116	33.07141	31824.27	48.29716	47.53397	164.2511	175.5906364	5.320204	30.15153	42.23584	1.034877	-138.154103	1.134044
bulkleft_007.hys	42.84892	168.5446	31.21791	31116.68	47.43273	46.89814	156.7986	166.3615173	5.416536	24.03072	40.9822	1.095754	-138.152553	1.134044
bulkleft_008.hys	48.19479	168.143	38.52823	35695.24	52.10449	51.46791	180.6794	196.4382331	4.710515	10.8806	45.04411	1.471946	-138.151003	1.134044
bulkleft_009.hys	50.39173	164.6312	34.14759	37649.06	54.77101	54.00761	155.9257	165.2896923	4.372785	5.535912	46.09869	1.640457	-138.155366	1.133875
bulkright_000.hys	52.53625	166.8213	45.24111	39597.28	56.01307	55.30178	201.4352	223.813562	4.212949	7.066695	48.97986	1.714474	-138.1511	1.126292
bulkright_001.hys	47.47425	168.188	42.8989	35063.64	51.15384	50.41467	202.9796	225.8986544	4.796648	6.162893	43.63923	1.72818	-138.14955	1.126292
bulkright_002.hys	45.78929	167.8241	37.31676	33604.36	50.12172	49.16226	180.3603	196.0264842	4.994117	37.16579	44.65769	1.001619	-138.148	1.126292
bulkright_003.hys	49.49465	167.8148	40.62547	36846.13	53.08798	52.59274	187.5156	205.3236984	4.554475	15.51245	46.92355	1.372425	-138.1511	1.124742
bulkright_004.hys	46.88166	167.8382	42.38959	34547.61	50.47339	49.85123	202.0622	224.6592179	4.858172	17.50885	44.50983	1.349036	-138.14955	1.124742
bulkright_005.hys	45.82495	167.953	46.64978	33634.99	49.10338	48.52517	225.3662	256.9077777	4.993401	3.343276	41.36286	1.989368	-138.148	1.124742
bulkright_006.hys	48.90775	167.8988	41.78829	36324.65	52.56827	51.92113	194.2624	214.2182151	4.622173	41.71088	47.90017	1.000775	-138.1511	1.123192
bulkright_007.hys	45.54763	167.9836	41.21603	33397.09	49.15731	48.60439	199.8236	221.6449073	5.029887	39.14972	44.44193	1.021292	-138.14955	1.123192
bulkright_008.hys	47.07868	168.3343	44.14937	34718.83	50.51434	49.93831	209.9311	235.3689052	4.848501	5.548926	43.14666	1.781259	-138.148	1.123192
bulkright_009.hys	47.96345	168.4891	35.52775	35491.96	52.39492	51.5203	167.085	179.1369822	4.747246	35.06636	46.75361	1.005108	-138.152163	1.125281
gb 000.hys	25.39461	171.1014	32.3038	17825.99	30.06865	29.36708	214.3688	241.4884168	9.598422	0.097054	14.64549	2.779423	-138.158112	1.12825
gb 001.hys	41.04756	168.6061	41.80082	29629.29	44.49517	44.07273	215.1588	242.5838931	5.690522	1.251528	35.072	2.23146	-138.15828	1.128043
gb 002.hys	46.66655	168.2794	44.26133	34361.04	50.45307	49.51801	211.5564	237.6033941	4.89739	3.192933	42.0307	1.969335	-138.158768	1.127848
gb 003.hys	28.87601	171.1497	34.21792	20284.42	33.39954	32.62733	212.8664	239.4101181	8.437497	0.604056	21.08202	2.308251	-138.159159	1.127809
gb 004.hys	53.29366	167.5427	47.43986	40295.1	56.73793	55.94242	209.3882	234.6242117	4.157893	2.441168	48.50125	2.106976	-138.159589	1.127711
gb 005.hys	29.91465	170.2584	27.8341	21035.55	35.13031	34.50232	170.0338	182.8488411	8.093845	4.277005	24.65127	1.610465	-138.160018	1.127652
gb 006.hys	32.46712	169.7461	37.18644	22917.12	36.9507	35.89067	217.6404	246.0373172	7.406956	4.069777	27.76299	1.780538	-138.160507	1.127555
gb 007.hys	42.27239	168.4908	32.16709	30637.63	46.80725	46.20088	162.8242	173.8127725	5.499473	32.16709	40.96289	1	-138.160917	1.127457
gb 008.hys	47.21538	167.7532	34.80534	34837.84	51.52325	50.83019	165.2171	176.797216	4.815258	20.24433	45.03151	1.203108	-138.161425	1.12734
gb 009.hys	53.60092	166.635	43.28877	40579.63	57.29874	56.48796	190.3952	209.1046236	4.10637	2.239246	48.50289	2.074376	-138.161893	1.12732
gb left 000.hys	31.95589	170.7638	39.01622	22536.15	36.19383	35.23844	230.2715	263.9047687	7.577326	9.727992	28.60872	1.514765	-138.149428	1.133504
gb left 001.hys	34.94614	170.4656	41.94718	24794.19	38.79495	37.994	236.0275	272.2113582	6.875222	2.288082	29.70894	2.038739	-138.14926	1.133328
gb left 002.hys	39.09886	169.3474	38.21182	28051.24	43.55605	42.42271	202.142	224.76688	6.037075	6.827384	35.21693	1.625924	-138.149675	1.133059
gb left 003.hys	43.17123	168.7227	38.22154	31385.74	47.13466	46.48199	191.1511	210.1008839	5.375775	16.25757	40.63396	1.32478	-138.150112	1.132801
gb left 004.hys	40.96321	169.6015	33.00277	29560.32	45.44083	44.81746	170.0712	182.8960881	5.737471	17.64753	38.50572	1.228203	-138.150487	1.132504
gb left 005.hys	40.92349	168.8097	36.88791	29527.86	44.86355	44.35571	190.1967	208.8432421	5.716962	4.072164	36.22315	1.777108	-138.15076	1.132207
gb left 006.hys	42.02989	169.2687	35.53081	30436.98	45.74447	45.60289	180.4426	196.1326795	5.561284	14.60781	39.27615	1.328031	-138.151581	1.131957
gb left 007.hys	42.88085	168.2423	33.65391	31143.3	47.17321	46.63024	168.9616	181.4966634	5.402199	33.6276	41.62955	1.0003	-138.15144	1.131652
gb left 008.hys	47.55725	168.542	40.12751	35136.17	51.07568	50.70737	189.6705	208.1510255	4.796823	1.896183	41.99895	2.073355	-138.151831	1.131363
gb left 009.hys	52.34797	166.8089	35.92809	39424.6	56.36981	55.83011	160.3191	170.7039218	4.231087	21.99698	50.319	1.187008	-138.152128	1.131074
gb left 010.hys	44.49989	168.9798	42.74805	32504.3	48.41911	47.46459	210.0781	235.5706884	5.198692	5.675385	40.53483	1.753072	-138.152487	1.130824
gb right 000.hys	46.25938	167.9463	37.63574	34009	50.11081	49.60619	180.8166	196.6152593	4.93829	37.44645	45.13477	1.002019	-138.153026	1.129789
gb right 001.hys	49.28509	167.8932	39.46266	36659.58	53.7	52.47596	182.6112	198.9363444	4.57979	15.24841	46.67222	1.364146	-138.152858	1.129535
gb right 002.hys	49.52492	167.2919	35.55725	36873.11	53.63626	53.05357	164.062	175.3547752	4.536961	21.34013	47.43869	1.19342	-138.153729	1.129262
gb right 003.hys	48.25266	168.0354	46.89121	35746.15	51.745	50.94029	219.7413	248.9753931	4.700797	12.51934	45.46623	1.527569	-138.154042	1.129008
gb right 004.hys	50.37205	166.6621	35.57486	37631.36	54.63373	53.88567	162.4812	173.3861173	4.428809	35.57486	49.20084	1	-138.153932	1.128832
gb right 005.hys	48.72504	167.3621	43.50586	36162.93	52.53394	51.61021	202.6986	225.5187201	4.628001	16.02529	46.24068	1.39581	-138.154303	1.128578
gb right 006.hys	50.96965	167.1574	40.10933	38170.08	54.86416	54.09531	181.8941	198.0078646	4.379279	11.02763	47.88915	1.489164	-138.154635	1.128344
gb right 007.hys	48.66551	167.2147	37.09061	36110.3	53.10496	52.04672	172.9352	186.523071	4.630666	28.11642	47.05027	1.108283	-138.155448	1.128109
gb right 008.hys	50.6161	167.8774	43.13796	37850.98	54.49207	53.53483	196.4517	217.1315795	4.43522	6.330372	46.83063	1.722718	-138.15578	1.127856
gb right 009.hys	51.63192	167.089	38.11141	38770.77	55.47405	54.92009	171.4895	184.689639	4.309663	11.09336	48.51641	1.460617	-138.156112	1.127621

References

1.   Jones R., Stress-Corrosion Cracking, Corrosion: Fundamentals, Testing, and Protection. ASM Handbook, ASM International (2003) 13A: pp. 346-366.

2.   Kane R., Corrosion in Petroleum Refining and Petrochemical Operations, Corrosion: Environments and Industries. ASM Handbook, ASM International (2006) 13C: pp. 967-1014.

3.   http://ece-www.colorado.edu/~bart/book/fcc.gif.

4.   Pace L., Scenna R & Childs J. NRC"s Response to the February 15, 2000, Steam Generator Tube Rupture at Indian Point Unit 2 Power Plant, 2000.

5.   http://www.nrc.gov/reading-rm/doc-collections/fact-sheets/steam-gen.html.

6.   Eisenhut D., Transmittial of NUREG-0916 relative to the restart of R. E. Ginna Nuclear Power Plant, 1982.

7.   Long S., Information Notice No. 84-49: Intergranular stress corrosion cracking leading to steam generator tube failure, 1984.

8.   Murphy E., NRC Information Notice 92-80: Operation with steam generator tubes seriously degraded, 1992.

9.   Conrad, H., NRC Information Notice 94-05: Potential failure of steam generator tubes with kinetically welded sleeves, 1994.

10.   Connor L., United States Nuclear Power Plant Steam Generator Replacement Experience, 1997.

11.   Was G., Fundamentals of Radiation Materials Science: Metals and Alloys. Springer, 2007.

12.   http://www.met-tech.com/metallography.htm.

13.   Watanabe T., The impact of grain boundary character distribution on fracture in polycrystals. Materials Science and Engineering (1994) A176: pp. 39-49.

14.   Tsurekawa S., Nakamichi S. and Watanabe T., Correlation of grain boundary connectivity with grain boundary character distribution in austenitic stainless steel. Acta Materiala (2006) 54: pp. 3617-3626.

15.   Tan L., Sridharan K. and Allen T., Effect of thermomechancal processing on grain boundary character distribution of a Ni-based superalloy. Journal of Nuclear Materials (2007) 371: pp. 171-175.

16. Tan L., Sridharan K., Allen T., Nanstad R & McClintock D. Microstructure tailoring for property improvements by grain boundary engineering. Journal of Nuclear Materials (2008) 374: pp. 270-280.

17. Fricano J., Chemical and Structural Analysis of Grain Boundaries in Inconel 690 for Corrosion Resistance. Massachusetts Institute of Technology. 2009.

18. Langitan F, and Lawn B., Hertzian fracture experiments on abraded glass surfaces as definitive evidence for an energy balance experimentation of Auerbach's law. Journal of Applied Physics (1969) 40: pp. 4009-4017.

19. Wynick G. and Boehlert C., Use of electropolishing for enhanced metallic specimen preparation for electron backscatter diffraction analysis. Materials Characterization (2005) 55: pp. 190-202.

20. Oliver W. and Pharr G., An improved technique for determining hardness and elastic modulus using load and displacement sensing indentation experiments. Journal of Materials Research (1992) 7: pp. 1564-1583.

21. Hysitron Probe Tip Selection Guide.

22. Gouldstone A., Chollacoop N., Dao M., Li .J, Minor A.M. and Shen Y., Nanoindentation across size scales and disciplines: Recent developments in experimentaton and modeling. Acta Materialia (2007) 55: pp. 4015-4039.

23. Fischer-Cripps A., Nanoindentation: Second Edition. Springer Science and Business Media, 2004.

24. Nix W. and Gao H. Indentation size effect in crystalline materials: a law for strain gradient plasticity. Journal of the Mechanics and Physics of Solids (1998) 46: pp. 411-425.

25. Vlassak J. and Nix W., Measuring the elastic properties of anisotropic materials by means of indentation experiments. Journal of the Mechancis of PhysicalSolids (1994) 42: pp. 1223-1245.

26. Gjostein N., Diffusion. ASM (1973) 8: pp. 241-274.

27. Soifer Y, Verdyan A., Kazakevich M and Rabkin E., Nanohardness of copper in the vicinity of grain boundaries. Scripta Materialia (2002) 47: pp. 799-804.

28. Soer W., Aifantis K. and De Hosson J., Incipient plasticity during nanoindentation at grain boundaries in body-centered cubic metals. Acta Materialia (2005) 53: pp. 4665-4676.